Application of Minimum Quantity Lubrication (MQL) in Plane Surface Grinding

Łukasz Barczak

A thesis submitted in partial fulfilment of the requirements of Liverpool John Moores University for the degree of Doctor of Philosophy

February 2010

Abstract

The aim of this research was to acquire and formalise understanding of the Minimum Quantity Lubrication (MQL) technique in the surface grinding operation. The investigation aimed to show through experiment and theoretical study the effects of MQL on grinding process performance, measured in terms of tangential and normal forces, temperature and surface finish.

A comparison of conventional, dry and MQL fluid delivery methods was performed. The experimental study was undertaken on a CNC grinding machine with integrated monitoring. A Taguchi methodology was employed to provide qualitative evidence of the strength of process parameters on performance indicators.

The usefulness and promise of MQL was established. The study identified regimes of grinding where MQL can be employed successfully. This outcome is supported by results showing, in some applications, that MQL is comparable in performance to grinding under conventional fluid delivery. It was found that for some conditions MQL outperformed conventional fluid delivery. This was particularly so in the case of the tests with material EN8, (approximately 32 HRC), where MQL was found to outperform conventional fluid delivery in almost all measures. As expected, not all conditions were in favour of MQL delivery and the reasons for this are discussed in detail in the thesis.

A theoretical explanation for the efficient process performance is developed in relation to the experimental results obtained. The effects of variables such as DOC, dressing conditions, wheel speeds, workpiece speed and workpiece material are considered.

It is reasoned that the MQL technique achieves efficient performance due to effective lubrication and effective contact region penetration by the fluid. Effective lubrication conditions were confirmed by highly competitive specific energy and grinding force measurements.

Dedicated to my Parents, Wife and Children

Acknowledgments

I would like to thank my Director of studies, Dr Michael Morgan, for his support and efforts put in this study, to make it a successful and valuable work.

Gratitude is also due to Dr Andre Batako whose invaluable assistance and limitless support throughout the project has been critical. Particular thanks go to Professor Bogdan Kruszynski for 'planting' my interest in MQL and whose practical help and theoretical guidance were vital.

I express my thanks to the Liverpool John Moores University who provided the finance and laboratory resources to support the research work. Thanks are also due to the staff of AMTReL and GERI for their help and support during this project.

I would also like to thank the technical staff without whom none of this work could have been accomplished, particular thanks go to Mr Paul Wright and Mr Peter Moran, for priceless support throughout the time of this study.

Finally, I would like to thank my friends and family, particularly my parents and my wife, who have provided critical emotional support and guidance throughout the course of this venture.

Nomenclature

Symbol	Meaning	Units
a	Applied depth of cut	m
a_e	Real/actual depth of cut	m
a_{ed}	Dressing depth	m
a_{sw}	Wheel wear depth	m
a^*	Effective 'contact radius' of a rough surface	m
a_0	Contact radius for smooth surfaces	m
b_s	Wheel width	m
b_w	Contact/workpiece width	m
c_s	Wheel specific heat capacity	kJ/(kg·K)
c_w	Workpiece specific heat capacity	kJ/(kg·K)
d_e	Equivalent wheel diameter	m
d_s	Wheel diameter	m
d_w	Workpiece diameter	m
e_c	Specific energy	J/m^3
e_{ch}	Energy of chip formation	J/m^3
e_p	Energy of ploughing	J/m^3
e_s	Energy of sliding	J/m^3
E_s	Wheel Young's modulus	MPa
E_w	Workpiece Young's modulus	MPa
E^*	Elastic properties of two surfaces	MPa
F_n	Normal grinding force	N
F_n'	Specific normal grinding force	N/mm
F_t	Tangential grinding force	N

F_t'	Specific tangential grinding force	N/mm
h	Height	m
h_{eq}	Equivalent chip thickness	m
h_f	Fluid convection coefficient	$W/(m^2 \cdot K)$
h_r	Real thickness of removed material	m
k_s	Wheel thermal conductivity	$W/(m \cdot K)$
k_w	Workpiece thermal conductivity	$W/(m \cdot K)$
l_c	Contact length	m
l_e	Real contact length	m
l_f	Deformation contact length	m
l_{fr}	Rough surface deformation contact length	m
l_g	Geometric contact length	m
l_k	Kinematic contact length	m
L_w	Workpiece length	m
m	Mass	kg
n_d	Number of dressing passes	-
p_a	Absolute atmospheric pressure	bar
P	Grinding power	W
Pe	Peclet number	-
q_{ch}	Heat flux dissipated to grinding chips	W
q_f	Heat flux dissipated to grinding fluid	W
q_s	Heat flux dissipated to grinding wheel	W
q_t	Total heat flux generated in the grinding zone	W
q_w	Heat flux dissipated to the workpiece	W
Q_w	Volumetric removal rate	m^3/s
Q'_w	Specific volumetric removal rate	$m^3/m/s$

R_r	Roughness factor	-
R_w	Partition ratio of workpiece	-
R_{ws}	Partition ratio of workpiece-wheel	-
r_0	Effective radius of contact of grains	m
r_s	Wheel radius	m
t_s	Dwell time	s
s	Feed per cutting edge	m
z	Workpiece height	m
v_{air}	Air velocity	m/s
v_{fad}	Dressing feedrate	m/min
v_f	Feedrate	m/min
v_{sd}	Dressing wheel speed	m/s
v_s	Wheel surface speed	m/s
v_w	Workpiece surface speed	m/s
μ_s	Wheel dynamic viscosity	kg/(m·s)
μ	Friction coefficient/force ratio	-
υ	Kinematic viscosity	m^2/s
ρ	Density	kg/m^3
θ	Absolute temperature	°C
θ_{amb}	Ambient temperature	°C
θ_{av}	Average surface temperature	°C
θ_{max}	Maximum background temperature	°C
θ_{mp}	Melting point temperature	°C

Acronyms and Abbreviations

AED	Aerodynamic Equivalent Diameter
AMTReL	Advanced Manufacturing Technology Research Laboratory
CNC	Computer Numerically Controlled machine
DOC	Depth of cut
DRY	Dry machining
EPA	Environmental Protection Agency/Authority
FEM	Final Element Method
GERI	General Engineering Research Institute
HEDG	High Efficiency Deep Grinding
HRC	Hardness Rockwell C
LDA	Laser Doppler Anemometry
MQL	Minimum Quantity Lubrication
NDG	Near Dry Grinding
NDM	Near Dry Machining
PVD	Physical Vapour Deposition coating
WET	Conventional flood cooling

Contents

ABSTRACT ..... **I**

ACKNOWLEDGMENTS ..... **II**

NOMENCLATURE ..... **III**

ACRONYMS AND ABBREVIATIONS ..... **VI**

CONTENTS ..... **VII**

LIST OF FIGURES ..... **XIII**

LIST OF TABLES ..... **XVII**

CHAPTER 1. INTRODUCTION **1**

1.1. Background 2

1.2. MQL Benefits and Limitations 4

1.3. Project Aim and Objectives 5

1.4. The Scope of the Investigation 5

CHAPTER 2. PROCESS FLUIDS, FLUID DELIVERY AND GRINDING WHEELS **7**

2.1. Process Fluids 8

2.1.1. The Function of Fluids in the Grinding Process *8*

2.1.2. Fluid Types in Grinding *9*

2.1.3. Oil-based Coolants *11*

2.1.4. Water-based Coolants *12*

2.1.5. Alternative Lubrication Techniques *13*

2.2. Fluid Influence on the Working and Natural Environment 14

2.3. Fluid Delivery 16

2.3.1. Fluid Delivery into Grinding Zone *16*

2.3.2. Boundary Effect *19*
2.4. Grinding Wheels 21
2.4.1. Abrasive Materials *21*
2.4.2. Bond Materials *22*
2.4.3. Wheel Composition and Parameters *23*
2.4.4. Wheel Wear and Dressing *24*
2.5. Summary 26
CHAPTER 3. MINIMUM QUANTITY LUBRICATION 27
3.1. Introduction 28
3.2. Minimum Quantity Lubrication Background 29
3.3. Economics of Minimum Quantity Lubrication 30
3.4. Classification and Design of Minimum Quantity Lubrication Systems 31
3.5. Results for MQL in Machining 34
3.5.1. MQL in Milling *35*
3.5.2. MQL in Turning *36*
3.5.3. MQL in Sawing *37*
3.5.4. MQL in Drilling *37*
3.5.5. MQL in Grinding *39*
3.6. Advantages and Disadvantages of MQL Systems in Grinding 45
3.7. Aspects of Health and Environment Hazards 49
3.8. Lubricants for MQL 49
3.9. Summary 50
CHAPTER 4. GRINDING THEORY AND KEY RELATIONSHIPS 52
4.1. Grinding Mechanics, Geometry and Kinematics 53
4.2. Contact Length 54
4.2.1. Geometric Contact Length *54*
4.2.2. Kinematic Contact Length *55*
4.2.3. Real Contact Length *56*
4.3. Thermal Models in Grinding 59
4.3.1. Power and Specific Energy *59*

4.3.2. Equivalent Chip Thickness *61*
4.4. Heat Transfer in Grinding 61
4.4.1. Heat Flux Into the Workpiece *62*
4.4.2. Heat Flux Into the Chips *63*
4.4.3. Heat Flux Into the Process Fluid *63*
4.4.4. Heat Flux Into the Wheel *64*
4.5. Temperatures in Grinding 64
4.6. Summary 65

CHAPTER 5. PRELIMINARY EXPERIMENTAL STUDIES 66
5.1. Aims and Objectives 67
5.2. Scope 67
5.3. Experimental Set-up and Equipment 68
5.3.1. Grinding Machine *68*
5.3.2. MQL System *69*
5.3.3. Data Collection System *72*
5.3.4. Grinding Wheel *73*
5.3.5. Grinding Fluids *73*
5.3.6. Workpiece Material *74*
5.4. Experimental Work 74
5.4.1. Experiment Procedure *75*
5.5. Results 77
5.5.1. Tangential Force Results: EN31 ..... *78*
5.5.2. Tangential Force Results: EN9 ..... *78*
5.5.3. Tangential Force Results: M2 ..... *79*
5.5.4. Surface Roughness Results: EN31 ..... *80*
5.5.5. Surface Roughness Results: EN9 ..... *80*
5.5.6. Surface Roughness Results: M2 ..... *81*
5.6. Discussion 82
5.7. Summary 83

CHAPTER 6. EXPERIMENTAL WORK 84
6.1. Aims and Objectives 85
6.2. Scope 85

6.3. Equipment 86
6.3.1. Grinding Machine 86
6.3.2. MQL System and Nozzle Arrangements 87
6.3.3. Data Acquisition System 89
6.3.4. Grinding Wheel and Fluid Delivery 90
6.3.5. Workpieces and Temperature Measurements 90
6.4. Experimental Work 91
6.4.1. Experiment Procedure 91
6.4.2. DOC Measurements 92
6.4.3. Surface roughness measurements 93
6.4.4. Laser Doppler Anemometry in Air Boundary Layer Measurements 94
6.5. Summary 96

CHAPTER 7. RESULTS 97
7.1. Introduction 98
7.2. Real Depth of Cut a_e and Equivalent Chip Thickness h_{eq} 99
7.2.1. Trial 1: v_s=25m/s, a=5μm, v_w=6.5m/min, Coarse Dressing, EN8 100
7.2.2. Trial 2: v_s=25m/s, a=5μm, v_w=15m/min, Fine Dressing, EN31 101
7.2.3. Trial 3: v_s=25m/s, a=15μm, v_w=6.5m/min, Coarse Dressing, EN31 ... 102
7.2.4. Trial 4: v_s=25 m/s, a=15 μm, v_w=15 m/min, Fine Dressing, EN8 103
7.2.5. Trial 5: v_s=45m/s, a=5μm, v_w=6.5m/min, Fine Dressing, EN31 104
7.2.6. Trial 6: v_s=45m/s, a=5μm, v_w=15m/min, Coarse Dressing, EN8 106
7.2.7. Trial 7: v_s=45m/s, a=15μm, v_w=6.5m/min, Fine Dressing, EN8 107
7.2.8. Trial 8: v_s=45m/s, a=15μm, v_w=15m/min, Coarse Dressing, EN31 108
7.2.9. Trial 2, 3, 5 and 8: Hard Material M2 109
7.2.10. Taguchi and ANOVA Analysis 110
7.3. Friction Coefficient 115
7.3.1. Trial 3: v_s=25m/s, a_e=15μm, v_w=6.5m/min, Coarse Dressing, EN31 .. 115
7.3.2. Trial 4: v_s=25m/s, a_e=15μm, v_w=15m/min, Fine Dressing, EN8 116
7.3.3. Trial 7: v_s=45m/s, a_e=15μm, v_w=6.5m/min, Fine Dressing, EN8 117
7.3.4. Trial 8: v_s=45m/s, a_e=15μm, v_w=15m/min, Coarse Dressing, EN31 ... 118
7.3.5. Trials: 3 and 8 for Hard Material M2 119

7.3.6. Taguchi Analysis *119*
7.4. Surface Roughness R_a 122
7.4.1. Trial 3: v_s=25 m/s, a_e=15μm, v_w=6.5 m/min, Coarse Dressing, EN31 123
7.4.2. Trial 4: v_s=25m/s, a_e=15μm, v_w=15m/min, Fine Dressing, EN8 ..... *124*
7.4.3. Trial 7: v_s=45m/s, a_e=15μm, v_w=6.5m/min, Fine Dressing, EN8 ..... *125*
7.4.4. Trial 8: v_s=45m/s, a_e=15μm, v_w=15m/min, Coarse Dressing, EN31 ... *126*
7.4.5. Trials: 3 and 8 for Hard Material M2 ..... *126*
7.4.6. Taguchi Analysis *127*
7.5. Grinding Process Temperature 130
7.5.1. Trial 3: v_s=25m/s, a_e=15μm, v_w=6.5m/min, Coarse Dressing, EN31 .. *130*
7.5.3. Trial 4: v_s=25 m/s, a_e=15 μm, v_w=15 m/min, Fine Dressing, EN8 ..... *132*
7.5.4. Trial 7: v_s=45m/s, a_e=15μm, v_w=6.5m/min, Fine Dressing, EN8 ..... *133*
7.5.5. Trial 8: v_s=45m/s, a_e=15μm, v_w=15m/min, Coarse Dressing, EN31 ... *133*
7.5.6. Trial 8: v_s=45m/s, a_e=15μm, v_w=15m/min, Coarse Dressing, M2 ..... *134*
7.5.7. Taguchi Analysis *135*
7.6. Specific Energy 138
7.7. MQL Process Economics 141
7.8. Discussion 145
7.9. Summary 147

CHAPTER 8. THERMAL ANALYSIS 148
8.1. Introduction 149
8.2. Calculations of Estimated Temperature 149
8.2.1. Contact Length *150*
8.2.2. Power, Material Removal Rate and Specific Energy *151*
8.2.3. Thermal Partition Model *151*
8.3. Results From Measured and Predicted Temperature 153
8.3.1. Results for Hardened Steel EN31 ..... *154*
8.3.2. Results for Hardened Steel M2 ..... *156*
8.3.3. Results for Mild Steel EN8 ..... *157*
8.4. Analysis of Predicted Temperatures Under Varying Assumptions 158
8.5. Discussion 160
8.6. Summary 161

CHAPTER 9. CONCLUSIONS 163

CHAPTER 10. FUTURE WORK 168

REFERENCES 171

BIBLIOGRAPHY 179

APPENDIXES 185

APPENDIX 1. STANDARD MARKING SYSTEM 186

APPENDIX 2. MQL SYSTEM 188

APPENDIX 3. MQL OIL SAFETY DATA SHEET 190

APPENDIX 4. MQL NOZZLE 194

APPENDIX 5. LABVIEW PROGRAM 195

APPENDIX 6. EQUIPMENT CALIBRATION PROCEDURE 196

APPENDIX 7. EXPERIMENTAL STUDIES WORKPIECE 198

APPENDIX 8. EXPERIMENTAL PROCESS SCREENS 200

APPENDIX 9. ANOVA RESULTS TABLES 201

APPENDIX 10. 5 μM DOC RESULTS CHARTS 206

APPENDIX 11. MATERIALS PHYSICAL PROPERTIES 209

APPENDIX 12. 5 μM DOC RESULTS CHARTS 210

List of Figures

Figure 2-1. Temperature of a workpiece as a function of wheel speed 10
Figure 2-2. Influence of fluid properties on specific normal force and roughness 11
Figure 2-3. Disposal of cutting fluids in cutting technology 15
Figure 2-4. De-oiling scheme 16
Figure 2-5. Examples for coolant supply strategies 17
Figure 2-6. Effect of coolant flow rate and nozzle cross-section on tensile residual stresses 19
Figure 2-7. Effect of boundary layer 20
Figure 2-8. Fluid flow vectors around an anti-clockwise rotating wheel 20
Figure 2-9. Wheel structure: a) soft, b) hard, c) open, d) compact 24
Figure 3-1. Manufacturing costs for crankshaft at a German car builder 28
Figure 3-2. Lubricating methods cost comparison for a coolant and MQL 31
Figure 3-3. Mixing methods: (a) inside and (b) outside nozzle 32
Figure 3-4. Working principle of excess pressure spraying MQL system 32
Figure 3-5. Principle of operation of MQL system 33
Figure 3-6. Examples of nozzles used with MQL systems (MicroJet). 33
Figure 3-7. Single segment and a rail build from segments used with MQL systems 34
Figure 3-8. MQL Systems solutions for 1) internal, 2) external drilling. 37
Figure 3-9. Diametral wear after 90 cycles using Al_2O_3 and CBN grinding wheels 40
Figure 3-10. Roughness R_a after 90 cycles using Al_2O_3 and CBN grinding wheels 41
Figure 3-11. Comparative results of residual stress 41
Figure 3-12. Influence of coolant supply method on function of normal forces and the DOC and specific material removal rate 43
Figure 3-13. Influence of coolant supply method 43
Figure 3-14. Variation of tangential force 44
Figure 4-1. Comparison of cutting speeds and angles for turning and grinding 53
Figure 4-2. Schematic presentation of single grain working 53
Figure 4-3. Stages of chip formation 54
Figure 4-4. Illustration of surface grinding with visible l_g 55

Figure 4-5. Analysis of the elastic deflection between the wheel and the workpiece ...57
Figure 4-6. Two features of wheel-workpiece body contact 58
Figure 4-7. Illustration of cutting force components, for surface face grinding 59
Figure 4-8. Graphical representation of equivalent chip thickness.....61
Figure 5-1. Elliot toolroom grinding machine 68
Figure 5-2. General schema of Steidle Lubrimat L50 MQL system.....69
Figure 5-3. Principle of operation of Steidle Lubrimat L50. 70
Figure 5-4. Nozzle used for initial investigation 71
Figure 5-5. Elliot Grinding Machine with MQL and conventional nozzles 72
Figure 5-6. Picture of the workplace 72
Figure 5-7. Workpiece before test and after test with a datum strip left.....74
Figure 5-8. Calibration chart dependence of frequency on MQL System flow rate.....75
Figure 5-9. General view of workplace for surface roughness measurements 76
Figure 5-10. DOC measurements 77
Figure 5-11. Tangential force as a function of real DOC for EN31.....78
Figure 5-12. Tangential force in the function of real DOC for EN9.....79
Figure 5-13. Tangential force as a function of real DOC for M2 79
Figure 5-14. Surface roughness as a function of DOC for EN31 80
Figure 5-15. Surface roughness as a function of DOC for EN9 81
Figure 5-16. Surface roughness as a function of DOC for M2 81
Figure 6-1. CNC Jones&Shipman Dominator 624 Easy 86
Figure 6-2. Nozzle and MQL system arrangement 87
Figure 6-3. Airflow velocity measurement workplace.....88
Figure 6-4. MQL System characterisation 88
Figure 6-5. A view of DAQ system 89
Figure 6-6. Thermocouple assembly and principle of operation 90
Figure 6-7. Mount of measuring clock gauge. 93
Figure 6-8. General view of Taylor Hobson Surtronic Duo roughness checker.....94
Figure 6-9. Equipment arrangements 94
Figure 6-10. MQL grinding process boundary layer 95
Figure 7-1. Specific tangential force as a function of DOC and specific removal rate, Trial 1. 100

Figure 7-2. Specific tangential force as a function of DOCand specific removal rate, Trial 2. 102
Figure 7-3. Specific tangential force as a function of DOC and specific removal rate, Trial 3. 103
Figure 7-4. Specific tangential force as a function of DOC and specific removal rate, Trial 4. 104
Figure 7-5. Specific tangential force as a function of DOC and specific removal rate, Trial 5. 105
Figure 7-6. Specific tangential force as a function of DOC and specific removal rate, Trial 6. 106
Figure 7-7. Specific tangential force as a function of DOC and specific removal rate, Trial 7. 107
Figure 7-8. Specific tangential force as a function of DOC and specific removal rate, Trial 8. 108
Figure 7-9. Specific tangential force as a function of DOC and specific removal rate for M2 and EN8. 109
Figure 7-10. Direct effects chart for specific tangential force with EN31 and EN8.... 112
Figure 7-11. Direct effects chart for specific tangential force with M2 and EN8..... 113
Figure 7-12. Coefficient friction in function of specific removal rate for EN31..... 116
Figure 7-13. Coefficient friction in function of specific removal rate for EN8..... 117
Figure 7-14. Coefficient friction in function of specific removal rate for EN8..... 118
Figure 7-15. Coefficient friction in function of specific removal rate for EN31..... 118
Figure 7-16. Coefficient friction in function of specific removal rate for M2..... 119
Figure 7-17. Direct effects chart for force ratio with EN31 and EN8..... 120
Figure 7-18. Direct Effects chart for force ratio with M2 and EN8..... 122
Figure 7-19. Surface roughness in function of specific removal rate for EN31. 123
Figure 7-20. Surface roughness in function of specific removal rate for EN8. 124
Figure 7-21. Surface roughness in function of specific removal rate for EN8. 125
Figure 7-22. Surface roughness in function of specific removal rate for EN31. 126
Figure 7-23. Surface roughness in function of specific removal rate for M2. 127
Figure 7-24. Direct effects chart for surface roughness with EN31 and EN8. 128
Figure 7-25. Direct effects chart for surface roughness with M2 and EN8. 129
Figure 7-26. Temperature as a function of specific removal rate for EN31. 131

Figure 7-27. Temperature as a function of specific removal rate for M2. 131
Figure 7-28. Temperature as a function of specific removal rate for EN8. 132
Figure 7-29. Temperature as a function of specific removal rate for EN8. 133
Figure 7-30. Temperature as a function of specific removal rate for EN31 134
Figure 7-31. Temperature as a function of specific removal rate for M2 135
Figure 7-32. Direct effects chart for temperature with EN31 and EN8. 136
Figure 7-33. Direct effects chart for temperature with M2 and EN8. 137
Figure 7-34. Direct effects chart for specific energy with EN31 and EN8. 140
Figure 7-35. Direct effects chart for specific energy with M2 and EN8. 141
Figure 7-36. Comparison of fluid delivery systems 142
Figure 8-1. Experimental & predicted temperature as a function of DOC for EN31 .. 155
Figure 8-2. Experimental & predicted temperature as a function of DOC for M2 157
Figure 8-3. Experimental & predicted temperature as a function of DOC for EN8 ... 158

List of Tables

Table 2-1. Comparison of different fluids properties. 12
Table 4-1. Heat flux distribution according to various researchers 62
Table 6-1. Set of parameters and Taguchi array 91
Table 7-1. Example of ANOVA results table for EN31 and EN8 for WET for F_t' 111
Table 7-2. Specific energy values for WET and MQL 139
Table 7-3. Fluid usage and power consumption 142
Table 7-4. Cost comparison in production conditions – local systems. 143
Table 7-5. Cost comparison in production condition – centralised facility. 145
Table 8-1. Experimental conditions values. 149
Table 8-2. Typical results for tangential force for the same test conditions 159
Table 8-3. Worst and typical case values of temperature 159
Table 8-4. Literature and obtained values comparison 160
Table 9-1. Table showing MQL and WET grinding process performance. 165

Chapter 1. INTRODUCTION

1.1. Background

Grinding is used for machining materials with challenging mechanical and chemical properties e.g. hardened steels, high-temperature resistant steels, sintered aluminium oxide and sintered carbides. Grinding may be used for rough machining replacing turning and/or milling. It may also be used as a precision process for achieving smooth surfaces, high accuracy and good size holding. More commonly, grinding is a finishing operation.

Currently, it is estimated that 25 per cent of all machined components, at some time in their production, require the grinding process. This number is likely to grow due to the requirements of more accurate and precise parts, the use of new materials and improved machine tool capability (Webster, 2004). A further factor that is adding to the growth in abrasive machining is the broader use of new alloys based on hard fusible components, sintered metals and sintered ceramics. These newer materials cannot be machined economically by any other machining method (Filipowski and Marciniak, 2000).

Although grinding has traditionally been regarded as a finishing process, more recent experience from the automotive and aerospace industries have convinced production engineers of the potential of grinding as a primary material removal process. This has led to recent process developments including: 'creep feed', 'one cut' or 'one pass' and most recently High Efficiency Deep Grinding (HEDG) in which large volumes of material are removed at very high wheel speeds of 120-140 m/s (Challis and Stanton, 1982; Rowe, 2001).

There are many types of grinding operation – rough and precision, internal, external, surface, centreless, using a wheel or a belt, and conventional and super abrasives. Nevertheless, all these different operations have in common the fact that there is a moving abrasive surface that contacts the workpiece. If the force is high enough, material will be removed from the part and the abrasive surface will wear. The force and its level determines how fast the mutual removal rates will be, how rough the remaining surface will be, and whether the workpiece will be metallurgically damaged or not (King and Hahn, 1986). In this context metallurgical damage would typically exhibit

itself as either: discoloration, burning, cracking, excessive tensile stress levels, tempering, hardening or surface oxidation.

The grinding process itself is very complex due to the stochastic nature of abrasive tool geometry. Adding to this complexity are the high cutting speeds, cutting resistance, force ratios, the variable compliance and the structure of the grinding wheel and many other varying parameters. There has been series of studies into abrasive machining many of which were deterministic, based on experiments and experience, and that is why it is often said that grinding is more of an art rather than a science (Marinescu *et al*, 2004).

In abrasive machining, a key objective is to maximise material removal whilst minimising wear of the abrasive. Although grinding can take place without lubrication it is often preferred to use wet grinding wherever possible to achieve this objective due to reduced frictional losses and improved quality of the surface produced. There are two main types of fluids used in grinding: emulsions and neat oil (Marinescu *et al*, 2004).

Emulsion is a diluted concentrate of oil in water. To protect the machine and parts, other constituents are added to the base fluid such as: anti-wear additives, anti-corrosion additives, anti-mist additives, antioxidants and emulsifiers.

Neat oils contain base oils and a mixture of additives to provide enhanced corrosion resistance and lubrication. They normally consist of 80-95 per cent basic oil (natural fatty oil/mineral oil/synthetic oil).

However, the use of fluids also represents a significant part of manufacturing costs. Furthermore, those fluids may have a detrimental effect on worker health as well as on the natural environment. As a result, dry machining would be desirable (Brinksmeier *et al*, 1999).

Near Dry Machining (NDM) is an alternative to conventional flood delivery. It covers areas of lubrication, where a minimised or micro amount of fluid is employed and this is commonly termed Minimum Quantity Lubrication (MQL). MQL in drilling, turning and milling has attracted extensive research however there has been only a limited research on MQL in grinding. Consequently, the efficiency of this fluid delivery method is

unclear. Preliminary studies have been promising and the need for further work has been established.

1.2. MQL Benefits and Limitations

Many innovations have been made in grinding – wheel speed and feed have increased, materials have changed, grinding has become more accurate. However, fluid delivery remains an important issue requiring further research effort. The rising cost of cutting fluid usage and disposal is a key driver for research into alternative fluid delivery techniques. As a result, the introduction of dry machining and minimum quantity lubrication techniques in machining processes is increasing.

The principle of MQL is to mix pressurised air and lubricant and deliver it directly to a machining zone using as little of fluid as possible. As a comparison fluid quantities in wet machining are typically 5000-25000 ml/min, in MQL they may be as little as 30-50 ml/h (0.5-0.8 ml/min). Relatively extensive research has been undertaken concerning MQL applied to milling, turning and drilling, however, MQL in grinding remains little understood. The small number of research publications on the subject suggest that the MQL system is sufficiently flexible for application in grinding, however very little is understand regarding the issue of where MQL would be most usefully employed.

There are number of reasons why attention should be paid to the MQL. These include environment and economic factors such as environmental friendliness, initial purchase cost, delivery cost to the contact region (high velocity and high pressure systems), and subsequent disposal costs.

The potential key benefits of MQL may be:

- reduced environmental impact – no need for waste disposal, no air and water pollution, smaller energy consumption,
- economical benefits: purchase, waste disposal, production unit price costs are reduced,

- no thermal shock for workpiece and the grinding wheel,
- cleaner work place and less hazardous to machine environment,
- storage space and costs are limited to minimum – on-time deliveries possible.

1.3. Project Aim and Objectives

The purpose of this research was to investigate the performance of MQL and to compare it to both the dry and wet conditions. The work was to set out to test the hypothesis that under some conditions MQL can deliver a process efficiency approaching that of conventional wet grinding. A key objective was to identify a grinding regime where MQL can demonstrate successful application. Grinding performance was established from process parameters that included grinding forces, workpiece surface roughness and grinding temperature.

1.4. The Scope of the Investigation

The work presented in this thesis describes advances made in the understanding of the MQL fluid delivery method in grinding. Fundamental interactions between the fluid system and the grinding system were investigated. The effects of workpiece material, wheel and workpiece speed and cooling/lubricating system provide the basis for the fundamental studies.

The research was focussed on plane surface grinding in the fine grinding and shallow cut regime. For this study, fine grinding refers to depth of cut (DOC) in the range: $0.5\ \mu m < DOC < 1\ \mu m$ and shallow cut grinding up to 15 μm.

Wheel speeds were varied in the range 20-45 m/s and a general purpose aluminium oxide grinding wheel was used throughout. A range of materials widely used in manufacturing industry: M2 steel hardened to approximately 51±2 Hardness Rockwell-C (HRC), EN31 approximately of 62±2 HRC and steel EN8 of 32±2 HRC, were selected for the study.

Preliminary experiments were undertaken on a manual grinding machine. Experiments for the full parametric study were undertaken on an advanced high precision CNC grinding machine.

Importantly, the real DOC is identified as a critical parameter in the assessment of MQL performance, and methods to determine this value in plane surface grinding are proposed. The work also presents new insight into temperature effects in MQL and the validity of accepted thermal models for MQL analysis has been established. A brief study on process economics provides further confirmation of the potential benefit of the MQL delivery method.

Chapter 2. PROCESS FLUIDS, FLUID DELIVERY AND GRINDING WHEELS

2.1. Process Fluids

2.1.1. The Function of Fluids in the Grinding Process

The family of process fluids includes dry fluids, liquids and some gases – used either as a cooling medium or as a carriage medium for oils. However, in most instances, water based or oil, liquid process fluids are preferred to gaseous fluid. In some cases, dry grinding may be considered where the workpiece material does not allow for use of a fluid containing even a trace amount of water (e.g. magnesium alloys) or it is desirable to contain the debris such as that from cast iron, brass, and similar materials, to avoid contamination of the machine (Dmochowski, 1983; Marinescu *et al*, 2004).

The chip formation process in the contact zone is influenced by the use of coolant. The coolant develops a thin film at the interface, thus lowering the friction forces, cooling the material and tool surfaces. According to Brinksmeier *et al*, (1999) as the lubrication effect increases, there is a corresponding increase in elastic-plastic deformation under the cutting edge of the abrasive grain, leading to a decrease in workpiece roughness. By reducing friction forces, friction heat is reduced and therefore also the total process heat. However, excess fluid delivery can have a negative thermal effect, as the efficiency of the cutting process may be reduced and relatively more energy is used in the shearing and deformation processes. The reason for this may be an effect of air boundary layer. When excessive fluid delivery takes place, a larger normal force is required to overcome the effect of the boundary layer between the wheel and the workpiece. Although this is not a common occurrence (Brinksmeier *et al*, 1999).

The different functions of the cutting fluid can be summarised as follows (King and Hahn, 1986; Malkin, 1989; Marinescu *et al*, 2004; Oczos and Porzycki, 1986; Dmochowski, 1983; Milton, 1996):

1. Cooling function – increases heat transfer from machining area. The cooling efficiency is higher when properties: thermal conductivity, specific heat and latent heat and are higher. Cooling occurs within and outside the contact area.

2. Lubricating function of the abrasive contact – decreases friction between grain and part, and between flank and chip. Efficiency of lubrication depends mainly on fluid

type and how effectively the fluid penetrates the faces. This is important for the case of Near Dry Machining.

3. Flushing function – is an important function as it removes detached/fractured grains and chips from machining area. Cutting fluids have very good flushing properties and particles are carried with the fluid flow. This property also beneficially influences the machined surface and wear of the wheel. However, it is generally not possible to achieve bulk cooling, swarf removal, wheel cleaning, contact zone lubrication and process cooling by using only one nozzle. Many processes use multiple nozzles and each nozzle is set up for a particular purpose.

4. Entrapment and cleaning function – is a function wherein the abrasive dust and metal process vapour are collected and entrapped in fluids. The cleaning function also aids wheel cleaning and helps prevent wheel glazing thus extending wheel life and time periods between wheel dressing operations.

2.1.2. Fluid Types in Grinding

Every grinding application operates under different conditions, thus the cooling and lubrication requirements differ. Coolants should, ideally, be composed to suit each specific case. Every coolant consists of a basic fluid, to which are added other products such as anti-wear, anti-corrosion or emulsifying agents. Fluids used during abrasive process can be categorised as: gases, mixture of gas and fluids, liquid fluids, liquid fluids mixture with solid lubricants and pastes. Liquid fluids are most common and they can be further divided into cutting oils and soluble oils (Silva *et al*, 2005; Rahman *et al*, 2001).

There is a general tendency to use cutting oils where lubrication is critical for form and finish. However, special precautions and equipment may be necessary for grinding with cutting-oils (Silva *et al*, 2005) as they produce a mist and fumes in the atmosphere, and may also present a fire hazard. Their use may also be restricted due to pollution and safety considerations, (October 2009) e.g. http://www.hse.gov.uk/index.htm, http://osha.europa.eu/, http://www.iso.org/.

It is shown in Figure 2-1, how a general purpose wheel, wheelspeed and different cooling/lubricating medium can influence the process temperature. Lowest temperatures are achieved with oil. It should be mentioned, that depending on workpiece material, its hardness, process parameters, grinding wheel, etc., grinding temperature may behave differently from this general chart.

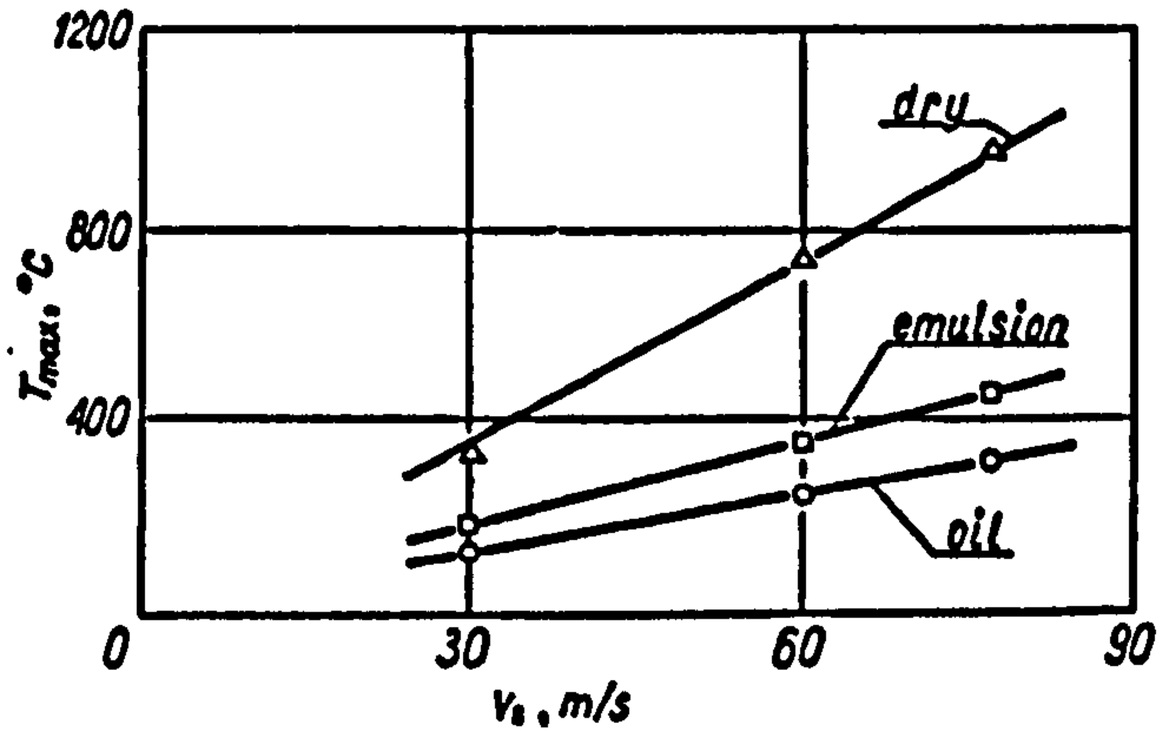

Figure 2-1. Temperature of a workpiece as a function of wheel speed (Oczos and Porzycki, 1986).

It should be mentioned, that according to the state-of-art in fluid delivery in grinding, there can be no entirely uniform statements made as to the comparison of oils, emulsions and solutions concerning roughness and residual stresses. The results show that in almost every case, oil is characterised by lower grinding forces, lower wear and higher values of the G-ratio. There are no such clear statements for the roughness. Thus, it can be only stated that a reduction of tool wear by the use of oil due to increased lubrication effect is clear. The merit of water-based fluids is their ability to aid control of workpiece bulk temperature such that part-to-part size variation is reduced (Brinksmeier *et al*, 1999).

Due to process complexity and qualities expected from fluid, it is not possible to create one universal fluid highly effective for both cooling and lubricating – thus there is a need for fluids, with different properties that are able to perform specific requirements. Different wheel and workpiece combination create various grinding conditions and for instance, when grinding titanium alloy with aluminium oxide wheels, wheel wear rate and surface roughness are outside tolerable levels with common grinding fluids, due to chemical reactivity between workpiece and wheel. (Nee, 1979; Tawakoli *et al*, 2007).

In Figure 2-2 the influence of using either oil or emulsion on specific normal force and surface roughness is presented in terms of specific material removal rate.

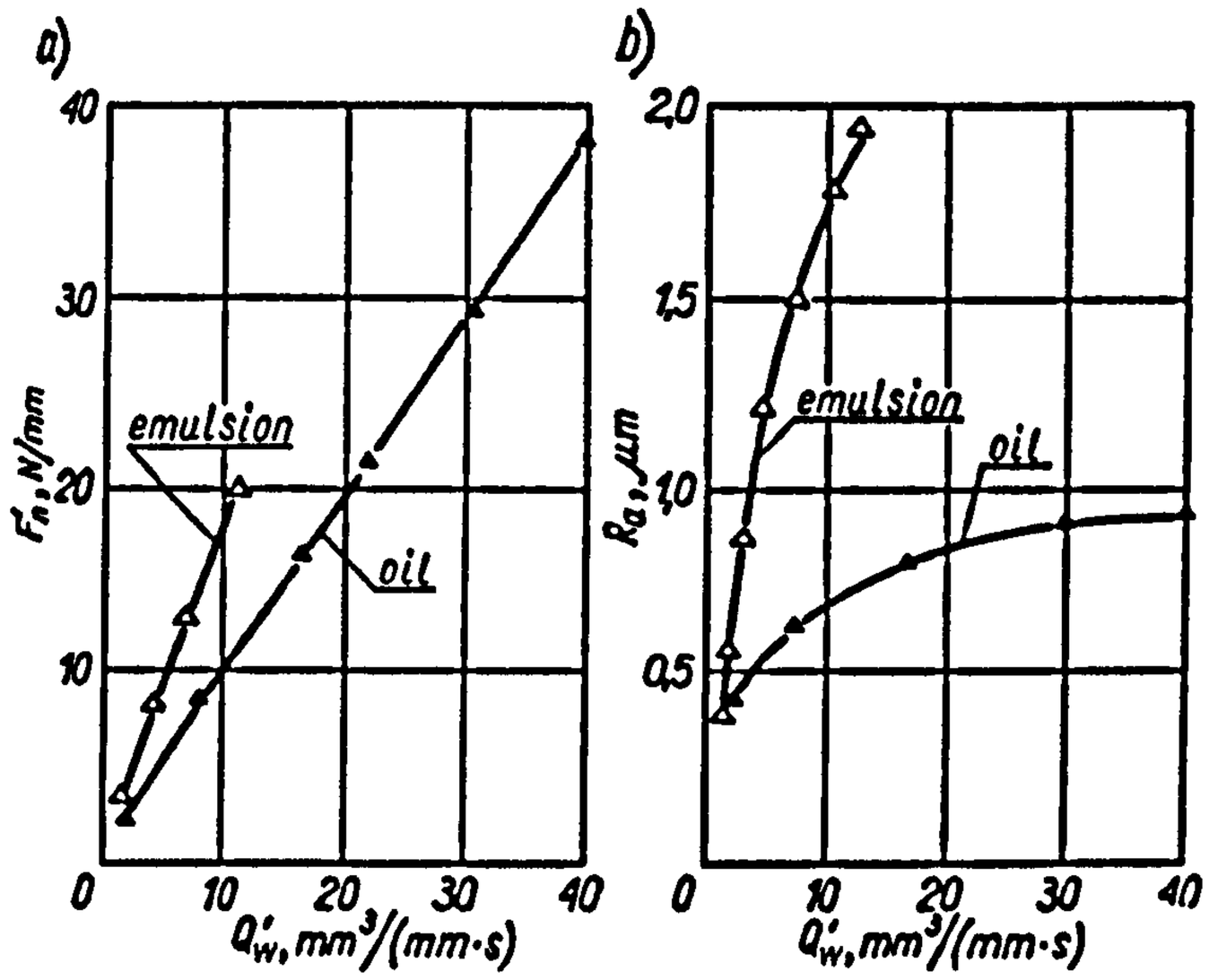

Figure 2-2. Influence of fluid properties on (a) specific normal force and (b) roughness, with specific material removal (Oczos and Porzycki, 1986).

2.1.3. Oil-based Coolants

A few researchers found that grinding wheel wear and surface roughness are often reduced with the use of oil compared with that achieved using an emulsion. In general, higher compressive residual stresses are found after use of oils in comparison to emulsion. This is due to the more favourable cutting conditions resulting from oil usage.

It is also advised to use oil as a coolant for high-speed grinding, as it reduces tangential forces as well as a large portion of friction heat. However, it has been reported that oil does not always reduce surface roughness in comparison to emulsion in the case of high-speed grinding (Brinksmeier *et al*, 1999).

Oil-based fluids owe their excellent lubrication properties to a high kinematic viscosity that is over 50 times greater than water. The viscosity is in the range of ν = 20-60 mm^2/s depending on fluid specification. However the heat capacity for oil based fluids is typically 1.95 kJ/(kg·K) and heat conductivity approximately 0.13 W/(m·K) and

therefore oil-based fluids have poor cooling properties compared to water based fluids (Brinksmeier *et al*, 1999; Oczos and Porzycki, 1986).

2.1.4. Water-based Coolants

Water-based fluids are widely used in abrasive machining, and are produced in form of concentrate and water is used to dilute the different substances. Emulsion i.e., oil plus water, combine some of the advantages of both water and oil. However, this symbiosis is never completely successful. The main disadvantage of water based fluids are micro organisms making high maintenance costs unavoidable. Furthermore, the water and oil phases must be separated before disposal (Marinescu *et al*, 2004; Brinksmeier *et al*, 1999).

When using water-based fluids, there is a need to ensure that the fluid film boiling temperature is not exceeded as this leads to a drastic reduction of heat transfer coefficient between workpiece and coolant. Film boiling occurs at approximately 120 °C, and leads to evaporation of the coolant solution. Film boiling also occurs with mineral oils, although at higher temperatures and above a certain temperature range, because oil exhibits an evaporation range. Due to the rise of the evaporation range, increasing coolant pressure in the contact zone leads to a delay of the film boiling effect. This effect is especially important because film boiling has a direct effect on the thermal damage of the workpiece subsurface layer (Shaji and Radhakrishnan, 2002; Shaji and Radhakrishnan, 2003; Alves and Gomes de Oliveira, 2006).

Properties	**Water**	**Emulsion**	**Oil**	**Air**
Kinematic Viscosity [cSt at 40°C]	0.66	~ 0.66	20-80	16.97
Density [kg/m^3]	1000	930-1000	850-1100	1.20
Heat Conductivity [W/(m K)]	0.60	0.63	0.15	0.02
Heat Capacity [kJ/(kg K)]	4.22	4.18	1.95	1.00

Table 2-1. Comparison of different fluids properties.

Water-based coolants are common for metal grinding operations. Their physical properties are similar to water. Heat capacity is 4.18kJ/(kg K) and is twice that of oil. Heat conductivity is 0.63 W/(m K). Their principal use is in cooling and flushing. Lubrication is a less important issue.

2.1.5. Alternative Lubrication Techniques

Alternative techniques of lubrication in abrasive machining tend to be neglected, however, some examples of techniques are given below: (Shaji and Radhakrishnan, 2002; Shaji and Radhakrishnan, 2003):

- Spray (i.e.: gases like argon, air, helium, nitrogen or carbon dioxide), mist or active chemical vapour lubrication. Due to requirements of decreasing conventional cutting fluids, gases seem to play a more important role nowadays. However they have some limitations due to their poor cooling and/or lubrication properties and they require special tools (i.e.: CBN wheels for grinding) to achieve lower temperatures and keep the machining process efficient. One of the most important spray techniques is MQL and this is shown in some cases to provide good lubrication. However, the usefulness of this method within grinding still needs to be determined and is investigated in this research.
- Surface layers with self-lubricating properties are being used with some success in milling and turning though operations they do provide sufficient cooling for grinding. This solution also requires special preparation (deposition or conversion on a half-finished product before grinding), thus increasing costs of the production process.
- Introduction of solid lubricants into the bond of the abrasive tool and/or into the composition of the workpiece material. This method requires the lubricant to be incorporated in the tool or workpiece at the time of initial fabrication. Self-lubricating materials may be introduced to enhance the effects of a process fluid or as an alternative to a process fluid. The effective role of graphite as a lubricant was proven in some studies, however, the method still needs many improvements as wheel clogging is a major problem.

- Dry abrasive machining where the process takes place exclusively in air, though, it is not usually possible to satisfy all the technical and economic requirements of a modern industrial process. Due to the lack of cooling, this process is very demanding and there is high risk of thermal damage. This machining method also demands state-of-the-art tools as dry machining with conventional grinding wheels causes high wear and clogging, leading to poor surface properties. However due to key developments in tool technologies dry machining is commonly used with materials (e.g. copper) that cannot be used in the presence of cutting fluids.

2.2. Fluid Influence on the Working and Natural Environment

The impact of machining and process fluids on the working environment is a matter of increasing legislation. These concerns range from potentially carcinogenic effects of ingesting workpiece material particles or ingesting process fluid, and extend through to the irritant effects of metals, oils, and bacteria through inhalation or direct contact with the skin. Machine operator's health can be affected by contact with various substances within the cutting fluid. Their health can be impaired by skin contact or by swallowing the substance but also by breathing oil mist and vapours. Increasingly, the answer to these problems is seen as total machine enclosure with fume extraction systems. The debate also ranges over the benefits of oil versus water-based fluids and desirability of minimum fluid application (Sokovic, 2001; Marinescu *et al*, 2004).

The impact on the natural environment is mainly caused by the disposal of waste coolant, as well as cutting fluid losses during the machining process, contamination of water for cleaning the workpiece and other related activities. The waste disposal of coolant, contaminated with abrasive particles and machining debris causes ecological problems and is also linked with rising costs. That is why nowadays, specialist disposal of waste oil and emulsion is becoming increasingly more important and there are several ways of dealing with this problem.

Figure 2-3 summarises how cutting fluids may be disposed. Stricter environmental regulations and guidelines support this development. Various options are now available to companies interested in conditioning these materials, regardless of whether this is conducted within the company or externally (Sokovic, 2001; Brinksmeier *et al*, 1994).

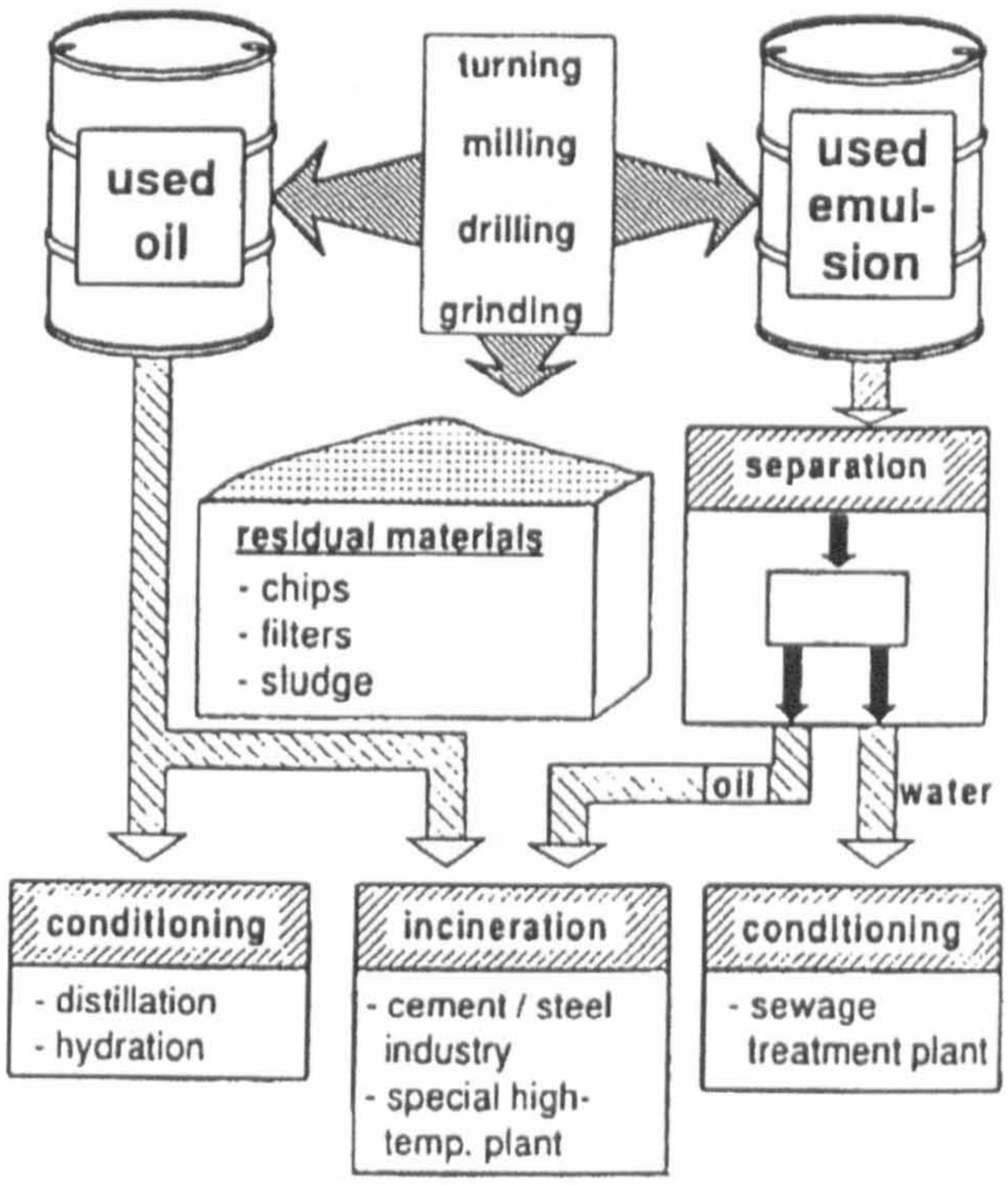

Figure 2-3. Disposal of cutting fluids in cutting technology (Sokovic, 2001).

There are different approaches to avoid some of the above issues, such as dry grinding, minimal quantity lubrication and use of biodegradable fluids as a part of green manufacturing. However, a complete reunification of cutting fluids is unlikely in the foreseeable future due to dependency on manufacturing for machined materials (Sokovic, 2001).

A very important issue is the safe disposal of grinding swarf. The swarf contains abrasive grains, bond materials, machining debris and lubricant. During the separation of the cooling lubricant from the pollutants, there invariably remain some traces of the pollutants in the fluid discharged. This discharge can amount up to 40 per cent of the disposal weight. In Germany the metal-working industry produces a volume of grinding swarf of around 130,000 tons per year. Therefore, the separation of the oil-contaminated grinding swarf into its main raw materials (i.e. oil, metal chips) and the recycling of these contents is economically as well as ecologically sensible and required. The whole

process after extraction leads to simple products: oil and metal powder (Brinksmeier, 1994). An example of oil and grinding swarf separation is presented in Figure 2-4.

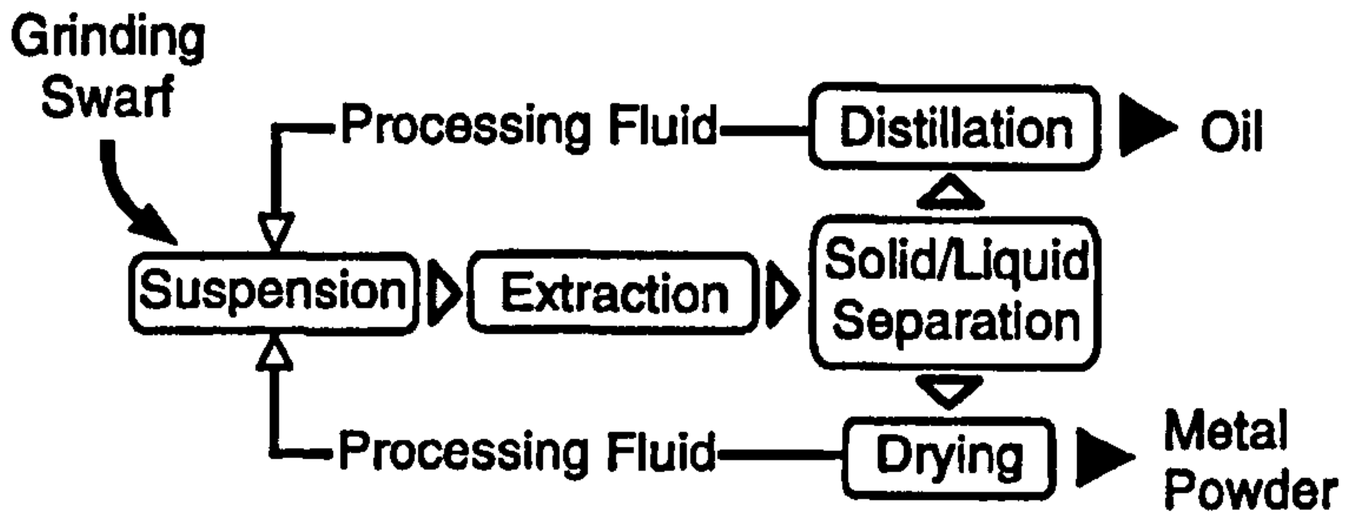

Figure 2-4. De-oiling scheme (Brinksmeier, 1994).

2.3. Fluid Delivery

2.3.1. Fluid Delivery into Grinding Zone

A process fluid by itself does not assure high workpiece quality and grinding process efficiency, thus its importance should not be overstated. It is known however that cutting fluids lower temperatures in grinding mainly by reducing friction. Lubrication depends on fluid entering the contact region between the grinding wheel and the workpiece. It does not necessarily mean a large volume of fluid has to be used, however lubrication may be ineffective if no fluid enters the grinding zone at all (Marinescu *et al*, 2004).

Previous research on fluid supply to the grinding zone has identified the basic methods of fluid delivery and their possible combinations. Methods of delivery include flood supply, pressurised fluid supply, fluid supply through porous grinding wheel, submerged grinding, fluid supply with ultrasound vibration (megasonic) and contact fluid supply (Oczos and Porzycki, 1986).

To achieve the highest possible cooling and lubricating qualities a correct nozzle arrangement is required. Specialised nozzles have been developed for different grinding applications and broadly they may be classified into the following groups as illustrated in Figure 2-5. Most common nozzles are free jet and shoe nozzles. (Brinksmeier *et al*, 1999).

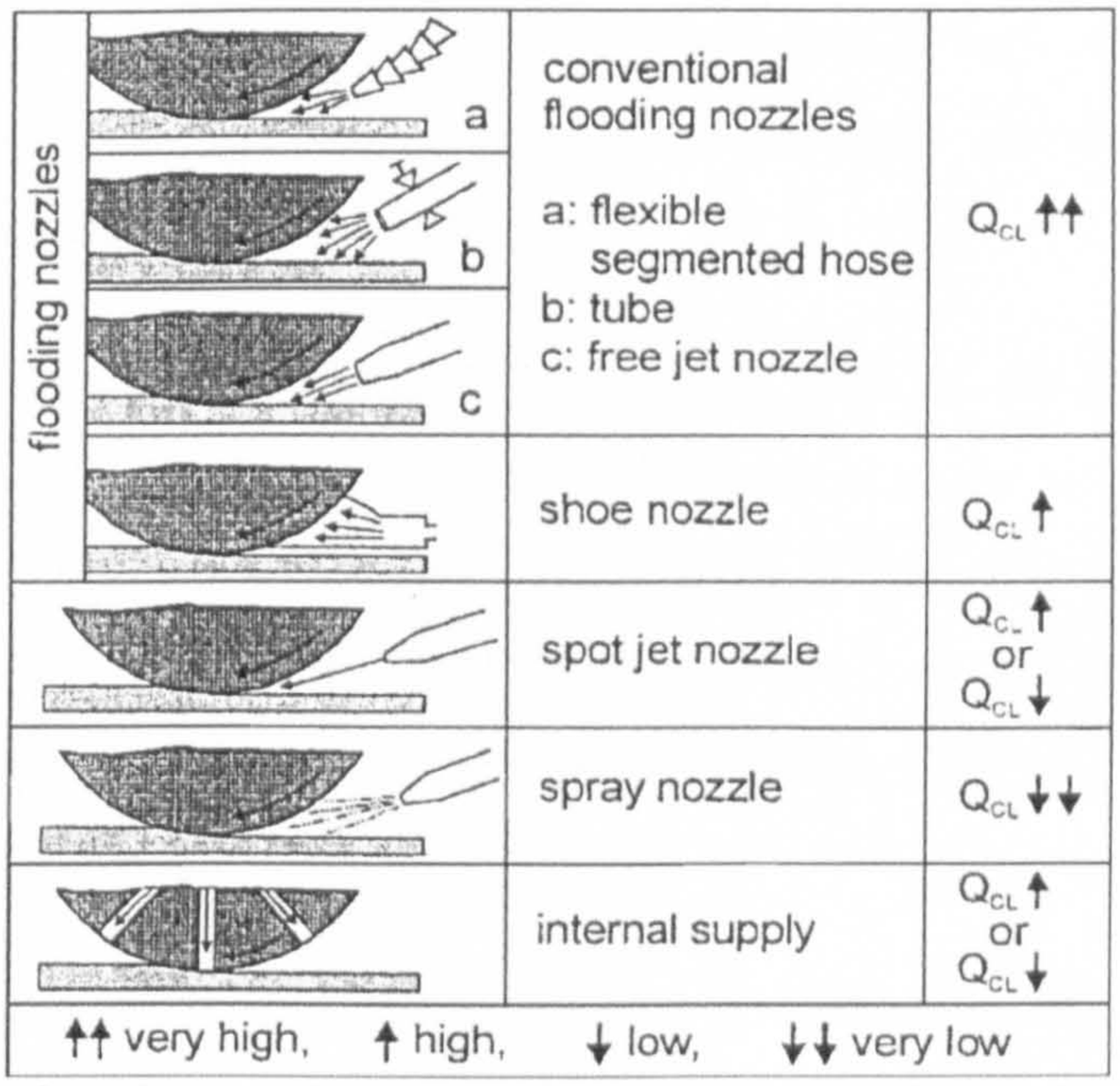

Figure 2-5. Examples for coolant supply strategies, where Q_{CL} coolant quantity (Brinksmeier et al, 1999).

Free jet nozzles are widely used, especially with universal grinding machines with coolant pressure around 0.1 MPa. Low pressure is required, when bulk cooling and swarf removal from the bed of the machine only is expected. However, low pressure nozzles are ineffective for high speed grinding. To achieve high velocity at the nozzle exit, it is necessary to use a pump of adequate flow rate and power. Ott (1991, from Brinksmeier *et al*, 1999) suggested using coolant jet velocities in the range of 0.6-1.0 times of cutting speed to achieve good jet adhesion to the grinding wheel (Oczos and Porzycki, 1986; Webster *et al*, 1995).

Another common flooding nozzle is the shoe nozzle. This type of nozzle characterises, that it fits to the wheel and encloses the grinding wheel on three sides. In comparison to the free jet nozzle, shoe nozzle leads to lower tool wear and less burning, with generally lower pressures and coolant flow rates (Marinescu *et al*, 2007).

In some grinding conditions (high wheel-speeds for instance) a single flood nozzle may not be sufficient to satisfy the various functions expected from the process fluid. Therefore, it is worth considering whether the various functions of bulk cooling, swarf removal, wheel cleaning, contact zone lubrication, and cooling may best be served with multiple nozzles. A medium flow rate nozzle with a medium pressure head, for example, 0.4 MPa, may be used to supply the fluid in the grinding arc. In addition, an 8.0 MPa high-

pressure nozzle may be used as a cleaning jet to force fluid at high velocity into the pores of the wheel. Each nozzle can then be designed to achieve a particular purpose in the most cost-effective way (Marinescu *et al*, 2004).

Finally, there are the spray nozzles, which provide reduced coolant flow rates. One spray cooling method is MQL, with coolant flow rates as much as 20,000 times lower, compared with flooding coolant supply methods. It has been proposed that MQL may possibly only be used for fine grinding due to the reduced cooling potential (Marinescu *et al*, 2004; Brinksmeier, 1999). However, this hypothesis requires further research and it is the subject of this investigation.

A further factor that plays a very decisive role with respect to efficiency of a coolant system is the position of the nozzle. It has a significant influence on the useful flow rate and according to Webster (1995) determines if the flow in the entry region is laminar or turbulent. Studies examining the optimal nozzle position have shown that the nozzle should be positioned as close to the contact zone as possible, to ensure optimum use of jet coherence. In addition to the distance, the orientation of the jet in relation to the grinding wheel should be considered. However, in free jet grinding, it was proposed that the flow should not hit the grinding wheel tangentially, but approximately at an angle of 10° to 25° in front of the grinding arc (Brinksmeier *et al*, 1999).

Other studies have proposed tangential flows (Ebbrell *et al*, 2000; Jackson, 2008). However, there is at present no hard and fast rule for angle of inclination despite it being the subject of many studies and the conclusion given by Baines-Jones (2005) is that each operation needs to be assessed independently to identify optimal angle.

In their work, Brinksmeier *et al* (1999) mentions that different researchers have found that increasing coolant pressure with an optimal nozzle geometry reduces the workpiece surface roughness. This happens because higher jet velocity provides better coolant penetration into the grinding wheel pores and more coolant can be carried into the grinding arc. This therefore reduces friction and temperature which in turn reduces wheel wear. It was also shown that tensile residual stresses at the workpiece surface were dramatically reduced. An example of how coolant flow rate and nozzle cross can affect tensile residual stresses is presented in Figure 2-6.

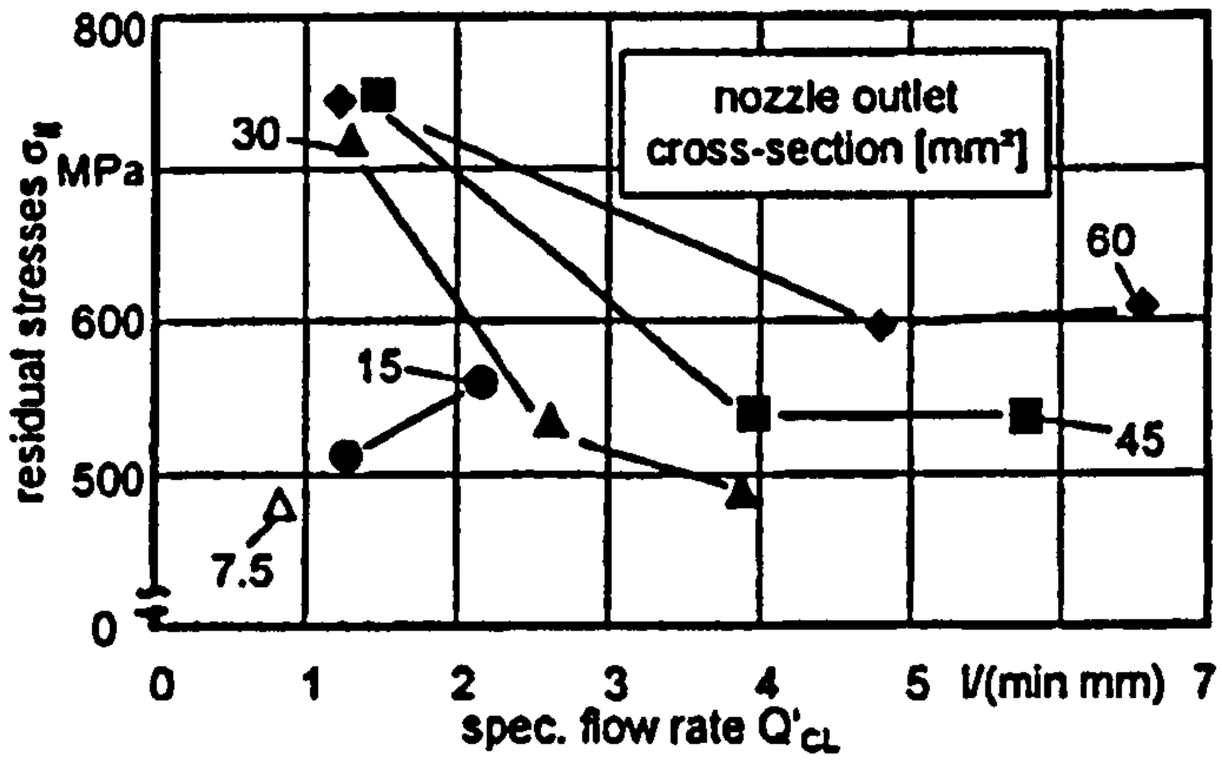

Figure 2-6. Effect of coolant flow rate and nozzle cross-section on tensile residual stresses, (Brinksmeier et al, 1999)

For the current investigation wet grinding was carried out with a conventional flood delivery nozzle. The nozzle produced a velocity of approximately 26 m/s and a flow of approximately 12 l/min. It was directed tangentially to the wheel according to suggestions made by Jackson (2008). In the case of MQL, a special purpose nozzle design, partially based on Silva's (2005) design, was used. More details about the delivery system for wet and MQL grinding can be found in Chapter 6, section 6.3.4.

2.3.2. Boundary Effect

A boundary layer of air develops around a rotating grinding wheel and occurs particularly due to the high surface speed of the wheel. This boundary layer effect is generally formed with wheel speeds at v_s > 20 m/s (Oczos and Porzycki, 1996). The thickness of the boundary effect strongly depends upon wheel speed, wheel surface topography (roughness) and wheel guarding (Trmal and Kaliszer, 1976).

In some situations the turbulent motion of the air above the wheel/work interface allows only a fraction of the coolant delivered to be drawn into the grinding arc. The strong fluid deflecting effect of the boundary layer is pictured in the work of Ebbrell and Rowe (Figure 2-7) (Ebbrell *et al*, 1999). In this figure it is seen that the boundary layer (red circle), is so strong (v_f ~ zero, gravity fed system) that no fluid is carried directly into grinding zone between the grinding wheel and workpiece.

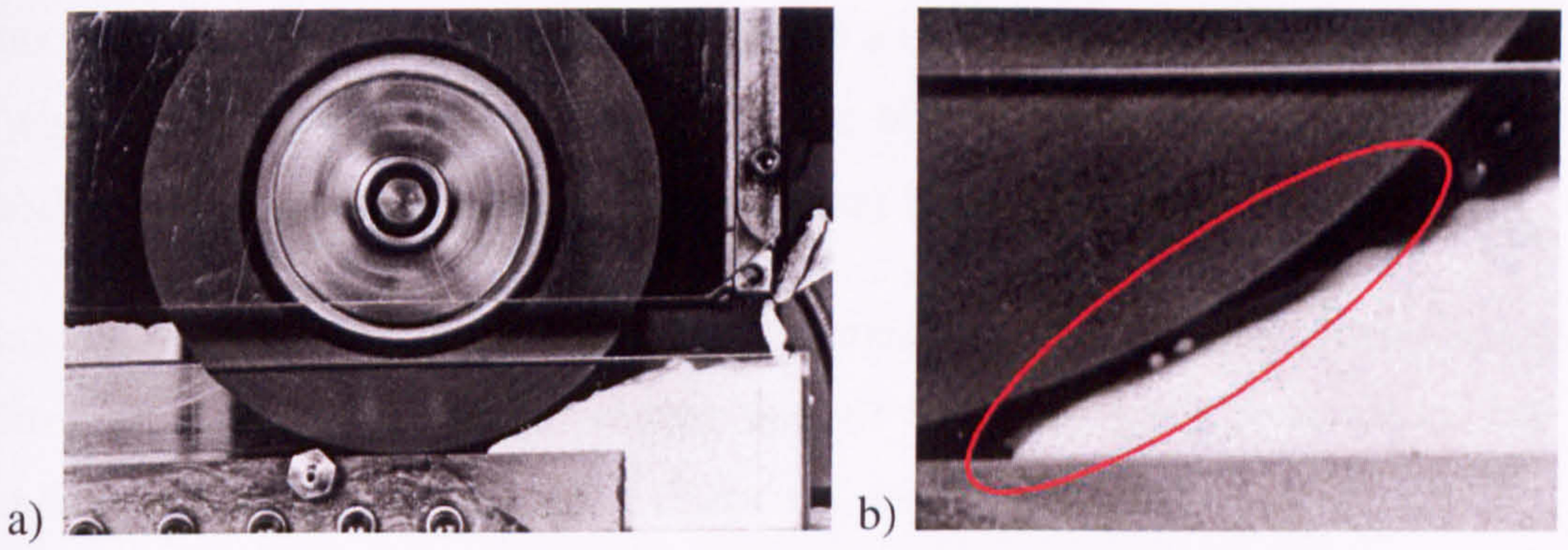

Figure 2-7. Effect of boundary layer, a) influence of air barrier on coolant supply, b) magnification, where boundary layer is visible in a red circle.

A large number of patents and papers regarding elimination or reduction of the air barrier are available. A common recommendation is to match the speed of the coolant jet to the peripheral speed of the grinding wheel. This should ensure good penetration of the air barrier and a decrease of the power loss due to fluid drag. The nature of the flows in the region immediately prior to the contact engagement was investigated by Wu, (2009), using Laser Doppler Anemometry (LDA) techniques and a representative result is shown in Figure 2-8.

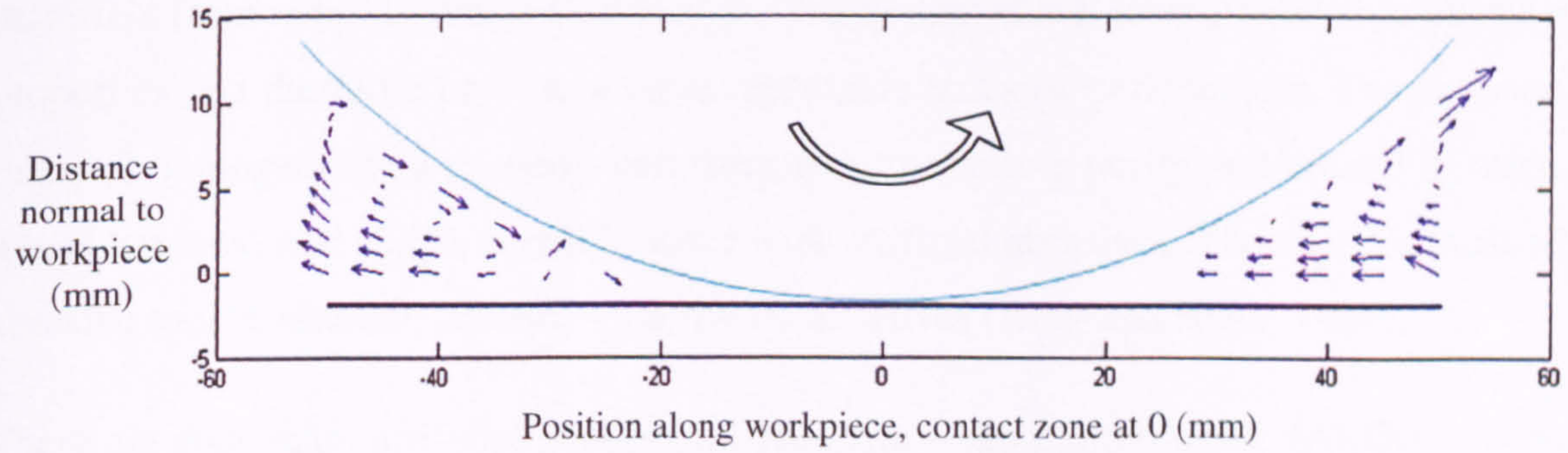

Figure 2-8. Fluid flow vectors around an anti-clockwise rotating wheel in a spark out position (Wu, 2009).

Another relatively simple method to reduce the negative effects of the boundary layer is by the use of a scraper. The scraper is designed and located to divert the air barrier before the fluid approaches the grinding zone. A disadvantage with the scraper, particularly in high removal rate operations with conventional abrasives is that it needs continual adjustment to compensate for wheel wear, thus use of this method in industrial conditions is questionable (Ebbrell *et al*, 1999; Trmal and Kaliszer, 1976).

In this study the MQL aerosol was delivered at a constant speed that (*i*) matched that of the wheel i.e. at $v_s = 45$ m/s or (*ii*) in the case of lower speed tests i.e. at $v_s = 25$ m/s exceeding wheel speed, to ensure MQL boundary layer penetration.

A series of tests using the Laser Doppler Anemometry method were also completed to confirm an efficient workpiece wetting and air boundary layer penetration. The test procedure and results are reported in Chapter 6, section 6.4.4.

2.4. Grinding Wheels

2.4.1. Abrasive Materials

There are five main types of natural abrasive materials commonly used in machining: diamond, corundum, emery, quartz and garnet. All apart from the diamond have low strength, are problematic in quality control and reproduction, thus when compared to artificial materials their role is rather minor. What differentiates artificial abrasive materials from natural ones is that they are easily controlled, have predictable physical properties and therefore provide a more repeatable abrasive performance. For instance, material homogeneity, a property very sensitive to abrasive purity and crucial to retain wheel hardness and shape, is much better with artificial abrasives. Therefore, almost all abrasive tool production is based on artificial abrasives (King and Hahn, 1986).

There are four main artificial abrasives: corundum – aluminium oxide (Al_2O_3), silicon carbide (SiC), and the superabrasives: cubic boron nitride (CBN) and diamond. Virtually all conventional abrasives used currently for grinding wheels are synthetic materials based on either aluminium oxide or silicon carbide (Malkin, 1989).

Aluminium oxide (alumina) abrasive consisting of crystalline aluminium oxide is made from bauxite. Depending on source it contains 85-90 per cent of alumina, 2-5 per cent of TiO_2 and up to 10 per cent iron oxide, silica and basic oxides. The bauxite is fused in electric-arc furnace at 2600 °C. Advantages of aluminium oxide are: heat resistance (melt point at about 1900-2000 °C depending on purity), chemical and acid resistance.

A further important property, used to determine grain quality, is its cleavage ability (Burnat, 1962).

Silicon carbide (SiC) is another commonly used abrasive. It has a hardness of 9.5 Mohs scale. It has better heat resistance compared to aluminium oxide and a higher melting point at approximately 2500 °C. However, SiC did not feature in this study and further information can be found literature.

Similarly superabrasives did not feature in this study and a detailed explanation of their properties and use is outside the scope of this work. The reader is referred to Rowe (2009) if they require more information on superabrasives.

2.4.2. Bond Materials

The role of the bond in the grinding wheel is to provide a matrix to support the grains so that they can remove material and are able to withstand grinding forces and temperatures. The bond-grain matrix should include porosity to provide for the transport of fluid, chips and debris. The bond needs to be resistant to usage of various cooling and lubricating fluids and should not be overly sensitive to large temperature gradients. The two most common bond materials for conventional abrasive wheels are: vitrified and resinoid.

Vitreous bonds are basically a glass bond formed from mixtures of clay, a feldspar and a frit. Approximately half of all conventional abrasive wheels are of this bond type. Vitrified wheels act hard and are relatively fragile with grains being held rigidly in place. They are largely resistant to heat and the influence of coolants at conventional grinding temperatures, typically 100 °C to 325 °C. However, they are sensitive to any mechanical impact and side load. Currently, it is possible to use this bond type at peripheral speeds up to 80-90 m/s (Burnat, 1962; Malkin, 1989). Resinoid bonded wheels are generally used for heavy stock removal processes and cut-off applications due to their durability.

The wheel employed for this study was a vitrified bonded alumina. The wheel selected was a general purpose wheel with the following specification: WA 100 JV. The general

purpose wheel was selected to provide a reasonable performance over the chosen range of work materials and hence provide a basis for comparison.

2.4.3. Wheel Composition and Parameters

Grinding wheels are made from many types of grain in a wide range of sizes, in conjunction with many bond materials and compositions, therefore a grinding wheel company may produce dozens of thousands of nominally different products to customer satisfaction (for example, Saint-Gobain have a range approaching 250,000 wheels). It is thus convenient to refer to the standard marking system for specifying conventional and superabrasives grinding wheels. The wheel specification defines the following parameters: the type of abrasive in the wheel, the bond type, the abrasive grain size, the wheel hardness, the wheel structure, any other marker's identification codes. Superabrasives use somewhat different wheel specification, where the wheel structure is replaced by abrasive concentration and addition of the superabrasive layer depth to the end of marking symbol (Malkin, 1989).

The conventional wheel marking system is explained in Appendix 1. Key wheel parameters denoted are:

1. Abrasive size – physical properties and amount of abrasive in a unit volume have a large influence on grinding wheel cutting quality. Cutting efficiency, smoothness of the workpiece, together with wheel durability and shape holding depend strongly on the abrasive. These are the main properties that can be controlled by changing volume percentage and size of the grain (Burnat, 1962).
2. Wheel hardness – describes the force needed to pull out the grain from the grinding wheel. The stronger the grain is held in the place the harder it is to pull it out and hence the harder the wheel. However, wheel hardness is influenced by many factors, and two grinding wheels with the same hardness, for instance vitrified and resinoid may produce different cutting abilities.

The difference between a 'hard' acting wheel and a 'soft' acting wheel is that the 'soft' acting wheel cannot endure the same bluntness as the 'hard' acting wheel The softer wheel therefore wears more quickly. However, very hard wheels have

some disadvantages. Hard wheels are more susceptible to wheel 'vitrification' (glazing) which is detrimental to performance and workpiece quality (Malkin, 1989).

3. Wheel structure – determines the grain, bond and porosity matrix and volumetric percentage of each. The higher the volumetric percentage of abrasive in the matrix, the higher the cutting edge density. Simplified illustrations of grinding wheel structure are shown in Figure 2-9. An open structured wheel provides clearances for removal of chips and debris, and for transport of fluid and as a consequence the risk of smearing and elevated temperatures is reduced. This leads to the conclusion that an open structure may provide better grinding, however this must be considered with the reduction in cutting edge density (Burnat, 1962; Malkin, 1989).

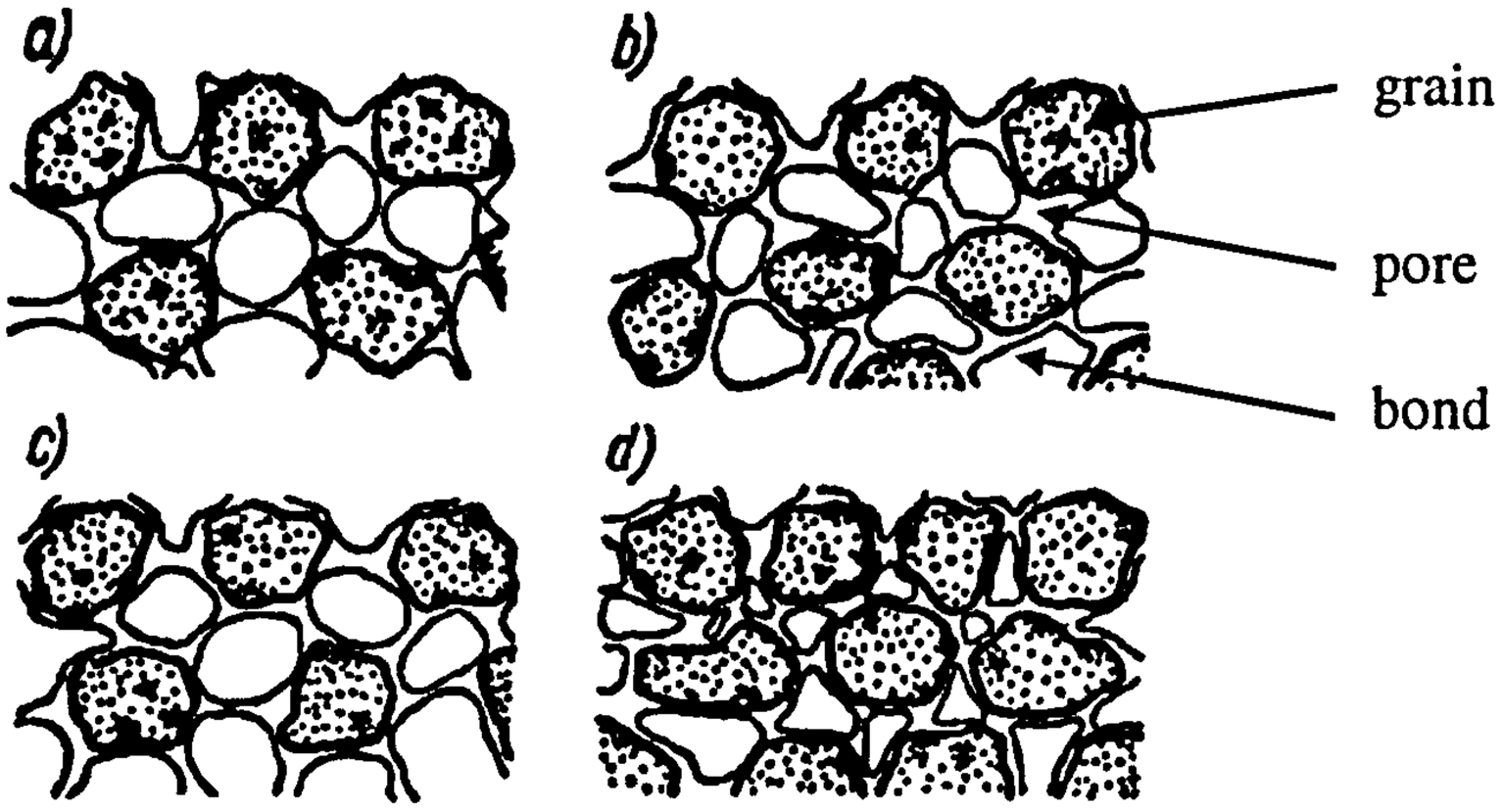

Figure 2-9. Wheel structure: a) soft, b) hard, c) open, d) compact (Burnat, 1962).

2.4.4. Wheel Wear and Dressing

There have been many studies performed regarding monitoring of abrasive wear and some key outcomes have been reported for instance in papers by: Rowe (1997, 2004), Brinksmeier and Werner (1992), Gotou and Touge (1996) and Liao *et al* (2007). The wheel wear rate has been shown to depend on many factors such as: abrasive type, grain cleavage, grain dissolution in ground material or due to chemical reactions, grinding conditions and process type, fluid type, grinding machine stiffness, operator experience and other variables including dressing conditions. Reasons for rapid wheel wear may include: too soft wheel, improperly balanced wheel, machine vibration, excessive DOC,

excessive workpiece speed, insufficient fluid delivery (Burnat, 1962). Wheel durability is defined by the dressing interval and varies due to its dependence on the operating factors influencing workpiece finish, geometry and quality.

The hardness of the wheel also has a great influence on wheel wear rate. A soft wheel generally wears more quickly than a hard one however due to better self sharpening qualities, dressing periods are often longer for a softer wheel. The main disadvantage with soft wheels is they do not retain their shape as well as hard wheels. Therefore, when shape-holding is not critical, a soft wheel may be more economical than a hard wheel owing to longer re-dress periods. Also, in general wheels with large grains wear more quickly than wheels with smaller grains (King and Hahn, 1986).

Wheel wear rate also changes with wheel speed. In general, increasing the wheel speed at a constant removal rate, reduces forces on the grains and therefore reduces the self-sharpening ability of the wheel. Self-sharpening however is an attribute that is important to maintain a free cutting surface and cutting edge density and to maintain grinding temperatures. However, the influence of wheel speed on wear rate decreases at very high speeds i.e. $v_s > 100$ m/s as cutting edges cannot be replenished at sufficient speed.

The topography of the grinding wheel is important in an analysis of the grinding process as the wear of a grinding wheel in grinding has a direct effect on workpiece quality and process efficiency as a result of a loss of cutting ability of the wheel. Geometric and functional characteristics of the grinding wheel are restored periodically by the process known as dressing. There are three goals to be obtained by dressing: equalisation of wheel shape, to shape it and to change cutting efficiency. The surface profile of the wheel formed by dressing is determined by the relative motion between the diamond and the wheel, the characteristics of the wheel and the shape of the diamond. Because of the random nature of the dressing process the interrelation between dressing and other grinding parameters are difficult to establish. It can be argued that dressing is the least understood yet one of the most influential aspects of the grinding process. Wheel wear due to dressing is often much higher than due to grinding, therefore dressing should remove only small layer of abrasive to avoid needless wheel and dresser usage (Buttery *et al*, 1978; Chen and Rowe, 1995; Chen et al, 1997).

2.5. Summary

In this chapter the functions of fluids and the types used in grinding were discussed. The following functions of fluids were described: cooling, lubricating, flushing and cleaning. Fluid types discussed were: oil based, water based and alternative lubrication/cooling. Fluid application techniques described were: spray, surface layers, solid lubricants in the bond, surface layers with self-lubricating properties and dry machining.

Also different delivery of fluids and potential issues with fluid delivery, such as air boundary layer were presented.

Finally a basic discussion about grinding wheels was provided. Grinding wheel abrasive and bond materials were discussed and how wheel composition influenced performance. Wheel wear and dressing were also discussed.

In the following chapter, the MQL delivery system is described in detailed together with the results for machining and grinding currently available.

Chapter 3. MINIMUM QUANTITY LUBRICATION

3.1. Introduction

It is widely recognised that cooling lubricants are very important in metal machining. However due to economical and ecological reasons, efforts are being made to reduce use of coolants. In the UK, the purchase, management and disposal of metal working fluids (including processes other than grinding) contribute approximately 15 per cent of overall manufacturing costs. Moreover, 10 per cent of the UK total oil sales for 1999 (1,000,000 tonnes a year) can be attributed to metalworking. A 5 per cent reduction a year would bring 7000 tonnes reduction which would have a significant environmental impact (Mortimer, 2005).

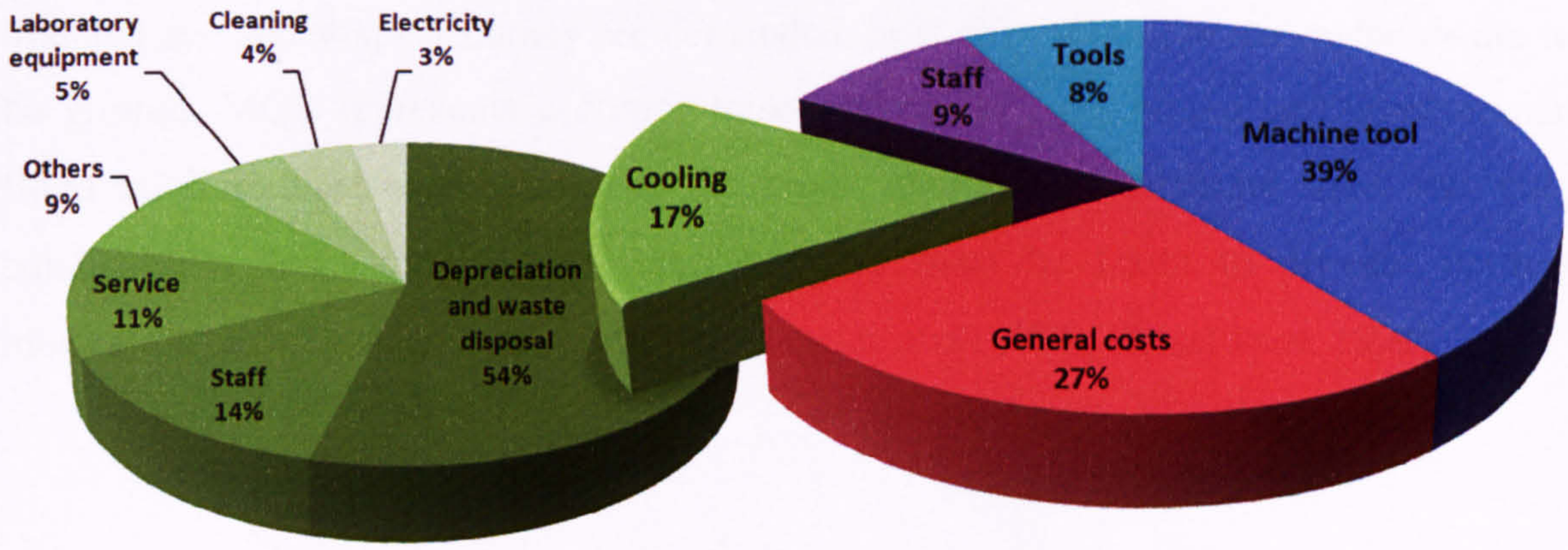

Figure 3-1. Manufacturing costs for crankshaft at a German car builder (Brinksmeier et al, 1999).

For illustration, the costs of the production of camshafts in a German automotive manufacturer are shown above. It can be seen that the costs of process fluid are close to one fifth (17 per cent) of all costs of camshaft production and are very similar to cost in the UK. When considering this, it seems incomprehensible that all innovation and activity directed towards cost improvement in the last few years have focused on tools and not really on decreasing or minimising fluids usage (Brinksmeier *et al*, 1997; Brinksmeier *et al* 1999).

What is alarming, is that the cost of machining fluid use continues to rise. It includes the costs associated with procurement, filtration, separation, disposal and record keeping for the EPA. Used cutting fluids are not safe for the environment as they always contain a

certain amount of additives that may be dangerous when they contact with water. Moreover, used fluids contain a large amount of fine particles of processed materials (swarfs) and facilitate the culture of bacteria. Furthermore, coolants may have unhealthy effects on workers as well as on the environment. Great effort is made to retrieve solid contamination and to allow for a safe disposal of used cutting fluids as already the costs for disposal of coolant are higher than the initial cost of the coolant, and they are still rising (Brinksmeier, 1999; Quaile, 2005).

Thus, considering the above issues, an interest in dry machining and the minimum quantity lubrication method, which provide a reduction or a complete avoidance of coolants, is increasing as these are interesting alternatives and quite competitive to conventional flood cooling methods. However when narrow tolerances and a high dimensional and shape accuracy are demanded, or if critical hard to cut materials are to be ground, MQL represents a compromise between dry machining and conventional flood cooling lubrication. In MQL the small amounts of lubricant used can only conditionally fulfil the cooling task, and care must be taken to provide optimal lubrication (Brinksmeier *et al*, 1997; Brinksmeier *et al*, 1999; Heisel *et al*, 1994).

3.2. Minimum Quantity Lubrication Background

Minimum Quantity Lubrication (MQL) is a near dry lubrication method. It aims to use a minimum amount of cutting fluid to satisfy the requirements of the process. It is generally accepted that MQL is achieved within the range of flow rates from 10-500 ml/hour (Brinksmeier *et al*, 1999; Autret *et al*, 2003; Braga and Diniz, 2002; Silva *et al*, 2005).

The basic principle of MQL is simple – a minute amount of lubricant is mixed with compressed air and delivered to the grinding zone by a nozzle as a fine spray. Due to better lubrication properties, oil is the principal lubricant used in industrial practice. The air pressure supplied to an MQL system typically has a pressure in the range of 0.4-1.0 MPa. As the quantities of oil and air are very small (typically 10-100 ml/h of oil), MQL systems are very compact.

The mixture of oil and air supplied to the grinding zone provides lubrication. This potentially reduces frictional heat generated between the wheel grains and the workpiece. The heat energy consumed by evaporation of lubricant can also contribute to the cooling of the workpiece and the wheel. Additionally, the decompressing air is able to carry away some heat (Silva *et al*, 2005). However, cooling by convection itself is rather low (Brinksmeier *et al* 1997).

In oil spray generation tests it has been found that almost all oil particles are in the size range 0.4 to 0.9 μm AED. According to Heisel (1994) the work diameter of droplets considered for oil mist generation process varies between 0.5 and 5.0 μm. These two results demonstrate the efficiency of the atomisation process for MQL method.

According to Shamin work (1995) as the viscosity of the lubricating oil increases the amount of oil in the larger particle size ranges increases and the amount of oil in the lower particle size ranges decreases. Moreover, generally an increase in oil viscosity reduces the mass concentration of oil in the mist. The type of oil and the presence of the stray mist reducing oil additives have significant influence on the droplet mass-size distribution and the mass concentration of oil in the generated mist. The larger particles are more desirable than the smaller particles because they do not contribute significantly to stray mist (Anand and McFarland, 1989).

3.3. Economics of Minimum Quantity Lubrication

In terms of process economics, the application of MQL to grinding must be thoroughly investigated to establish basic gains in surface quality compared to wet grinding, tool life and mist supply to the cutting zone.

Tadashi Makiyama (2000) in his work produced a bar chart (Figure 3-2) showing a cost comparison for drilling, when considering fluid consumption, staffing expenses, cost of waste liquid treatment, energy consumption for compressed air and coolant pump, and depreciation of equipment. Comparison is made for processes that require medium to high coolant pressures. The chart shows that MQL provides a drastic cost reduction,

reaching up to 65 per cent. Components such as depreciation of equipment, power consumption, disposal and cleaning constitute a major part of costs. MQL provides saving due to its cheapness, low cost of equipment maintenance and low power consumption.

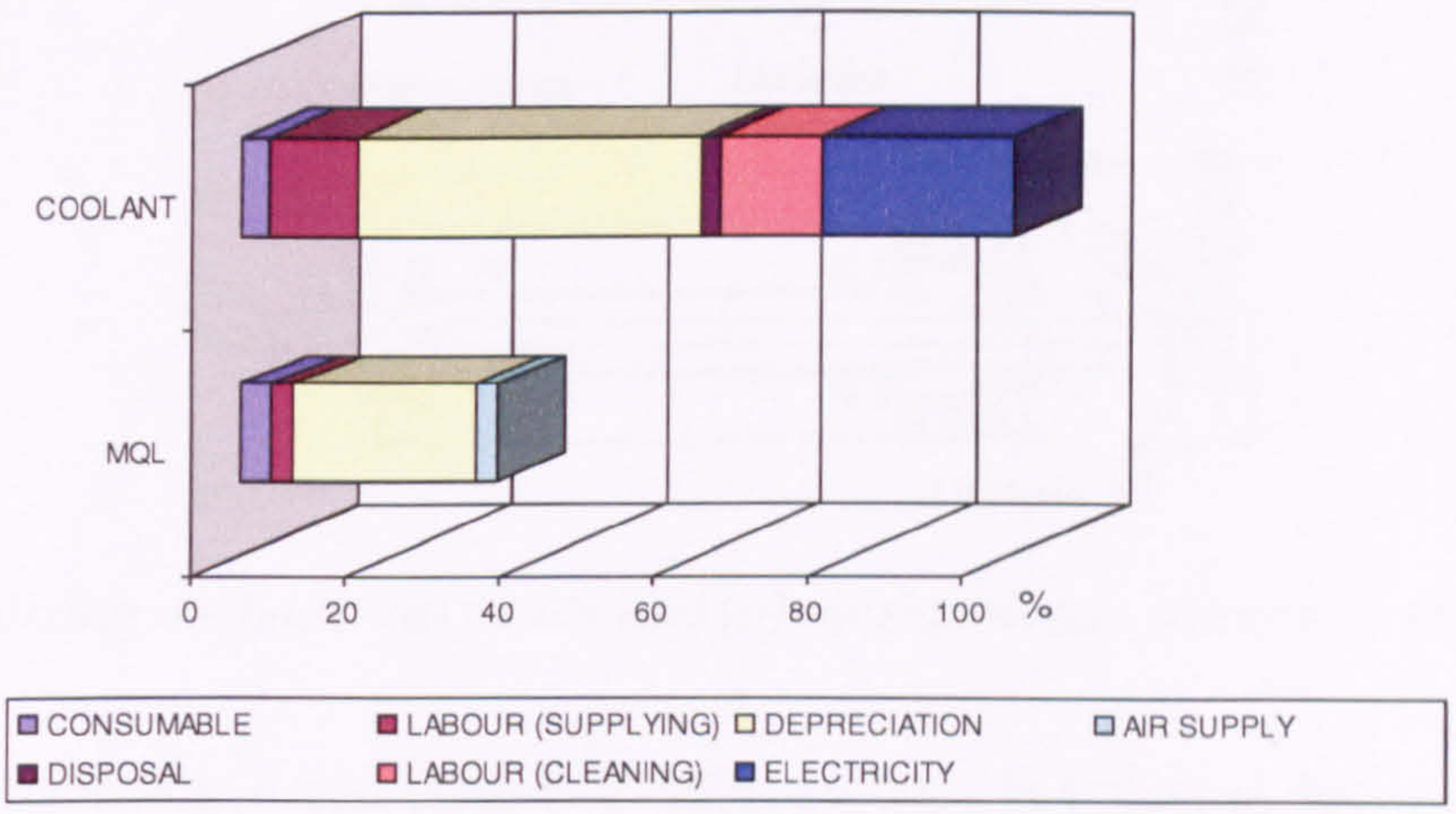

Figure 3-2. Lubricating methods cost comparison for a coolant and MQL (Makiyama, 2000).

In a different research Dorr and Sahm (from Silva, 2005) compare costs of wet and MQL machining, based on investments and annual fixed and proportional costs at the BMW company. The comparison of the total investment costs in the transfer line, including chip cleaning equipment, confirmed 22 per cent financial advantages of machining with MQL technology.

3.4. Classification and Design of Minimum Quantity Lubrication Systems

There are three types of MQL system available for end users: excess pressure spraying system (mixing inside nozzle), lubrication through spraying (mixing outside nozzle in the reservoir), and low-pressure spraying system (based on the Venturi nozzle principle). However, only the first two types are most common in industry, and most users employ the first one. These systems are based upon the principle of total loss

lubrication with dry chips and dry workpiece following the machining process (Brinksmeier, 1999).

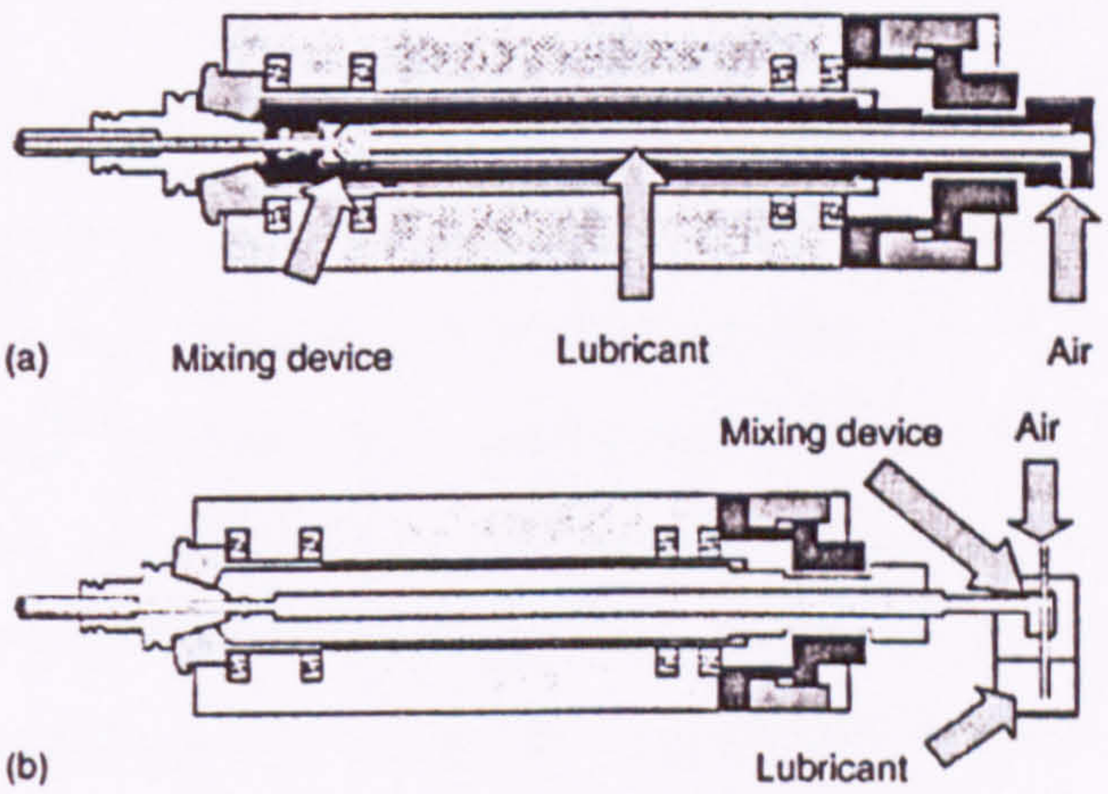

Figure 3-3. Mixing methods: (a) inside and (b) outside nozzle (Attanasio et al, 2005).

The main difference between these two MQL systems is a mixing device (Figure 3-3). The working principle of a pressure spraying system is shown in Figure 3-3 (a) and Figure 3-4.

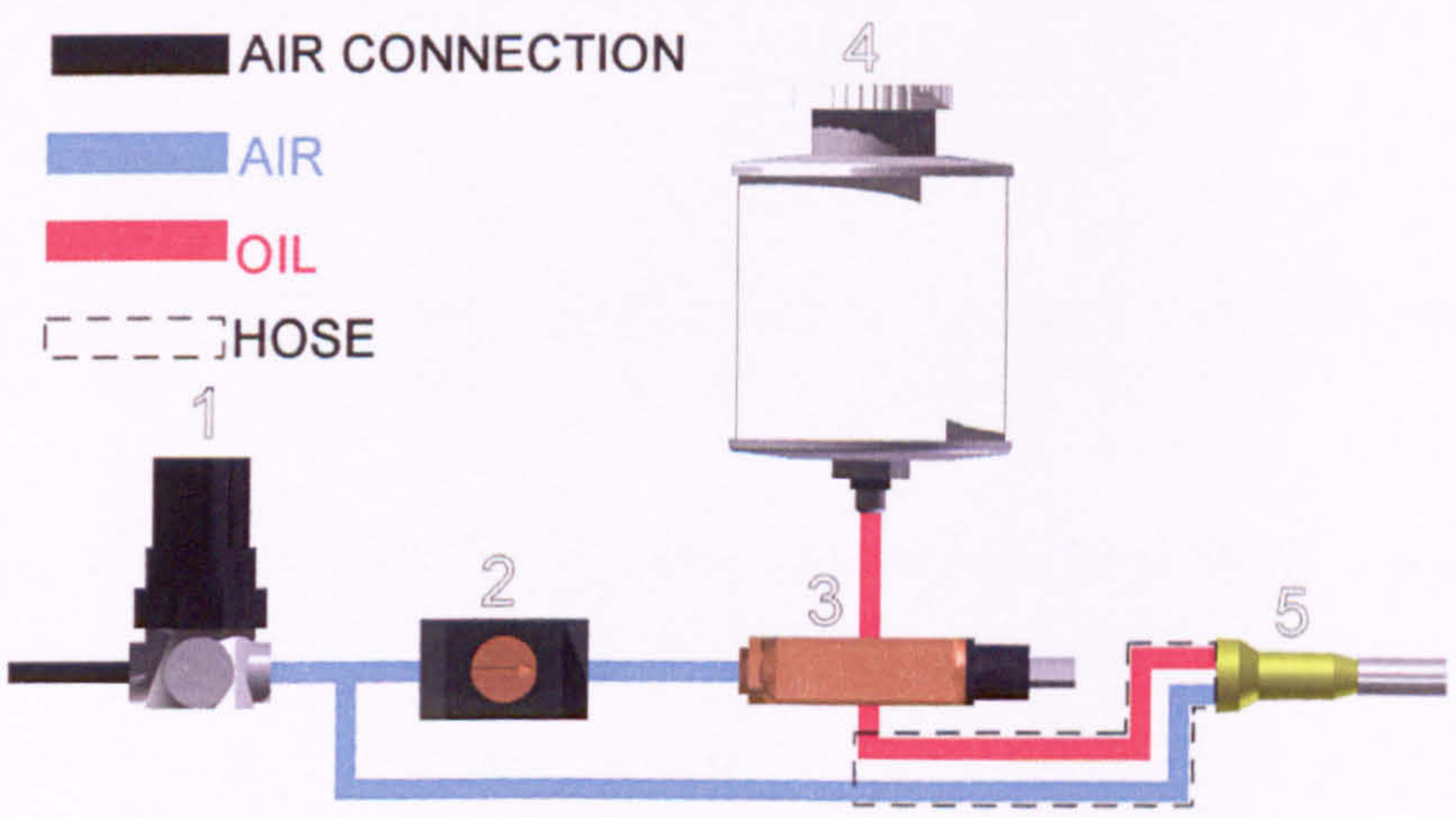

Figure 3-4. Working principle of excess pressure spraying MQL system – 1 – air valve, 2 – impulse generator, 3 – oil pump, 4 – reservoir, 5 – nozzle.

In this situation, the air is supplied from air connection and through a valve (1) the amount may be adjusted. Passing the valve, the air is divided into two lines – one goes straight to the nozzle (5), and the other one powers up a impulse generator (2) that generates delays in air delivery, that is supplied for an oil pump (3). The oil under gravitational force goes down from the reservoir (4) to the pump, where it is pumped to the nozzle by air impulses from the generator. The amount of oil used is controlled by

changing the piston stroke in the pump, as well as by the frequency of air supplied. Both, oil and air go separately to the nozzle where they meet at the end of the nozzle. Here the mixing device is located that mixes the two media.

For an MQL system using lubrication through spraying – see Figure 3-3(b) and Figure 3-5, the principle of operation is different. The air supplied from the line goes through the valve (1), that controls the amount and pressure of the flow at the end of nozzle. However in the first place it is carried inside of reservoir (2) that is filled with oil. The oil and air are mixed inside of this reservoir and then, as the mixture is carried to the choke (3), that is used to adjust the oil amount. The mixture goes to the nozzle via a hose, that may be supplied with another mixing device. The main work of mixing oil and air is done during the "reservoir" phase.

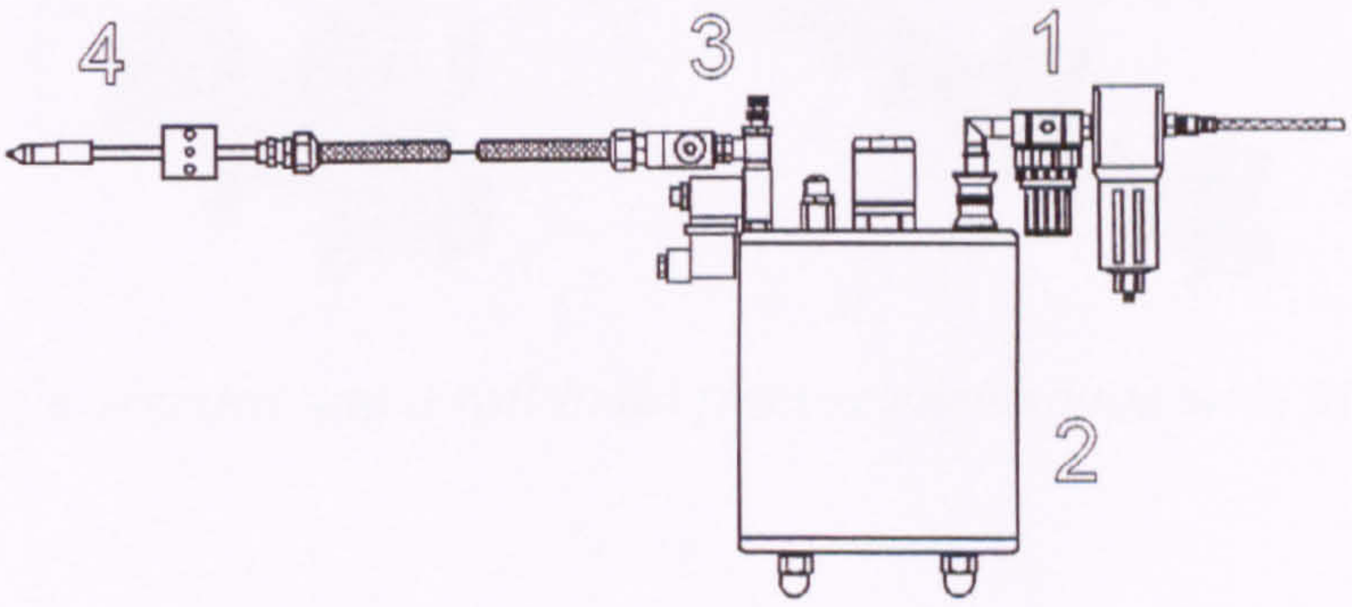

Figure 3-5. Principle of operation of MQL system using lubrication through spraying. 1 – main air valve, 2 – oil reservoir, 3 – choke, 4 – nozzle (MicroJet).

All systems mentioned can be found in many variations, with larger reservoirs, fully- or semi automated air and oil valves and chokes, combinations and different nozzles shapes (Figure 3-6 and Figure 3-7). However, in its simplest form, the MQL system does not require electrical connection and can operate based only on the air supplied from an airline – this makes it very flexible and easy to operate.

Figure 3-6. Examples of nozzles used with MQL systems (MicroJet).

It is not possible to state which one of those systems is better or achieves the best results, as there is no evidence of any comparative work carried out in the past. However, it should be mentioned that excess pressure spraying systems appear to be more common in industry. Also in the opinion of the author of this work, this system provides greater flexibility and assures better working conditions. For instance with lubrication through spraying MQL systems, the mixing reservoir has to be close to the machine, as when the oil mist is carried to various points of lubrication by hoses and pipes, the droplet size and oil concentration change. With excess pressure spraying MQL systems, there may be one large oil reservoir supplying oil to all MQL devices via a pump, as the mixing occurs in the nozzle.

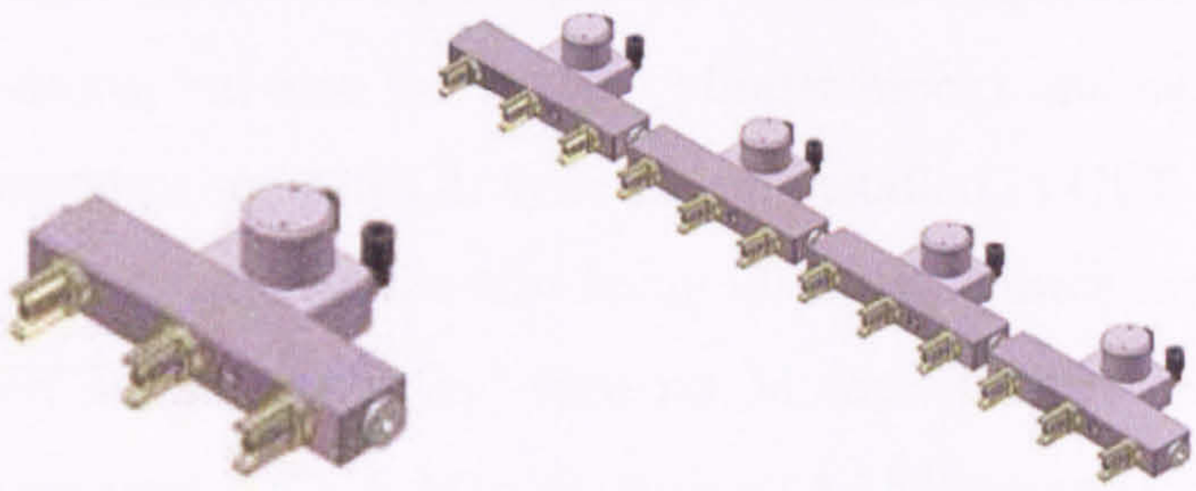

Figure 3-7. Single segment and a rail build from segments used with MQL systems (by Microjet).

It is highly desirable, to obtain a very good atomisation in order to achieve good wetting of the grinding zone. However, it involves high risks to the health of workers, due to exposure to aerosols. It should not be such a large problem with the new generation of grinding machines fully enclosed and ventilated, though it is a concern when machining is carried out without efficient ventilation with open grinding machines.

3.5. Results for MQL in Machining

MQL systems are very flexible and can be broadly used in machining such as milling, turning, drilling, sawing and grinding. Their flexibility is based on a simple construction and thus simple adaptation to different machining methods. However, there are differences in the mechanics of various machining methods, so there is a need for different delivery systems.

The tribology of MQL in machining is not well understood and has been investigated by only a few researchers, however MQL has found its place within many industrial applications. For instance John Mortimer (2005) in his article "Less coolant can be more" explains how MQL is being adopted in machining throughout the world. In the chase for environment protection and cost savings, dry machining was initially considered and implemented. Since then MQL has been identified as not only an alternative to dry machining, but as an alternative to conventional flood cooling. At GTF's (Getrag Ford Transmissions) Halewood plant in the UK, there has been a production of six-speed transmissions for Transit vans, involving 14 machines tools and modest dry machining of gears in small batches. In 2005, Ford considered MQL for a new transmission line. Ford was interested not only in implementation of MQL for machining transmissions, but also for engine cylinder blocks and heads, with both cast iron and aluminium components. MQL systems are installed in GFT in Cologne as well as at Volkswagen in Germany and are also being installed at three major automotives in the USA – DaimlerChrysler, Ford and General Motors. Other American automotive suppliers such as American Axle & Manufacturing (AAM) recently purchased an MQL machining line to produce aluminium transfer casings (Mortimer, 2005).

In Japan, Horcos claims to have installed over 250 MQL machines, including transfer lines that use MQL. Horcos use MQL technology for deep hole drilling of oil ways in crankshafts. In 2005 at the International Manufacturing Technology Show in Chicago, the company unveiled its RM80H near-dry horizontal machining centre, that uses 55 ml of cutting fluid per hour, mixing air with the fluid in the spindle. The company claims a 15 per cent reduction of machining cost and cutting feed rates of over 1 m/min (Mortimer, 2005).

3.5.1. MQL in Milling

Some sources (e.g. Mortimer, 2005) claim, that many milling operations are not well suited to MQL due to the difficulties of getting the aerosol directly into the cutting edge and that the ideal machining process for MQL is boring. However Rahman *et al* (2001, 2002) in his work examined MQL in end milling. As a conclusions MQL may be regarded as an attractive alternative to flood cooling. The tool wear obtained in MQL

was comparable to that for flood cooling at low feed rates and low speeds and depths of cut. In almost all cases, the surface roughness generated by MQL was almost equivalent to that obtained by flood cooling. No significant difference in cutting force was observed between that of flood cooling and MQL. However, at higher depths of cut, the cutting force increased for MQL. Fewer burrs were formed during machining with MQL which is a distinct advantage compared to dry cutting and flood cooling method.

A study by Liao and Lin (2007) considered the mechanism of MQL in high speed milling. It was found that the tool life was increased with MQL compared to dry machining and for some conditions tool life was over twice long. It was also found that for extremely high-speed cutting there was no protective layer of oxide that occurred for lower speeds. That resulted in thermal cracks, and hence MQL application was not suggested by the authors for this range of speeds, despite it still resulting in an increase of tool life. This was confirmed by the work of Rahman (2001, 2002).

3.5.2. MQL in Turning

A UNIST manufacturer of MQL systems performed a study (CS20070802S) for a company that was using a CNC lathe with no coolant due to nature of the machining application. The installation of an MQL system resulted in savings of 41 per cent of tool inserts and the annual insert cost was reduced by $3,800 to $5,555 on one machine. Tool life was extended from 600 cuts to an average of 900 cuts a day.

Another investigation by Sreejith (2007) was concerned with the effect of the coolant on tool wear. It was shown that the application of coolant did not necessarily reduce tool wear since in MQL conditions the tool wear was found to be lower. The cutting forces were found to be dependent on the coolant system and if an improved quality of the workpiece surface was expected, coolant was necessary. It was found that MQL was able to produce results comparable with that of flood cooling.

3.5.3. MQL in Sawing

According to industry experts, MQL technology has equal applicability compared with the machining-centre applications widely used. MQL plays an important role in sawing and Neuwirth for instance implements this technology further. It is estimated that around 75 per cent of its structural-fabrication cutting is done with MQL. The main advantage of this is no cleanup time and disposal issue with near dry lubrication systems as there is no need to clean out a sump in the saw or dispose the coolant. However, there are some limitations for MQL use. One of them is the distance of the nozzle from the saw blade that needs to be reduced. The other concern is how the saw is lubricated and direction of lubrication as in some operations (vertical band-saw), MQL nozzle cannot be used in the same way as conventional cooling due to technical limitations. Finally the material is a limitation for the MQL – it is hard to obtain adequate cooling when sawing with solid, thick and hard materials (such as titanium) (Heston, 2007).

3.5.4. MQL in Drilling

In drilling there may be used two types of MQL systems: internal and external – Figure 3-8. The difference between these systems is, that with the internal system air and oil mixture is transported directly to the machining zone and with external there are nozzles that supply oil mist to the tool (Figure 3-8 (2)). Internal MQL systems are found to be more efficient. The internal delivery is generally considered as most efficient in MQL machining systems.

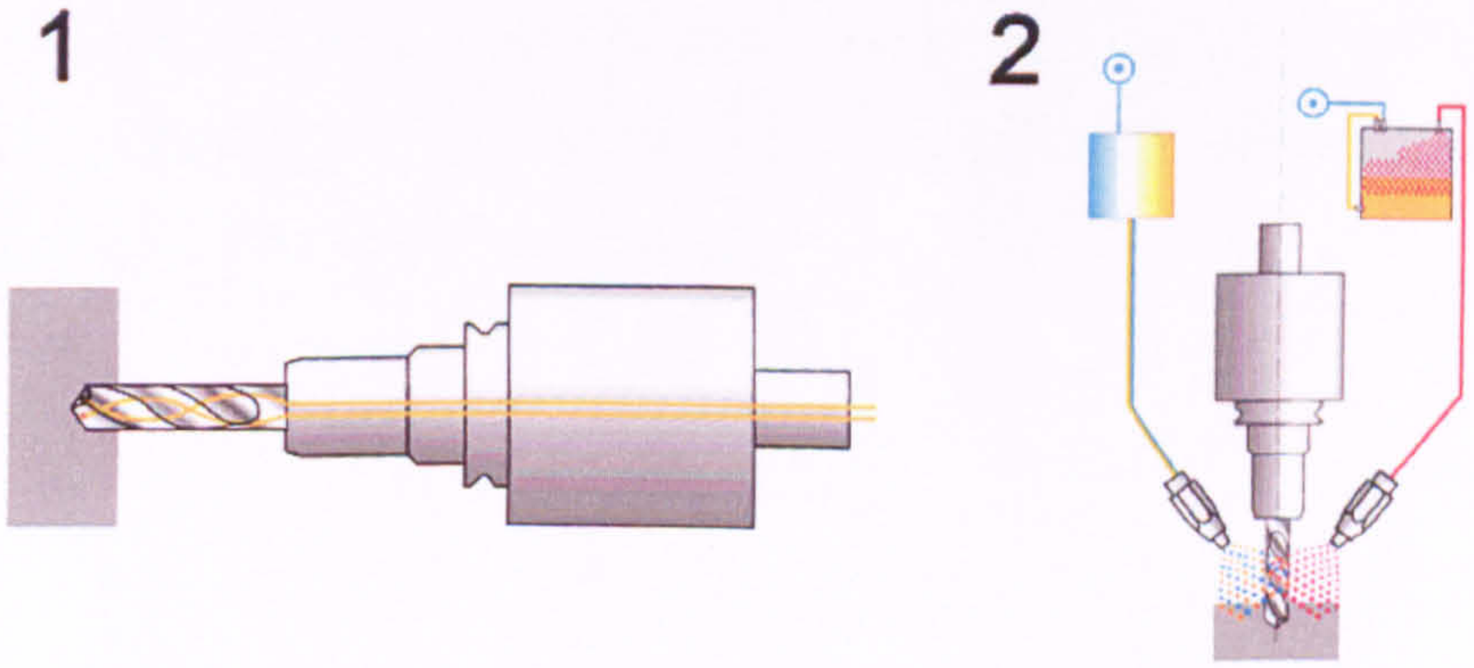

Figure 3-8. MQL Systems solutions for 1) internal, 2) external drilling.

Trials on crankshafts at Ford in the US with Sumitomo drills achieved feed rates of 650 mm/min for oil holes, Guhring and Ex-Cell-O have pushed this figure up to between 1,200 mm/min and 1,400 mm/min with associated good tool life. It was claimed by Guhring, that they have optimised flute profiles to generate chips and good chip flow. With feed rates of 1,098 mm/min, Guhring reported a 0.18 mm wear rate after 100 m – some 20 per cent better than a leading competitor (Mortimer, 2005).

Ford engineers focused on the productivity potential of near dry machining centre with high-speed linear motor driven slides, dual-channel MQL delivery systems and dry filtration. The baseline for assessing the gains was a Horcos NDM centre that processed 4,200 cast aluminium housings for a Ford 4x4 transmission. Such a system produced 139 parts per shift at a machining cost of $3.40 per part, but the optimised MQL system could produce 460 parts per shift at a machining cost of $2.00 per part. Thus, the new system could double production at a 41 per cent lower unit cost. In addition, the number of tools used fell from twelve to eight or six. An important factor was, that the air quality, measured by oil content, improved from 0.23 mg/m^3 to 0.20 mg/m^3 (Mortimer, 2005).

Another case from the industry is described in Modern Application News, April 2005 (Unist, 2005). One of national shops in USA, Central Florida, that concentrated on cutting and holemaking used annually 330 gallons of coolant that cost $6,600. Further costs were incurred due to disposal of the coolant, plus the costs associated with cleaning. The twist-drills used were lasting for only 100 holes, before re-sharpening. After MQL system provided by Unist, Inc., together with a new type of drills, a significant advantage of a change to MQL was avoidance of a disposal or environmental compliance cost to be paid. Further, cost reduction was realised by eliminating $6,430 annual cost for new coolant, as new coolant acquisition cost was $170 a year. Finally this technology change was claimed to allow 22,000 holes before a drill has to be replaced compared to 100 with old technology.

3.5.5. MQL in Grinding

From both an ecological and economical point of view MQL is highly desirable. However, due to the large amount of heat produced during chip removal there is a high risk of thermal damage and a solution providing both effective cooling and lubrication is required. As MQL cannot provide good cooling properties it must provide extremely efficient anti-frictional properties to help reduce heat generation. However, MQL remains a relatively new concept in processes with undefined cutting edges and there is a lack of information regarding the effectiveness of MQL in grinding. It is not yet possible to answer questions such as: Which wheel is the most suitable for MQL? What oils perform best with MQL? What are MQL limitations for machining various materials? Therefore, it is hard to say if MQL provides the desired anti-frictional effects. In spite of the lack of knowledge concerning MQL there are some publications that demonstrate that MQL may perform well in grinding and some tentative explanations are presented.

Klocke (2000) in his publication considers MQL as a flexible system for grinding and other applications. He explains MQL's good performance as a factor of low coolant flow rate that is able to get exactly to the grinding area and provide very good lubrication reducing friction conditions. It is due to the lack of pressure build up in the grinding gap and hence the lubricant can be transported through the grinding zone in the pores.

Silva *et al* (2005, 2007) in their work do not focus on MQL mechanics but provide very promising practical results. Their study, based on the evaluation of the technical performance of MQL in grinding using aluminium oxide and superabrasive CBN grinding wheels, consisted of an experimental analysis of the behaviour of the tangential cutting force, G ratio, roughness and residual stresses.

In Silva *et al* comparison of the two cutting fluid application systems it was revealed that the CBN grinding wheel and the aluminium oxide grinding wheel produced similar tangential cutting force. However, in the initial cycles, the CBN wheel presented higher tangential cutting force under all lubrication and cooling conditions tested.

There was a microeffect of MQL system causing the cutting edges of the CBN grinding wheel to be renewed continually during the grinding process, therefore maintaining the grinding wheel sharpness and leading to a gradual decrease in the tangential cutting force during the tests. Nevertheless, this condition led to substantial wear.

Figure 3-9 illustrates grinding wheel wear and reveals the substantial CBN wheel wear. It can be also noticed that the application of MQL produced a superior result when compared with the use of conventional cutting fluid, possibly due to the excellent lubricating capacity in the region of contact between the grinding wheel and the work piece.

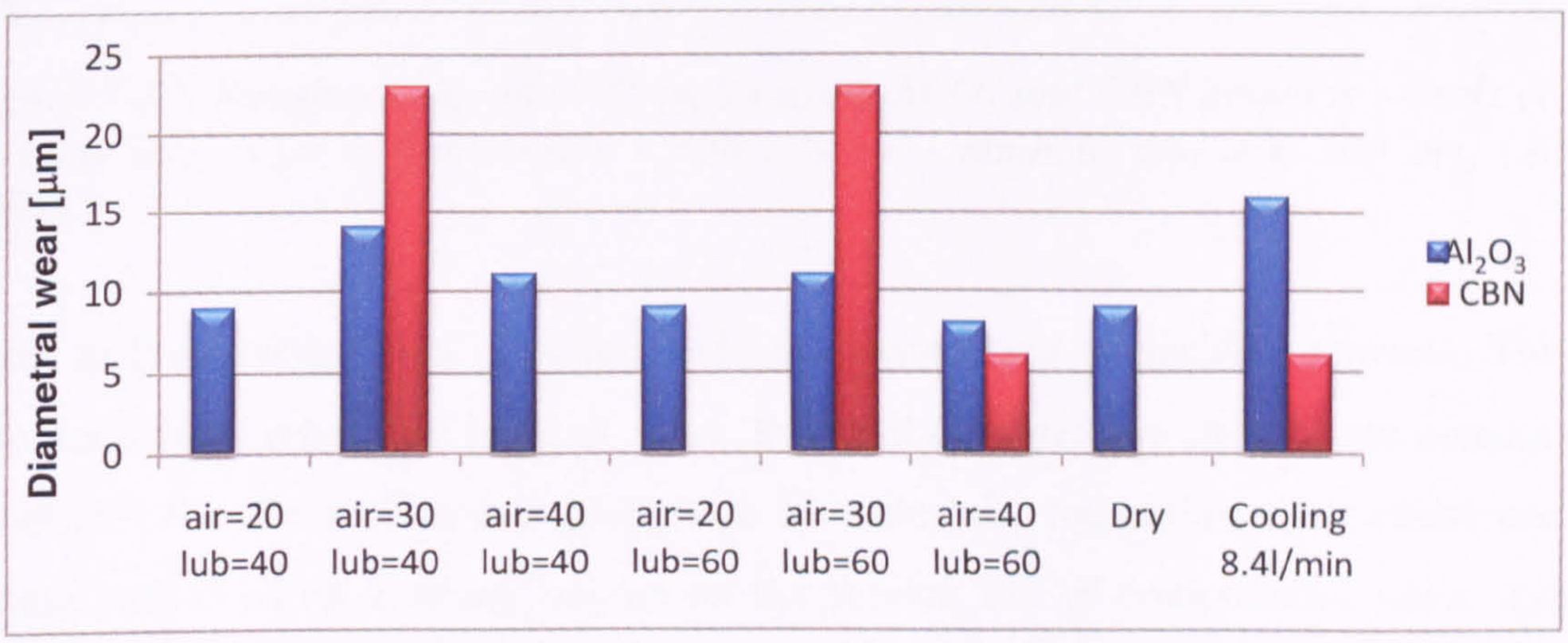

Figure 3-9. Diametral wear after 90 cycles using Al_2O_3 and CBN grinding wheels (v_{air} = variable m/s, v_{lub} = variable ml/h, v_s = 30m/s, v_f = 1mm/min, a = 100 µm and t_s = 10s) (Silva, 2005).

Figure 3-10 presents the results of comparison of mean roughness values R_a with Al_2O_3 grinding wheel using the conventional flood cooling against the results obtained under MQL technique. In general the MQL technique produced lower surface roughness under most lubrication and cooling conditions using the Al_2O_3 grinding wheel, most likely because of the effective lubrication in the cutting region. With MQL, the lowest surface roughness R_a was 0.41 µm, using the Al_2O_3 grinding wheel, compared with 0.60 µm in the flood cooled condition. In these experimental conditions using conventional cooling with the CBN grinding wheel led to a better finish than with MQL in two of three cases. A possible reason is that the extremely high tool hardness, causes it to exhibit macro-wear that leads to greater surface roughness. However, in favour to the wheel manufacturer, the CBN abrasive has been designed to perform under aggressive

machining conditions with flood cooling of oil and the tests do not fully examine MQL under such conditions.

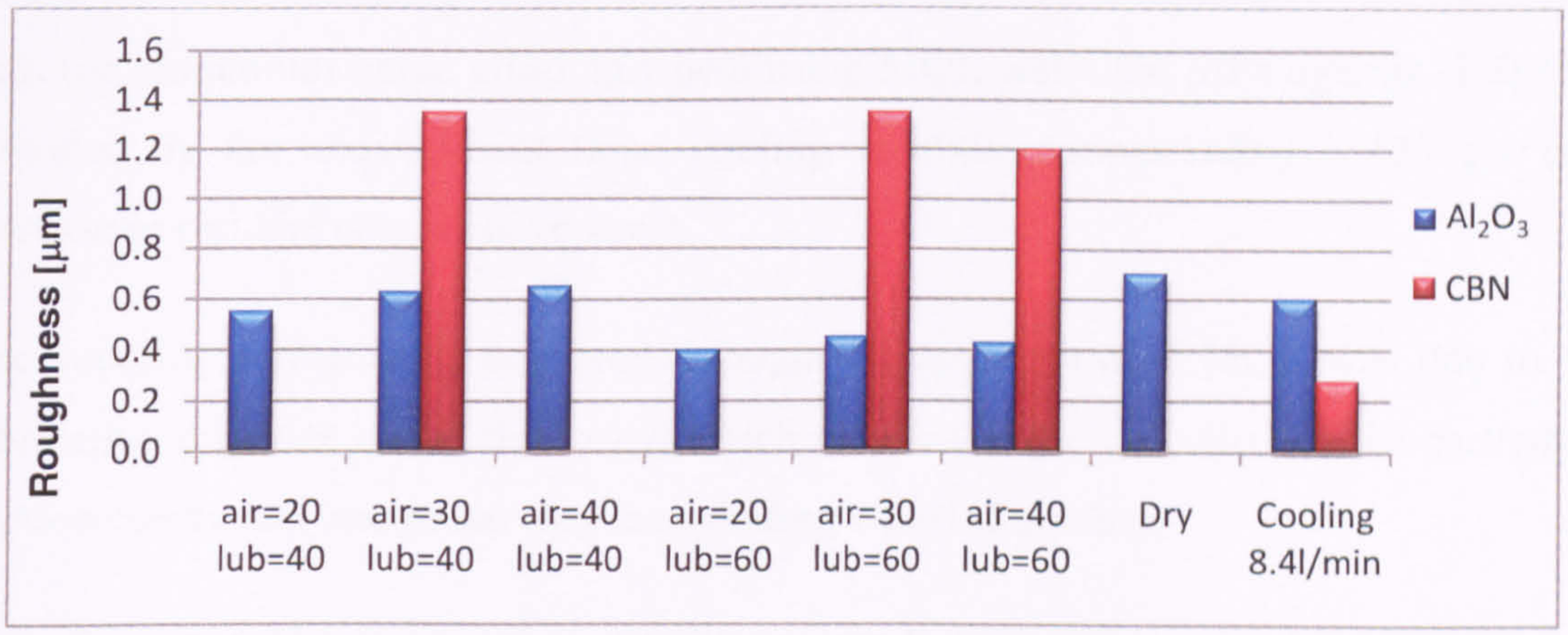

Figure 3-10. Roughness R_a after 90 cycles using Al_2O_3 and CBN grinding wheels (v_{air}= variable m/s, v_{lub}= variable ml/h, v_s=30 m/s, v_f=1 mm/min and a = 100 µm) (Silva, 2005).

Later in their work Silva *et al* focused on measurement of residual stresses. This is important from reliability point of view. Residual compressive stresses are considered beneficial for the mechanical properties of materials, increasing their resistance to fatigue and exerting a strong impact on the service life of components, while tensile stresses compromise the mechanical strength, corrosion and wear resistance. They may be caused by factors: influence of thermal expansion and influence of microstructural transformations in the part.

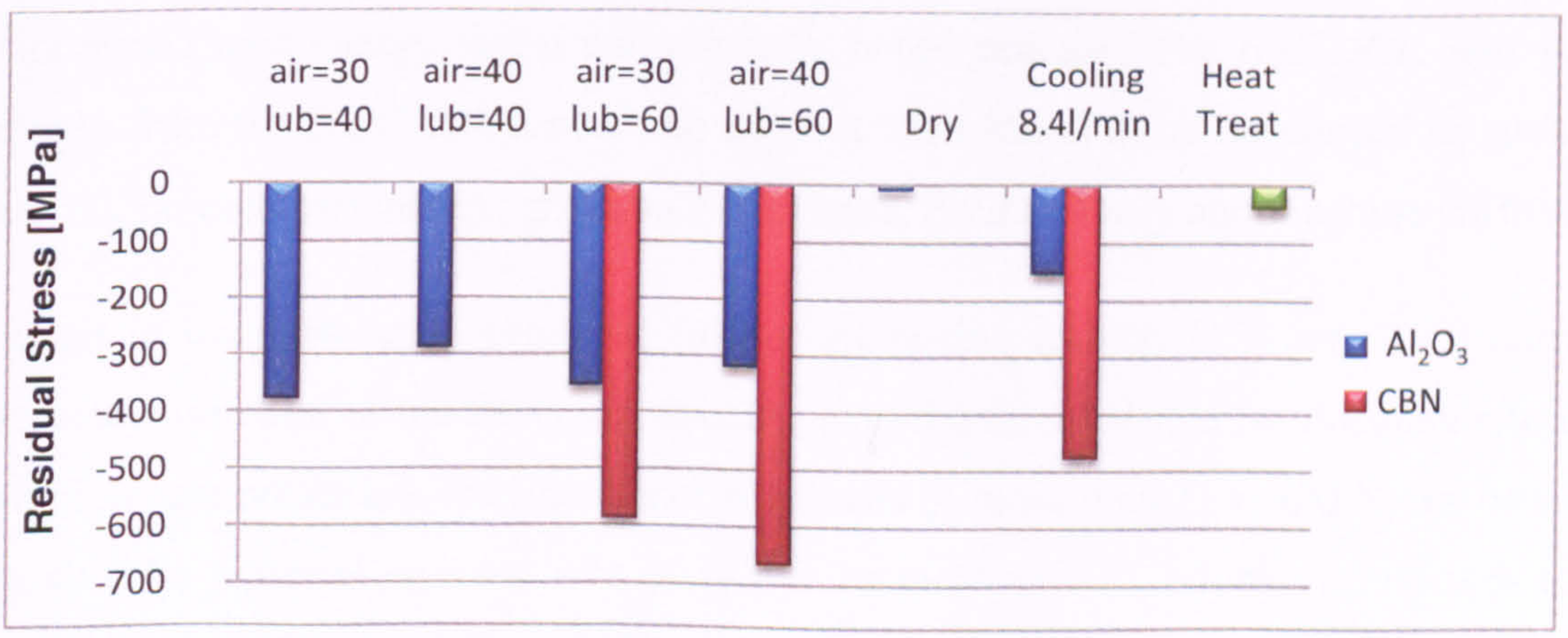

Figure 3-11. Comparative results of residual stress at a depth of aprox. 10µm below the surface after 90 cycles using Al_2O_3 and CBN grinding wheels (v_{air}= variable m/s, v_{lub}= variable ml/h, v_s= 30m/s, v_f=1 mm/min and a = 100 µm)(Silva, 2005).

The results of residual stresses are shown in Figure 3-11. The use of the MQL technique was found to give rise to higher negative values of residual compressive stresses under all the lubrication/cooling conditions. The lowest residual compressive stress obtained with the aluminium oxide grinding wheel using MQL was -376 MPa against -160 MPa provided by the conventional flood cooling condition, representing a 135 per cent increase in residual compressive stress.

The superior performance achieved through the application of MQL was due to the lubrication qualities of the fluid used which resulted in the reduction of the part/wheel friction coefficient and preserving the grinding wheel sharpness.

In a further study Silva *et al* (2007) analysed the workpiece microstructure and microhardness. They concluded that the MQL technique efficiency was also verified in the microstructure, reinforcing the hypothesis that MQL has substantial effects on both cooling and lubrication, and that it provides a positive effect on workpiece surface integrity. The microhardness measurements for the two lubricating and cooling conditions did not indicate important subsurface modifications.

However, it remains unclear whether or not the studies reviewed have considered the real DOC. The DOC is recognised as a critical parameter in grinding studies as it has a strong effect on tangential force and chip properties. This is because the DOC is largely responsible for the contact length, which increases with larger DOC. However to produce higher DOC, higher forces are required which requires higher power and leads to increased heat energy and a consequently hotter process. The real DOC will vary strongly from the DOC set on machine and has been found to be influenced by ground material, process parameters, grinding wheel used, fluid delivery and machine stiffness.

Weinert in his publication produces further interesting results. In Figure 3-12 normal forces as a function of the DOC and specific material removal rate for different cooling conditions are presented. Maximum normal forces of more than $F_n = 900$ N can be seen at a specific material removal rate of $Q'_w = 14$ mm³/(mm s), which corresponds to a DOC of $a_e = 140$ µm. When MQL is applied under the same grinding conditions thermal damage occurs at lower specific removal rates for $Q'_w < 1$ mm³/(mm s). In comparison to the flood coolant supply, the normal force increases more quickly when using MQL and chip shapes changed significantly and

were characterized by great quantities of fragmented chips, indicative of a deterioration of the chip removal because of wheel loading (Weinert *et al*, 2004). This would lead to a conclusion that MQL is applicable only at low DOC.

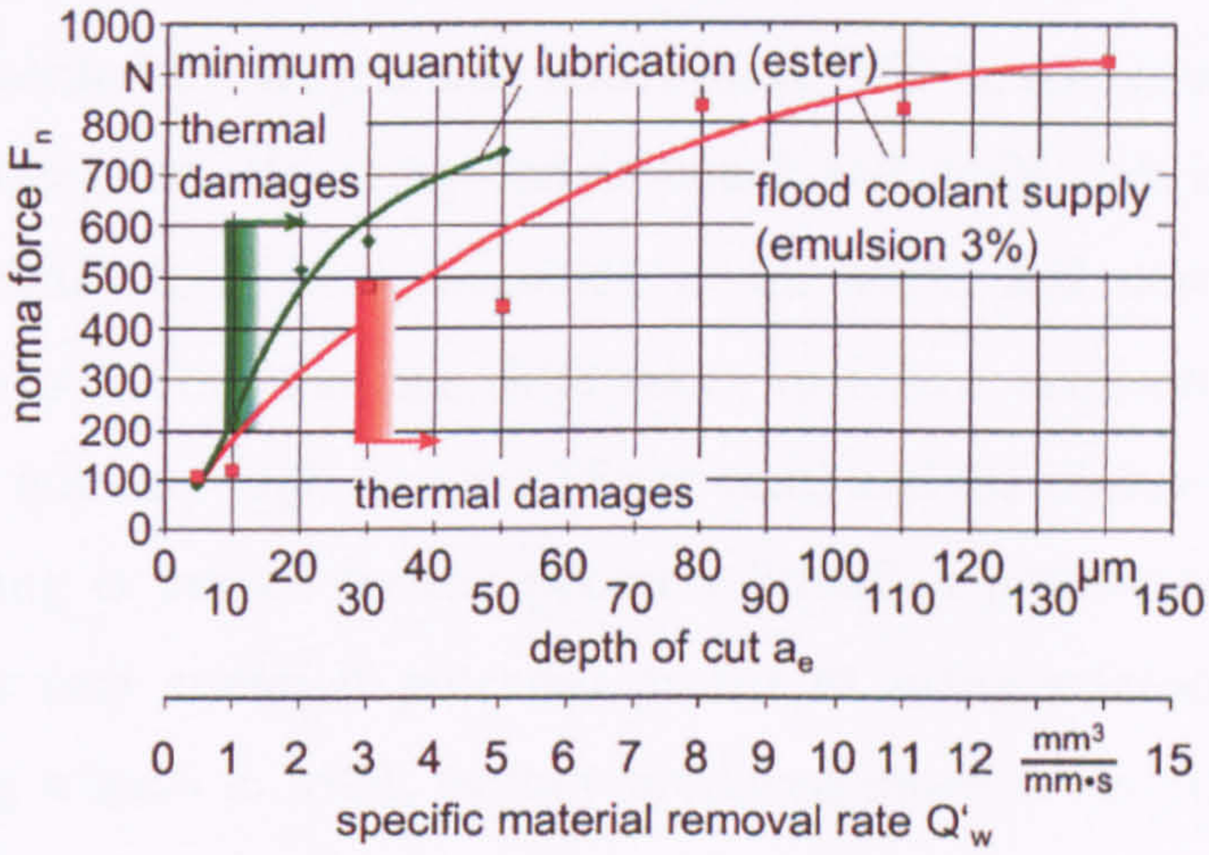

Figure 3-12. Influence of coolant supply method on function of normal forces and the DOC and specific material removal rate for different cooling conditions (Weinert et al, 2004).

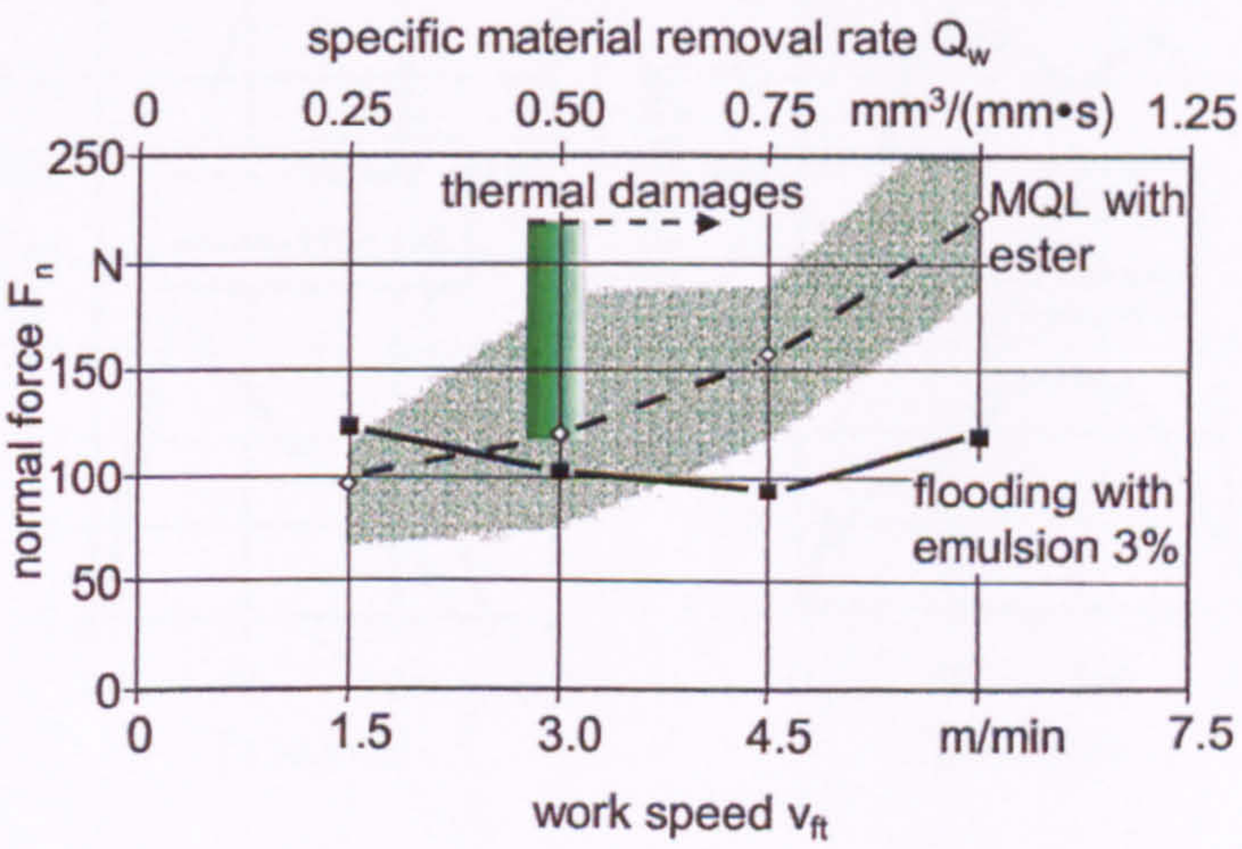

Figure 3-13. Influence of coolant supply method on relation of normal force to the workpiece speed (Weinert et al, 2004).

In Figure 3-13 the normal force in relation to the work speed is presented. It is evident when the flood coolant emulsions are applied to the contact zone, the normal force remains nearly constant and no thermal damage is observed. However, the use of MQL leads to a continuous increase in the normal forces with a great deviation in the results, maybe due to reduced process stability with this coolant supply. At the same time,

thermal damage occurs at a low removal rate of $Q'_w < 0.5$ mm³/(mm·s). Thus it is concluded in pendulum grinding with MQL a maximum removal rate of $Q'_w = 0.5$ mm³/(mm·s) or $Q'_w = 0.25$ mm³/(mm·s) is achievable without thermal damage to the workpiece surface layer (Weinert *et al*, 2004).

Another study presented by Wojcik and Kruszynski (2003), consisted of grinding with two different grinding wheels using conventional and MQL lubrication systems. A variation in tangential force was measured under MQL and conventional cooling, Figure 3-14. They point out that the differences in forces between conventional and MQL grinding are not very high (around 15 per cent) and the higher forces observed in conventional cooling is caused by the poorer lubrication properties of the emulsion. Their work brings into attention potential profits of using microcrystalline sintered corundum grinding wheels in MQL as they produced much lower forces and provided better surface quality.

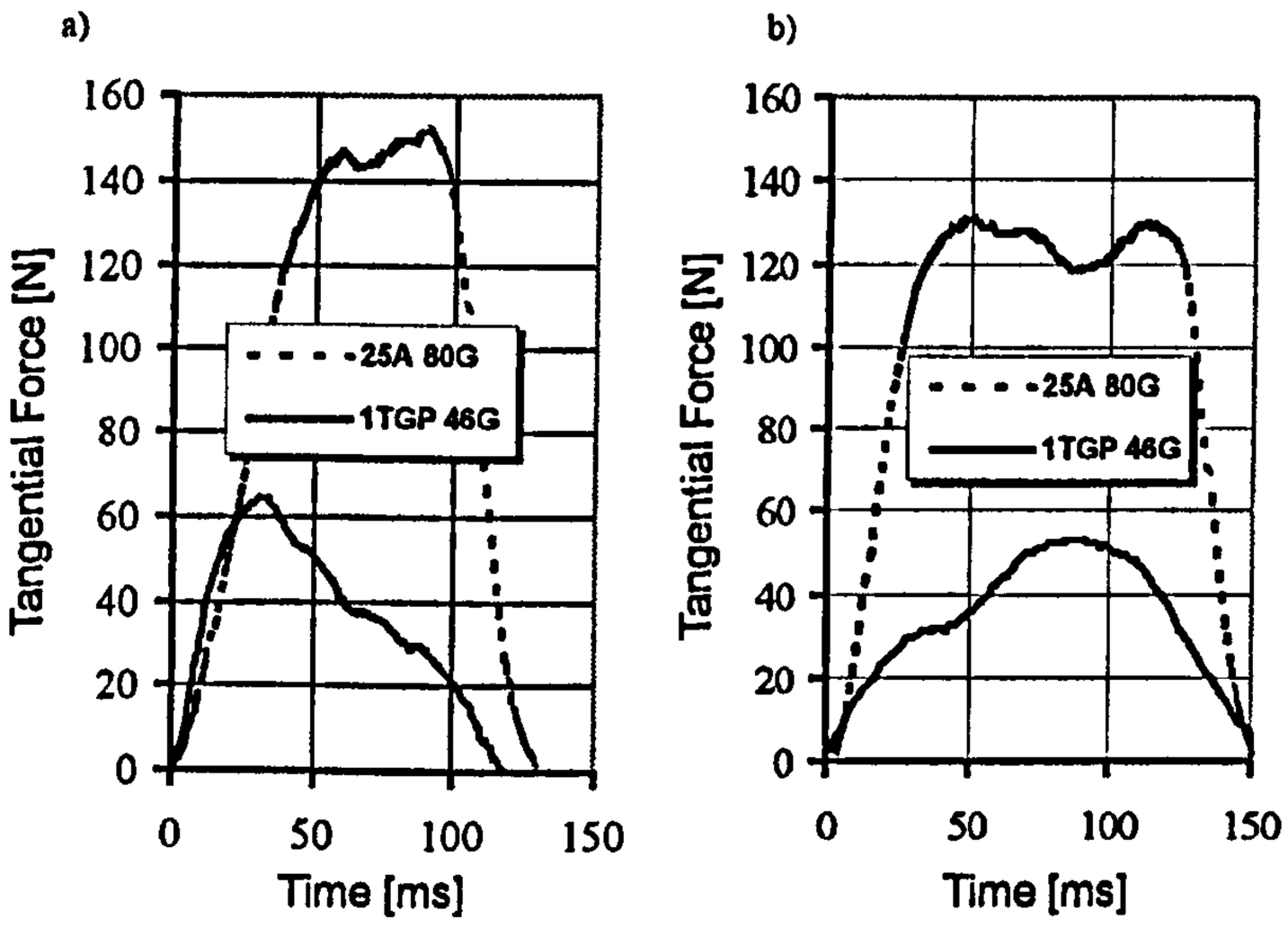

Figure 3-14. Variation of tangential force for a) conventional flood cooling and b) MQL, where $v_w = 0.5$ m/s, $a = 50$ μm, $v_s = 25.5$ m/s, when using aluminium oxide (25A 80G) and microcrystalline sintered corundum (1TGP46G) wheels (Wójcik and Kruszyński, 2003).

Later in their work Wojcik and Kruszynski (2003) also checked differences in internal stresses for conventional and MQL cooling method. They reported that there were no major differences in compressive stresses if grinding was undertaken with a conventional aluminium oxide grinding wheel. However grinding with microcrystalline

sintered corundum grinding wheels produced compressive stresses that were lower (higher negative values) for MQL than compared to conventional flood cooling.

This result, when alumina wheel is taken into account, presents a different outcome when compared with the results of Silva *et al* (2005). However it is difficult to comment on this and make a direct comparison as different alumina wheels were used (Silva 38A60KV – medium grain size and harder grade, Wojcik and Kruszynski 25A80G – fine grain size and softer grade). Also different materials and types of grinding were employed – Silva *et al* cylindrical grinding, Wojcik and Kruszynski plane surface grinding. However, it may be summarised that when using a specific grinding wheel and material and process conditions, MQL can induce more favourable compressive stresses compared to conventional fluid delivery.

3.6. Advantages and Disadvantages of MQL Systems in Grinding

As recent legislation put more pressure on industry for more environmental friendly cooling/lubricating process, the MQL technique which is in fact approximately 50 years old, is now more considered. But what does this technique offer over dry or conventional flood cooling methods? There are a number of advantages of MQL systems. All of them are based on the opinions of users and manufacturers of MQL systems (e.g. Vogel's FAQ, Unist, MicroJet, Steidle) as well as on conclusions resulting from research.

First, and probably most economical and attractive, is the very small quantity of lubricant that is used during the machining process. As mentioned earlier amounts range in the order of: 10-500 ml per hour. However amounts like 10-100 ml/h are most common. When this amount is compared to conventional flood cooling, typically in the range of 60-1200 litres per hour (1-20 l/min) it becomes obvious that usage of MQL oil is reduced by orders of magnitude. It leads directly to the conclusion, of disproportion in costs of money. As an example given earlier, a small workshop saves $6,430 on

purchase cost alone. For large companies it may mean enormous expenses just on coolant.

Disposal costs are the next consideration. Very often contaminated fluid is treated as toxic, with potential dangerous implications for the natural environment. As a result they often have to be stored in specially prepared places. All this generates costs, that are comparable or sometimes higher than the cost of fluid purchase. With MQL these problems are almost reduced to nil as the process is generally considered to be one of total loss.

Another important issue connected with environment damage is energy consumption. With conventional flood cooling electrical energy can make up to 25 per cent of the total cost of workpiece production, whereas MQL uses only a comparatively small amount of energy for the delivery and control apparatus.

Another cost, arising from using conventional flood cooling systems is that associated with the monitoring of condition of the fluid, as fluid properties change with time due to evaporation and chemical changes. When emulsion is used there is the possibility of bacteria growth. All this requires laboratory equipment/services and continuous monitoring, and results in further costs. There is also a requirement to prepare a coolant (an emulsion), and this may lead to frequent contact with the fluid. There can be also a contact with fluid during machining that can cause a health issues for staff, such as an irritation of skin or respiration system. With the MQL system there is little need for coolant preparation and monitoring.

Another very costly factor with conventional delivery is coolant cleaning and enrichment, at times accounting for up to one third of total machine cost. When costs of filters and other moving parts, and maintenance are taken into account, it is evident that conventional delivery systems are expensive. There may be further costs resulting from loss of coolants due to excess of coolant that often goes to floor and parts, and leakages. With MQL there is no excess of fluid and possibly more importantly, there are no expensive fluid cleaning systems and hence total machine footprint is reduced. They also require lower maintenance, as MQL systems require only periodic cleaning and minimum maintenance of pressurised elements.

Perhaps importantly for additional savings there is no requirement for storage of new and/or used fluids.

The total purchase cost of a MQL system and its components, is only a fraction of that of a conventional flood system. A basic MQL systems price starts from around £1,000 (October 2009). The price depends on the complexity of the system, and the more advanced systems tend to use less oil and perform with higher efficiency.

Depending on the machining process, MQL can be more or less efficient than conventional delivery methods, however it is very common, that the productivity is higher.

Though the role of coolant is to keep the workpiece and tool temperature low, it sometimes can lead to a negative effect such as thermal shock during bulk cooling. Thermal shock for material and tool is significantly reduced when MQL is used.

A definite advantage of MQL systems, is that systems can be readily adapted for grinding machines not built for usage with MQL in mind. However, it may be more challenging to adapt older machines, and the economics of such integration may need to be assessed.

Though there appear to be many benefits associated with MQL there are some economics of MQL that have to be established. These relate to productivity and quality.

There is a limited information concerning surface quality produced by MQL in grinding. However there is no strong evidence to indicate that the surface produced by MQL is inadequate for purpose. On the other hand, one of the biggest bearing manufacturers SKF, use a VOGEL's MQL system in production of their bearing balls, to the highest levels of accuracy, surface quality and roughness so it can be assumed that MQL is capable of producing highly specified surfaces.

Another limitation of MQL system is the material range appropriate for its application. MQL is not suited to machine materials with low thermal conductivity. For instance grinding of copper is a problem for MQL due to insufficient heat dissipation. There may be also problems with abrasive process of titanium alloys and magnesium.

Finally, there is a potential issue with removal of chips and debris from the working area, the contact area and the wheel surface. Such issues are readily resolved in drilling, either using vacuum or gravitational solutions, however it is considerably more complicated in grinding, especially with complex forms.

Removal of chips and partially fractured grains from the wheel surface presents a challenge. Wheel clogging may be ruled out up to some degree by using high porosity wheels but as it is not always possible, other solutions are necessary.

It was found during the preliminary tests presented in this thesis that chips and debris may be removed from the working area by using systems of brushes or brushing of the work area by the operator during workpiece interchange. However, this is not a permanent solution and may be impracticable in production conditions. The wheel loading was found to be the most important issue requiring further work, however this was considered outside the scope of this work. There are solutions using high pressure air and/or water systems and their use in MQL requires full investigation. Another sophisticated method is use of a high frequency base vibrating for the workpiece that has been found very beneficial in some conditions for workpiece surface quality – so not only wheel loading could be avoided but surface quality of the workpieces can be improved. Such a solution is in its early design and development stage at Liverpool John Moores University. Other innovative wheel cleaning solutions such as microwave plasma or laser devices may also be found useful. However, these are only futuristic solutions that need research and development before they can be successfully employed in MQL systems.

Wheel loading may be removed by the process of dressing, however, this solution leads to another issue – near dry wheel dressing. It was found in the experimental tests that dressing with MQL did not provide the same surface as was obtained with flood coolant dressing. It was found that debris was not entirely removed from the surface pores and hence wheel performance was affected deleteriously. It was necessary therefore to employ flood coolant delivery to achieve required surface topography.

3.7. Aspects of Health and Environment Hazards

It has been recognised that MQL system produces oil spray containing fine particles (0.4-5.0 μm (Heisel *et al*, 1994; Shamim, 1995)). These particles are dangerous for the human respiratory system. According to Uwe Heisel *et al* injuries to human organs can only be caused by particles that are able to get into and remain in the lungs. The diameter of such a particles is considered to be between 0.5-5.0 μm. Particles with diameters greater than 5 μm are pre-filtered by the human nose and particles with a diameter smaller than 0.5 μm are mostly exhaled during breathing. The smallest particles are considered harmless due to no evidence of injuries of the respiratory track. It is also recommended that a single concentration of oil mist should not exceed 5 mg/m^3 (Heisel *et al*, 1994) whereas MQL systems are based on generation of exactly this kind of oil mist. To decrease this hazard it is advised efficient ventilation systems should be available both, in the working area and the machine enclosure.

The chips and debris can be directly taken for recycling without the need of additional processing. There is also no waste of water that would be used in large volumes for flood cooling. It is also claimed by MQL fluids manufacturers (such as VOGEL), that there is no environmental damage due to additives in the oil and that those fluids are of Water Hazard Class 1 which means it is not hazardous for waters.

In general the MQL technique may be considered as a harmless and safe technique for both the natural environment and human beings. However, it is important for the safety and health of the operator and those in the environment local to the machine tool that precautionary measures are in place to ensure that inhalation of droplets is avoided wherever possible. This may be achieved through the Health and Safety Personal Protection Equipment, monitoring and additional exhaust equipment.

3.8. Lubricants for MQL

As the main tasks for conventional fluids is to reduce and dissipate generated heat from the tool-work contact together with transporting chips, MQL lubricants are unable to

transport chips and are capable only of reducing heat by reducing friction. There are different expectations (apart from very good lubricating qualities providing effective cutting) from cutting fluids used with MQL (Weinert *et al*, 2004).

Oils used for MQL differ depending on the application. For instance different types of fluids are required for aluminium and copper, as due to deoxidation process stains can be formed. Their composition is based on amino alcohol of fatty acids (esters), fatty acids, emulsions that neither contain mineral oils nor compounds such as chlorine, sulphur or heavy metals; hydrocarbons and modified vegetable oils. Vegetable-based oils have a better biodegradable characteristics. Synthetic esters provide a wide range of biodegradability depending on their combined molecular structures of acids and alcohols. If one compares the degrees of biodegradability of various synthetic esters, then monoester, diester and polyol ester can be regarded as biodegradable. Since polyol esters may probably have suitable viscosities for MQL machining, several polyol esters have been examined as lubricants. Based on the reported test results synthetic biodegradable polyol esters were found to be superior to vegetable oils. In terms of secondary characteristics, biodegradable polyol esters were identified as the preferred lubricant for MQL machining (Klocke *et al*, 2000; Weinert *et al*, 2004).

An important quality of vegetable oil, unlike petroleum products, is that it is a polar fluid. When the vegetable oil contacts a metallic surface, its molecules align themselves according to their polarity. This is what gives it the superior lubricity characteristics.

However, there is a lack of information regarding specification of oils for MQL systems. It is not clear why some oils are suggested for some machining processes. At this stage this area needs further research as it is clear that properly chosen oil may change things and either improve or worsen machining conditions.

3.9. Summary

A broad review of Minimum Quantity Lubrication delivery was presented in this chapter. MQL background and economics were discussed, together with potential savings. MQL systems classification was provided with explanations about differences

between excessive pressure lubrication and lubrication through spraying systems. Literature review results for MQL delivery in machining, particularly in milling, turning, sawing and drilling were presented, leading to the conclusion that MQL may extend tool life and provide substantial savings on tools and fluid costs.

Importantly results for MQL delivery in grinding were also presented and discussed.

Advantages and disadvantages of MQL delivery were discussed, together with consideration of MQL aspects on hazards to health and the environment.

Finally, lubricant selection in MQL delivery systems is briefly discussed.

The following chapter will discuss abrasive material removal process theory and key relationships in terms of grinding mechanics, thermal models and temperatures in grinding.

Chapter 4. GRINDING THEORY AND KEY RELATIONSHIPS

4.1. Grinding Mechanics, Geometry and Kinematics

The grinding process is stochastic in nature and the number of active grains and their geometry is unknown. The grains present rake angles which are, in general, more negative than those normally used in milling or turning (Figure 4-1).

	Turning (a)	*Grinding (b)*
Cutting speed	*0.25-15 m/s*	*5-90 m/s*
Rake angle γ	*+20° to -10°*	*0° to -60°*
Clearance angle α	*6° to 10°*	*0° to 60°*

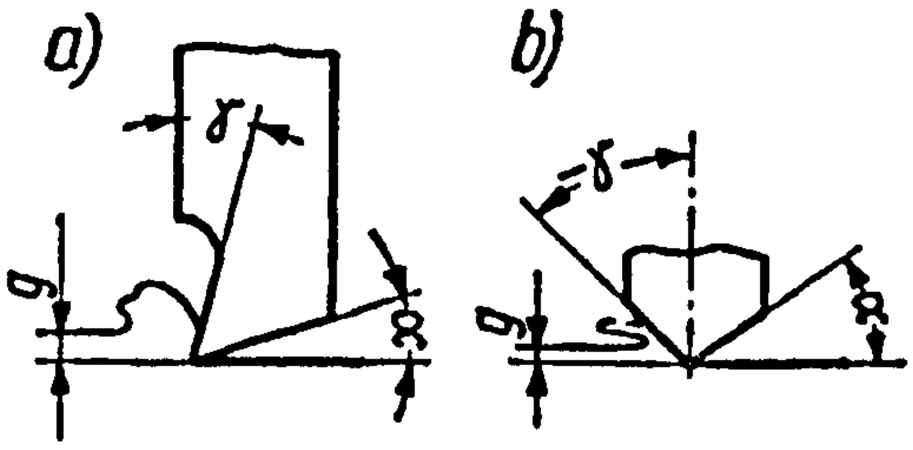

Figure 4-1. Comparison of cutting speeds and angles for (a) turning and (b) grinding (Filipowski and Marciniak, 2000).

To perform efficient cutting, a large negative rake angle of the grain requires a normal force that can be 2-3 times higher than in turning. This results in high power consumption and leads to the generation of high temperatures. However, negative rake angle ensures good surface roughness. During the grinding process as the grain wears, clearance angles decrease to 0° causing higher friction and therefore higher temperatures (Rubinstein, 1972; King and Hahn, 1986).

A schematic presentation of a single grain working is shown in Figure 4-2.

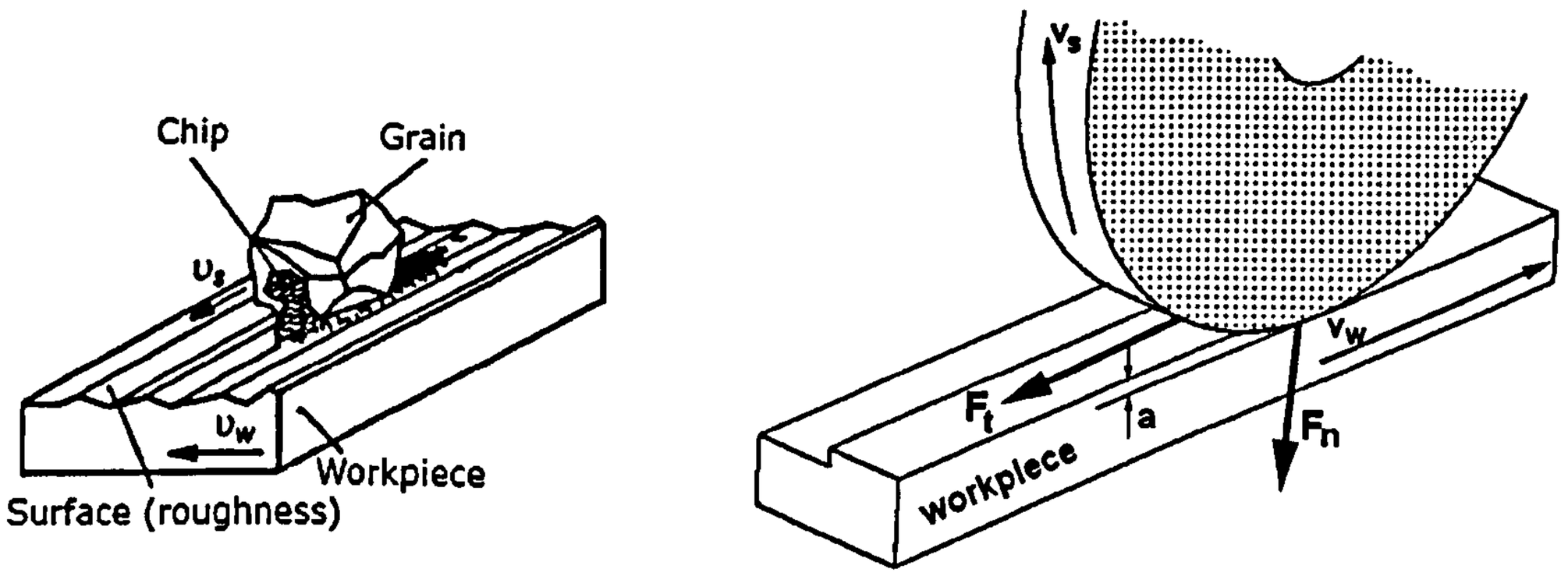

Figure 4-2. Schematic presentation of single grain working (left figure)(Filipowski and Marciniak, 2000), where: v_s – wheel speed, v_w – workpiece speed, a – depth of cut, F_t – tangential force, F_n – normal force, (right figure).

The following analysis considers the interaction of a single grain with the workpiece. The stages of chip formation recognised by Hahn (1966) and now generally accepted are shown in Figure 4-3.

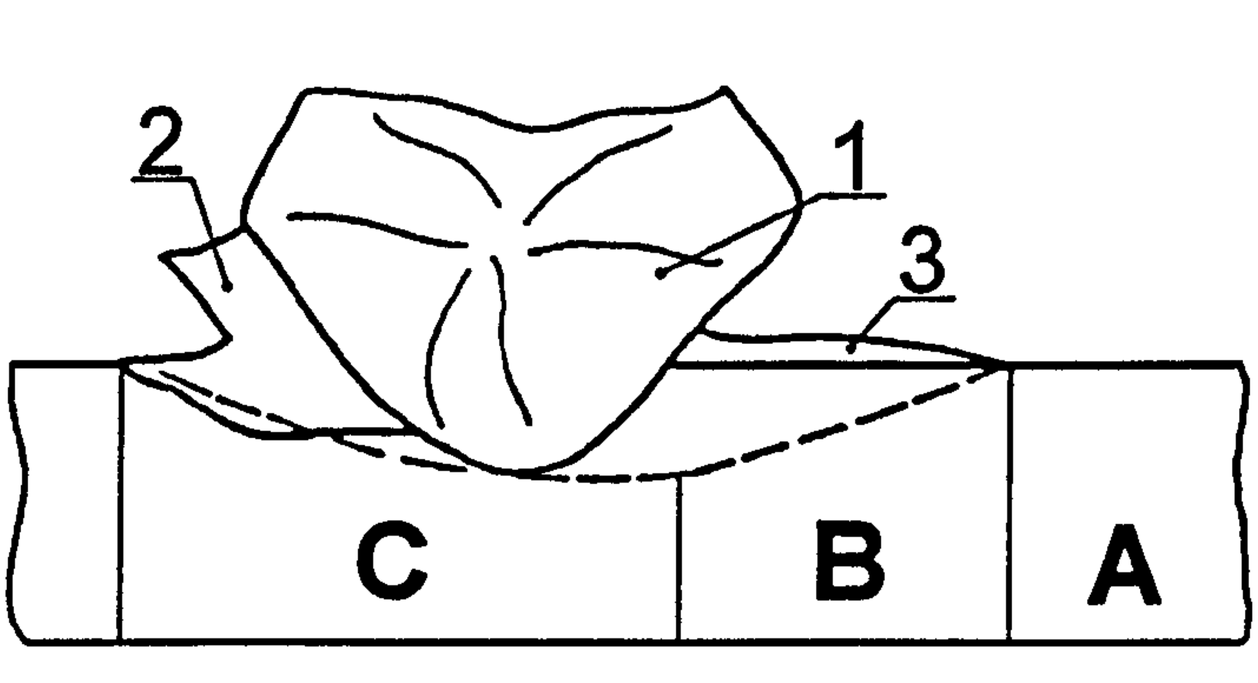

Figure 4-3. Stages of chip formation, where: A – rubbing, B – ploughing, C – cutting; 1 – grain, 2 – chip, 3 – burr (Oczos and Porzycki,1986).

First stage (A), rubbing or sliding phase, consists of elastic deformation and friction between the grain and workpiece material. During stage (B), ploughing, plastic deformation occurs with an internal friction in the workpiece material. The deformed material is moved to the sides. The third stage (C), cutting or chip formation begins with material being cut and removed from the workpiece.

4.2. Contact Length

4.2.1. Geometric Contact Length

The geometric contact length l_g is determined from the analysis of the contact geometry between a grinding wheel and workpiece. In the surface grinding process, the wheel has a diameter d_s and rotates with a wheel speed v_s, whereas the workpiece moves with a speed v_w. A layer of material of a thickness equivalent to the DOC, a is removed. For the purpose of calculation a_e, the real DOC, should be used instead of the applied DOC a.

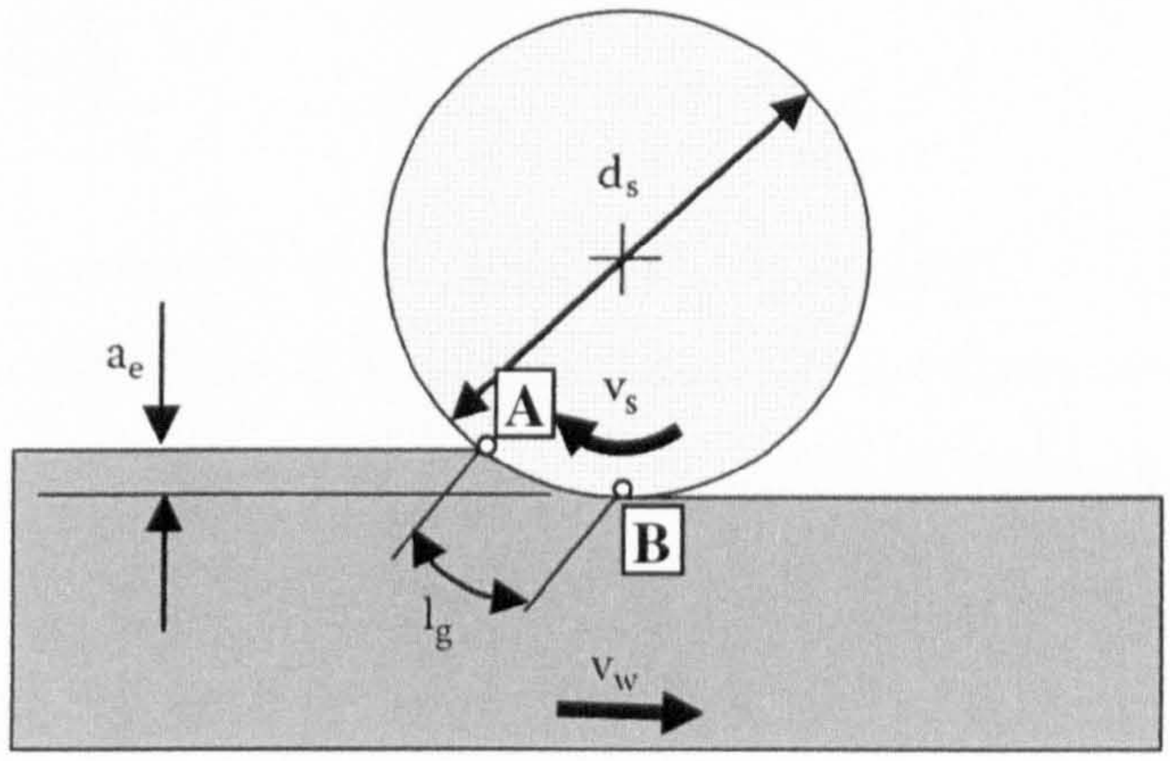

Figure 4-4. Illustration of surface grinding with visible l_g (Marinescu et al, 2007).

The geometric length of contact between the grinding wheel and workpiece is defined from:

$$l_g = \sqrt{a_e \cdot d_s} \tag{4.1}$$

This simplified expression for the geometrical contact length is almost identical to the length of the chord AB (Figure 4-4). The geometric contact length neglects the motion and any deformation or deflections caused by the applied grinding forces (Rowe, 2009).

4.2.2. Kinematic Contact Length

The kinematic contact length, l_k is the length of the arc of the contact between grinding wheel and workpiece, which includes influence of wheel speed and workpiece speed. The feed per cutting edge, t_s depends only on the work speed ratio and the grain spacing L. The feed per cutting edge, t_s, can be derived with:

$$t_s = \frac{v_w}{v_s} L \tag{4.2}$$

The larger the value for t_s, the larger the maximum chip thickness. As the speed ratio decreases, the chip thickness decreases also (Kasprowicz, 2007).

The kinematic contact length is given by:

$$l_k = \left(1 \pm \frac{v_w}{v_s}\right) l_g + \frac{t_s}{2} \qquad (4.3)$$

The cutting path is longer for up-grinding (plus sign) than for down-grinding (minus sign), although the difference is extremely small for most practical workpiece/wheel speed ratios. Also the contribution of $t_s/2$ to the total path length may be negligible. Therefore, it is assumed that $l_k \approx l_g$ (Marinescu *et al*, 2004).

4.2.3. Real Contact Length

The penetration of the grinding wheel into the workpiece results in an apparent area of contact where the cutting action occurs. The length of the grinding contact zone is the length over which a grain enters in contact with the workpiece. Real contact length varies from geometric contact length due to deformations. The contact length is governed by a number of factors including: the thickness of uncut chips, the kinematic roughness of the workpiece, the time of contact of abrasive with the workpiece material, the number of active grains, temperature and the wear of the grains. The heat energy distribution into the workpiece is a function of the real contact length. Errors in contact length computation may result in severe errors in predicted temperature and it is therefore a key parameter in grinding analyses (Rowe *et al*, 1993).

Rowe *et al* (1993) in their work considered the effect of deformations of the contact area in grinding and produced a new approach to understanding contact length. It is based on Hertz theory for the grinding contact, where it is assumed, both, grinding wheel and workpiece surfaces are smooth. An analysis of such deflection is shown in Figure 4-5. The contact curve due to a load has a diameter d_3, and the undeformed diameter of contact curve of the workpiece is d_2 and the undeformed diameter of the wheel body is d_s. Thus, when under load, the contact length l_c is the length of the arc ABC. However, when grinding force is zero the workpiece returns to its undeformed shape.

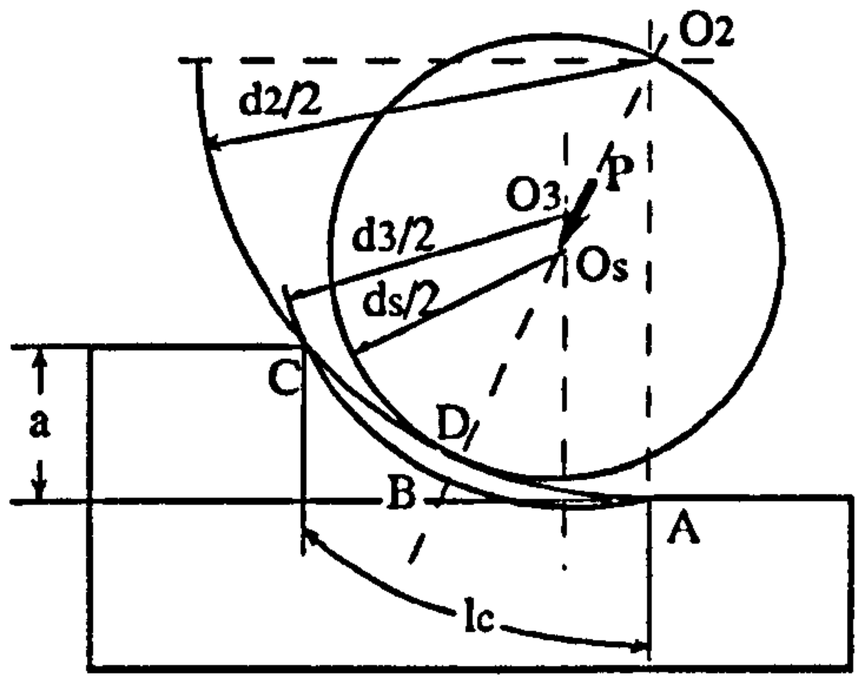

Figure 4-5. Analysis of the elastic deflection that occurs between the wheel and the workpiece (Rowe et al, 1993).

According to Hertz theory, the contact length for cylindrical contact is represented by equations:

$$l_c = 2\sqrt{\frac{2\,p\,d_3}{\pi\,E^*}} = 2\sqrt{2\,p\,d_3\,(K_s + K_w)} \qquad (4.4)$$

where: $\frac{1}{E^*} = \frac{1-v_s^2}{E_s} + \frac{1-v_w^2}{E_w}$; $K_s = \frac{1-v_s^2}{\pi\,E_s}$; $K_w = \frac{1-v_w^2}{\pi\,E_w}$ and $\frac{1}{d_3} = \frac{1}{d_s} \pm \frac{1}{d_2}$

Thus, as $d_3 = l_c^2\,d_s/(l_c^2 - a_e\,d_s)$ contact length between is:

$$l_c = \sqrt{8\,p\,(K_s + K_w)\,d_s + a_e\,d_s} \qquad (4.5)$$

As the average pressure p can be assumed to be equal to the specific grinding force $F_n' = F_n/b$ (where b is width of grinding contact), equation (4.5) can be written as:

$$l_c = \sqrt{8\,F_n'\,(K_s+K_w)\,d_s + a_e\,d_s} \qquad (4.6)$$

And finally:

$$l_c^2 = l_f^2 + l_g^2 \qquad (4.7)$$

Where l_f is the contact length due to deformation as a result of applied force. l_g (geometric length of cut) equation (4.8) is related to the contact length due to the geometry of the DOC.

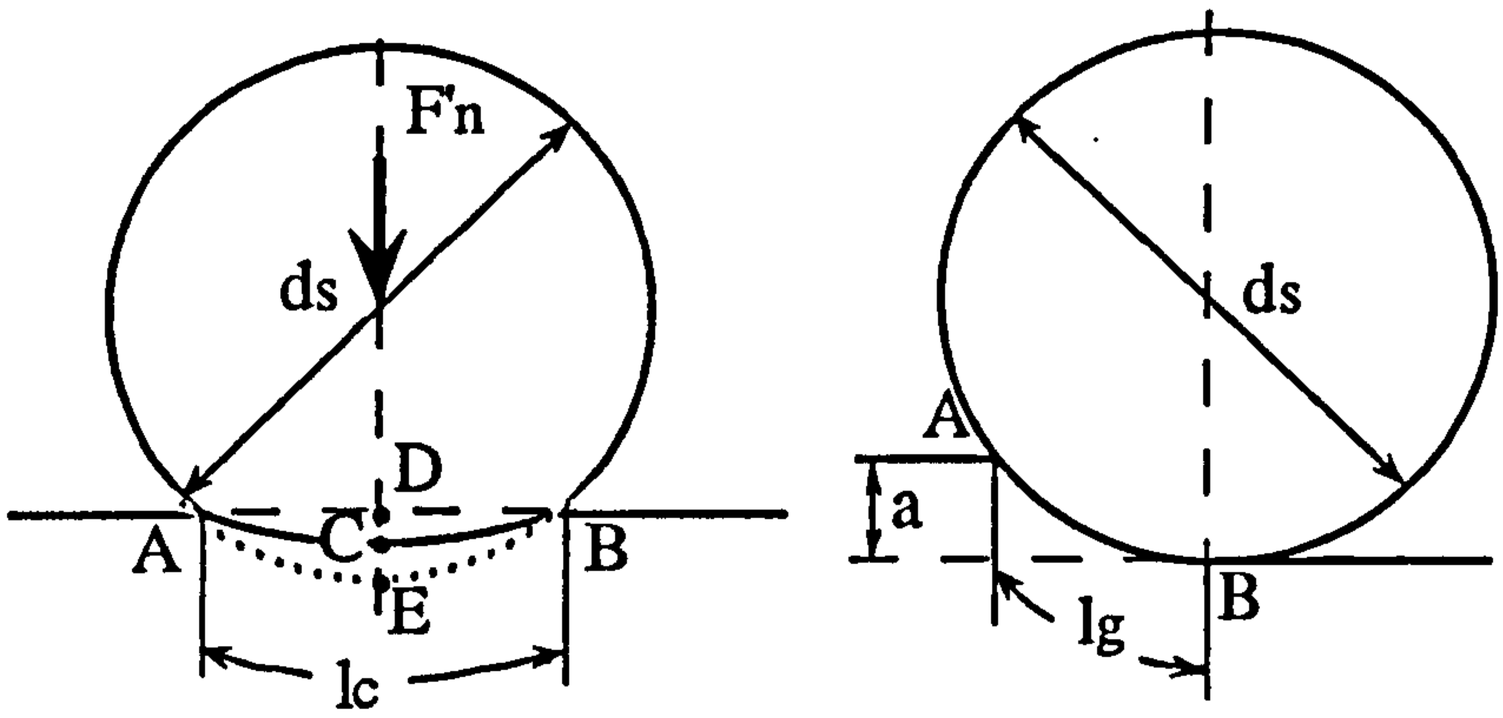

Figure 4-6. Two features of wheel-workpiece body contact (Rowe et al, 1993).

When the DOC is very small, DOC a approaches zero and $l_c = l_f$ - see Figure 4-6 (a). However when the normal force is very small (Figure 4-6 (b)), the contact condition is likely to reduce to:

$$l_c = l_g = \sqrt{a_e\, d_s} \tag{4.8}$$

However, in normal grinding conditions both, wheel body and workpiece are not smooth and have some roughness. Therefore:

$$l_c^2 = l_{fr}^2 + l_g^2 \tag{4.9}$$

And the contact length for rough surfaces is hence:

$$l_c = \sqrt{R_r^2\, l_f^2 + l_g^2} = \sqrt{R_r^2 8\, F_n'\, (K_s{+}K_w)\, d_s + a_e\, d_s} \tag{4.10}$$

Where $R_r = a^*/a_o$ is known as Roughness Factor (a^* - the effective 'contact radius' of a rough surface defined by Greenwood and Tripp (1967) and a_o - the contact radius for smooth surfaces given by Hertz theory).

The increase of the contact length can be observed with high workpiece speed and small DOC. This depends mainly on the workpiece material properties. There is no influence on the contact length due to the grain size, whereas wheel hardness has only minor meaning. Different mathematical models attempt to describe how the non-uniform wheel surface interacts with workpiece using either statistical models or computer simulations. (Malkin, 1989; Oczos and Porzycki, 1986; Rowe *et al*, 1993).

In this study, the measured temperature from actual grinding test was compared with a mathematical model, therefore the knowledge of the most critical factors for the model is required. It is essential to understand how to obtain accurate geometrical contact length, and therefore real contact length. An example of calculations for the temperature model is given in Chapter 8, section 8.2.

4.3. Thermal Models in Grinding

4.3.1. Power and Specific Energy

As grinding proceeds, forces between the grinding wheel and the workpiece are developed. Figure 4-7 illustrates a plane surface grinding action. The resultant force vector exerted by the workpiece against the wheel can be divided into a tangential force component F_t and a normal force component F_n (Kaczmarek, 1971; Shaw, 1996).

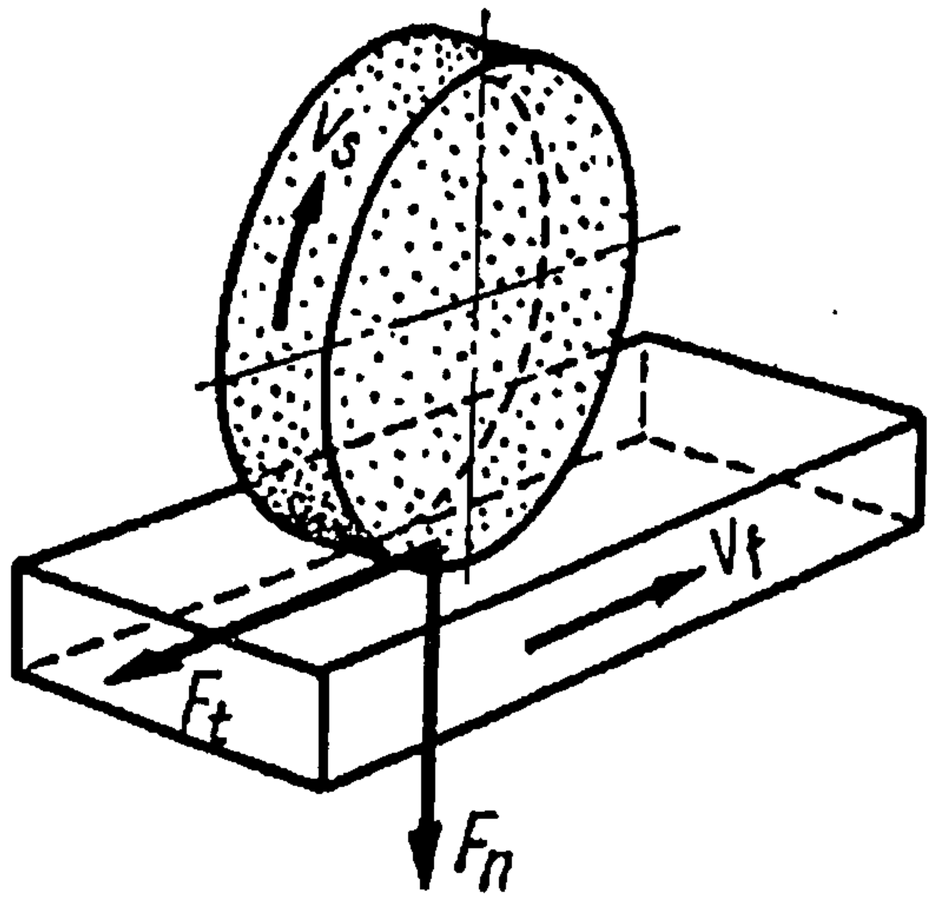

Figure 4-7. Illustration of cutting force components, for surface face grinding (Oczos and Porzycki, 1986).

The grinding power is a direct function of the tangential cutting force and therefore the power is expressed as:

$$P = F_t (v_s \pm v_w) \qquad (4.11)$$

The '+' sign is for up-grinding whereas '-' sign is for down-grinding. However, as v_w is usually much smaller, the workspeed is neglected and the grinding power is simplified to equation (4.12), that is sufficient for most grinding situations (Oczos and Porzycki, 1986):

$$P = F_t \cdot v_s \tag{4.12}$$

A very important factor of the power and machining condition is the specific energy. This is defined as the energy per unit volume of material removal. It is the energy needed to remove (convert to chips) a unit volume of cut material (Kaczmarek, 1971; Callis and Stanton, 1982; Shaw, 1996):

$$e_c = \frac{P}{Q_w} \tag{4.13}$$

The volumetric removal rate parameter is defined by:

$$Q_w = v_w \, a_e \, b \tag{4.14}$$

where a_e is the real DOC and b is grinding width.

The values of the specific energy for grinding of steels typically range from 20 to 60 J/mm^3, however higher values are not uncommon – especially in fine grinding (Rowe, 2009).

In their work Kannapan and Malkin (1972) proposed that the specific energy could be split into three components: chip formation e_{ch}, ploughing e_p, and sliding or rubbing e_s. The three components correspond to the three mechanisms proposed by Hahn (1966).

$$e_c = e_{ch} + e_p + e_s \tag{4.15}$$

A further detailed explanation of these energy components is provided in Malkin (1989).

4.3.2. Equivalent Chip Thickness

The equivalent chip thickness may be defined as the thickness of a continuous layer of material removed at a volumetric rate per unit width. Its graphic presentation is shown in Figure 4-8 (Dmochowski, 1983; Marinescu *et al*, 2004; Malkin, 1989; Oczoś and Porzycki, 1986; Shaw, 1996). Its value may be calculated by:

$$h_{eq} = \frac{Q'_w}{v_s} = \frac{v_w a_e}{v_s} \qquad (4.16)$$

Grinding results are often expressed in terms of equivalent chip thickness as it can readily be related to other grinding parameters. The relationship between h_{eq} and forces, surface quality and wheel life can also be stated. However, it can be seen that two identical values of h_{eq} may be obtained for very different grinding conditions and therefore care is needed in its use and interpretation of results. As a consequence, use of specific energy is now more commonplace.

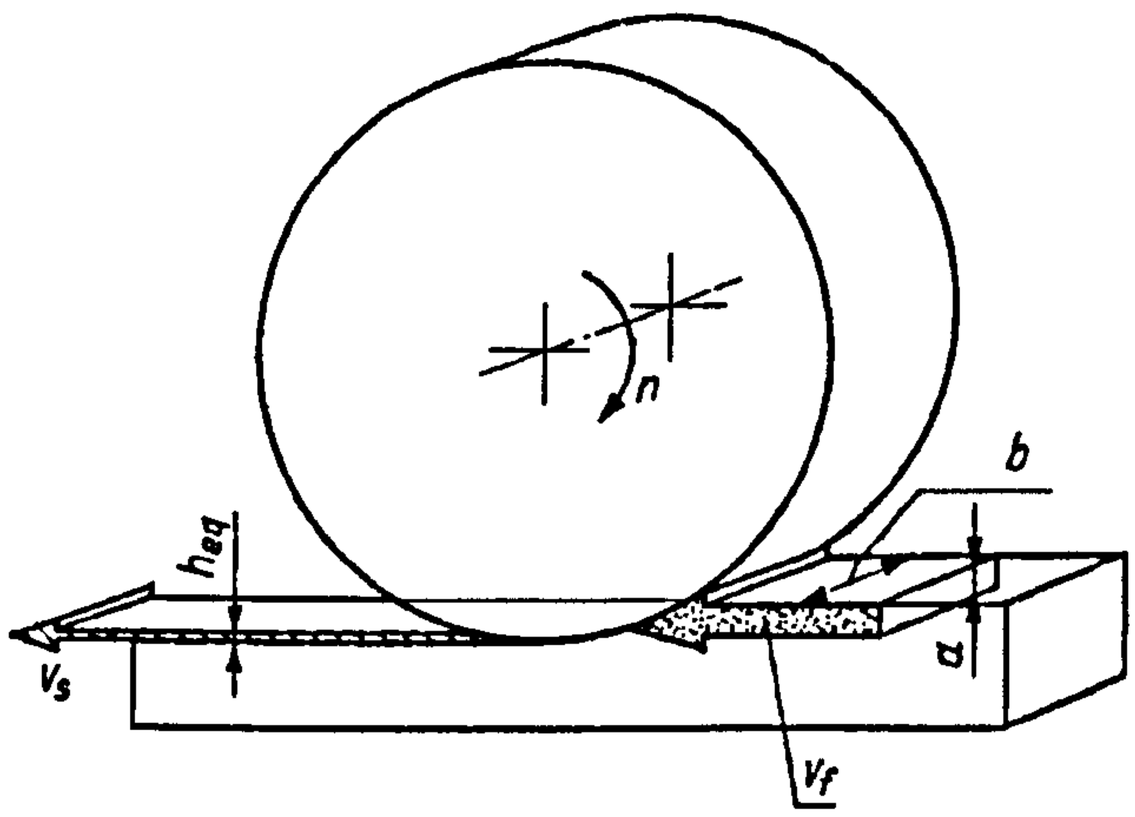

Figure 4-8. Graphical representation of equivalent chip thickness in surface grinding (Oczoś and Porzycki, 1986).

4.4. Heat Transfer in Grinding

The total heat flux generated in the grinding contact zone is partitioned between the workpiece, grinding wheel, grinding fluid and grinding chips:

$$q_t = q_w + q_{ch} + q_f + q_s \qquad (4.17)$$

where q_w is the heat flux which enters the workpiece within the contact zone, q_{ch} is the heat flux which is carried away by the chips, q_f is the heat flux which is carried away by the fluid within the contact zone and q_s is the heat flux which enters the grinding wheel or abrasive tool (Marinescu *et al*, 2004; Oczoś and Porzycki, 1986; Jin and Stephenson, 2006).

It is considered that when the length of cut is short as in shallow grinding (around 1 mm) just 5 per cent of energy input is taken away with the chips or fluid and the remaining heat is distributed between the grinding wheel and the workpiece (Chang and Szeri, 1998; Babic *et al*, 2005; Jin and Stephenson, 2006). Under deep-cut grinding, such as creep-feed conditions, over 90 per cent of the total heat can be taken away by the fluid and therefore the heat partition to the chips is negligible.

However, there are different views on how much of the heat goes into the workpiece, wheel, chips and/or fluid. This is evidenced by results summarised in Table 4-1.

Author	*Heat Flux Distribution percentage*			
	workpiece	*wheel*	*chips*	*coolant*
Rowe and Morgan	**55-90**		**45-10**	
Outwater and Shaw	**35**	**65**		**-**
Malkin	**60-80**	**40-20**		**-**
Sauer	**30-70**	**70-30**		**-**
Shafto and others	**<5**	**rest**		

Table 4-1. Heat flux distribution according to various researchers.

4.4.1. Heat Flux Into the Workpiece

The heat flux conducted into the workpiece is a proportion of the total heat flux, q_t, where this proportion is defined as partition ratio R_w. The actual distribution of q_w can

be identified from the measured grinding temperature. This approach has been proven by Rowe (1995).

The heat flux conducted into the workpiece is:

$$q_w = R_w q_t \tag{4.18}$$

The partition ratio R_w depends on factors such as type of abrasive, the workpiece material, the grinding efficiency, grinding fluid and contact length l_c. Thus in dry shallow-cut conditions the partition ratio may be as high as 90 per cent whereas in well lubricated shallow-cut processes R_w may be less than 5 per cent (Rowe, 1995; Chang and Szeri, 1998).

4.4.2. Heat Flux Into the Chips

The heat flux to the chips can be defined as a function of the density of the workpiece material ρ, the specific heat capacity c, the melting temperature θ_{mp} (there is an assumption the chips reach a temperature close to the melting point), the real depth a_e, the workpiece speed v_w, and the contact length l_c (Marinescu *et al*, 2004):

$$q_{ch} = \rho\, c\, \Theta_{mp} \left(\frac{a_e\, v_w}{l_c}\right) \tag{4.19}$$

This is the relationship assumed in the temperature analysis presented later in the thesis. The thermal properties used for the different materials were obtained from materials data literature (Appendix 11).

4.4.3. Heat Flux Into the Process Fluid

Heat flux to the process fluid depends on whether the contact zone temperature remains below the boiling temperature or whether it is substantially exceeded. Where the fluid boiling is avoided, the heat convected by the fluid is proportional to the average surface temperature T_{av}, the contact area $b \cdot l_c$ and the convection coefficient, h_f (Marinescu *et al*, 2004, Jin and Stephenson, 2006):

$$q_f = h_f \, T_{av} \tag{4.20}$$

The relationship of maximum contact temperature at the workpiece surface to the heat flux into different thermal elements is called the coolant convection coefficient h_f.

In the thermal analysis of the dry and MQL situations fluid convection is assumed to be zero. In the case of wet grinding convection to the fluid is calculated using convection coefficients reported by Morgan *et al* (1998).

4.4.4. Heat Flux Into the Wheel

The heat flux to the wheel q_s can be related to the maximum background temperature at the contact surface θ_{max}, that can be derived from thermal model presented by Rowe (1995) and Jin (2006):

$$q_s = h_s(\theta_{max} - \theta_{amb}) \tag{4.21}$$

Where θ_{amb} is the ambient temperature and h_s is the conduction coefficient for the abrasive grains. This calculation is based on the wheel bulk properties reported by Morgan (1995).

4.5. Temperatures in Grinding

Surface temperatures in grinding play a very important role in the efficiency of the process and in the quality of the output. In general there are two main temperature measurement techniques: non-contact – optical and fibre optic; direct contact – coating techniques and thermocouple techniques (Shaw, 1994).

Optical techniques include the thermo-camera (radiation thermometer) or pyrometer that captures the temperature field distribution on the side of the workpiece or via a hole. In the fibre Bragg technique, distortion in the sensor grating due to the heat causes variation of the wavelength of the reflected light (Batako *et al*, 2005).

One of direct contact measurement method is the PVD coating technique, which is based on covering the workpiece with a thin film layer (~200 nm). Low melting point materials and heat sensitive paints have been used to estimate temperatures in grinding (Walton *et al*, 2006).

Thermocouples may be placed either in the workpiece or within the surface of the grinding wheel, used as either single or double-pole based sensors (Batako *et al,* 2005).

The single-pole thermocouple technique has been proven to be the most reliable method for surface measurement (Rowe *et al*, 1998) and this is the method selected for this study.

The use of FEM analysis is often used as a tool to predict temperatures in grinding however, there is only limited benefit in such simulations as grinding temperatures need to be validated with measured temperatures and the visualizations are necessarily based on parameters derived from analytical models. FEM simulation therefore is only as good as the model adopted (Klocke *et al*, 2002; Shaw, 1996; Skuratow *et al*, 2007). However, such an analysis can provide interesting insights into temperature and stress fields.

4.6. Summary

In this chapter, more detailed grinding mechanics, geometry and kinematics of the abrasive material removal process were presented. An emphasis was put on the real contact length due to its importance to the thermal model.

The thermal model employed for this study was introduced.

Finally temperature measurement methods, such as: optical, contact - thermocouple and FEM analysis in grinding were briefly discussed. The single-pole thermocouple technique was chosen as the most appropriate for this study.

In the following chapter, preliminary experimental studies will be presented.

Chapter 5. PRELIMINARY EXPERIMENTAL STUDIES

5.1. Aims and Objectives

The purpose of this research was to study the effects of MQL in comparison to the wet and dry grinding situations. This would provide understanding of the needs of an MQL delivery system for further research and to acquire essential knowledge for the design and planning of optimal MQL systems.

As part of this work the MQL system described was fully calibrated to ensure that all processes were repeatable.

A further aim of this study was to gain and compare initial results with results from other researchers. The effects of MQL are rather broadly known and understood for sawing, milling and drilling as it is successfully employed in some companies. However, in grinding it is still rather unknown and only a few researchers have established work in this area. Preliminary results from literature indicate that MQL grinding systems do show promise (Silva *et al*, 2005; Silva *et al*, 2007), hence this early work was completed to gain insight as to the reasons for this conclusion.

5.2. Scope

Using a data acquisition system and other available instrumentation, the following parameters were measured: power, real DOC, surface roughness. The preliminary tests delivered results that allowed some initial conclusions to be drawn.

The experimental variables during preliminary tests were:

1) v_s – wheel speed – 21 m/s,
2) v_w – worktable speed – 9 m/min,
3) a – DOC – range of cuts adjusted on the grinding machine 10-30 μm,
4) material type – workpieces were made of: EN9, EN31, M2,
5) wheel type – aluminium oxide 73A 461 I 7V,
6) dressing – with single point diamond,
7) cut type – down-grinding,

8) fluid delivery state – using conventional fluid delivery, dry machining and MQL.

5.3. Experimental Set-up and Equipment

The aim was to prepare and use equipment and collect data in such a way, that very little would require change for undertaking the full tests. Initial tests were undertaken on a manual grinding machine and the setting of the MQL and acquisition systems were designed to be transferable to full tests that were scheduled on a CNC machine.

5.3.1. Grinding Machine

Grinding machine used for initial test, was ELLIOT Model 618 – a toolroom grinding machine – with 1.5 kW spindle power, 3 phase and a maximum wheel speed of 2950 rpm.

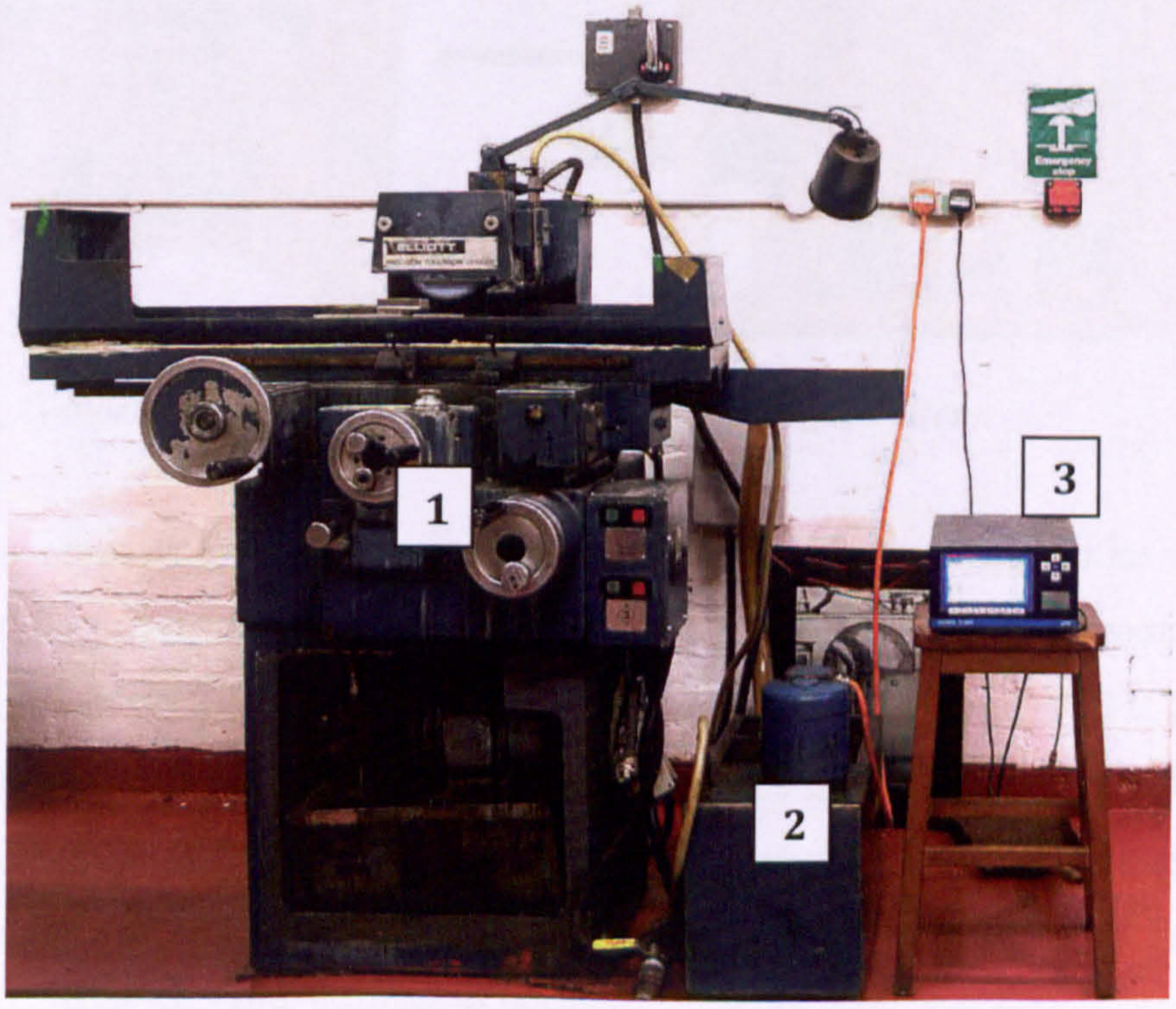

Figure 5-1. Elliot toolroom grinding machine, where: 1 – grinding machine, 2 – fluid supply and filtration system, 3 – power analyser.

The machine allowed for different depths of cut to be applied and three depths of cut were used – 10 μm, 20 μm and 30 μm – for each material and lubrication/cooling method.

5.3.2. MQL System

The MQL system used for the study was originally fabricated by a German company Steidle that specialises in manufacturing lubricating systems for machining. Though the range of lubricating systems from Steidle is very wide, the Lubrimat L50 (Figure 5-2, more information can be found in Appendix 2) model was used, because it adequately suited the test requirement and the purpose of this work programme.

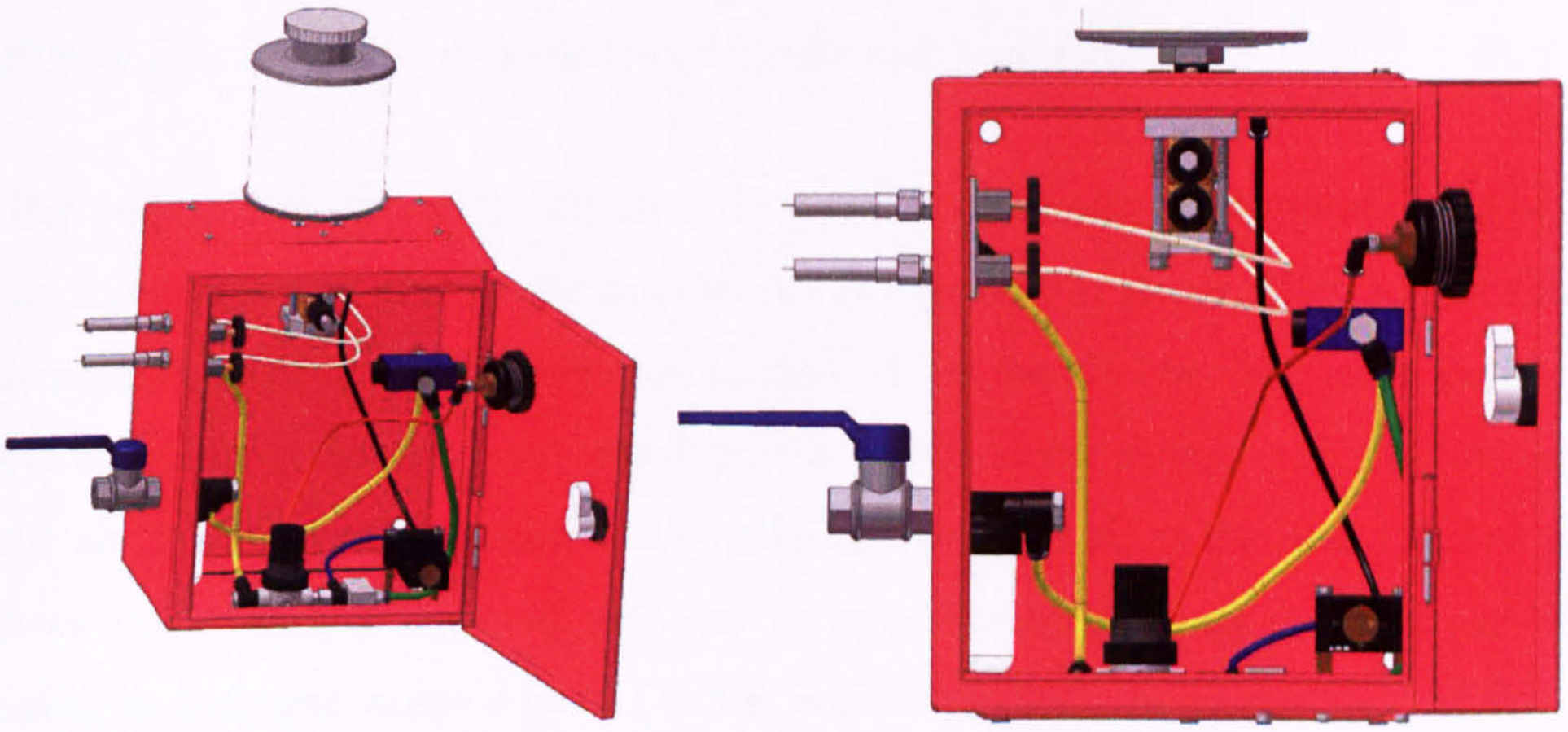

Figure 5-2. General schema of Steidle Lubrimat L50 MQL system.

The system consists of a piston pump that delivers metered quantities of liquid – 0-150 ml/h per nozzle. An impulse generator is used to fine-tune the amount of liquid carried at a given time. The generator operates in the frequency range of 0.1 to 4 Hz. It is also possible to adjust the flowrate of air that carries the oil particles and its pressure. The pressure range is 0.4-0.8 MPa. A relatively large reservoir provides sufficient oil for a constant working of the system for up to 8 hours, when one nozzle is used, however this kind of MQL system is easy to upgrade with a larger reservoir. It also enables work with up to four nozzles.

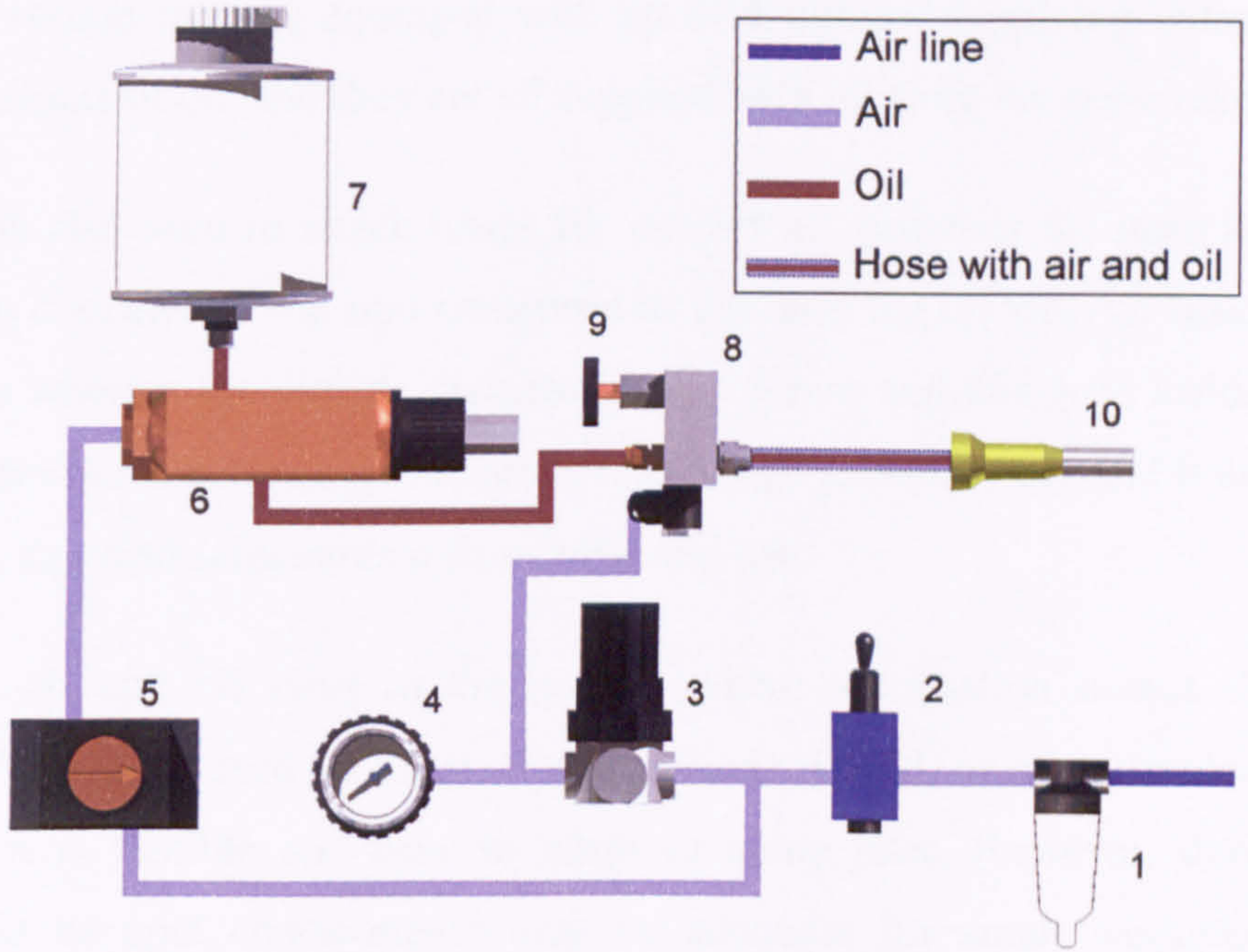

Figure 5-3. Principle of operation of Steidle Lubrimat L50.

The principle of operation (Figure 5-3) is based on mixing oil supplied by a pump and air supplied by air line in the nozzle. Air is supplied to an air filter *1*, that filters any remaining water and contamination carried within the air line. The main switch *2*, cuts off air access to pump ***6*** and impulse generator ***5***. If the switch is in the "on" position, the air flows in two branches. The first branch supplies air to the island ***8***. The pressure from this branch is adjusted with the valve ***3***. Readings of air pressure can be made using an analogue gauge ***4*** placed on the door of the MQL housing.

The island is equipped with two valves ***9***, that can independently change the pressure of the nozzles. However only two nozzles can be adjusted and there is no option for adjusting four different pressures. There are no gauges for those valves, however the system can readily be upgraded with such facilities.

The other branch of air, is supplied to the impulse generator, that may generate an air delay from 0.25 s to 10.00 s. The air coming from the impulse generator goes to the pump and allows it to pump oil from reservoir *7*. The oil gets to the pump by gravitation, and the exact amount of delivery can be adjusted on the pump. The pump has a special feature that allows changing of the piston initial position, and thus the volume of oil pumped. The oil is transported by a plastic hose to the nozzle ***10***.

This MQL system may be equipped with up to 4 pumps, supplying independently 4 different amounts of oil, and they are all supplied with oil from the same reservoir.

The island is also used to attach hoses for air and oil, however the hose for air has a larger inside diameter d_i = 8 mm compared to the hose for oil with an inside diameter d_i = 1.5 mm whereas the outside diameter is d_o = 3 mm and this goes inside the larger hose. Both are flexible, however the air hose is a high pressure hose and is strengthened with wiring, that also safeguards it from wear and tear.

Finally, the air and oil meet in the nozzle, where atomisation occurs. The nozzle geometry (Figure 5-4) used for the tests was a standard MQL nozzle provided with most systems as it is flexible and easy to adapt to many jobs. However, during tests it emerged that its spot characteristic may be adequate for small workpieces, but is insufficient for larger ones, and may cause a lack of oil distributed to the grinding zone. Therefore, a larger nozzle would be required for full tests.

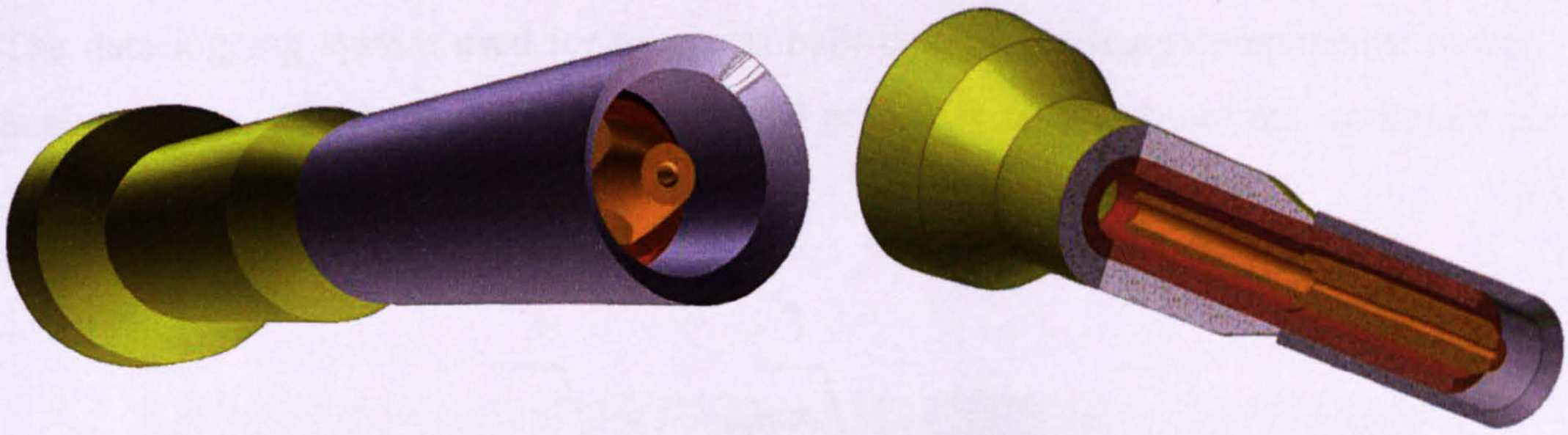

Figure 5-4. Nozzle used for initial investigation – general view and section.

The entire MQL system was supplied with air from a local line and did not require any electrical connection, however more advanced systems are equipped with electric valves and impulse generators that may lead to improved system control and automation of the process.

Preliminary tests were carried out with only one standard nozzle, that was situated on the machine as shown in Figure 5-5.

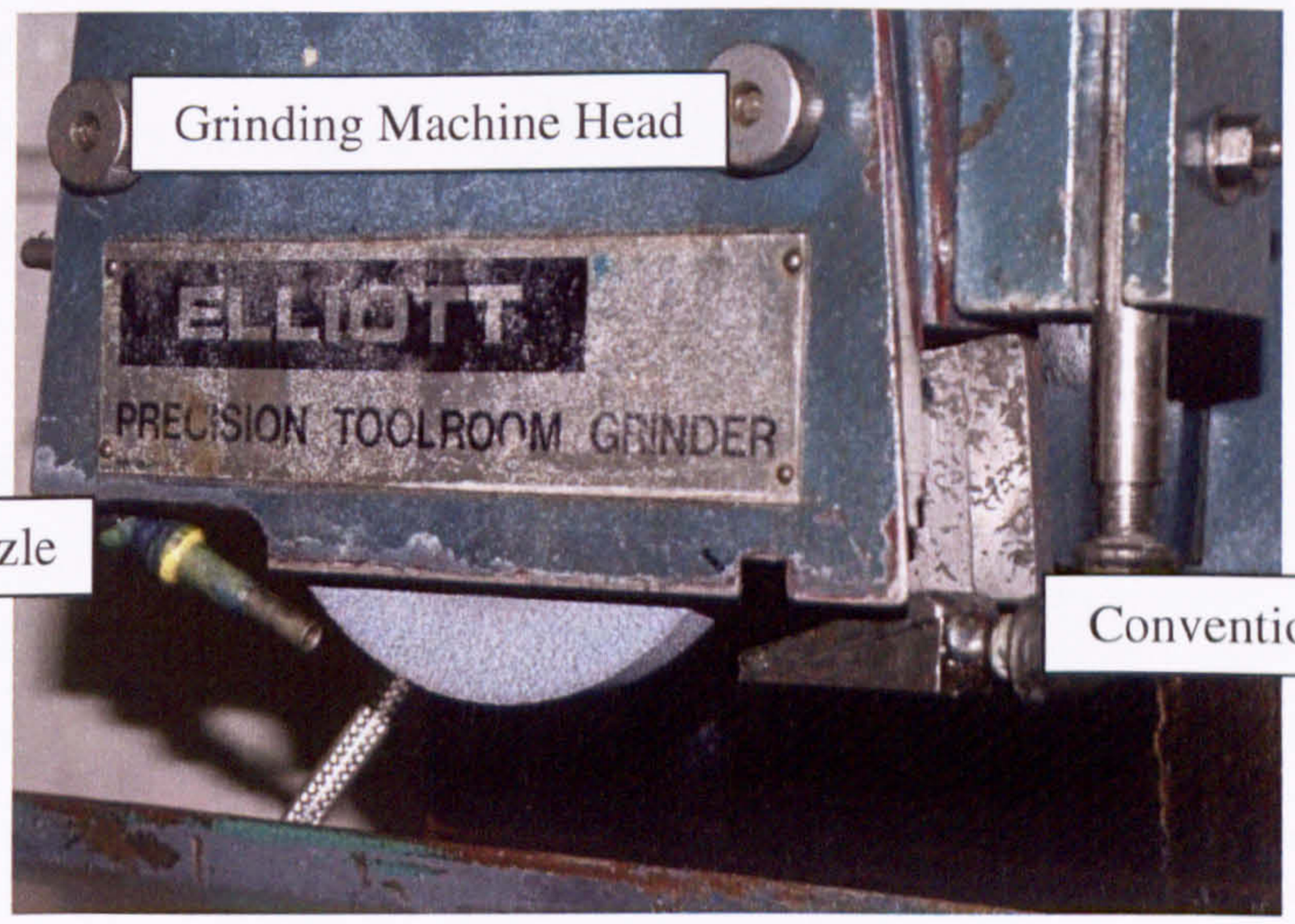

Figure 5-5. Elliot Grinding Machine with MQL and conventional nozzles placed on it.

5.3.3. Data Collection System

The data logging system used for tests was built using three main components: power analyser, data acquisition system and personal computer. Schematic of the workplace is shown in Figure 5-6.

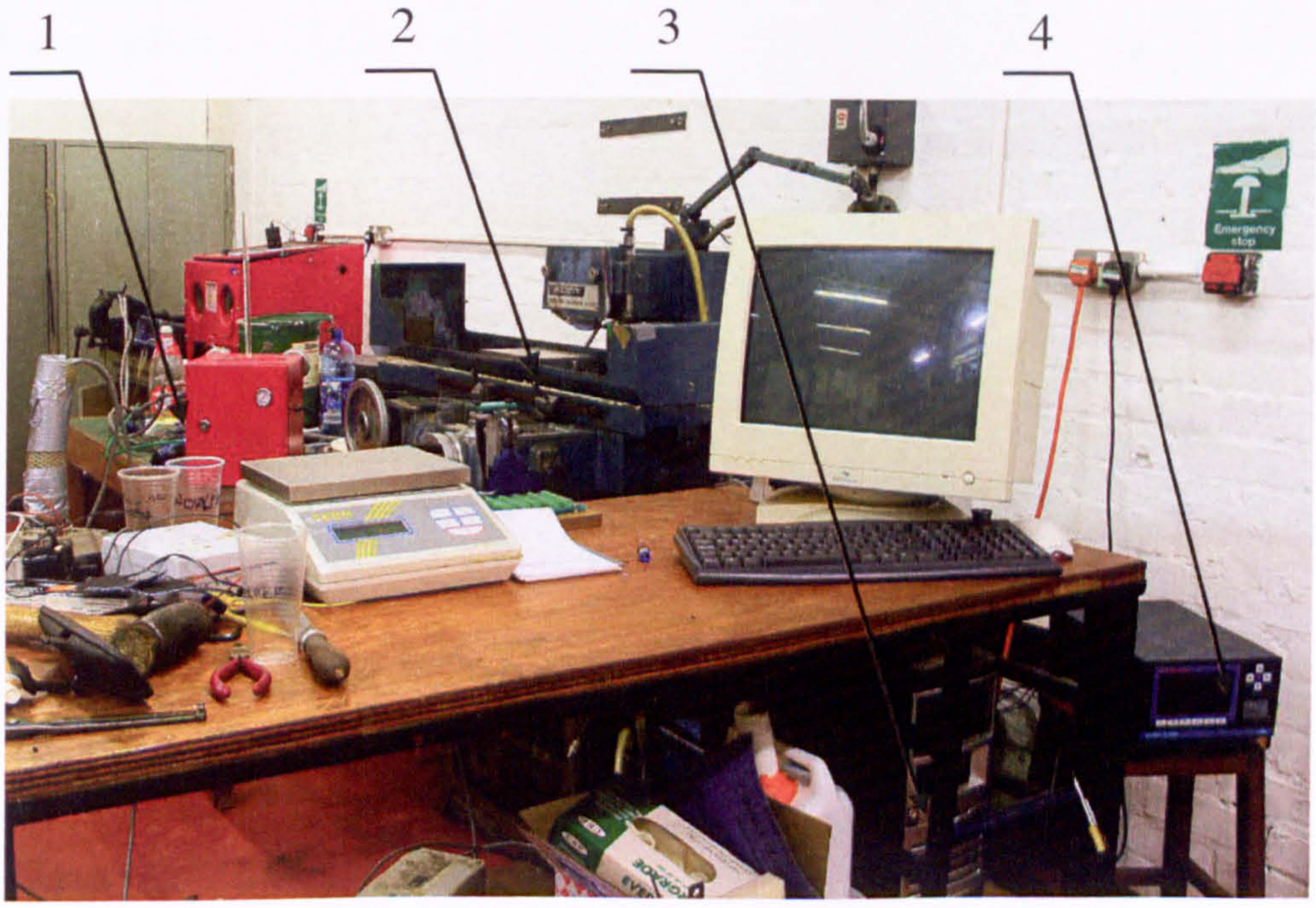

Figure 5-6. Picture of the workplace, where: 1 – MQL system, 2 – grinding machine, 3 – DAQ system, 4 – power analyser.

For the power the data logging system was based on LEM Norma GmbH D 4000 power analyser, with ability to measure and compute current (up to 100 A), voltage (0.3 V – 1000 V), power and energy simultaneously. Frequency measurement is in the range of 0.1 Hz to 300 kHz.

The data acquisition system used for initial tests was a bipolar Pico Logger ADC-42 that is a medium speed, single channel analogue to digital converter. A PC based on Intel P4 3.2GHz CPU and 2GB RAM, was used to collect all data. Communication with the data logger was based on Centronics printer input, with a PC working on Windows XP operating system.

The power analyser connection is shown in Figure 5-6. Power analyser *1* was connected to one of three current phases and analysed power consumed by the grinding machine *3*. The Power analyser was also connected to the data acquisition system *2* via the PicoLog.

5.3.4. Grinding Wheel

The grinding wheel used for initial tests was aluminium oxide, original diameter $\phi = 250$ mm, width = 10 mm, 73A 461 I 7V Universal Solos G wheel. Due to machine limitations, the working range of wheel speed was approximately $v_s = 21$ m/s, however it was capable of speeds around $v_s = 40$ m/s.

5.3.5. Grinding Fluids

No fluid was used in the dry grinding tests. Two different oils were used in the preliminary tests: one for conventional delivery and one for MQL delivery.

In the conventional delivery tests, a common emulsion of 5 per cent by volume of Castrol Hysol XF was used.

For grinding with MQL, pure synthetic oil Castrol Carecut ES1 was used. A full specification of this fluid is given in Appendix 3.

5.3.6. Workpiece Material

The materials used for the tests were – M2, EN9 and EN31. The selection of these materials was motivated by their common use in engineering industry. M2 is a typical high carbon tool steel, EN9 is medium carbon steel and EN31 is a bearing steel. The M2 steel had a hardness of approximately 61±2 HRC, EN9 32±2 HRC and EN31 63±2 HRC respectively. The workpieces were identical in dimensions: 125x16 mm as illustrated in Figure 5-7. One workpiece was used for each test, and each was marked with a unique code to ensure correct identification. Throughout all the initial tests, workpieces were fixed to the grinding table using a magnetic chuck.

To measure the real DOC, the following procedure was performed – the workpiece was ground flat across its whole width with several spark-out passes. The wheel was then moved across the workpiece width, such that a small strip of material was left not ground and that section thereafter could be used as a datum for DOC measurements.

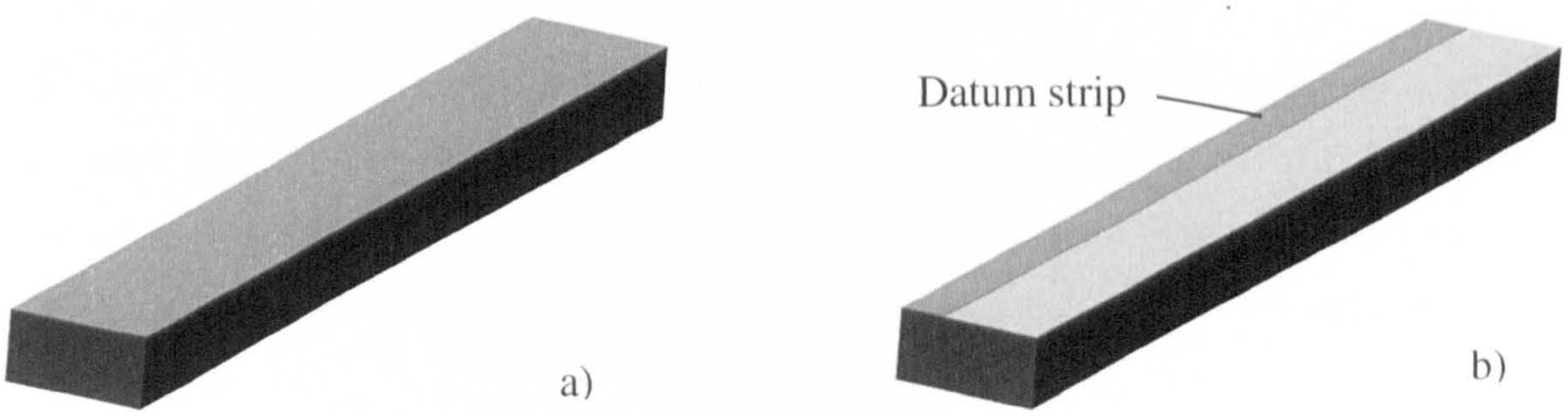

Figure 5-7. a) workpiece before test, b) after test with a datum strip left.

5.4. Experimental Work

Initial tests were undertaken in two stages. The first stage was based on machining, and second on measurements. All components of the experimental set-up were calibrated. The components requiring calibration were: MQL system, power analyser and data acquisition system. Calibration of MQL system consisted of a series of measurements, with different adjustments of the main air valve, pump piston and impulse generator. The results obtained allowed the production of performance charts showing system response characteristics. Three measurements were used to characterise the performance

of the MQL system, i.e. the dependence of MQL system, efficiency on 1) air pressure, 2) frequency, 3) pump piston opening. The use of these charts allows to define the flow rate of MQL system as a function of the frequency and the pump piston position (opening).

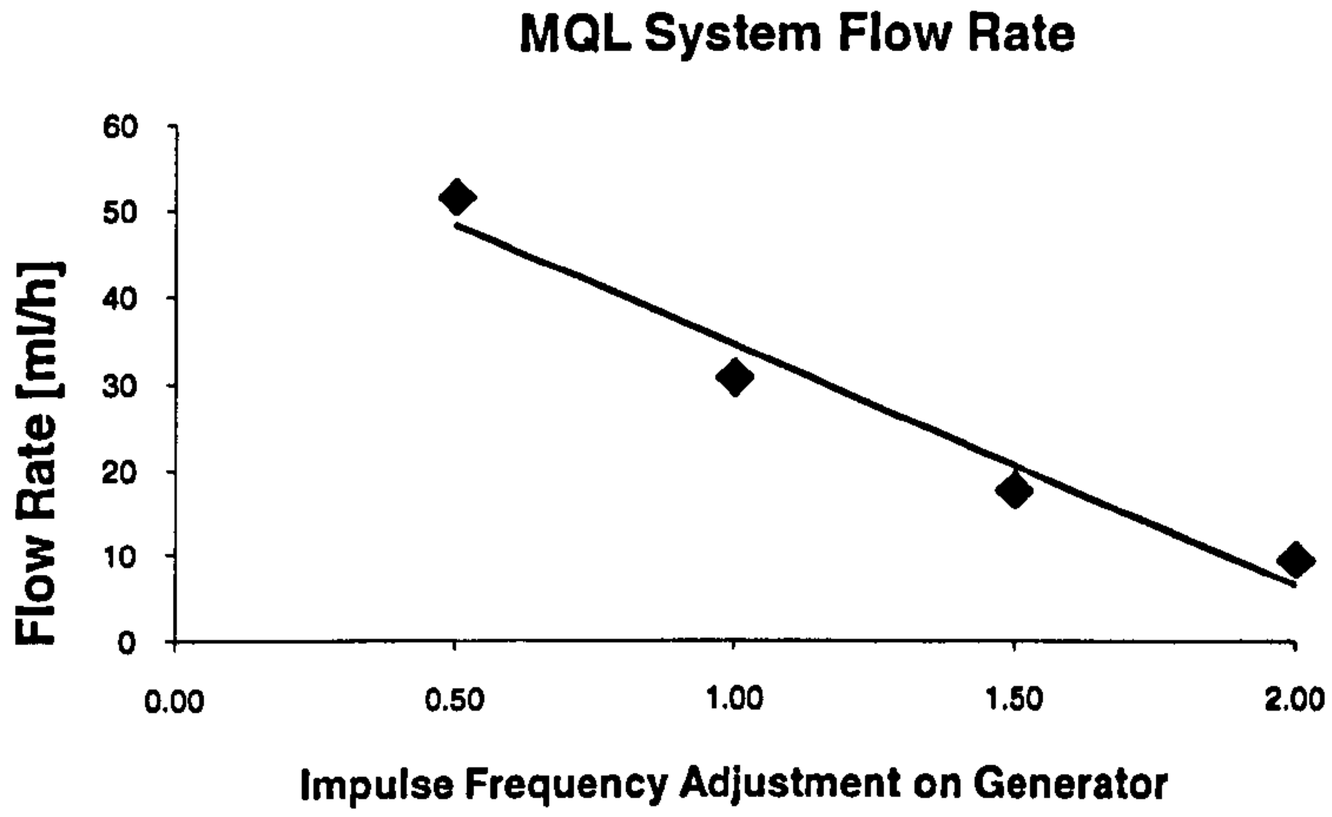

Figure 5-8. Calibration chart – dependence of frequency on MQL System flow rate – for air pressure 0.45MPa, pump piston opening = 20 revolutions.

To measure oil consumption, a transparent plastic pipe with a known inside diameter was used. The level of the oil in the pipe at the beginning and the end of each test was marked and the volume consumed was calculated. The error was estimated to be a maximum of 5 per cent, though typically would be expected to be within approximately 2 per cent.

Calibration of the data acquisition system and the power analyser was based on manufacturer information, and the set-up was performed in accordance with those data.

5.4.1. Experiment Procedure

Initially the grinding wheel was first dressed before use, and the call for redress was triggered by high forces. This was found later (second part of preliminary studies) to be unreliable. Therefore, the wheel was dressed after every three workpiece and then sparked out for 30-45 seconds. It provided reasonably repeatable conditions, as well as a consistently sharp wheel, producing lower tangential forces. Due to the mechanical limitations of the grinding machine, it was difficult to keep repeatable conditions for

feed rate and it was approximately 9 m/min, however this value was affected by the machine operating time and changes during studies. A further limitation was the achievable DOC, which was a maximum of 30 μm for the easier to machine material EN9. Beyond this DOC the power of the machine was not sufficient for the width of workpiece used. It was also found, that grinding with different feed rate was not practicable. This was a result of the machine behaviour. When the machine warmed up, the response to the machine controller became erratic when speeds were changed. To avoid this irregularity a single feed rate, three depths of cut, three fluid delivery methods and down grinding were adopted.

A single pass down-grind procedure was employed with the dry grinding first, MQL grinding second and wet grinding thirdly.

When all grinding was completed workpieces were taken for measurements of surface roughness (R_a) and real DOC.

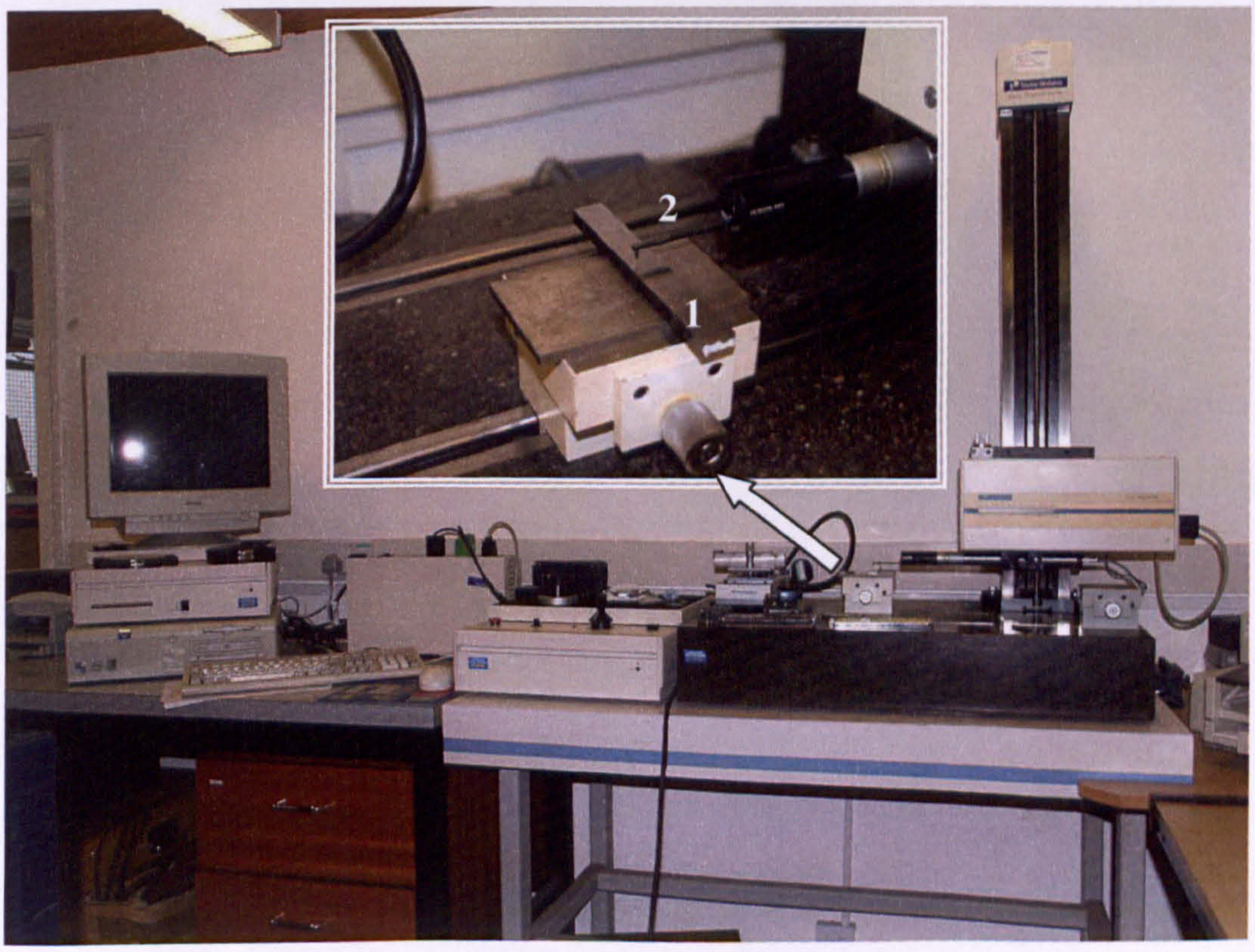

Figure 5-9. General view of workplace where measurements of surface roughness parameters R_a and R_z with Taylor Hobson were taken (1 – workpiece, 2 – stylus).

Measurements of roughness were taken on a Rank Taylor Hobson surface profilometer Form Talysurf Series 120 (Figure 5-9). The parameter measured was R_a in three places. Prior to measurement workpieces were de-magnetised, washed with solvent and the instruments warmed up for 1 hour.

Measurements for real DOC were taken on a Mitutoyo high precision digital height gauge (Figure 5-10). Workpieces were laid down flat on a high precision metrology support and then measured. Measurements were taken in three places on the ground area and on the reference datum strip of the workpiece. For consistency, the measurements were taken at the same location for all workpieces.

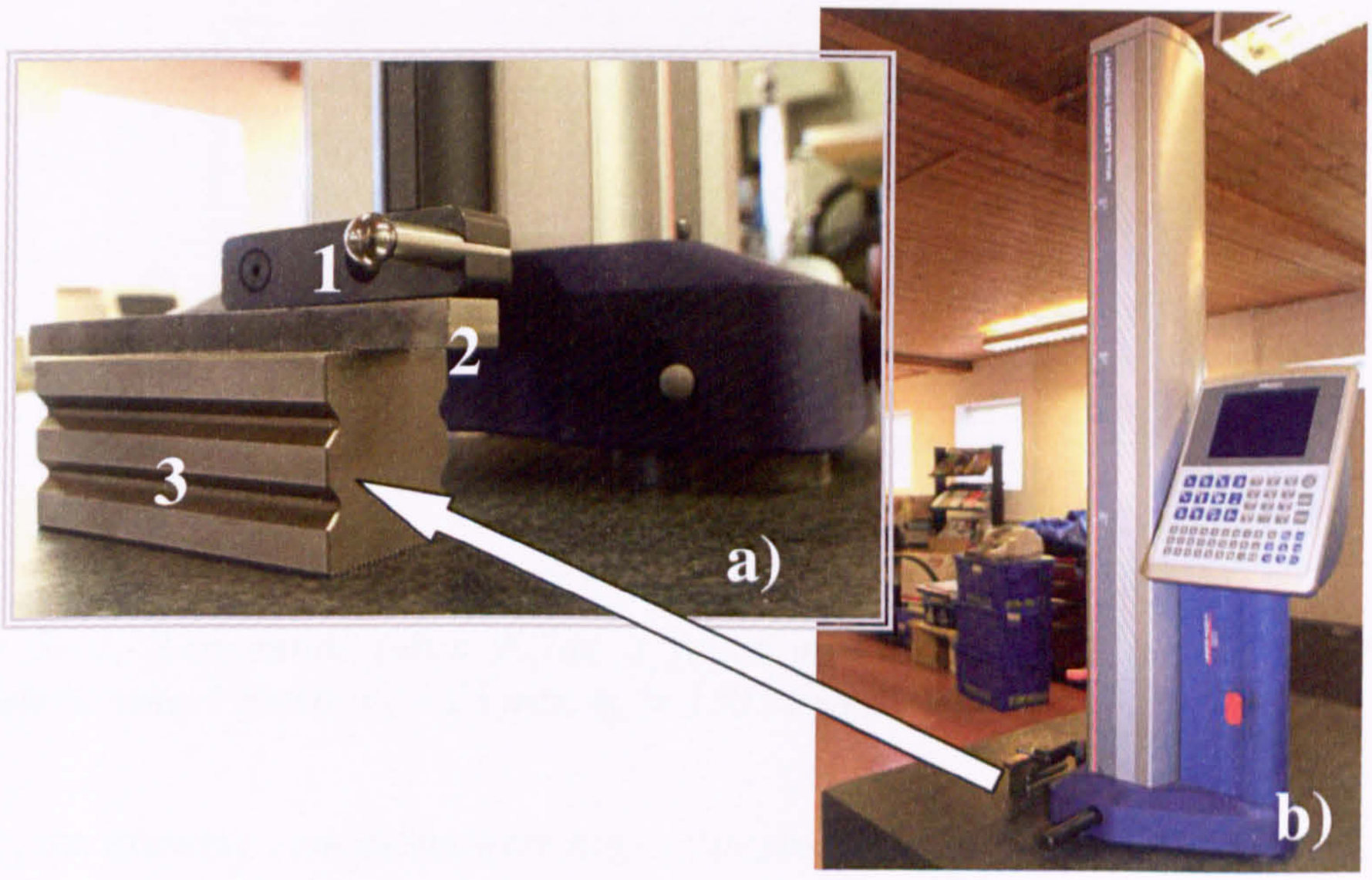

Figure 5-10.DOC measurements, where: a) base with the workpiece and b) Height gauge (1 – measuring head, 2 – workpiece 3 – support).

5.5. Results

The results are presented in two types of charts: (1) tangential force F_t is shown as a function of real DOC a_e and (2) surface roughness R_a is shown as a function of DOC a.

Visual inspection of ground workpieces showed no burn marks or any other visible thermal damage. The results in Figure 5-11 – Figure 5-13 are shown for grinding with

minimum quantity lubrication (MQL), dry machining (DRY) and conventional flood cooling (WET). Results are shown separately for each material.

5.5.1. Tangential Force Results: EN31

For a given DOC, forces in MQL were very similar to those measured for the case of dry grinding and only little benefit can be identified. It is difficult without further tests, to establish the reasons for this, however, the wheel used was a general purpose wheel and was not entirely appropriate for the difficult-to-machine EN31.

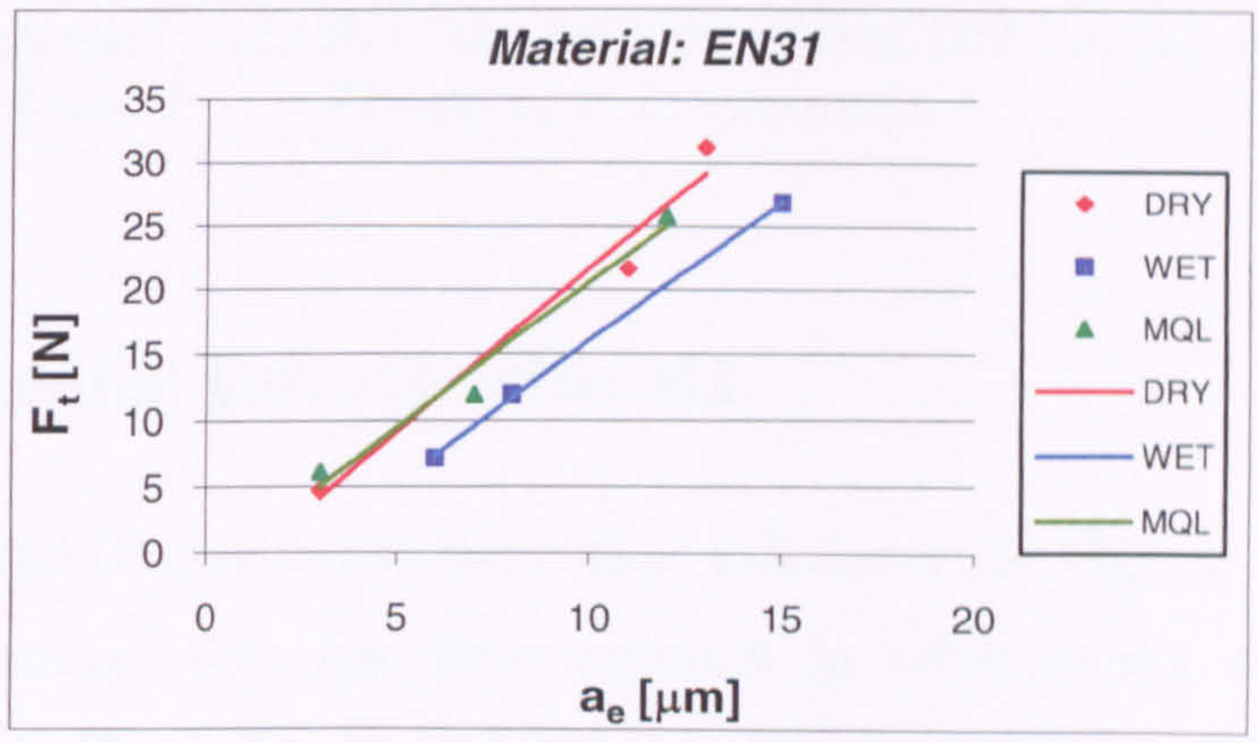

Figure 5-11. Tangential force F_t as a function of real DOC a_e for EN31, with parameters: wheel speed: v_s = 21 m/s, v_w = 150 mm/min.

Further, the dressing conditions were not optimized for each case. The improved cutting efficiency reportedly offered by MQL would be difficult to discern under such circumstances.

5.5.2. Tangential Force Results: EN9

For EN9 (Figure 5-12) very little difference is observed in the cutting efficiency under dry or wet grinding conditions. MQL is shown to be the least efficient of the three, though the difference is hardly significant. This set of results could be treated as erroneous. This is likely to have been a product of the problems encountered in trying to establish a workpiece datum in the wet condition wherein heating and cooling altered the height of the workpiece surface relative to the wheel and also due to effects resulting

from wheel wear as no dressing operation was undertaken for this test. It is worthwhile mentioning that the ratio of achieved DOC to applied DOC was different in each case.

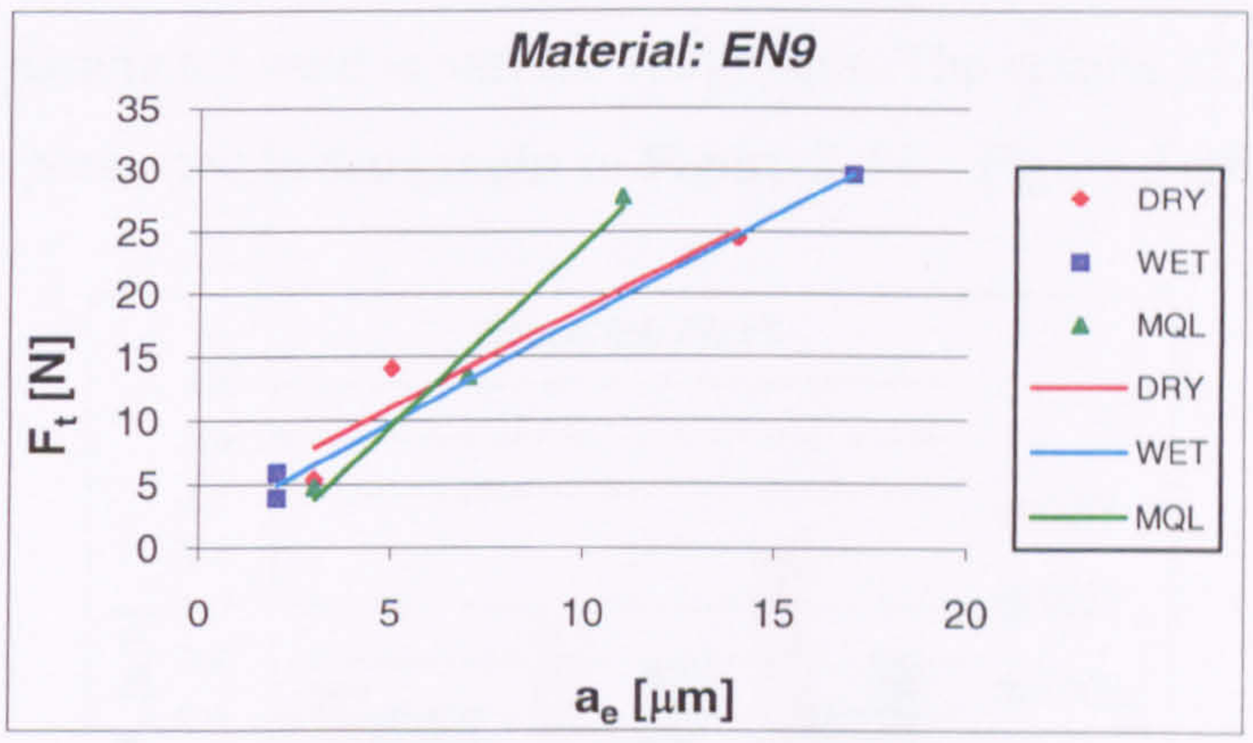

Figure 5-12. Tangential force F_t in the function of real DOC a_e for material EN9, with parameters: wheel speed: v_s = 21 m/s, v_w = 150 mm/min.

5.5.3. Tangential Force Results: M2

For the M2 material (Figure 5-13), the cutting efficiency for MQL is better than in the case of wet grinding. This has been reported in other works and a speculative explanation is the effect of reduced hydrodynamic forces. However further tests are required, as this provides some promise for the further work.

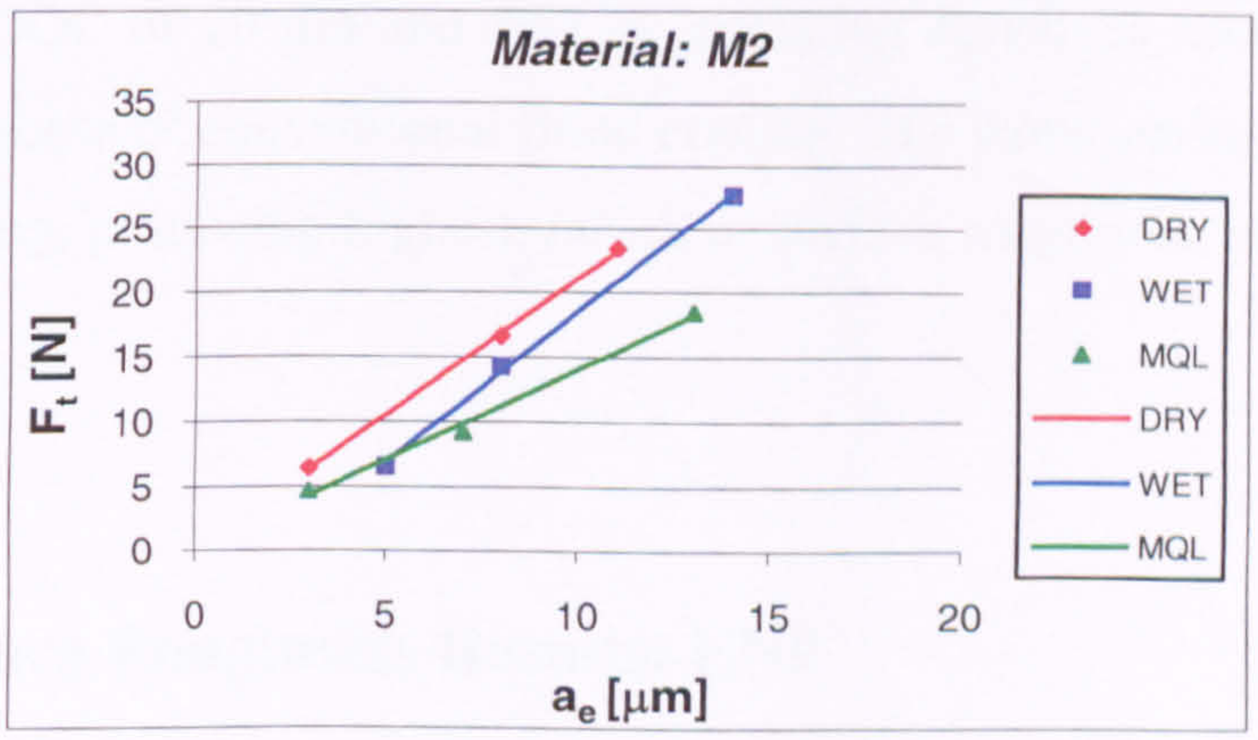

Figure 5-13. Tangential force F_t as a function of real DOC a_e for material M2, with parameters: wheel speed: v_s = 21 m/s, v_w = 150 mm/min.

5.5.4. Surface Roughness Results: EN31

A further performance indicator often used in industry is the workpiece surface quality, and the principal parameter used is surface roughness. The results of surface roughness measurements are presented in the graphs in Figure 5-14 – Figure 5-16.

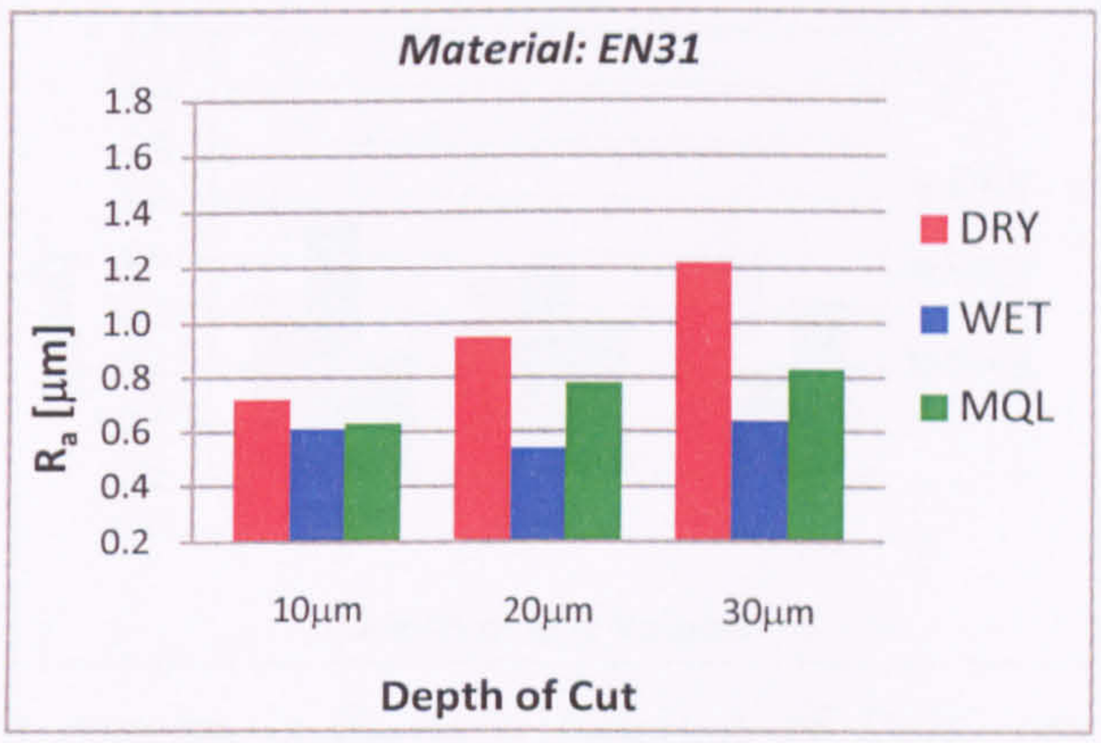

Figure 5-14. Surface roughness R_a as a function of DOC for material EN31, with parameters: aluminium oxide wheel, v_s = 21 m/s, v_w = 150 mm/min.

For material EN31 (Figure 5-14) the lowest surface roughness was measured for the range of DOC was approximately R_a = 0.6 µm. The surface roughness obtained from MQL was higher than the WET case, however for values of DOC a=10 µm the surface roughness was very similar to WET (difference of 1 per cent). However, MQL did not perform well at DOC of 20 µm and 30 µm producing R_a values about 25-30 per cent higher than in the case of conventional flood cooling. The worst performance was found with dry machining, producing highest values of surface roughness, reaching values of R_a = 1.2 µm.

5.5.5. Surface Roughness Results: EN9

For material EN9 (Figure 5-15) the situation looks a little different. The best results in terms of surface roughness are achieved by MQL for depths of cut 10µm and 20 µm. DRY machining produced similar forces, but worse surface roughness R_a = 0.9 and 1.0 µm. For some reasons WET machining performed badly and achieved R_a = 1.1µm - 1.0 µm. However the situation stabilised for a DOC a = 30 µm and the surface

roughness was similar to that achieved with EN31 material, where WET machining provided lowest surface roughness. The roughness achieved by MQL was similar and was around R_a = 0.8 μm similar to that from EN31 material. DRY machining produced higher surface roughness.

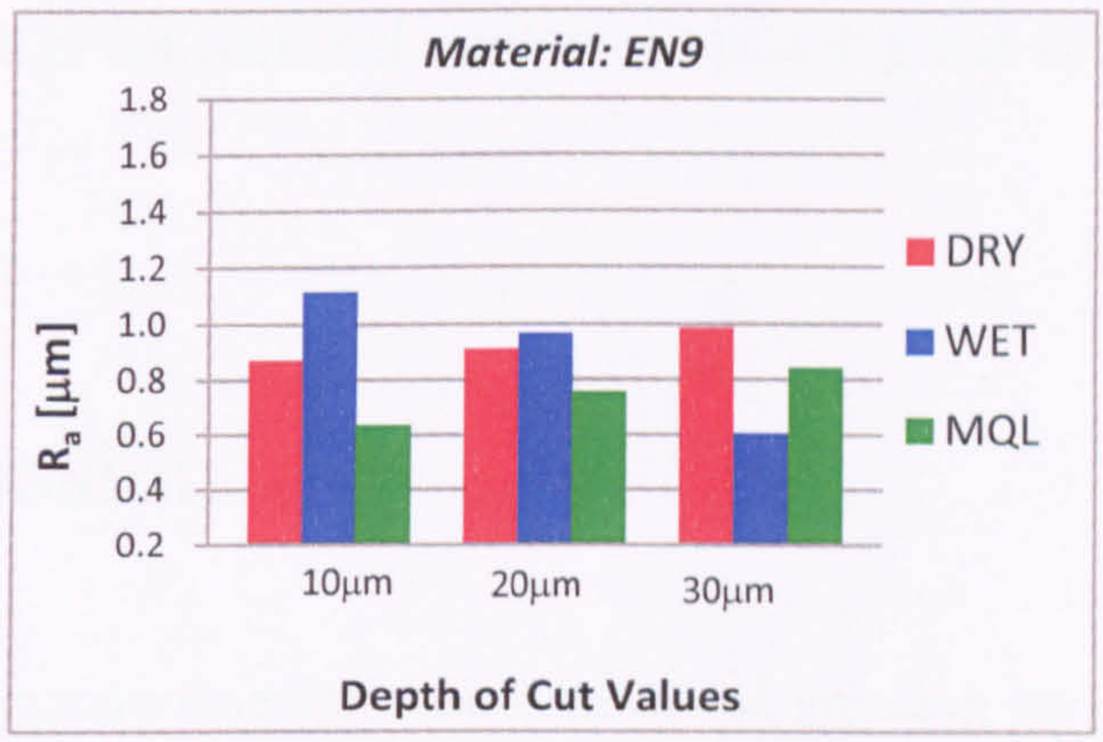

Figure 5-15. Surface roughness R_a as a function of DOC for material EN9, with parameters: aluminium oxide wheel, v_s = 21 m/s, v_w = 150 mm/min.

5.5.6. Surface Roughness Results: M2

For material M2 (Figure 5-16) the lowest surface roughness is again achieved in WET machining. WET machining generated surface roughness below R_a = 0.6 μm and reached R_a = 0.4 μm for DOC a = 30 μm. When WET is compared with MQL it is found, that MQL kept surface roughness below R_a = 0.8 μm. DRY machining produced the highest surface roughness reaching a value of R_a = 1.8 μm for DOC a = 30 μm.

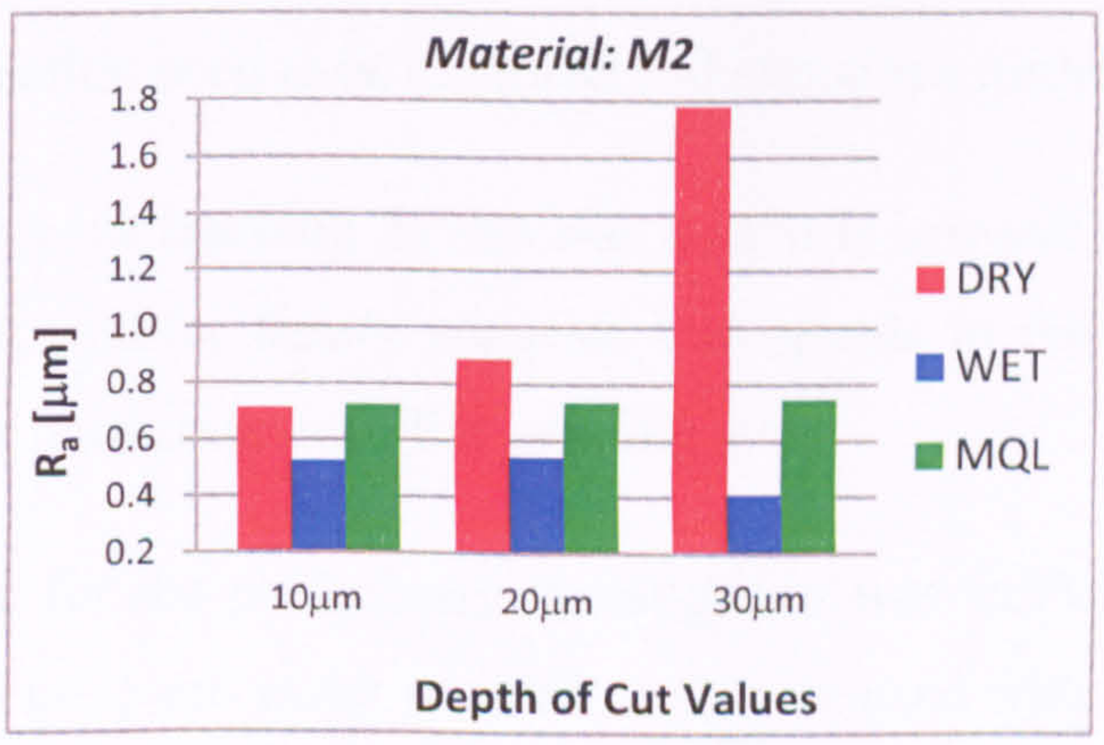

Figure 5-16. Surface roughness R_a as a function of DOC for material M2, with parameters: aluminium oxide wheel, v_s = 21 m/s, v_w = 150 mm/min.

It can be concluded that MQL performed very well compared with dry machining, and reasonably well compared with conventional flood cooling. For the whole test, MQL maintained the value of surface roughness at approximately R_a = 0.6-0.8 μm whereas the value for WET machining was generally in the rage R_a = 0.4-0.6 μm.

The promise of MQL in conventional shallow cut grinding was firmly established from this initial study.

5.6. Discussion

The aim of this preliminary research was to study the grinding performance of the three grinding methods MQL, dry and wet machining and to acquire and evaluate the understanding needed to apply MQL correctly in grinding. A further important aim was to establish system requirements for the planned full tests. Both aims were achieved.

Results achieved are of a good value and showed that MQL is efficient in lubricating the contact region and frictional forces can be maintained at a level that avoids thermal damage. Consequently, MQL shows its ability to compete successfully with wet grinding in a specified regime. MQL generally produces lower tangential forces and a better surface quality than that obtained in dry grinding.

Due to limited tests in this preliminary works it was not possible to investigate how MQL would perform under depths of cut higher than those employed. The effect of convection and lubrication need to be explored and explained further.

The range of wheel speeds reaching 21 m/s was relatively low and higher speeds should be investigated. Heat transfer theory suggests that speeds in the range of 40-60 m/s should produce lower temperatures in the grinding arc.

The spot nozzle used for the preliminary investigation was sufficient only for narrow workpieces (up to 10 mm) and wider nozzles need to be used with wider workpieces. It was planned to use the wider workpieces as higher forces and temperatures will be generated, resulting in tougher conditions for the full MQL studies.

5.7. Summary

In this chapter preliminary experimental studies were presented. The aims, objectives and scope were presented followed by discussion on experimental set up and equipment. A description of every piece of equipment employed for this part of the research is provided. Experimental procedure is explained and discussed.

Presentation of results and discussion of tangential forces and surface roughness for EN31, M2 and EN9 materials is given. Reasonably good results for MQL performance in terms of forces and surface roughness were noted, confirming possible regimes for MQL. The promise of MQL in conventional shallow cut grinding was firmly established from this initial study.

In the following chapter the experimental work and procedures will be presented.

Chapter 6. EXPERIMENTAL WORK

6.1. Aims and Objectives

The aim of this work was to fully evaluate MQL under a range of operating conditions identified in the preliminary study. The necessarily large matrix of tests was minimised employing the fractional factorial approach (Taguchi). This approach provides a qualitative indication of the effective strength of a parameter on the performance and identifies key interactions.

6.2. Scope

Using the data acquisition system and other available measuring tools, a measurement of the following parameters was undertaken: forces – normal and tangential, instantaneous power usage, temperature and surface roughness. The real DOC was obtained with a separate procedure, using workpieces ground under the same experimental conditions.

The following is the list of process variables employed in the experiments with their ranges:

1) v_s – wheel speed – 25 and 45 m/s,
2) v_w – worktable speed – 6.5 and 15 m/min,
3) a – applied DOC – 5 and 15 μm,
4) material type – workpieces were made of three various materials: EN8 (mild steel), EN31 and M2, both hardened,
5) wheel type – aluminium oxide WA 100 JV universal grinding wheel,
6) dressing – with multi-cluster diamond,
7) cut type – down grinding,
8) fluid delivery – conventional fluid delivery, dry machining and MQL.

6.3. Equipment

6.3.1. Grinding Machine

The grinding machine used for the experiment, was a full CNC surface grinding machine Dominator 624 Easy (Figure 6-1) manufactured by Jones and Shipman Renold Precision. This grinding machine is equipped with 3-phase motor of 11 kW and is capable of wheel speed up to 80 m/s, wheel carrier speed (X-axis) of 0-24 m/min (36 m/min in override feed rate) and 0-10 m/min (15 m/min in override feed rate) for creep feed grinding, whereas elevation speed (Y-axis) was 6 m/min and crossfeed (Z-axis) was 6 m/min. This specification makes this machine well equipped for creep and conventional grinding, with both conventional flood and near dry cooling machining. The general view of the Dominator with mounted equipment can be seen in Figure 6-1. More accurate view of arrangements is shown in Figure 6-2.

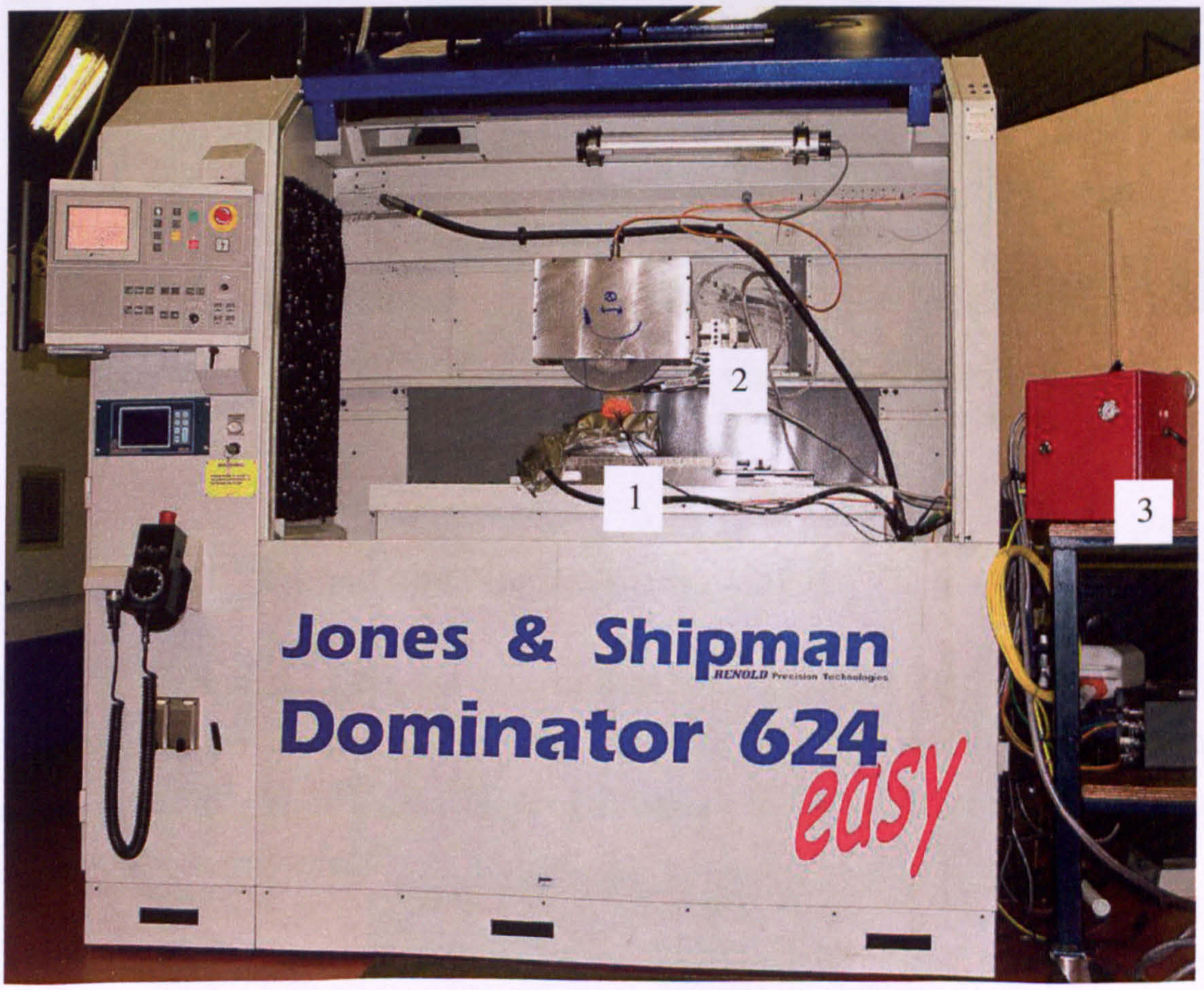

Figure 6-1. CNC Jones&Shipman Dominator 624 Easy with open front hosing: 1 – dynamometer, 2 – nozzle, 3 – MQL system.

The tests were performed using two programs: program one – slot cycle grinding when flat and sparked out surface was obtained and program two – creep feed grinding, when single pass grinding with data collection was performed. The nozzle arrangement is shown Figure 6-2.

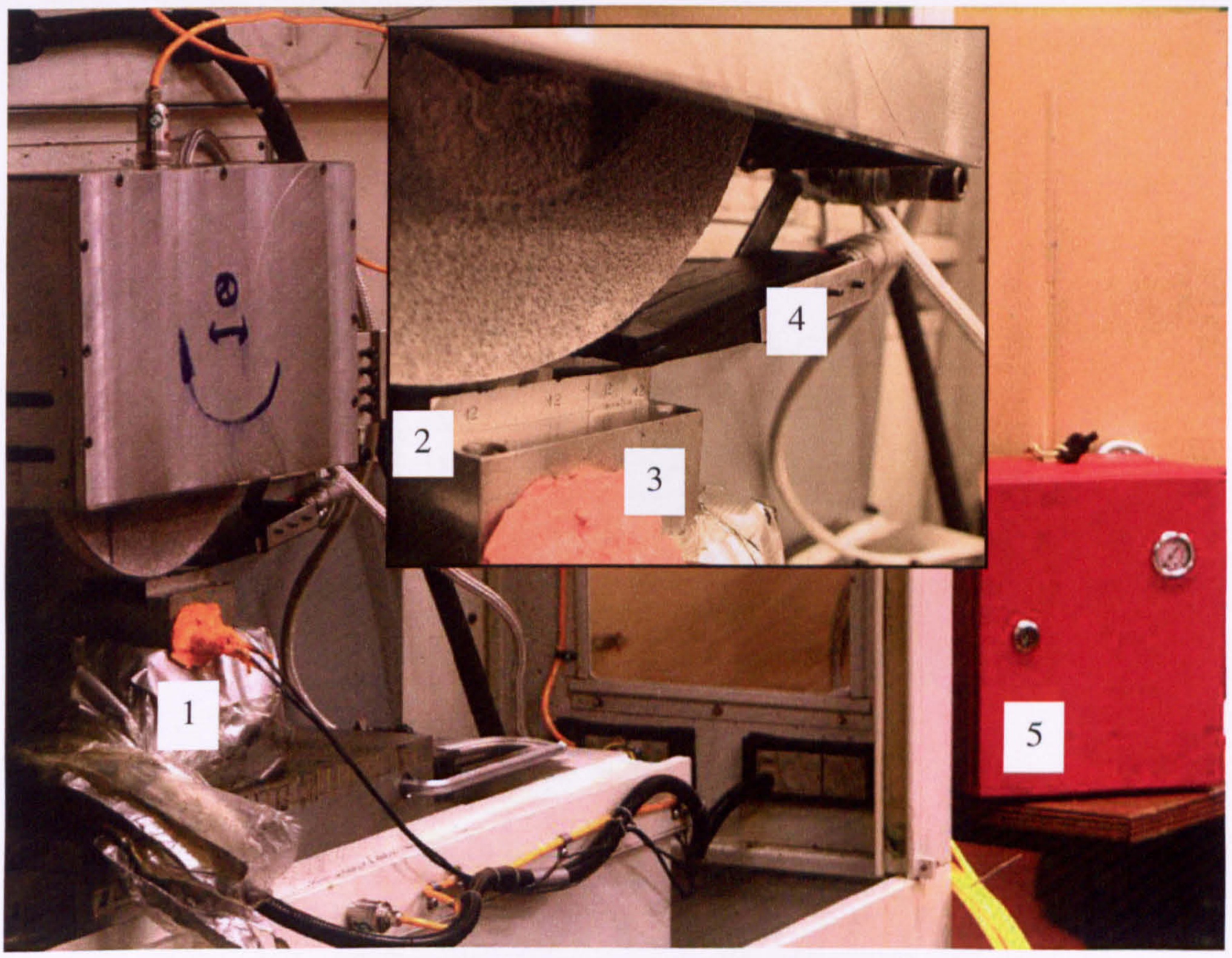

Figure 6-2. Nozzle and MQL system arrangement, where: 1 – dynamometer in plastic cover, 2 – workpiece, 3 – workpiece base, 4 – MQL nozzle, 5 – MQL system.

6.3.2. MQL System and Nozzle Arrangements

The MQL system used for the investigation was the same as that used for the preliminary studies (Chapter 5). The only differences were diameters of pipes supplying air to the main toggle and a specially designed nozzle that matched the wheel width and range of the wheel speeds.

As the nozzle was of a different design (Appendix 4) to those original nozzles delivered by the manufacturer it was necessary to establish nozzle flow rate. A series of tests were completed (Figure 6-3) to characterise velocity distributions at varying distance from

the nozzle outlet and air pressure supplied to the nozzle. Measurements of pressure were taken at 0.40, 0.45 MPa with air valves fully open. The pitot tube was placed at 4 points of the outlet at 5, 10, 15 and 20 mm. Distances from the nozzle outlet were in 10 mm increments from 0 to 90mm. It was established that the nozzle worked well and the pressures were the same at all points.

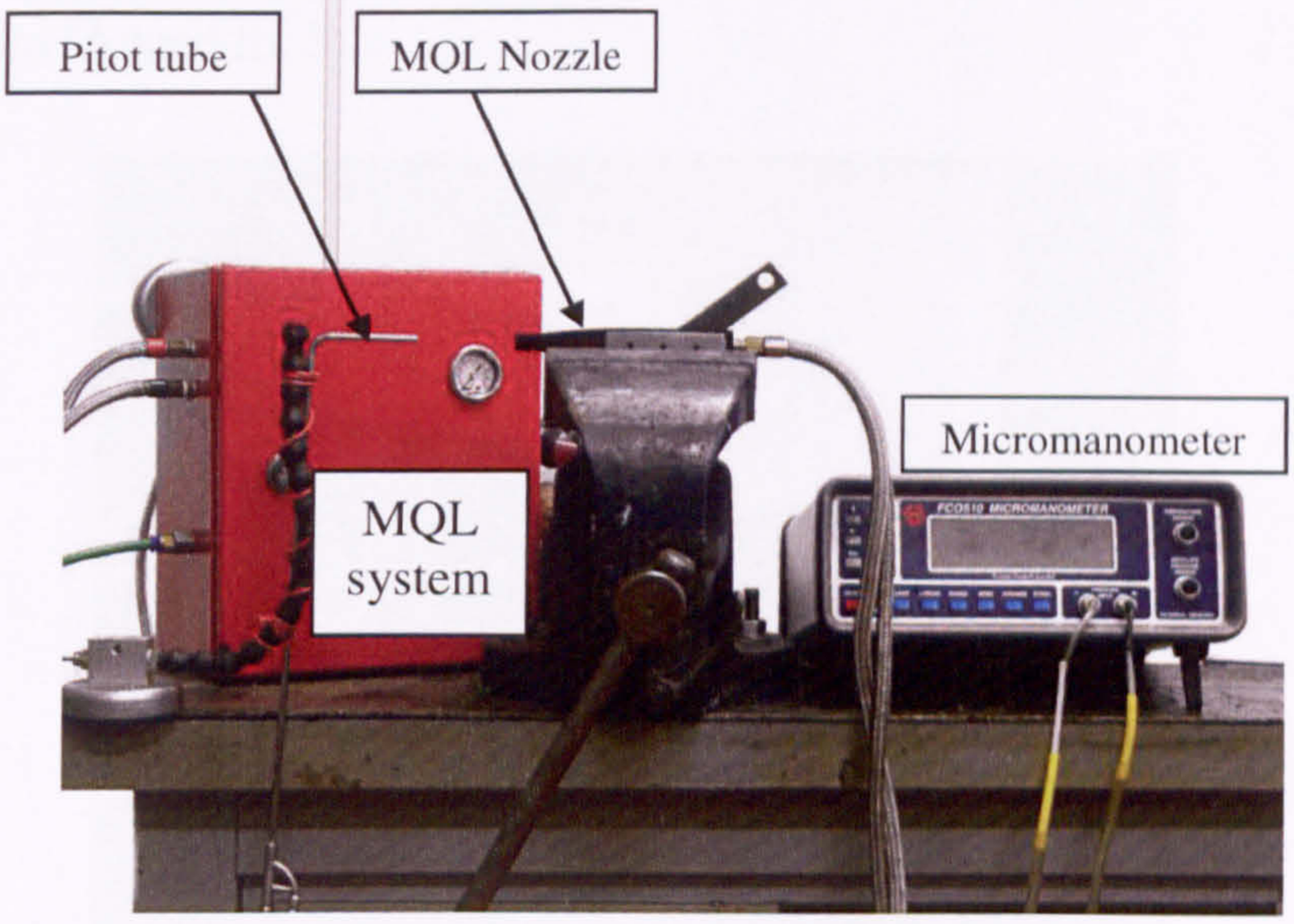

Figure 6-3. Airflow velocity measurement workplace.

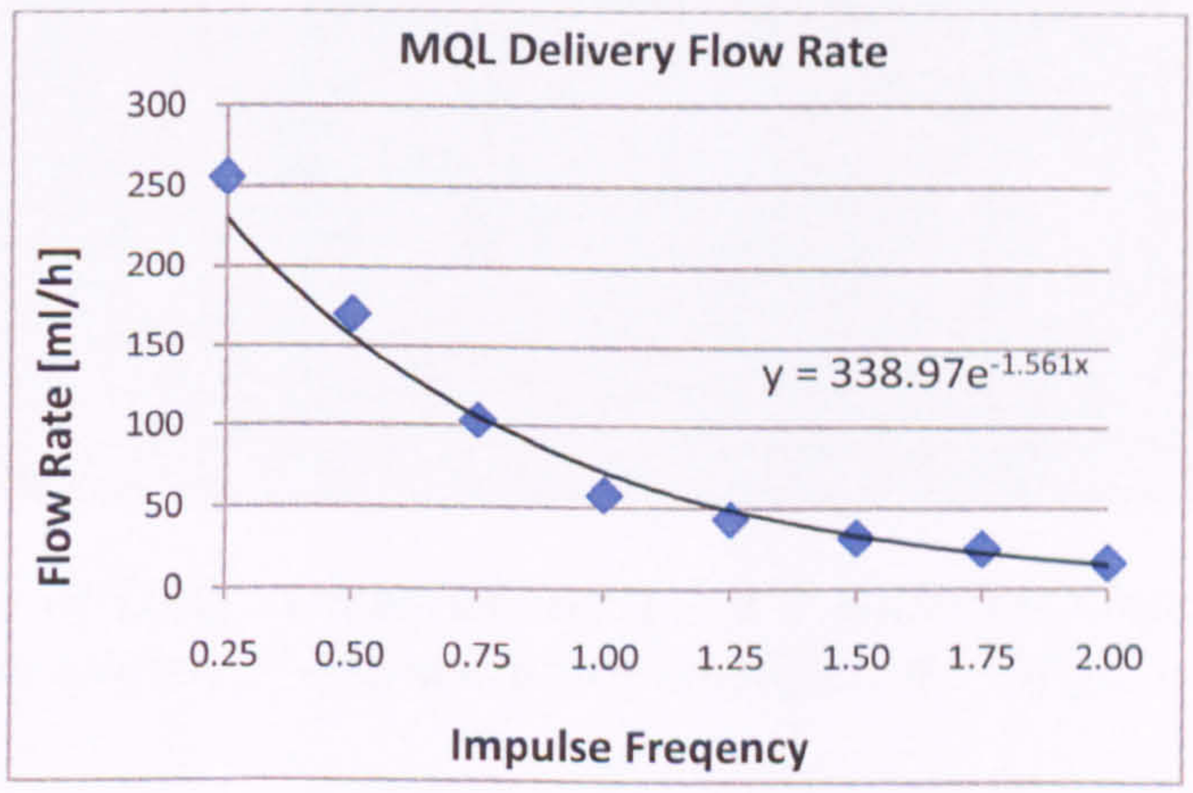

Figure 6-4. MQL System characterisation for 0.45MPa and impulse generator various settings.

It was then possible to prepare the MQL characterisation and to establish exact MQL system setting for required amount of oil – Figure 6-4. All air velocity results were confirmed and repeated in presence of LDA system where air and oil mixture in air boundary layer behaviour was checked.

6.3.3. Data Acquisition System

The data acquisition system was based on the National Instruments multichannel data acquisition NI6250. The power, grinding forces: normal and tangential and temperature were captured. The DAQ captured data at a frequency of 2000 Hz on a PC working on Windows XP OS. The DAQ system was controlled by LabView 7.1 with a purpose written program (Appendix 5).

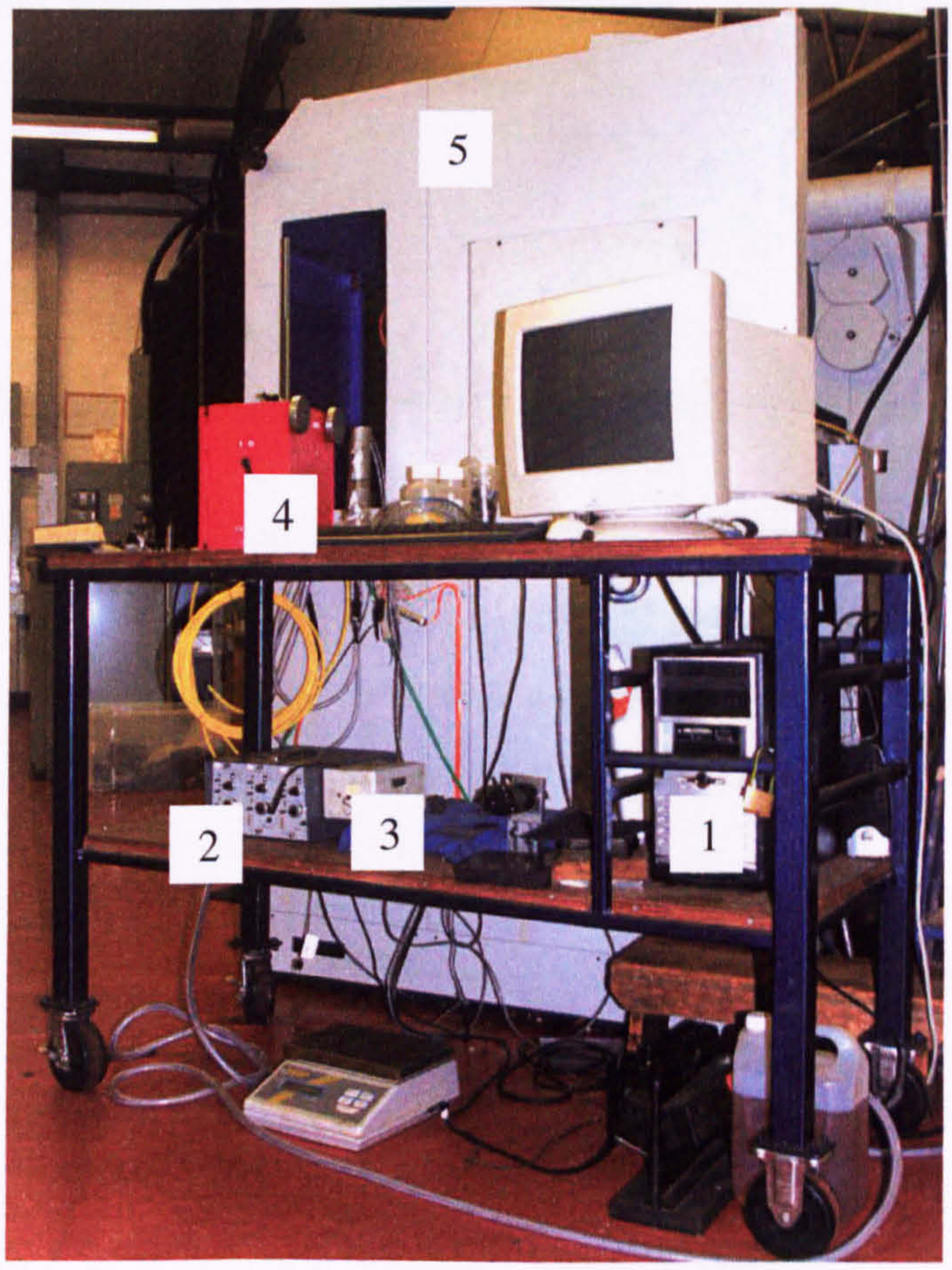

Figure 6-5. A view of DAQ system, where: 1 – PC with DAQ integrated, 2 – Kistler Type 5006 forces amplifier, 3 – temperature amplifier, 4 – MQL system, 5 – grinding machine.

Further processing of raw data was completed in the MS Excel 2007 and/or Matlab software environments. The related programs are given in Appendix 5.

The tangential and normal forces, were measured with the Type 9257A Kistler 3-component dynamometer together with Kistler Type 5006 amplifier. Prior to use the equipment was calibrated – see Appendix 6.

6.3.4. Grinding Wheel and Fluid Delivery

A general purpose utility wheel was used in this research: aluminium oxide, WA 100 JV.

The fluids used were those described for the preliminary studies, Chapter 5.

The coolant system used was an Arboga Darenth type 2210/3057. Maximum delivery conditions available were: 35 bar at a flowrate of 100 l/min. Filtering was undertaken via both a cartridge and centrifuge. Delivery conditions were: 1 bar pressure and approximately 27 m/s fluid velocity.

6.3.5. Workpieces and Temperature Measurements

Materials used were those used in the preliminary studies, namely EN31 and M2 (hardened steels) and EN8 (mild steel). Measurement of forces and temperatures required introduction of new workpieces and a purpose designed base to accommodate the dynamometer. Workpiece dimensions and arrangement are given in Appendix 7.

Hardness of EN31 was 62 HRC, M2 52 HRC and EN8 32 HRC. Dimensions were – 20 mm wide, 90 mm long, 20 mm high. The workpiece was sectioned and a slot prepared for installation of a thermocouple. The workpiece mounted is shown in Figure 6-6.

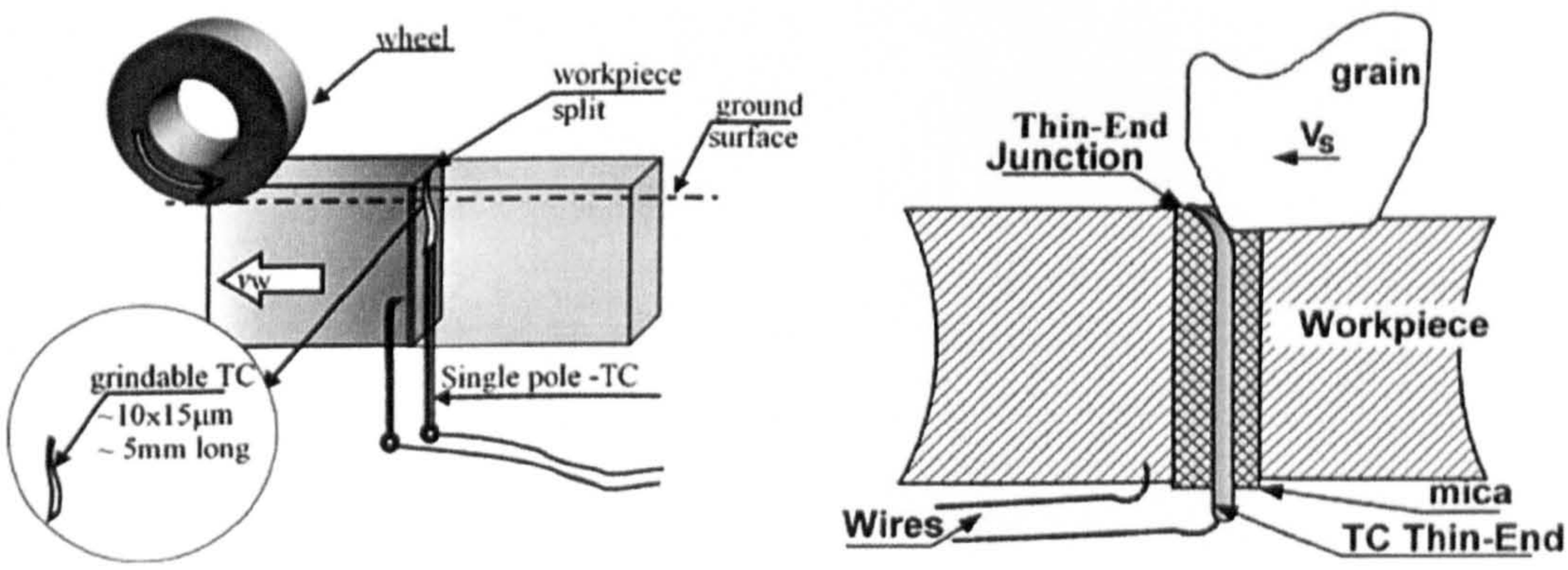

Figure 6-6. Thermocouple assembly and principle of operation (Batako, 2005).

An Omega CO2-T thermocouple was adapted to a single pole arrangement thermocouple. The J-type junction is formed when the grinding wheel passes over the

exposed single pole and smears it over the workpiece thereby forming a junction at the ground surface. Appendix 6 provides the thermocouple calibration details.

6.4. Experimental Work

It is important to recognise that the aim of this research was not to find optimal conditions for MQL but to compare MQL with dry and conventional machining using machine and equipment adapted for conventional flood cooling.

The experimental design approach was that based on the Taguchi method and yielded a high definition L_8 (2^7) orthogonal array.

	Parameter	Level 1	Level 2
A	Wheel speed	25m/s	45m/s
B	DOC	5μm	15μm
A x C	Interaction	-	-
C	Workpiece speed	6.5m/min	15m/min
B x C	Interaction	-	-
D	Dressing	coarse	fine
E	Materials	soft	hard

	v_s	a_e	·	v_w	·	*Dre*	*Mat*
	A	B	AxC	C	BxC	D	E
1	1	1	1	1	1	1	1
2	1	1	1	2	2	2	2
3	1	2	2	1	2	1	2
4	1	2	2	2	1	2	1
5	2	1	2	1	1	2	2
6	2	1	2	2	2	1	1
7	2	2	1	1	2	2	1
8	2	2	1	2	1	1	2

Table 6-1. Set of parameters and Taguchi array.

6.4.1. Experiment Procedure

The experimental work was performed in three stages – 1) conventional flood grinding, 2) dry machining and 3) MQL grinding. Each stage consisted on grinding three materials with all possible combinations of parameters according to the Taguchi's array (Table 6-1). As 'hard materials' in Taguchi's array it was meant: EN31 and M2, so in the end there were combinations of hard-soft materials as follows: EN31 vs. EN8 and M2 vs. EN8.

For conventional flood cooling there was no need for any preparations for the grinding machine. For dry and MQL machining, coolant nozzle had been disassembled. However, due to often wheel dressings a special nozzle was used for them. For MQL additionally conventional flooding nozzle had to be disassembled and MQL nozzle assembled in its place.

Before every single test the wheel was dressed. There were 2 types of dressings: fine and coarse – parameters can be found in Table 6-2.

The dressing process was based on 3 wheel cleaning passes (each a_{ed} = 10 µm with v_{fd} = 500 mm/min). After that the proper dressing process occurred according to Table 8-2.

Parameters	**Fine dressing**	**Coarse dressing**
Dressing wheel speed: v_{sd}	30 m/s	
Dressing feed rate: v_{fad}	100 mm/min	300 mm/min
Depth of dressing cut: a_{ed}	2 µm	10 µm

Table 6-2. Dressing parameters.

After dressing, the wheel needed to be conditioned. Wheel conditioning consisted of 2-5 passes (depending on process type) for 2 µm cut before programmed datum, 10 passes 1 µm form datum and 8 sparking out passes.

Then one down cut was performed according to Taguchi array's parameters.

The tests were repeated three times with the same settings to obtaining a more accurate mean value. However, it is possible to perform Taguchi's approach with only two repetitions for each trial.

6.4.2. DOC Measurements

The real DOC was obtained during a separate process after performing all tests.

In this process a 15 mm strip was ground from the 20 mm wide workpiece. This left an unground 5 mm width strip. The purpose of this 5 mm strip was to use it as a datum, where the '0' was obtained. The difference between the datum 'strip' and the ground 'strip' was measured using a clock gauge – Figure 6-7.

Figure 6-7. Mount of measuring clock gauge.

There were 12 points obtained and then a mean value of the real DOC calculated. This mean value represented the real DOC and was used in later calculations.

6.4.3. Surface roughness measurements

The roughness parameter used during this study was R_a. This is the most commonly referred to parameter for general surface measurement and provides a mean line average of the magnitude of peaks to valleys across the profile of the measured surface. A more complete discussion of surface roughness measurement was provided in Chapter 7.4. The instrument used was the Taylor Hobson Surtronic Duo, a high precision portable instrument, capable of 0.01 μm resolution (Figure 6-8). During the tests it was placed on the workpiece in three different locations ([*i*]approximately 10 mm from the start edge of the workpiece, [*ii*] the centre and [*iii*]approximately 10 mm from the end edge of the workpiece) using a 5 mm traverse length. The mean of these three measurements was used in further analyses.

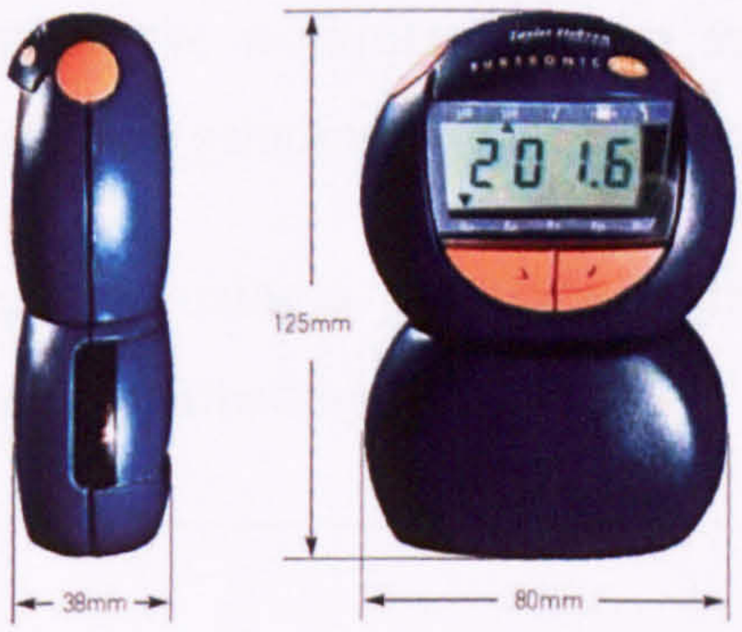

Figure 6-8.General view of Taylor Hobson Surtronic Duo roughness checker.

6.4.4. Laser Doppler Anemometry in Air Boundary Layer Measurements

A series of experiments were conducted to establish the interaction between the air and oil mix and the air boundary layer. The equipment and experimental arrangement is shown in Figure 6-9.

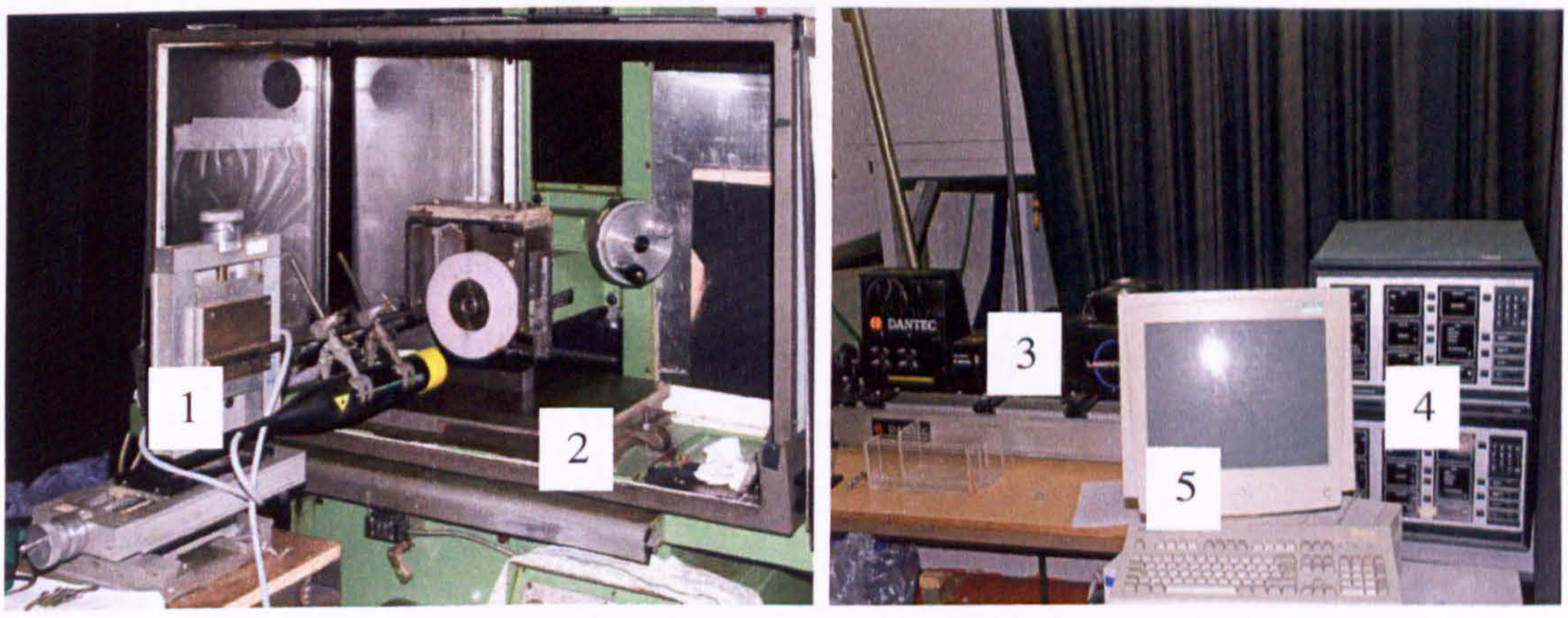

Figure 6-9. Equipment arrangements, where: 1 – laser probe, 2 – grinding machine, 3 – laser generator, 4 – BSA – burst spectrum analyser, 5 – Personal Computer with DAQ onboard.

Tests were performed on the Abwood Series 5020 surface grinding machine. The Laser Doppler Anemometry (LDA) system was based on the Dantec Argon-ion laser comprised of three main components: the Laser optical System, the Burst Spectrum Analyzers (BSA) and the PC. Wheel speed used for tests was kept constant at v_s = 35 m/s. Air velocity was varied: lower value v_{air} = 25 m/s, mid range value (equal to wheel speed) v_{air} = 35 m/s and higher value v_{air} = 45 m/s.

The wheel was rotated 2 mm above workpiece surface and the nozzle outlet set at a distance of 0mm to 50 mm from the grinding arc. Results can be seen in Figure 6-10.

Air velocities were first measured using a pitot tube method. The velocities obtained from pitot measurements were confirmed by LDA.

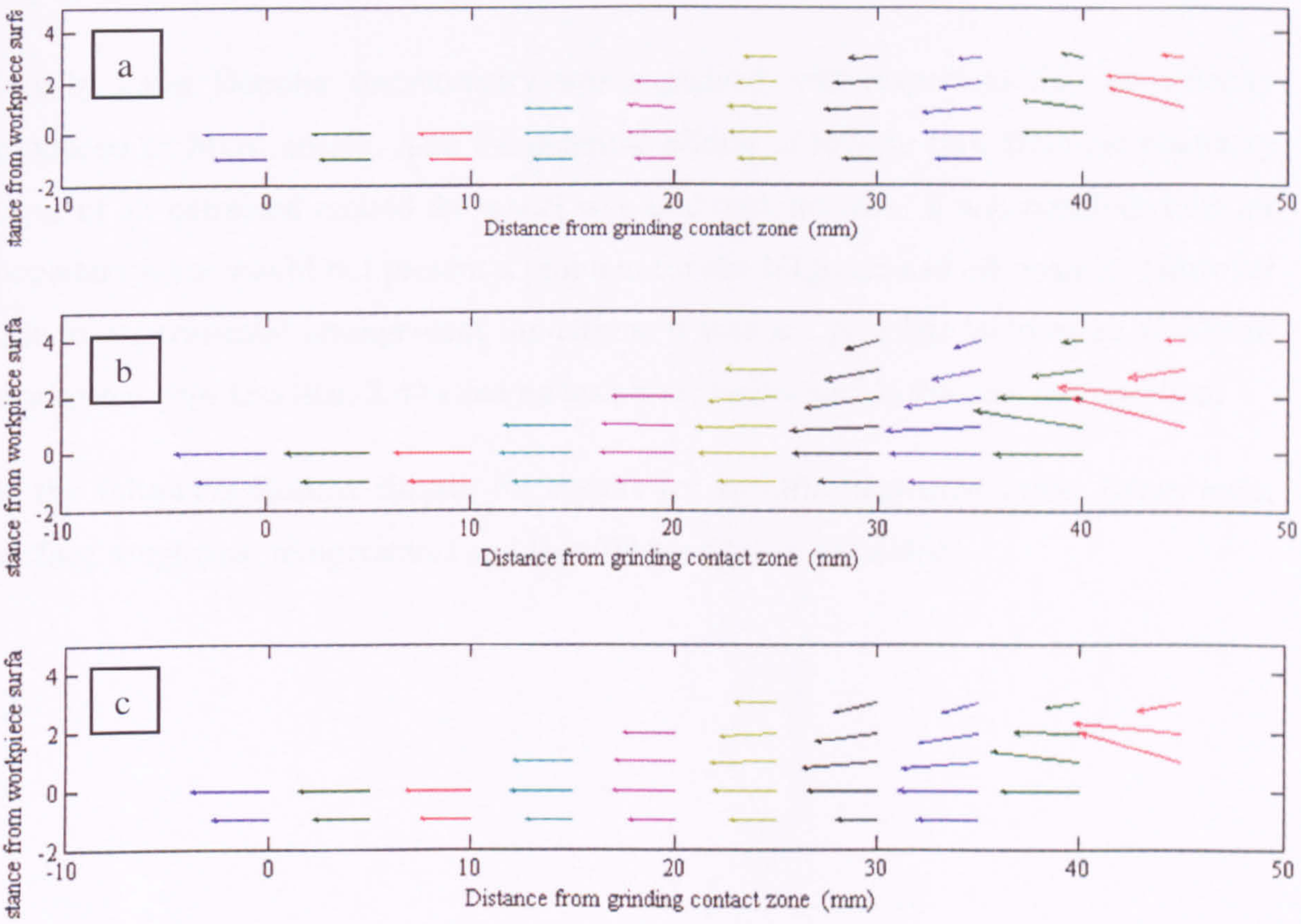

Figure 6-10. MQL grinding process boundary layer: a) v_{air} = 25 m/s, b) v_{air} = 35 m/s and c) v_{air} = 45 m/s to the wheel velocity v_s = 35 m/s.

For all three cases (Figure 6-10), there is no evidence of disturbance or reverse flow. It is reasoned therefore that the jet flowrate is sufficient for the air/oil mix to adequately penetrate the boundary layer. Due to limitations of the LDA instrumentation it was not possible to measure at wheel-workpiece gaps less than 2 mm and no tests were performed in the contact condition. However, these preliminary results were encouraging as they indicated that flow delivered is carried through the grinding arc and therefore able to provide lubrication. Such positive lubrication effects were supported in the results from the full experimental tests that follow.

6.5. Summary

In this chapter aims, objectives and scope together with equipment were presented. They were followed by discussion on experimental work and procedure. Explanation of depth of cut and surface roughness measurements were provided.

Use of Laser Doppler Anemometry was explained with respect to the air velocity produced by MQL nozzle. Also the potential effects of reverse flow from the boundary layer of air entrained around the wheel was analysed, however it was concluded the air boundary layer would not present a problem for the MQL air and oil mixture. However due to experimental arrangement limitations it was not possible to measure at wheel-workpiece gaps less than 2 mm and no tests were performed in the contact condition.

In the following Results chapter the results for specific tangential force, forces ratio, surface roughness, temperatures and specific energy are presented.

Chapter 7. RESULTS

7.1. Introduction

The aim of the main body of experimental work was to establish the efficacy of MQL in grinding and to gain further understanding of the effect of MQL on the grinding performance. Results obtained from a series of experimental tests are presented and discussed in this chapter. The aim of the investigation was to obtain data for the three different grinding cases using: conventional flood cooling (WET), dry machining (DRY) and MQL system (MQL) and to then compare the results and establish in which area they either differ or have similarities as this should then lead to possible explanations of MQL success in particular circumstances.

For ease of reference the reader is reminded of the Trial numbering identified in the Table below (Source: Table 6-1. Set of parameters and Taguchi array).

		Level	
	Parameter	**1**	**2**
A	Wheel speed	25m/s	45m/s
B	DOC	5μm	15μm
AxC	Interaction	-	-
C	Workpiece speed	6.5m/min	15m/min
BxC	Interaction	-	-
D	Dressing	coarse	fine
E	Materials	soft	hard

	v_s	a_e	-	v_w	-	*Dre*	*Mat*
Trial No	**A**	**B**	**AxC**	**C**	**BxC**	**D**	**E**
1	1	1	1	1	1	1	1
2	1	1	1	2	2	2	2
3	1	2	2	1	2	1	2
4	1	2	2	2	1	2	1
5	2	1	2	1	1	2	2
6	2	1	2	2	2	1	1
7	2	2	1	1	2	2	1
8	2	2	1	2	1	1	2

The results are presented in the following order to provide for discussion on the grinding performance of each regime under the conditions stated in the Table 6-1:

- 7.2. Achieved DOC (proxy equivalent chip thickness h_{eq}) and Specific removal rate *shown against* Specific tangential force.
- 7.3. Specific removal rate *shown against* Force ratio (F_t/F_n).
- 7.4. Specific removal rate *shown against* Surface roughness (R_a).
- 7.5. Specific removal rate *shown against* Measured temperature.
- 7.6. Specific energy results.

At the close of each sub-section results are presented using the Taguchi methods and direct effects charts.

The Taguchi approach was used to optimise the experimental programme and to minimise the number of practical tests. Two material groups were used in this study, hard materials EN31 and M2 and the soft material EN8. As a result there are combinational Taguchi arrays with EN31 and EN8, and also M2 and EN8 materials.

7.2. Real Depth of Cut a_e and Equivalent Chip Thickness h_{eq}

In this section, results are presented for the parameter real DOC, a_e and specific tangential force F_t. The achievable DOC with each material had an impact on the experimental methodology. For example, the actual DOC achieved at a programmed DOC of 15 μm varied between 3 μm to 13 μm dependent on material and machining parameters therefore fixing a programmed DOC to 10 μm for example, would not be beneficial. It is the actual achieved DOC, which is the important value in the tests.

What is worth pointing out is that a programmed DOC of 5 μm DOC did not perform very well throughout all the study due to grinding machine limitations. Additionally, the higher values of cut such as those between 20 μm and 30 μm were often impossible to achieve due to the power limitation of the machine. In some instances, a programmed DOC of 15 μm could utilise 75 per cent of grinding machine power capability. The differences in DOC achieved were therefore strongly dependent on the grinding situation, that is: speeds, applied DOC material and case (WET, DRY or MQL).

The equivalent chip thickness expressed in its simplest form was given previously in Chapter 4.1, equation (4.16) as:

$$h_{eq} = \frac{Q'_w}{v_s} = \frac{v_w}{v_s} \cdot a_e \qquad (7.1)$$

In the section that follows the speed ratio (v_w/v_s) remains the same and hence the relationship between equivalent chip thickness and specific tangential force is similar to

that between DOC and specific tangential force. Graphical results are presented therefore only for the parameter real DOC, though the tendency of results are similar for each parameter a_e and h_{eq}.

Specific tangential force was calculated by dividing the tangential force captured via the DAQ system by the workpiece width b:

$$F_t' = \frac{F_t}{b} \left[\frac{N}{mm}\right] \qquad (7.2)$$

The tangential force acts tangentially to the wheel surface and also the surface velocity of the tool. Due to the high speed of the wheel the tangential force in grinding is mainly responsible for power dissipation (Marinescu *et al*, 2004), where $P = F_t \cdot v_s$.

7.2.1. Trial 1: v_s=25m/s, a=5μm, v_w=6.5m/min, Coarse Dressing, Soft Material EN8

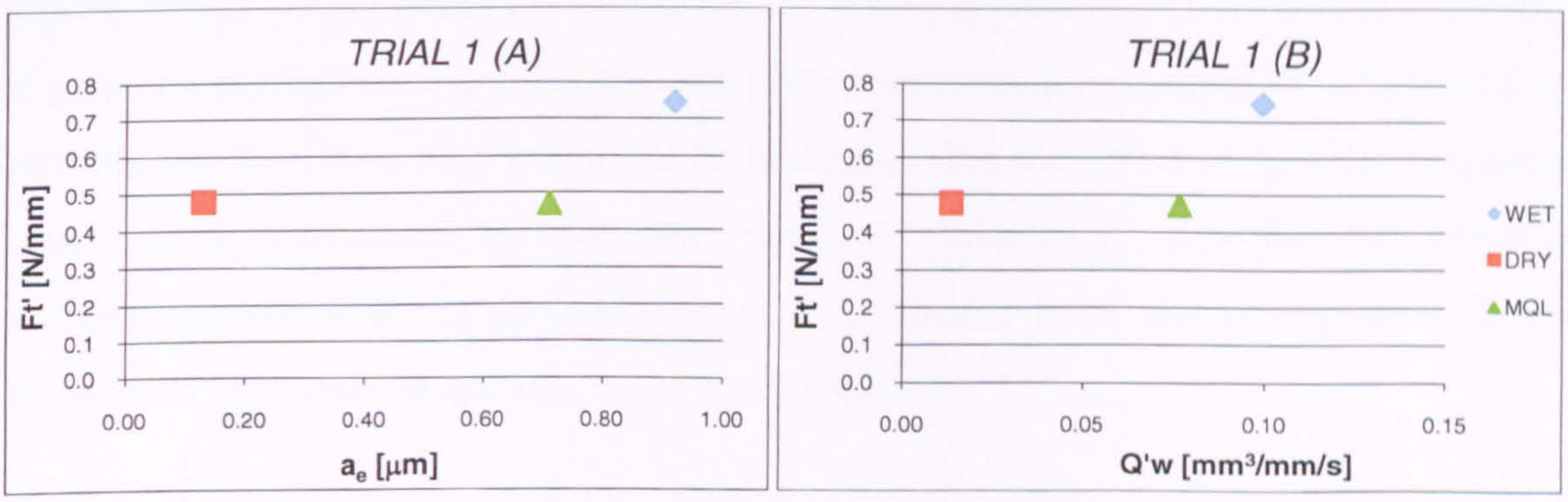

Figure 7-1. Specific tangential force as a function of DOC (A) and specific removal rate (B), Trial 1.

In this test the highest specific forces at F_t' = 0.7 N/mm were obtained for the WET case and it was found that the wheel barely scratched the workpiece surface. The lowest values were obtained under MQL, approximately 35 per cent lower than those for WET. It was a result of the achieved DOC a_e = 0.7 μm in MQL and for the case of WET a_e = 0.9 μm.

The values of h_{eq} ranged between h_{eq} = 0.001 μm (DRY) and h_{eq} = 0.004 μm (WET) *[h_{eq} values: WET = 0.004 μm; DRY = 0.001 μm, MQL = 0.003 μm]*. These values are

consistent with those published in literature for shallow cut operations using similar materials, machining parameters and abrasive tools.

The value of h_{eq} is a measure of the grain penetration depth. Grinding behaviour however cannot be explained by this parameter in isolation as two equivalent values may be obtained for very different chip shapes. Thus, the cutting edge density must also be considered when describing grinding behaviour in this context. In the case of DRY grinding it is possible that frictional wear was greater than in the other cases resulting in a reduction in cutting edge density. This would lead to a poorer grain penetration and result in force values similar to those in MQL.

The similarity in values of h_{eq} and real depth a_e for both MQL and WET would suggest that similar tribological processes occurred in both cases.

In Trial 1 it can be seen the highest Q'_w was achieved in WET however MQL provided the lowest specific tangential force: the difference in Q'_w for the two cases was approximately 20 per cent in favour of WET, whereas the difference in F_t' was approximately 40 per cent in favour of MQL. It may therefore be reasoned that in terms of grinding performance and for the two parameters considered there is little to choose between the two. It is also important to recognise that the value of specific tangential force, when considered in isolation, does not adequately describe the physical phenomenon and it is the ratio of tangential to normal force that is important. These results will be presented and discussed later in Chapter 7.3.

7.2.2. Trial 2: v_s=25m/s, a=5μm, v_w=15m/min, Fine Dressing, Hard Material EN31

In this test force values for the cases of DRY and MQL were in relatively close agreement with a DOC a_e = 0.5 μm and h_{eq} = 0.005 μm *[h_{eq} values: WET = 0.005 μm; DRY = 0.005 μm, MQL = 0.005 μm]* achieved throughout. The lowest force values were obtained in MQL and the highest in WET with a maximum difference of approximately 28 per cent.

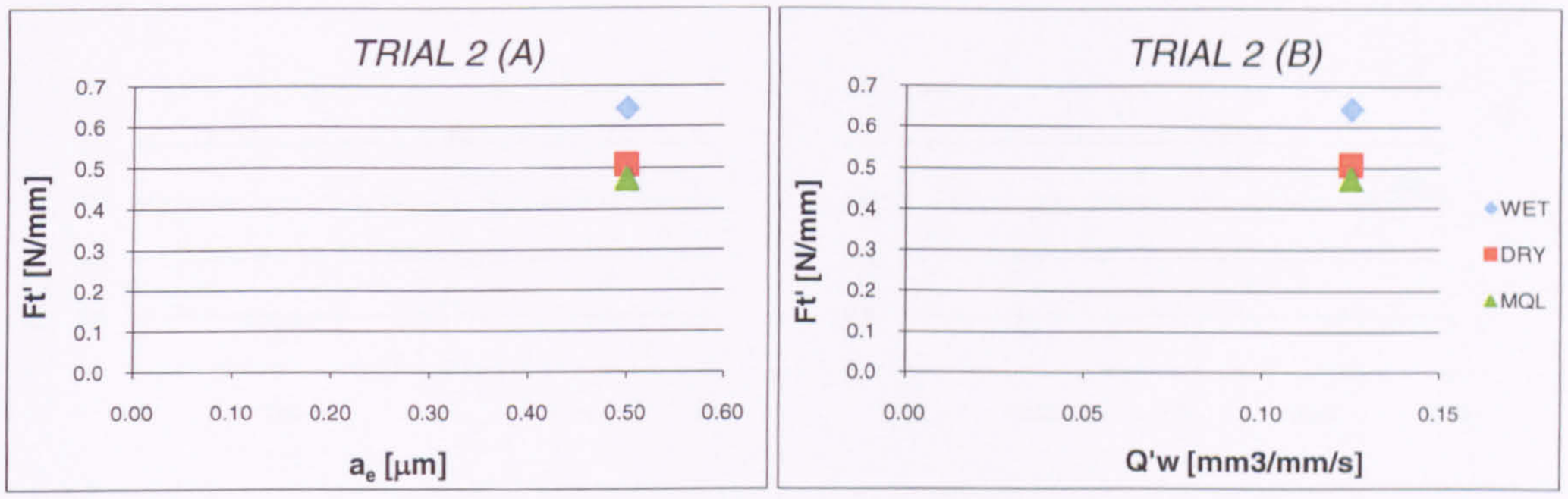

Figure 7-2. Specific tangential force as a function of DOC (A) and specific removal rate (B), Trial 2.

The similar level of specific tangential force in the cases of DRY and MQL may be a consequence of the very small DOC achieved. The marginally improved performance of MQL compared with DRY may be explained by improved lubrication.

The higher force values in WET can be explained by the requirement of the wheel to accelerate the fluid.

7.2.3. Trial 3: v_s=25m/s, a=15µm, v_w=6.5m/min, Coarse Dressing, Hard Material EN31

In this trial a DOC of approximately 7 µm was returned in both WET and MQL (resulting in h_{eq} = 0.030 µm) *[h_{eq} values: WET = 0.030 µm; DRY = 0.019 µm, MQL = 0.029 µm]* and slightly over 4 µm in DRY. Also a very close performance in both WET and MQL is observed in terms of specific removal rate and specific tangential force.

The highest values of specific tangential force occurred in DRY, approximately 22 per cent higher, and this is attributed to the lack of lubrication as in the previous test.

From the operator perspective, it was evident that the wheel, due to its low porosity and fine grain structure, was susceptible to visible loading and clogging with this material under DRY grinding. This would indicate an incorrect wheel selection for this material and the process parameters. Naturally, this would result in higher forces.

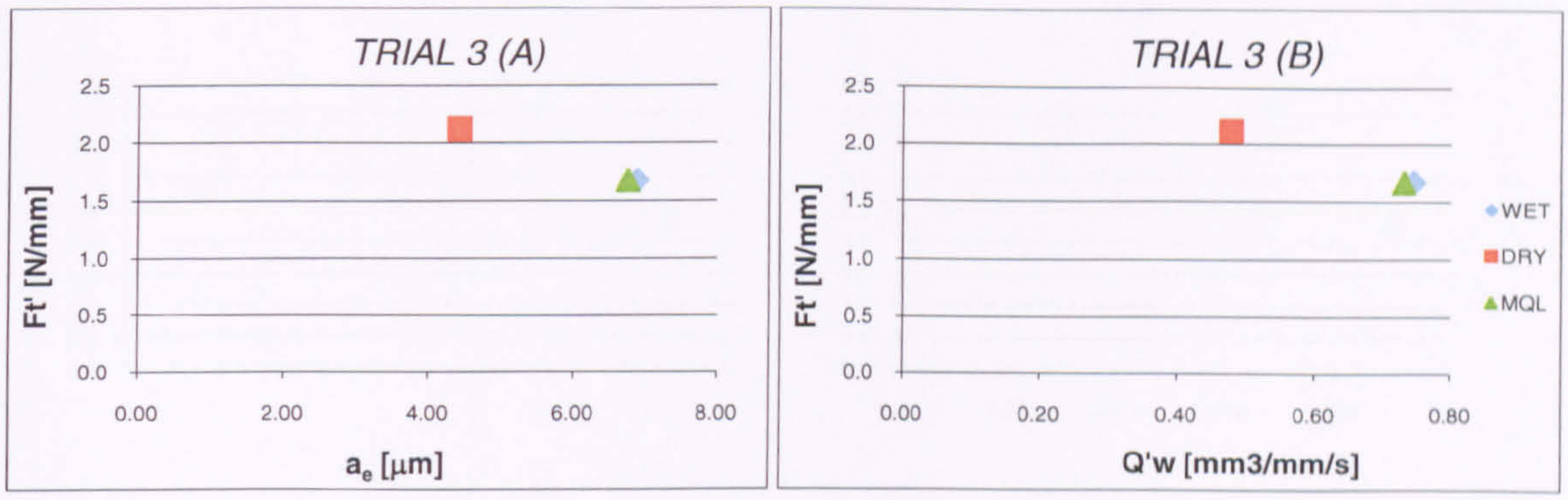

Figure 7-3. Specific tangential force as a function of DOC (A) and specific removal rate (B), Trial 3.

From this trial, it can be seen that MQL has potential to compete with WET under this combination of material, wheel and machining parameters.

The surface of the wheel had a similar though not identical appearance to that observed under DRY. It is argued that the visible appearance was due more to surface contamination rather than deeply impregnated physical loading. There is no evidence for this from topographical studies, however, the forces would support such an argument.

7.2.4. Trial 4: v_s=25 m/s, a=15 µm, v_w=15 m/min, Fine Dressing, Soft Material EN8

In the case of Trial 4, rather low DOC were obtained in all cases for an applied DOC of 15 µm: 4 µm for MQL, 3 µm for WET, and less than 1 µm for DRY.

A value of h_{eq} = 0.036 µm *[h_{eq} values: WET = 0.027 µm; DRY = 0.005 µm, MQL = 0.036 µm]* was established with MQL and this was the highest value obtained from within this series of 8 trials (Figure 7-4).

The MQL trial yielded the lowest forces at F_t' = 2.36 N/mm, approximately 42 per cent lower F_t' than in WET. The better results for MQL may be a result of hydrodynamic effects increasing power consumption in WET and the improved lubrication properties of the MQL oil.

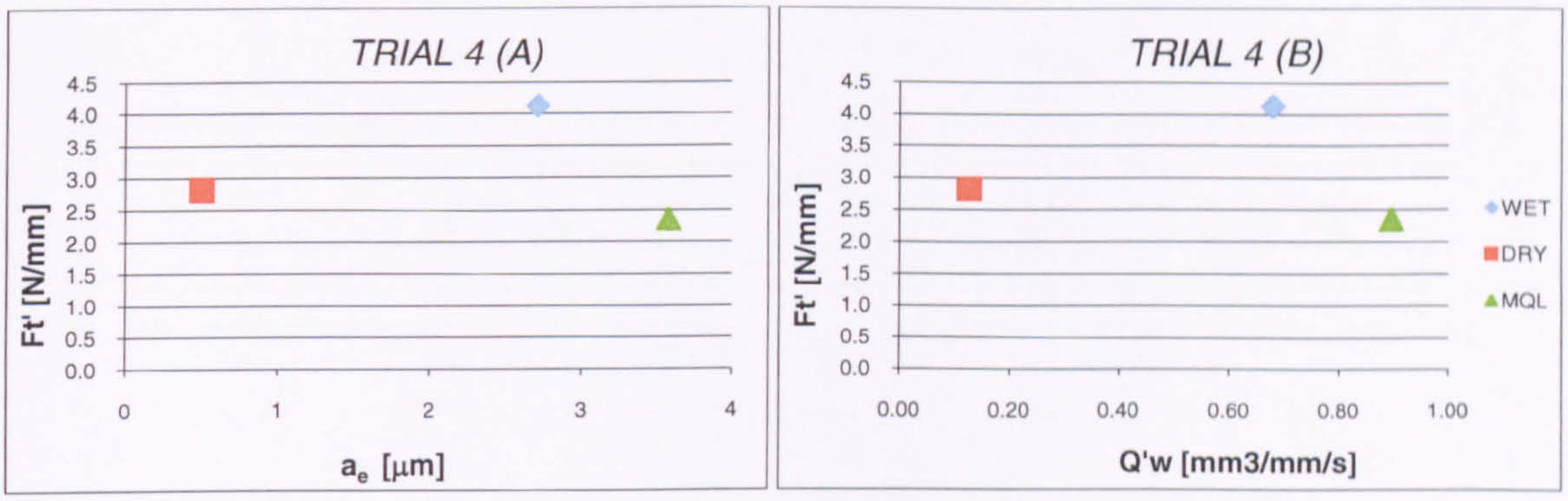

Figure 7-4. Specific tangential force as a function of DOC (A) and specific removal rate (B), Trial 4.

Low Q'_w under DRY was due to accelerated wheel loading under the fine dressing condition. The value of Q'_w in MQL exceeded that in WET by approximately 25 per cent.

The most reasonable explanation for the very low DOC is that accelerated wheel loading occurred in each case due to increased workpiece speed and that such a combination of parameters proved inappropriate for this wheel, material and dressing condition and consequently resulted in lowered process efficiency.

Such a good MQL performance in terms of cutting and energy efficiency may be a result of the combined effects of workpiece material hardness, which was relatively low in this trial and good lubrication properties of the MQL oil.

7.2.5. Trial 5: v_s=45m/s, a=5μm, v_w=6.5m/min, Fine Dressing, Hard Material EN31

In this trial, as in other trails at an applied DOC = 5 μm, only a low DOC was actually achieved in each of the different cases. The highest DOC was achieved under MQL. However, this value of a_e = 0.6 μm is still less than 15 per cent of the applied. The higher real DOC resulted in a higher Q'_w and specific grinding forces similar to those under DRY. The higher specific forces under WET are reasoned to be due to the hydrodynamic effects of delivered fluid. The effects of a higher wheel speed are seen in higher specific force values when compared to those obtained at lower wheel speed.

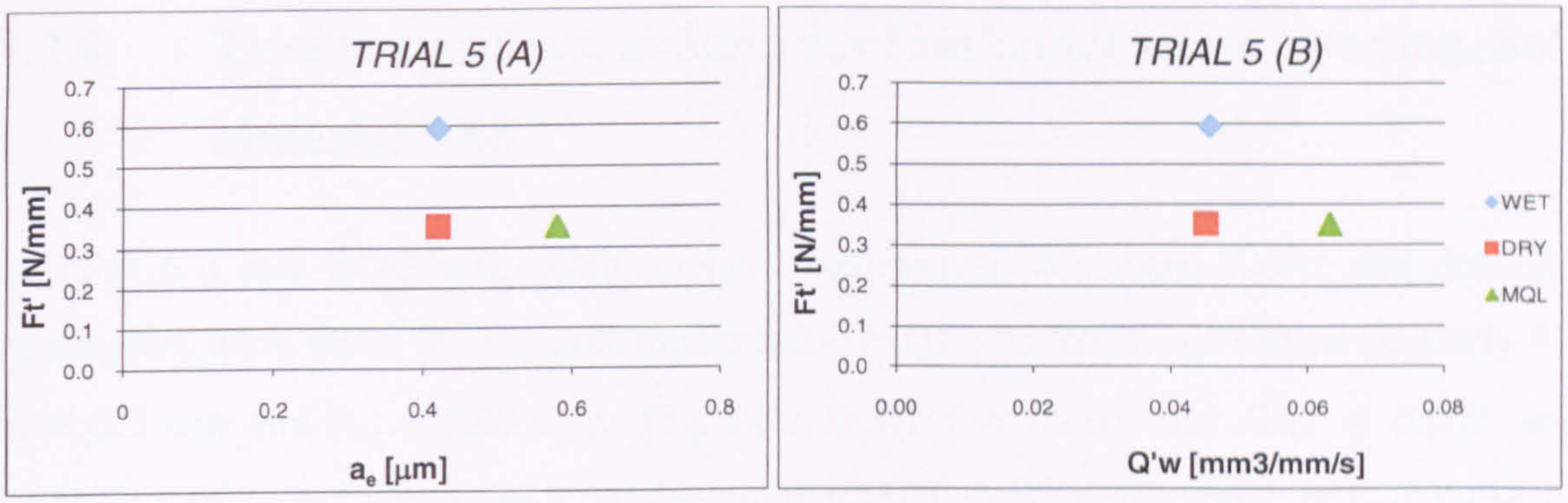

Figure 7-5. Specific tangential force as a function of DOC (A) and specific removal rate (B), Trial 5.

The wheel loading effect due to fine dressing conditions experienced in the previous case under DRY conditions are not apparent here with the harder material and lower DOC.

As discussed in the previous trials at low DOC a greater proportion of energy is consumed in ploughing and rubbing, rather than cutting compared with grinding at higher DOC and this is seen clearly in the lower Q'_w values.

In Trial 5 MQL delivered the best performance with lowest F_t' and highest Q'_w values *[h_{eq} values: WET = 0.001 μm; DRY = 0.001 μm, MQL = 0.001 μm]*. The explanation for this may partly be due to the dressing conditions and small DOC that were shown in previous Trials to be inappropriate for WET. Additionally, the vitrified wheel used required rather harder pressing into the workpiece to operate effectively but with such a small DOC it is not possible to press it hard enough to overcome hydrodynamic and air boundary layer effects. This is confirmed by the results for the DRY case, in which lower specific force compared to WET was generated.

It seems that suggestion is supported by the fact that in DRY only slightly higher F_t' value was obtained than in MQL but the resulting DOC was similar as for WET.

7.2.6. Trial 6: v_s=45m/s, a=5μm, v_w=15m/min, Coarse Dressing, Soft Material EN8

In Trial 6 a low DOC was again applied, however speeds were higher and dressing parameters were those for a coarse topography. MQL and WET performed similarly for a_e = 0.5 μm and h_{eq} = 0.003 μm *[h_{eq} values: WET = 0.003 μm; DRY = 0.001 μm, MQL = 0.003 μm]*, although F_t' values under MQL were approximately half those of WET. Coarse dressing with the softer material decreased specific tangential force in comparison to the values in Trial 5 for all the cases.

A very poor performance can be observed under DRY in comparison with MQL and WET.

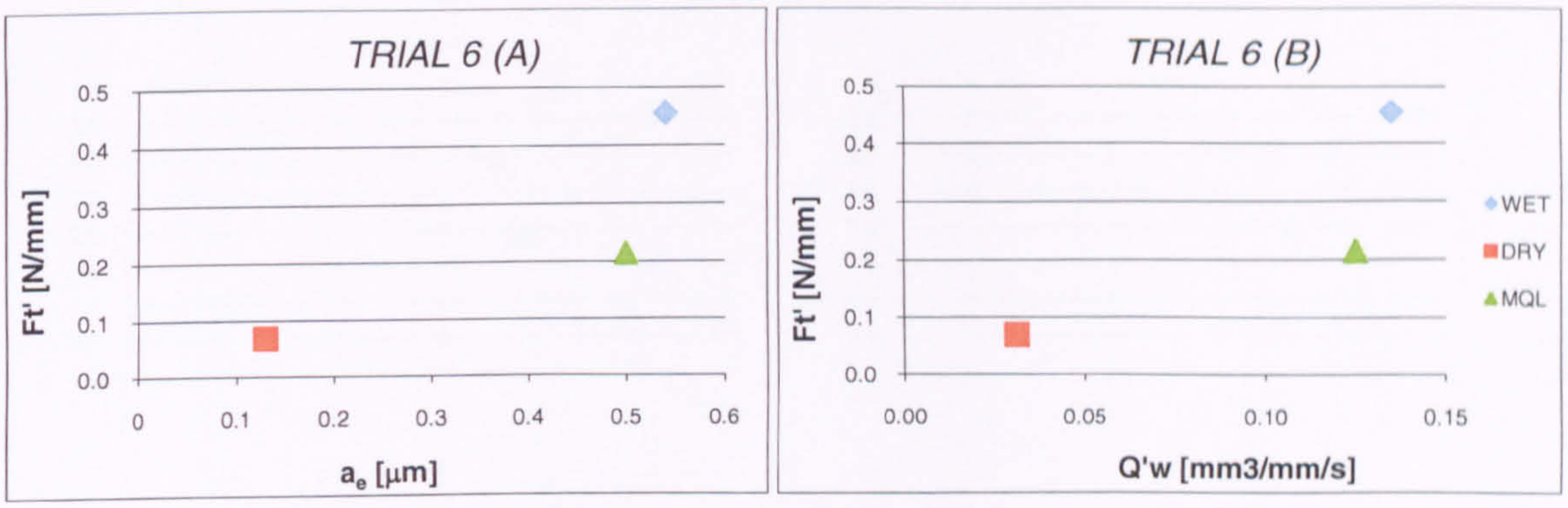

Figure 7-6. Specific tangential force as a function of DOC (A) and specific removal rate (B), Trial 6.

Poor performance and low Q'_w under DRY would suggest a higher ratio of ploughing and rubbing than in WET and MQL and perhaps may be explained by the value of friction coefficient.

The influence of the hydrodynamic effects were marginally weakened in this trial due to coarse dressing producing a relatively higher wheel surface porosity.

The results imply that effective lubrication takes place under MQL in these trial conditions and relatively efficient grinding occurs.

7.2.7. Trial 7: v_s=45m/s, a=15μm, v_w=6.5m/min, Fine Dressing, Soft Material EN8

In this trial much improved DOC values were achieved. In the case of WET the achieved DOC was a_e = 13μm and h_{eq} = 0.031 μm. The DOC under DRY and MQL were 9 μm and 10 μm respectively [h_{eq} = *0.022 μm and* h_{eq} = *0.024 μm respectively*].

It can be seen that the value of F_t' under WET is some 60 per cent higher than that under MQL with a difference in DOC of approximately 23 per cent. This leads to the conclusion that for only a marginal reduction in grinding efficiency MQL can perform at a level similar to that of WET but with lower forces and hence lower local temperatures.

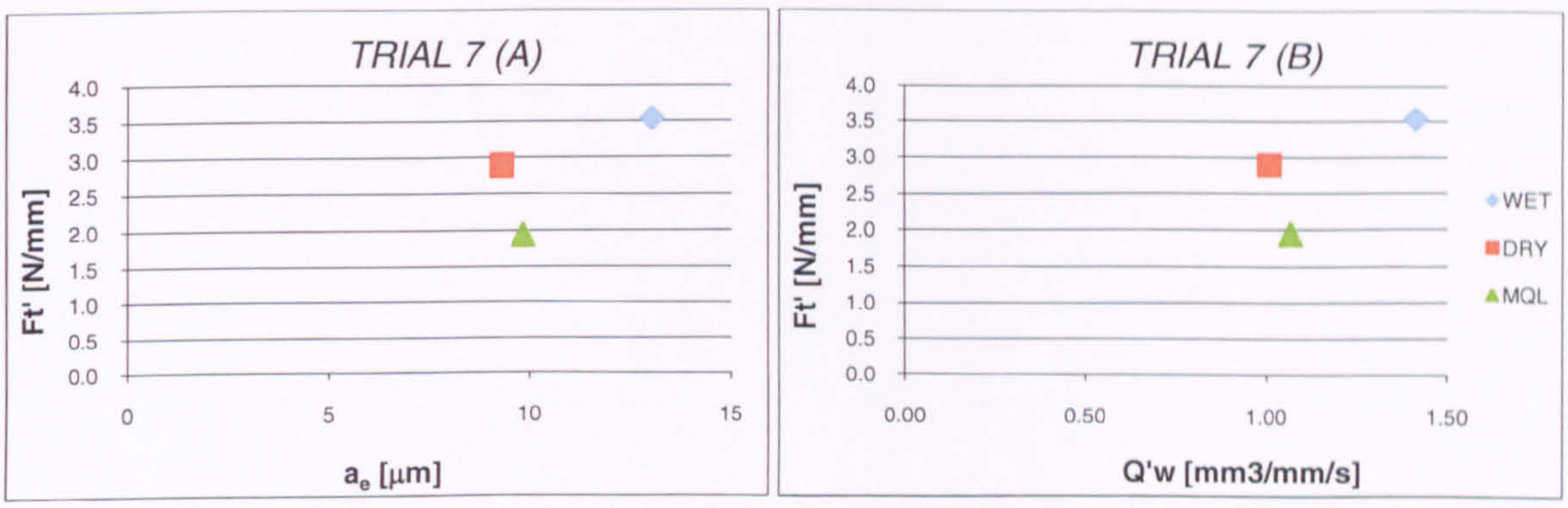

Figure 7-7. Specific tangential force as a function of DOC (A) and specific removal rate (B), Trial 7.

Though fine dressing was applied, good cutting efficiency was observed in each case. This results from the high wheel speed and low workpiece speed, combined with the softer material. As wheel speed is higher, the wheel should present better self sharpening properties, influencing its performance significantly, i.e. it is evident from equation (7.1) that doubling the wheel speed halves the equivalent chip thickness and by implication halves the grain depths of cut. Thus, increasing wheel speed will tend to reduce the stress on the abrasive grains and support increased removal rates. However, in the situation reported above, the lower DOC under MQL compared to WET may be caused by the process susceptibility to wheel loading, as with MQL there is a lack of efficient wheel cleaning and flushing.

In general terms MQL and WET each performed well, however MQL produced the lower F_t' and therefore a cooler process occurred.

7.2.8. Trial 8: v_s=45m/s, a=15μm, v_w=15m/min, Coarse Dressing, Hard Material EN31

In Trial 8 the performance of MQL is close to that of DRY *[a_e = 3 μm, h_{eq} = 0.017 μm,]*. The WET test resulted in the highest achieved DOC at approximately 60 per cent greater than that of the other cases. Notably the specific forces in WET were similar to those in DRY and in MQL despite the improved DOC and subsequent higher specific material removal rate.

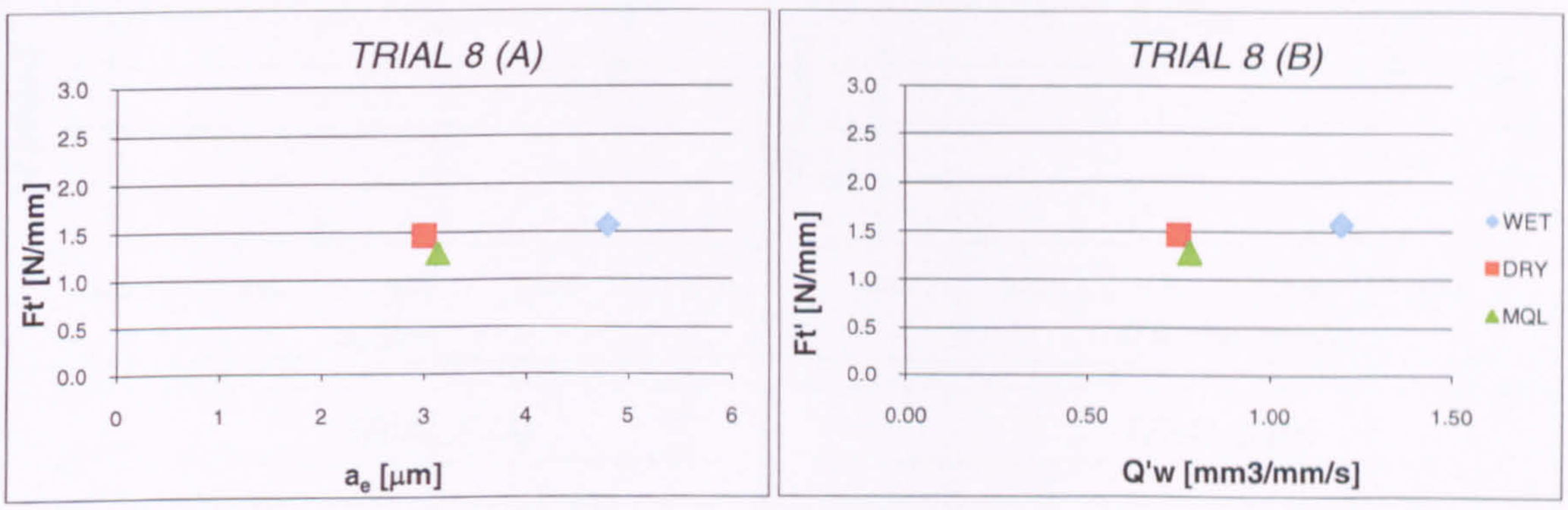

Figure 7-8. Specific tangential force as a function of DOC (A) and specific removal rate (B), Trial 8.

In Trial 8 the conditions appeared favourable for the WET case: hard material, fine grain and relatively soft wheel as good results were obtained in respect of material removal rate and specific tangential force.

Though there is not a large difference between WET, DRY and MQL in specific force values only WET was able to perform reasonably well. This is reasoned to be due to the effects of accelerated wheel loading in DRY and MQL under these conditions. As a result higher temperatures are expected to be seen in these cases.

7.2.9. Trial 2, 3, 5 and 8: Hard Material M2

Further results for specific tangential force as a function of real DOC and specific material removal rate were obtained for grinding M2 and are shown in Figure 7-9.

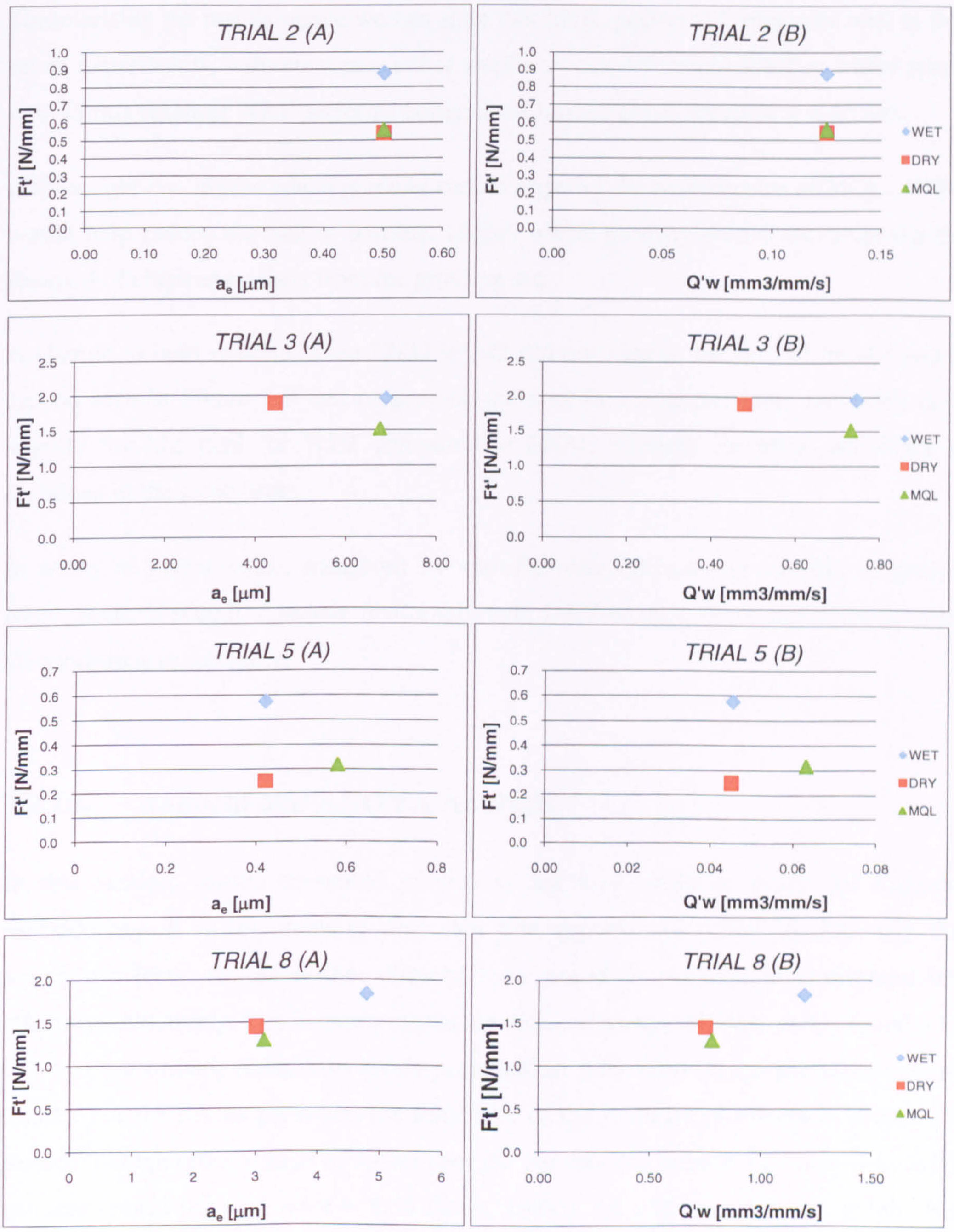

Figure 7-9. Specific tangential force as a function of DOC (A) and specific removal rate (B), for hard material M2 and soft material EN8.

Generally, the trends for DOC and hence h_{eq} and specific material removal rate Q'_w were very similar to those obtained for EN31. There are some minor discrepancies in the results but one can be reasonably confident in stating that EN31 and M2 performed comparably.

Summarising the results above we can state that MQL performed relatively well in this set of experiments, with outcomes either similar or outperforming WET at wheel speed v_s = 25 m/s whereas WET performs better at the higher wheel speed of v_s = 45 m/s.

It is thought that higher wheel porosity should improve the performance of MQL, as this would help reduce the rate of loading. Higher wheel porosity would also improve the removal of chips and debris from the grinding arc.

A change in hard material from EN31 to M2 did not change the overall trends, and it can be seen in Figure 7-9 that in general, the specific tangential force increased only slightly for M2 steel for WET compared to EN31, whereas for MQL and DRY it remained at the same level.

In terms of performance, measured by specific removal rate and specific tangential force, MQL is seen to compare favourably with DRY or to in fact outperform it under all conditions investigated.

7.2.10. Taguchi and ANOVA Analysis

In this section, results presented previously are now analysed using the Taguchi methodology. It is important to note that this approach identifies qualitatively the strongest effects, though further directed tests would be required to understand the effects quantitatively. The Taguchi results are checked using ANOVA analysis, and a F-test was performed. Reliability levels provided an indication of the usefulness of all results. For the results presented the reliability of the majority of effects is at least 95 per cent though often as high as 99 per cent (95 per cent confidence – F value = 4.49; 99 per cent confidence – F value = 8.53 (Ross, 1988)). As a large number of graphs has already been presented the full ANOVA table is not presented but only quoted where appropriate. However, an example ANOVA table is given in Table 7-1, where results

are presented for EN31 and EN8 for WET. In the presented ANOVA results case, it was found that C and interaction-AC effects are below 95 per cent reliability level thus cannot be taken into account. These results are shown highlighted in the direct effects charts that follow.

The full series of results are presented in the ANOVA Tables in Appendix 9.

ANOVA Results Table

Source	SS	ν	V	F
A	0.41	1	0.41	20.49
B	26.90	1	26.90	1355.54
C	0.02	1	0.02	1.20
D	7.43	1	7.43	374.59
E	7.21	1	7.21	363.13
AC	0.05	1	0.05	2.38
BC	0.20	1	0.20	10.14
e	0.32	16	0.02	
Total	**42.54**	**23**		

Table 7-1. Example of ANOVA results table for EN31 and EN8 materials for WET for F_t'. Key: SS – square sums, ν - degrees of freedom, V – variance, F – F ratio

The first analysis in Figure 7-10, is for EN31 and EN8 materials and show the value of specific tangential force against the Taguchi coordinate. The three different charts relate to the cases of WET (A), DRY (B) and MQL (C) respectively.

The second set of three charts, Figure 7-11 are for materials M2 and EN8, and similarly show the value of friction coefficient against the Taguchi coordinate. The three different charts relate to the cases of WET (A), DRY (B) and MQL (C) respectively.

As illustrated in graph (Figure 7-10 A) the DOC has the strongest effect in the case of WET. Strong effects also arise from the dressing mode and workpiece material. The effect of wheel speed, and the interaction between DOC and workpiece speed are less significant.

When a similar analysis is performed for the DRY case, it can be seen that the strongest effect is again seen as DOC and similarly to WET relatively strong effects are noted for the dressing mode and workpiece material. However, results for workpiece material and other effects fall below 95 per cent reliability level and are therefore to be rejected.

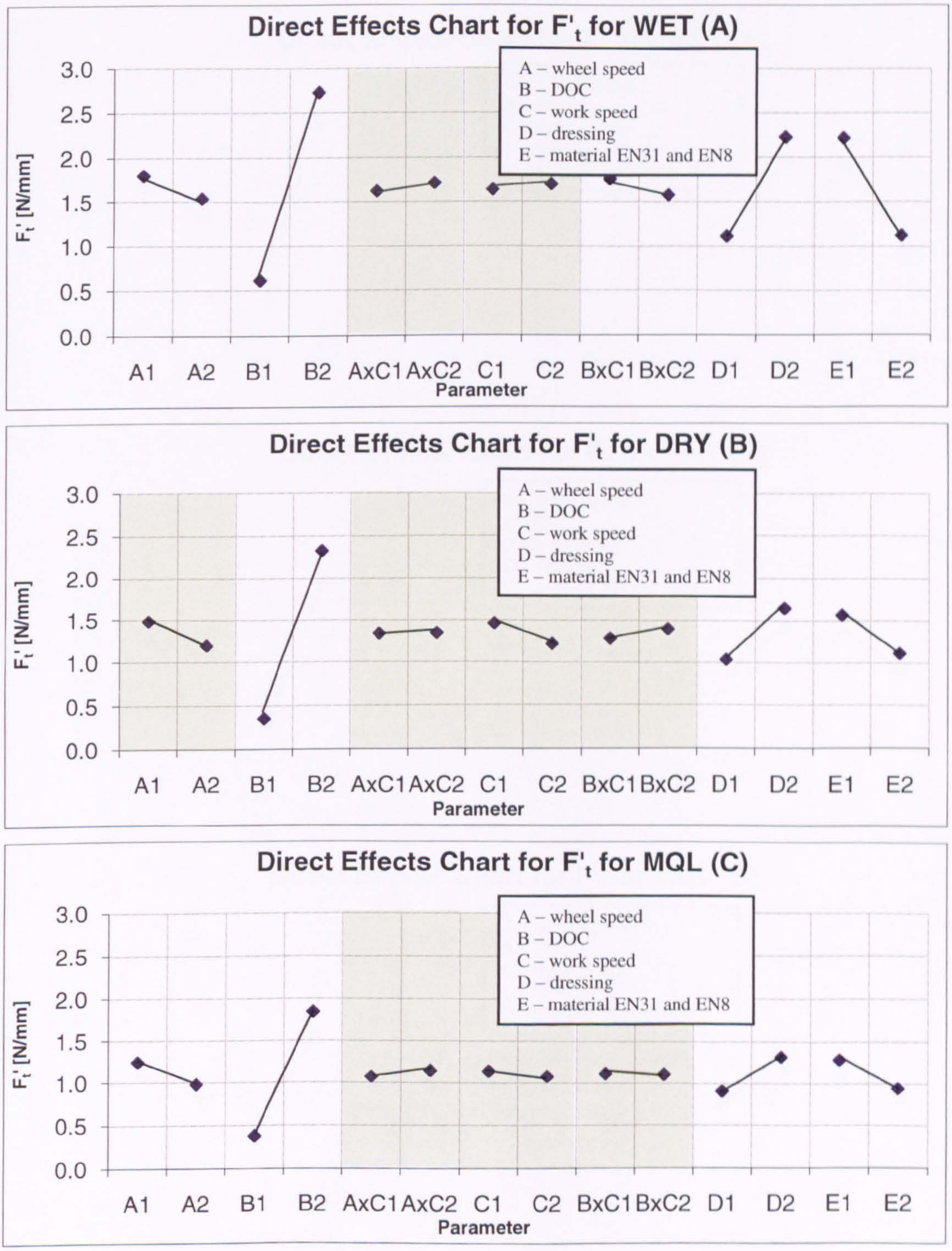

Figure 7-10. Direct effects chart for specific tangential force with EN31 and EN8.

The strongest effect on specific tangential force in MQL was DOC. All relationships follow the same tendency for the high(1) and low(2) Taguchi value (refer to Figure 7-10. Direct effects chart for specific tangential force with EN31 and EN8.) though magnitudes are highest in WET followed by DRY and finally MQL.

Graphs in Figure 7-11 illustrate the results obtained for M2 and EN8.

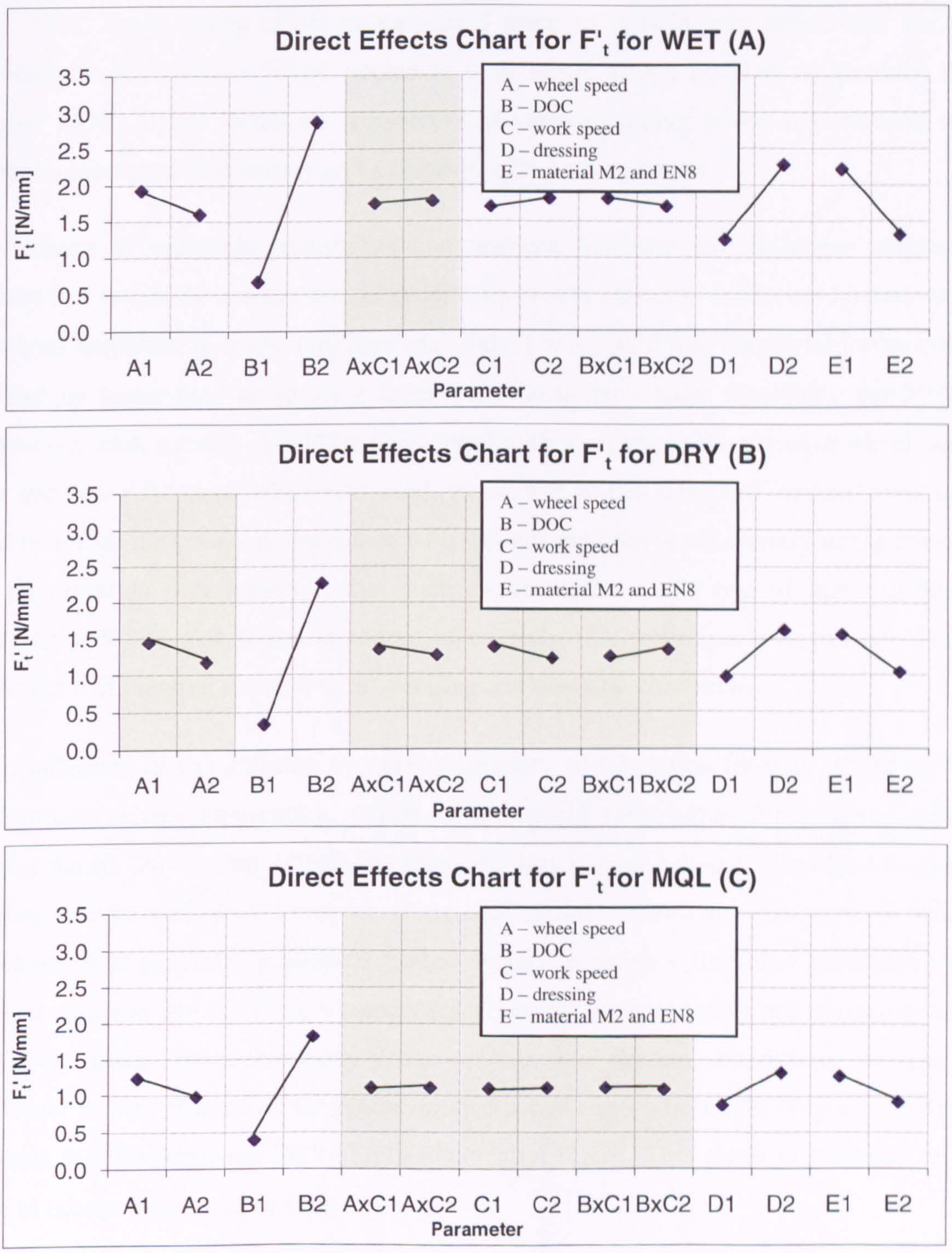

Figure 7-11. Direct effects chart for specific tangential force with M2 and EN8.

The trends for M2 and EN8 (materials have similar hardness values) are the same as those for EN31 and EN8. This demonstrates the correctness of the experimental tests and the correctness of the data obtained.

The Taguchi analysis yields results that are consistent with general understanding of grinding kinematics.

The DOC has a strong effect on tangential force as it is largely responsible for the contact length. Contact length increases with larger DOC, however to produce this higher DOC, higher forces are required. This involves higher power requirements and leads to increased heat energy and a consequently hotter process.

Mechanics of materials informs us that material hardness will influence tangential forces in a two body contact, and in general we would expect to see forces increase with material hardness. In trials with hard materials it was found that tangential forces could in fact be lower than those for a softer material under similar machining conditions. However, such a result should be considered with a regard to the abrasive wheel used. For each case the same wheel was used, which was in fact designed for hard materials, and therefore the poorer performance with the soft material is not entirely unexpected. It is important to note however, that such an outcome is only one of many different outcomes. It was also found in certain other trials, that wheel performance was better with the soft material depending on grinding and dressing conditions.

The influence of the dressing process parameters on tangential force is strong as this determines wheel topography, which is ultimately responsible for grinding wheel performance. More open wheel structures and larger grain wheels, often lead to lower forces due to ability to transport chips and coolant. However, this type of wheel structure will generally produce a higher surface roughness than that produced by a closed structure and therefore a compromise between process forces and surface quality has to be made. From this study it can be seen how dressing conditions can lead to different values of specific tangential force for the same wheel. The Taguchi analysis reveals that fine dressing led to higher tangential forces. This result is reasoned to be due to accelerated wheel loading.

The influence of wheel speed on grinding forces accords with theory and increased wheel speed results in a decrease in specific tangential force. This is due to a shorter period of contact with the workpiece material and therefore in the unit of time a single grain is engaged with the work material. Wheel speed also influences surface roughness this relationship will be discussed in later section of this chapter.

7.3. Friction Coefficient

In abrasive machining processes the ratio of F_t/F_n is commonly known as the force ratio (it has similarity to the coefficient of friction in mechanics) and is referred to by the symbol μ. The tangential and normal forces were measured during the study and thus it is possible to consider the effects of friction as a measure of process performance. Compressive stresses often result from machining situations of low friction, whereas tensile stress conditions may arise in the situation of high friction where higher surface temperatures occur at the interface of the sliding bodies.

The force ratio is indicative of the grain sharpness and also the ability of the grain to penetrate the workpiece material. Typical values of F_t/F_n in abrasive machining lie between 0.2-0.7. A value of 0.2 or lower corresponds to well-lubricated blunt abrasive grain in contact with the surface and very little penetration. High values correspond to sharp abrasive grains and deep penetration (Marinescu *et al*, 2004).

It is reasoned that since results for 5 μm DOC are hard to interpret in respect of quantities measured and are considered unreliable, further results at this DOC are not presented in the sections that follow. However, all results obtained at this DOC can be found in Appendix 10.

7.3.1. Trial 3: v_s=25m/s, a_e=15μm, v_w=6.5m/min, Coarse Dressing, Hard Material EN31

In Trial 3 the lowest value of μ is observed for MQL, the highest one for DRY. The specific material removal in DRY was lower than that for both WET and MQL and this implies a reduced penetration depth. In such a situation, the higher μ is due largely to an increased proportion of sliding and ploughing, which is inefficient and results in a higher interface temperature and hence accelerated loading and wear. The improved μ in WET and MQL is due to effects of lubrication. The better performance of WET is due to higher cutting efficiency and the effect of improved cleaning action of the larger volume of fluid. The lowest value of force ratio was obtained under MQL and this is

important in explaining the efficiency of the method. This is indicative of a situation of good lubrication, relatively high specific material removal and reasonable penetration depth. This outcome which is highly significant for MQL points strongly toward an applicable regime for MQL i.e. relatively shallow cut operations, for a range of material hardness.

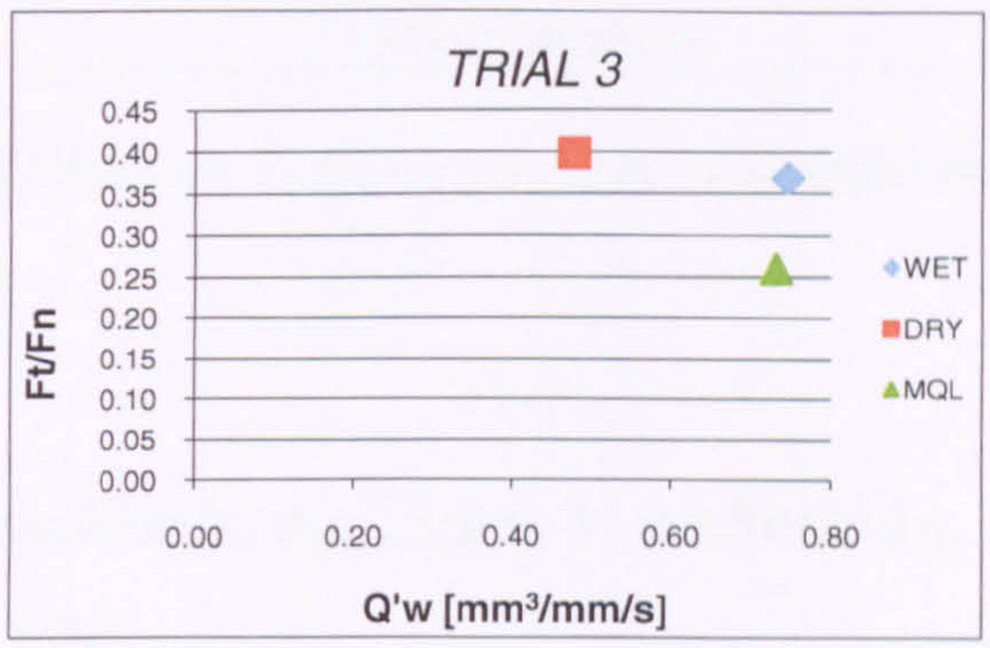

Figure 7-12. Coefficient friction F_t/F_n in function of specific removal rate Q'_w for hard material EN31.

7.3.2. Trial 4: v_s=25m/s, a_e=15µm, v_w=15m/min, Fine Dressing, Soft Material EN8

Results for Trial 4 are shown in Figure 7-13. As in the previous case the results for DRY show it be the least efficient method. The value of Q'_w for DRY in this Trial is much lower than in the previous Trial 3 (Chapter 7.3.1) and is reasoned to be due to the rapid loading (soft material, fine dressing and no flushing).

The performance of WET is not as effective as in the previous Trial 3 (Chapter 7.3.1). It is likely that the wheel loaded more rapidly with the softer material and this is supported by the fact that no increase in specific material removal rate was observed despite the higher workspeed. However, MQL is seen to yield an increased specific material removal rate and this indicates efficient cutting and results in the lower μ value.

The results from this Trial suggest that MQL is more suited to grinding of soft material in shallow cut with fine dressing than WET.

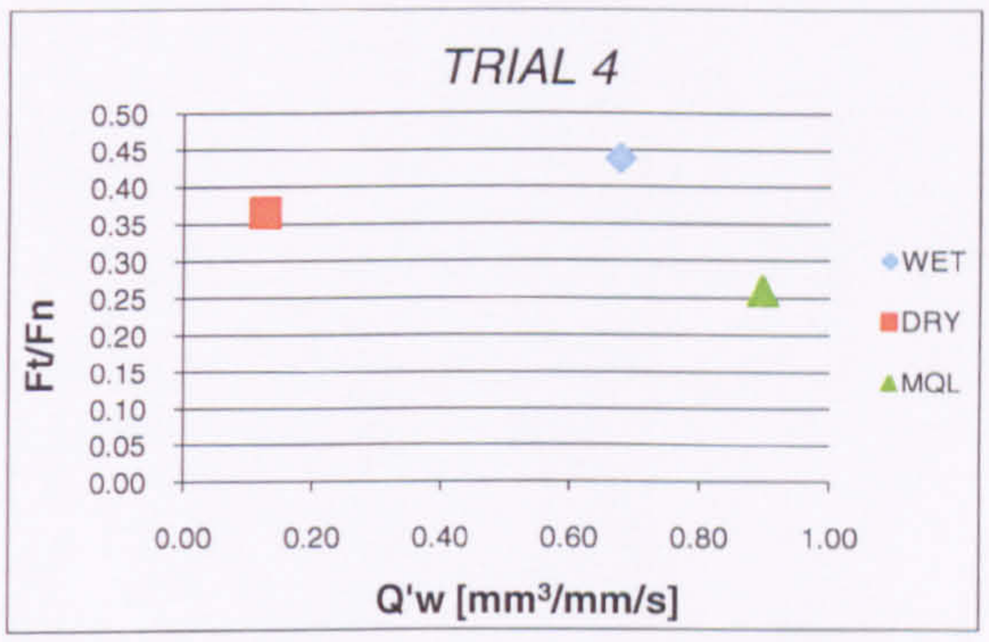

Figure 7-13. Coefficient friction F_t/F_n in function of specific removal rate Q'_w for soft material EN8.

7.3.3. Trial 7: v_s=45m/s, a_e=15μm, v_w=6.5m/min, Fine Dressing, Soft Material EN8

In Trial 7 the lowest μ was again obtained under MQL, and the highest again under DRY. WET performed with 18 per cent lower μ than DRY and 40 per cent higher than MQL.

The best cutting performance was produced by WET. The wheel did not experience excessive loading as in the previous Trial 4 (Chapter 7.3.2) even though in this trial a soft material and fine dressing were used, this was due to the high wheel speed which resulted in higher DOC, more effective cutting and an improved wheel cleaning situation.

The cutting efficiency of MQL was lower than that for WET (approximately 25 per cent) however, the value of μ was consistent with values from previous Trials.

Thus the value of μ in MQL is not as strongly affected as the other cases by dressing condition, speeds or material hardness. This is also the situation for specific material removal rate.

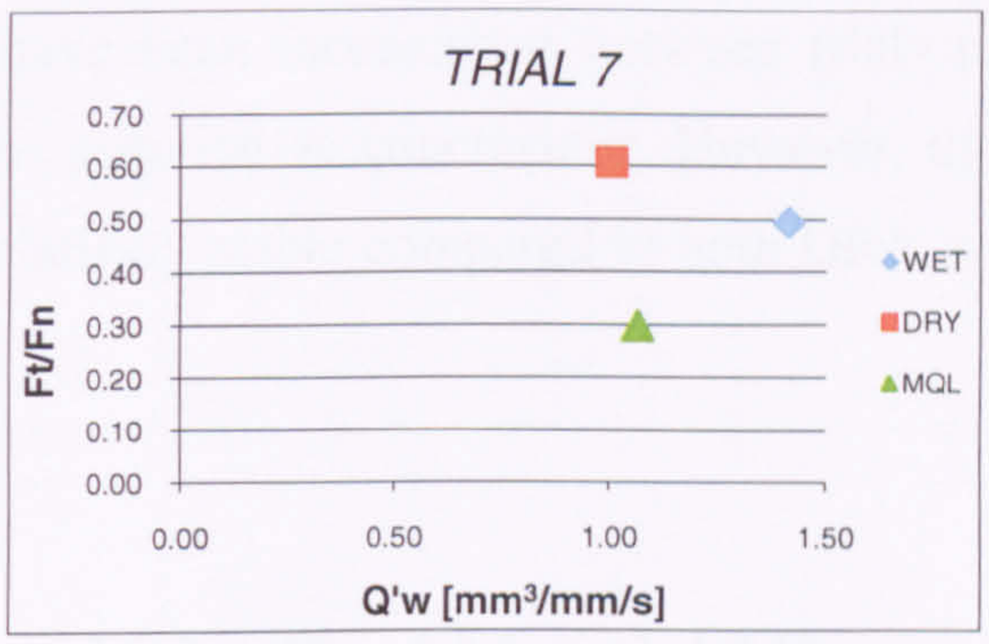

Figure 7-14. Coefficient friction F_t/F_n in function of specific removal rate Q'_w for material EN8.

7.3.4. Trial 8: v_s=45m/s, a_e=15μm, v_w=15m/min, Coarse Dressing, Hard Material EN31

In Trial 8 (Figure 7-15) the values of μ and Q'_w recorded for the case of MQL were very similar to those obtained in Trial 3 (Chapter 7.3.4). This result is consistent with other values i.e. speed ratio, material type and DOC in the two Trials being the same (or similar – speed ratio).

The value of Q'_w achieved in the case of WET however, was considerably higher in this trial than in Trial 3 despite the similar value of μ in both trials. This is difficult to explain in terms of speed effects due to the similar speed ratio in both Trials, though a difference in achieved DOC was recorded (6.9 μm Trial 3 – Chapter 7.3.1 and 4.8 μm Trial 8 – Chapter 7.3.4). Confusingly, the separate values of F_n and F_t in each trial were also very similar.

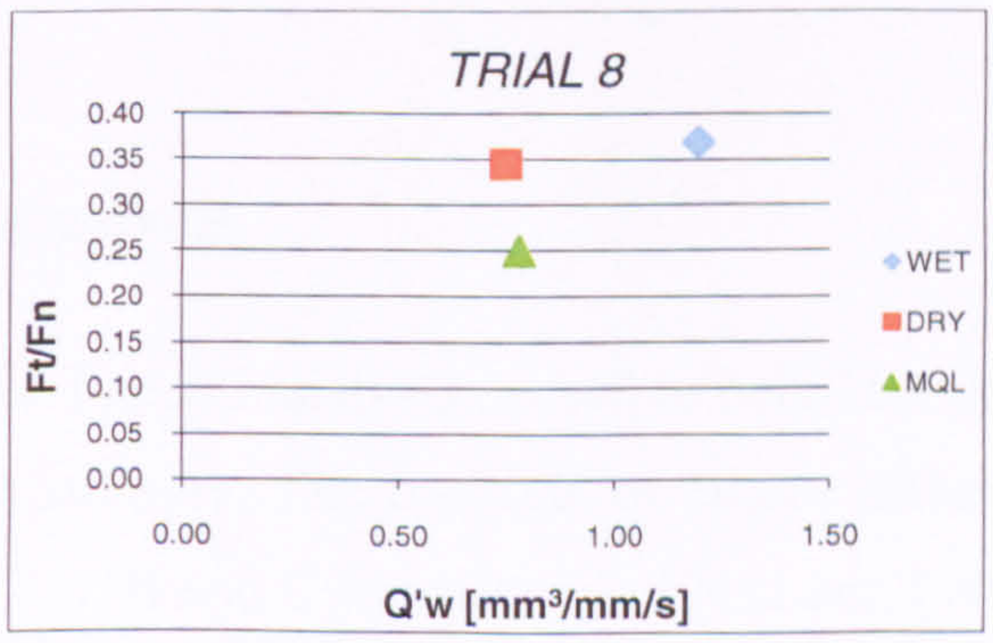

Figure 7-15. Coefficient friction F_t/F_n in function of specific removal rate Q'_w for hard material EN31.

The results for DRY have been inconsistent between trials presented and there are insufficient data to draw quantitative conclusions. However, the performance of MQL appears to have been relatively stable compared to both DRY and WET throughout the trials to this point.

7.3.5. Trials: 3 and 8 for Hard Material M2

The values of μ in Trial 3 compared to those values for the other hard material EN31 (previous section Chapter 7.3.1 – Trial 3) are seen to be very similar in all cases. The values of μ in Trial 8 compared to those values for the other hard material EN31 (previous section Chapter 7.3.4 – Trial 8) are also seen to be very similar in all cases.

The small discrepancies do not allow identification of any clear trend, however the results do inform us that there is no strong effect due to a difference in material hardness of the two 'hard' materials (EN31-HRC 62, M2 – 52HRC).

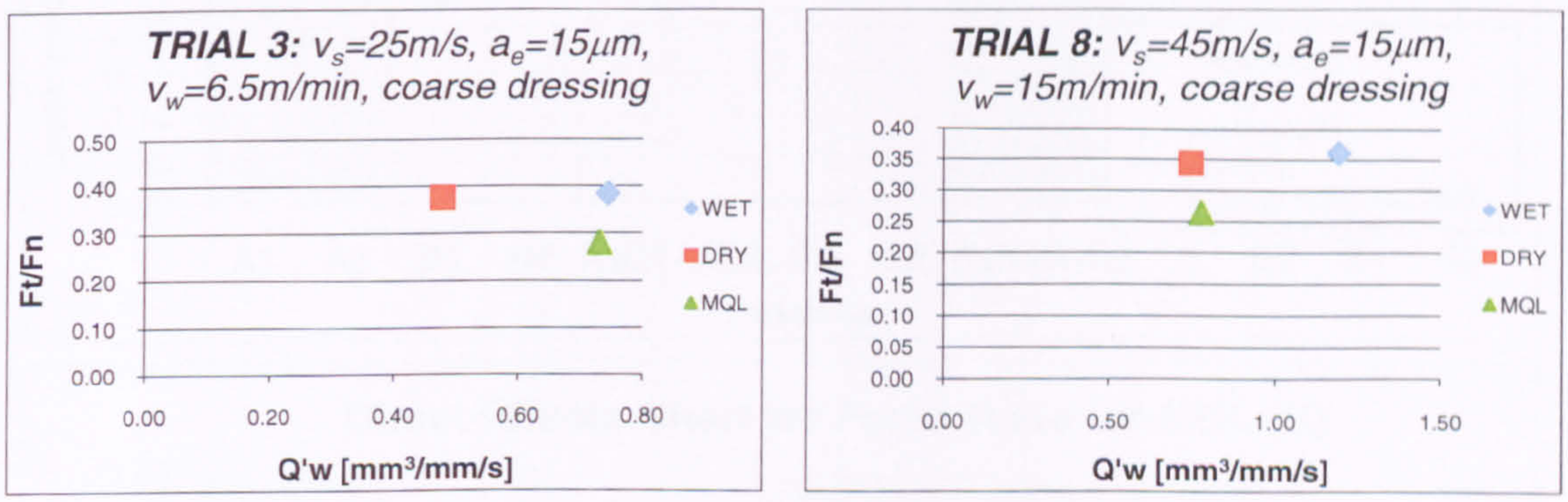

Figure 7-16. Coefficient friction F_t/F_n in function of specific removal rate Q'_w for hard material M2.

7.3.6. Taguchi Analysis

As stated previously, the Taguchi analysis is used to help identify those parameters that affect the process most strongly. The two sets of Direct Effects Charts generated are presented in Figure 7-17 A, B and C for materials EN31 and EN8 and Figure 7-18 A, B and C for materials M2 and EN8.

As discussed in section 7.2.10, a number of results were below the accepted threshold for reliability. Such results are highlighted in each direct effects chart. The full series of results are presented in the ANOVA Table in Appendix 9.

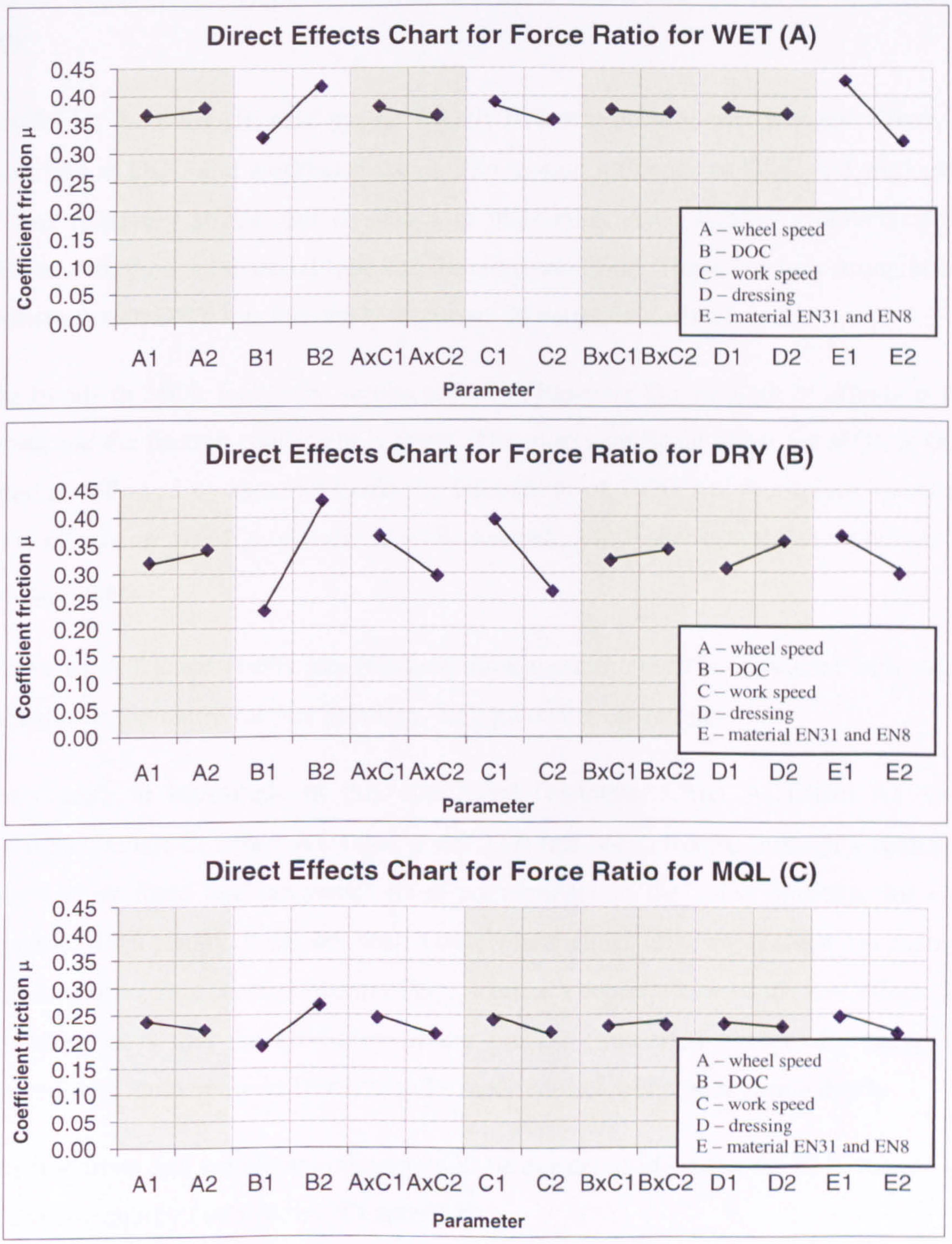

Figure 7-17. Direct effects chart for force ratio with EN31 and EN8.

In the case of WET (A) the material hardness produced the strongest effect. A similarly strong effect was observed for DOC. All other effects and interactions were weak. As identified and discussed in previous sections such effects would be expected to obtain a higher 'actual' DOC with soft material than for a harder material for an equal applied DOC.

Results for the DRY (B) case appear slightly different because the strongest effects are identified as DOC and workpiece speed. The mutual influence of DOC and workspeed is also relatively strong and is shown in interaction A-C. Further relatively strong effects were those of material type and dressing condition. These last two strong effects confirm that in DRY it is extremely important to maintain a wheel clean.

The trends in MQL look very similar to WET, however the strength of effects is less strong and the friction coefficient is lower. The most significant effect for MQL is DOC together followed by material hardness. Interaction of DOC and workpiece speed has some effects on the MQL process as well. According to Fisher criteria, other effects are not significant.

The value of friction coefficient obtained throughout the tests is consistent with values published in literature for fine grinding, high precision operations.

The change in magnitude of this coefficient (example: Chart A, Effect A1 value $\mu = 0.367$; Chart C, Effect A1 value $\mu = 0.237$) has been effected through a change in both normal force and tangential force components in the same direction for each situation. Importantly, it has not been a case where either force component has changed independently. This corresponds to effects seen as a consequence of the size effect. The size effect says that the efficiency of the process (measured by specific energy) is reduced with an increase in DOC, or to be more correct, grain penetration depth.

This important and significant outcome will be discussed in greater detail in the section on specific energy that follows (Chapter 7.6).

With the M2 and EN8 materials (Figure 7-18) the general performance is similar to that presented for EN31 and EN8.

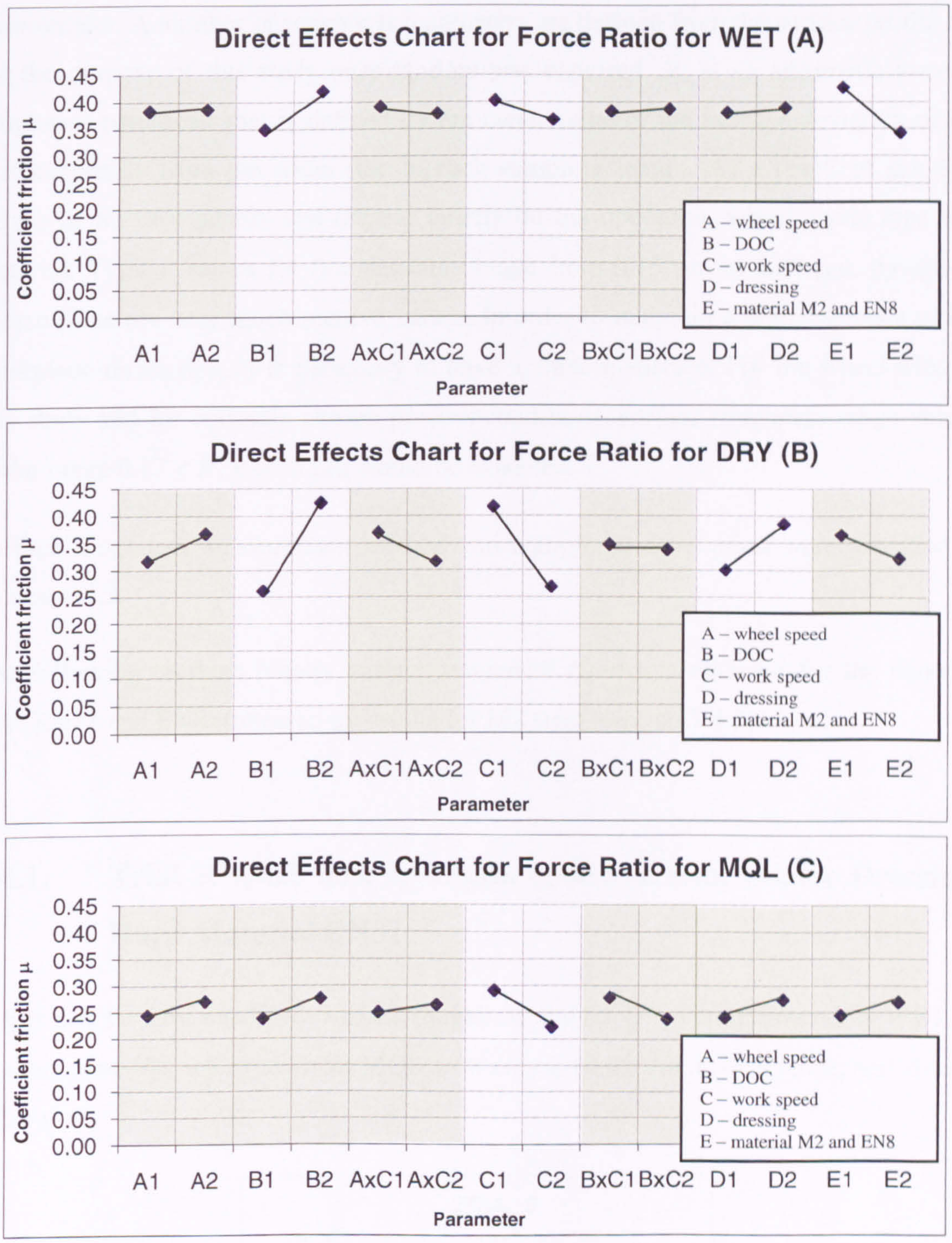

Figure 7-18. Direct Effects chart for force ratio with M2 and EN8.

7.4. Surface Roughness R_a

Surface texture refers to the characteristic pattern of undulations on the workpiece. The surface roughness requirement is often a consequence of the dimensional tolerance

requirement. A number of roughness parameters are defined from the surface profile but for the purpose of this study only R_a data was captured. R_a is an arithmetic average roughness parameter that is defined by the mean value of the average deviation of the surface profile from the mean line in each sampling length. As a result of grinding values of R_a vary greatly and depend largely on the operation, wheel, cycle type and material. Typical values for fine finishing range from 0.15 μm to 2.50 μm, though of course these are very much relative values. In order to maintain a high tolerance of the workpiece dimension, it is necessary to have a smooth surface. For the wheel used in this study and for correctly chosen process conditions, surface roughness range values in the range $0.17 < R_a < 0.25$ μm would be expected.

Surface roughness measurement method and equipment description were provided in section 6.4.3.

The following sections present surface roughness R_a results obtained for the material pair: EN31 and EN8, followed by results for M2 steel (section 7.4.5).

7.4.1. Trial 3: v_s=25 m/s, a_e=15μm, v_w=6.5 m/min, Coarse Dressing, Hard Material EN31

In this trial the best results for surface roughness and for Q'_w were produced by WET. A similar value was achieved under MQL with only a +0.02 μm R_a difference, and similar Q'_w value.

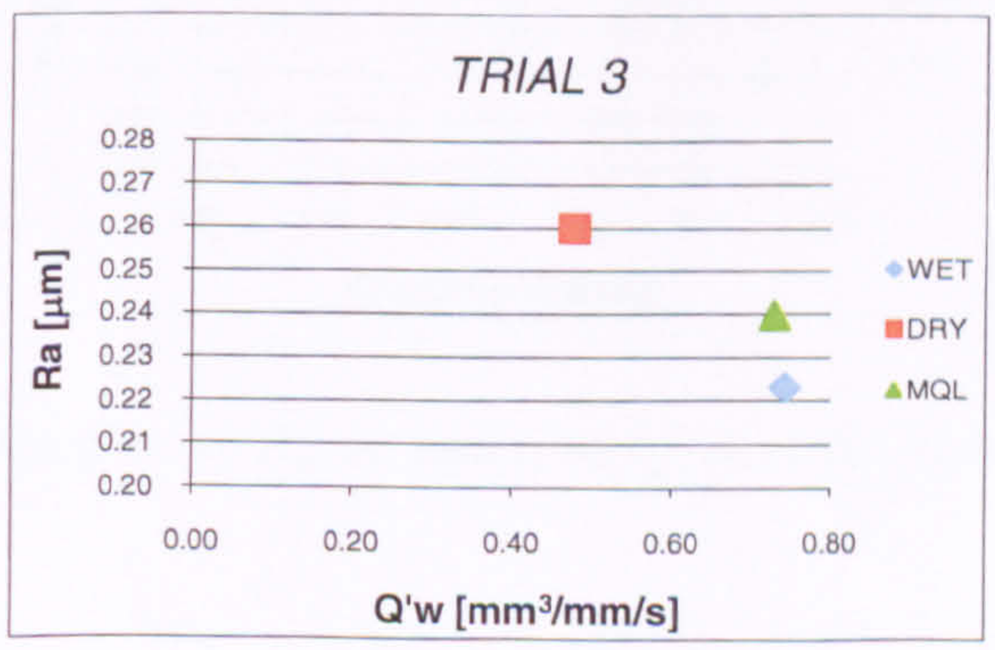

Figure 7-19. Surface roughness R_a in function of specific removal rate Q'_w for hard material EN31.

DRY produced a surface with 0.04 μm rougher R_a than that attained by either MQL or WET at a value of Q'_w 60 per cent lower. This poorer performance results from lack of lubrication, cooling and chips removal and consequent low Q'_w. In general however, the surface roughness for all grinding methods is very good and meets the R_a = 0.17-0.25 μm expectations.

7.4.2. Trial 4: v_s=25m/s, a_e=15μm, v_w=15m/min, Fine Dressing, Soft Material EN8

In this case the lowest surface roughness was obtained in MQL, which also achieved the highest Q'_w. The WET surface was 0.05 μm rougher and value of Q'_w approximately 25 per cent lower. The combination of soft material, fine dressing and low wheel speed resulted in the poorer WET surface roughness. However the conditions were favourable for MQL and though the wheel speed was low (grains need to remove more material in a unit of time when compared with higher wheel speed what leads to worse surface production) the good lubrication of the MQL oil and lack of hydrodynamic effects contributed to the better performance. Presumably, the surface roughness in MQL could have improved had efficient wheel cleaning been present. Again, in general WET, DRY and MQL produced very good surface roughness values.

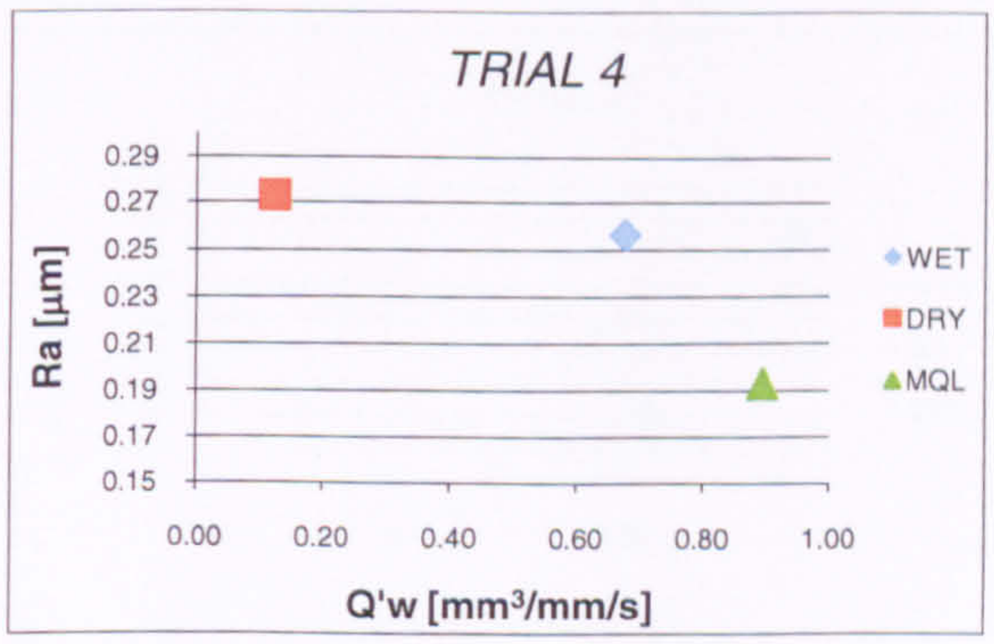

Figure 7-20. Surface roughness R_a in function of specific removal rate Q'_w for soft material EN8.

7.4.3. Trial 7: v_s=45m/s, a_e=15μm, v_w=6.5m/min, Fine Dressing, Soft Material EN8

In this trial, at the higher wheel speed, the WET case produced the highest R_a though also achieved the highest Q'_w.

MQL achieved the best surface finish though not quite as good as in previous trials. The reason for this is that at this higher wheel speed individual grains remove less material in each pass (in a single second a grain may make a number of passes resulting in a higher specific (unit time) material removal rate though lower material removal rate per pass – i.e. at v_s = 25 m/s single grain contact time will be $t \approx 38$ ms, whereas at v_s = 45 m/s contact time $t \approx 21$ ms, which leads to the conclusion that at v_s = 45 m/s the grain will pass 2 times more than at v_s = 25 m/s). In such a case a smoother surface is generated. The results, in contrast, do not show this tendency, though the difference in R_a between low speed and high wheel speed is marginal at 0.05 μm. This could be due to the experimental procedure used in which no spark out passes were applied.

Again, it is reasoned, that if efficient wheel cleaning was in place for MQL, it would have produced not only the best surface roughness but also the best cutting efficiency. In this case only MQL managed to fit into R_a = 0.17-0.25 μm, yet DRY and WET results still are very reasonable.

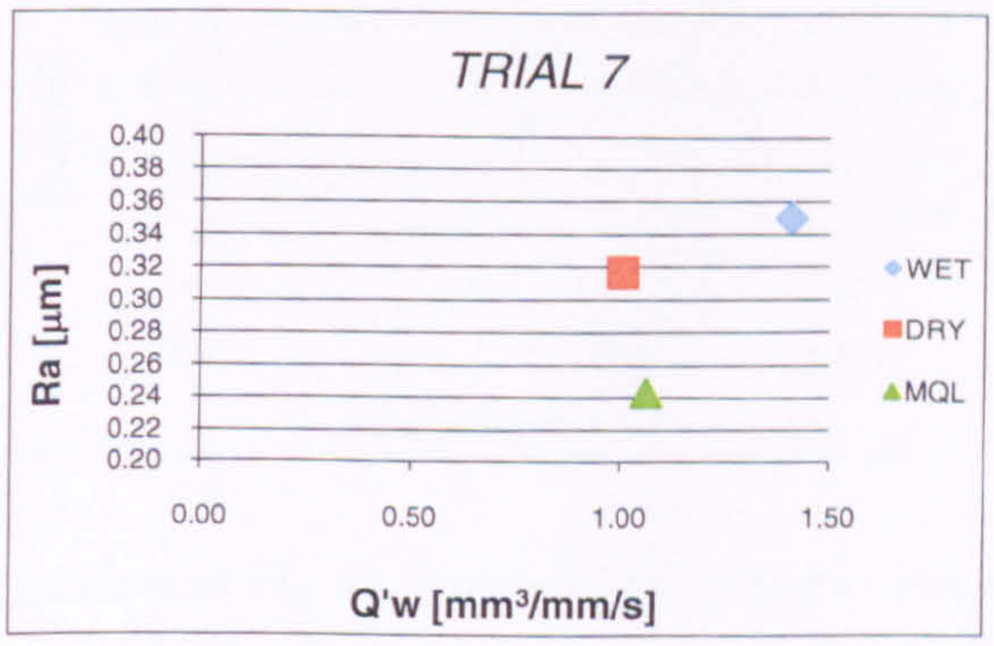

Figure 7-21. Surface roughness R_a in function of specific removal rate Q'_w for soft material EN8.

7.4.4. Trial 8: v_s=45m/s, a_e=15μm, v_w=15m/min, Coarse Dressing, Hard Material EN31

In Trial 8, WET performed the best by producing a good surface finish and high Q'_w. Despite a large DOC, coarse dressing and Hard material MQL did not perform as well as WET. Both DRY and MQL achieved only approximately 60 per cent of the Q'_w achieved in WET. The very good WET performance can be explained by the combination of high wheel speed and hard material favoured by this specific grinding wheel (WA100JV) with a purpose of delivering a fine finish. This is consistent with many of the previously discussed results that have suggested wheel loading in WET is more problematical with the soft material with this given wheel.

Conversely, similar Q'_w values for MQL and DRY may be a result of inefficient wheel cleaning and its specification (fine grains, low porosity). A partial wheel loading is assumed to increase surface roughness. The lubricating fluid in some way countered this effect in the case of MQL. It is reasoned therefore that if better wheel cleaning conditions were in place, both cutting efficiency and surface roughness would be improved. In general all grinding methods produced reasonably good results and only the DRY surface quality is outside (marginally) the range: $0.17\mu m < R_a < 0.25\ \mu m$.

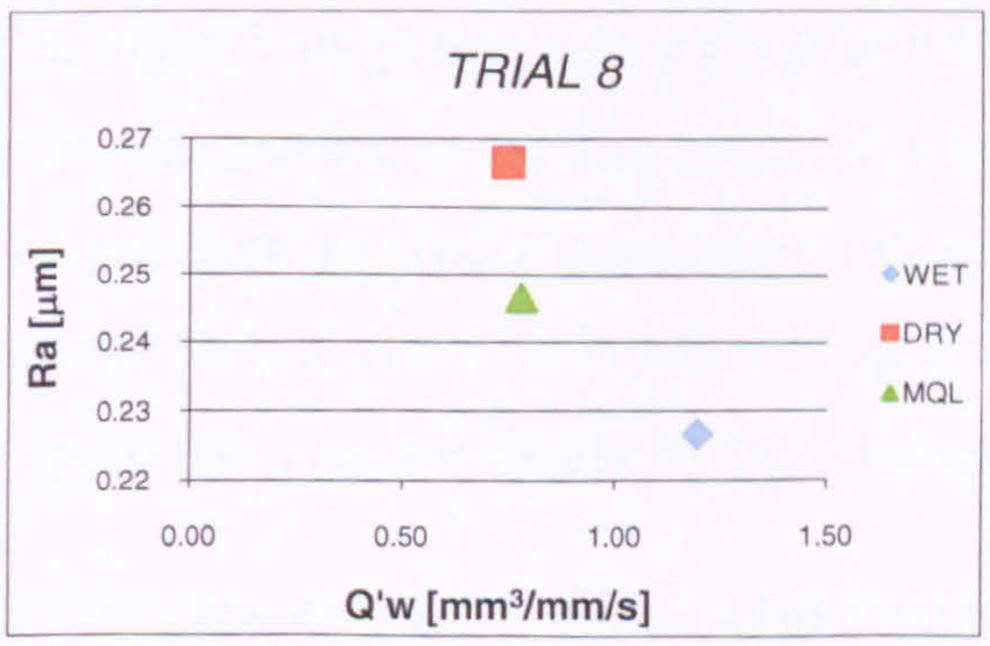

Figure 7-22. Surface roughness R_a in function of specific removal rate Q'_w for hard material EN31.

7.4.5. Trials: 3 and 8 for Hard Material M2

In Figure 7-23 in Trial 3 further differences in the performance of each method can be seen. MQL produced not only the finest surface finish but also the highest Q'_w. The

WET method achieved a similar Q'_w to that in MQL however the R_a value was approximately 0.05 μm higher. This situation was opposite to that obtained for EN31. A better R_a was achieved with M2 than EN31 under MQL, which is slightly softer than EN31. For the case of WET, the value of R_a was similar both for M2 and EN31, whereas for DRY it worsened. It is of note that surface finish results for MQL and WET are consistently within the range expected and vary only marginally across the series of tests.

Figure 7-23. Surface roughness R_a in function of specific removal rate Q'_w for hard material M2.

7.4.6. Taguchi Analysis

In Figure 7-24 direct effects charts are presented for EN31 and EN8 materials. For WET trials the strongest effect is material hardness. The effect of wheel dressing is relatively strong and this would be expected as wheel topography influences surface roughness directly. A further relatively strong effect is workpiece speed, though consideration needs to be given to the speed ratio, shown clearly by the interaction AxC.

For DRY effects look similar, however ANOVA analysis suggest that the effects from wheel speed and its interactions are less significant. The tendency of the effects and their strength are similar to those in WET.

The composition (strength and tendency) of the effects in MQL appear similar to those in WET. However, the strongest effect is the dressing condition and the second strongest effect material hardness. The DOC has a stronger effect in WET, though not as strong as for DRY. Based on ANOVA, the interaction of DOC and workpiece speed is not significant (less than 95 per cent) for this process.

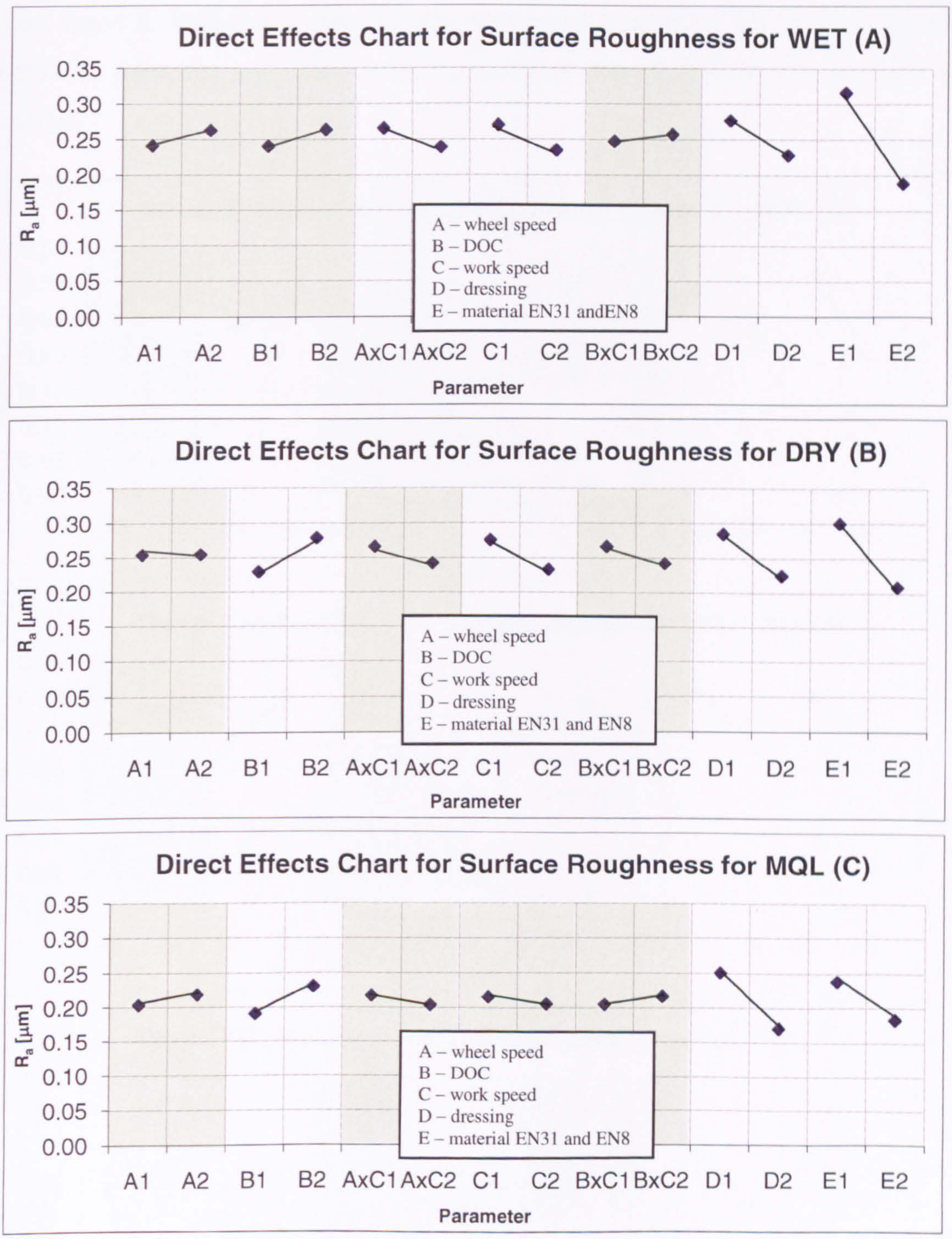

Figure 7-24. Direct effects chart for surface roughness with EN31 and EN8.

Finally Figure 7-25 gives a comparison of M2 and EN8 materials. For WET, the composition of the effects is similar to that determined for EN31 and EN8 materials. However the DOC, the wheel speed and the workpiece speed influence the process moderately. Also for MQL and for DRY the situation looks similar, however the material (soft-hard) and dressing conditions seem to have similar effect, whereas the

wheel speed in MQL has a greater influence on the process for EN31 than with EN8. The DOC does not have such a strong effect as was found for the previous hard material.

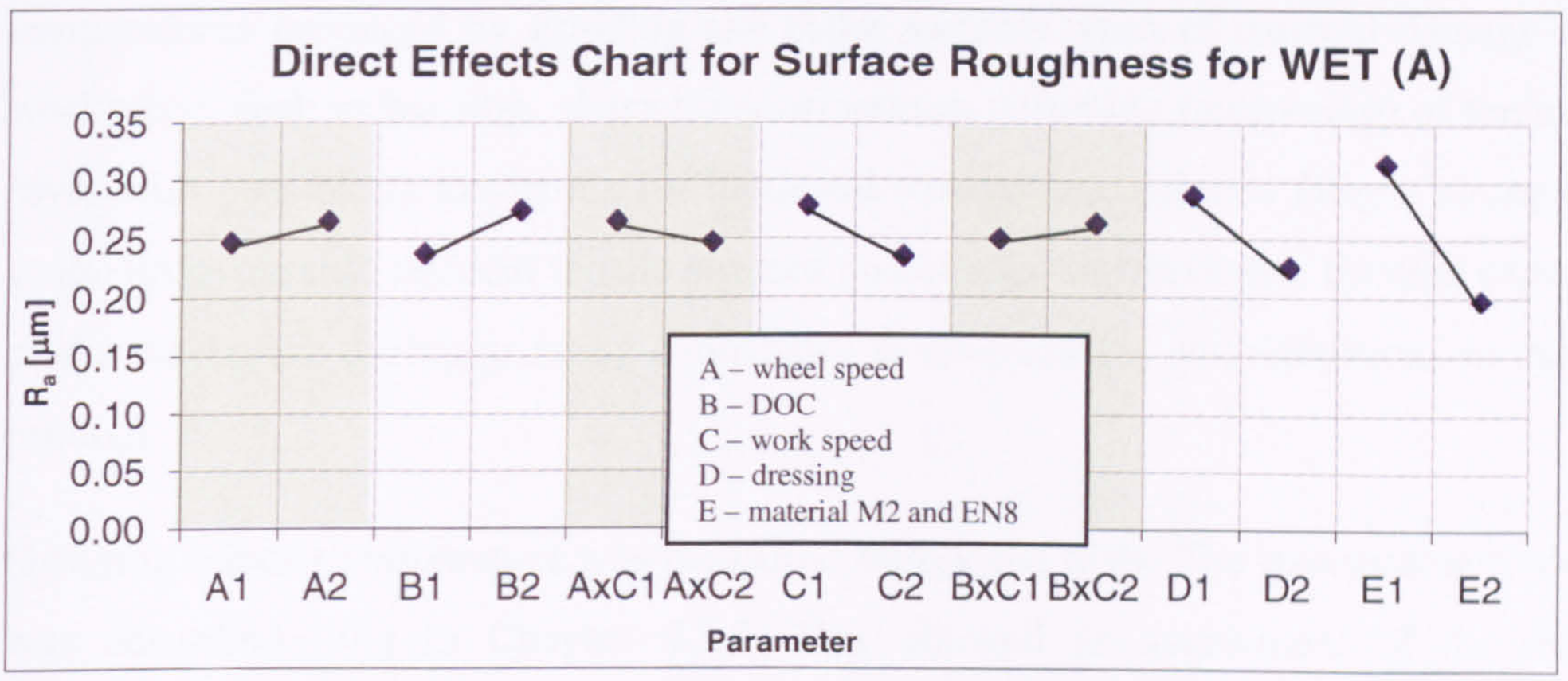

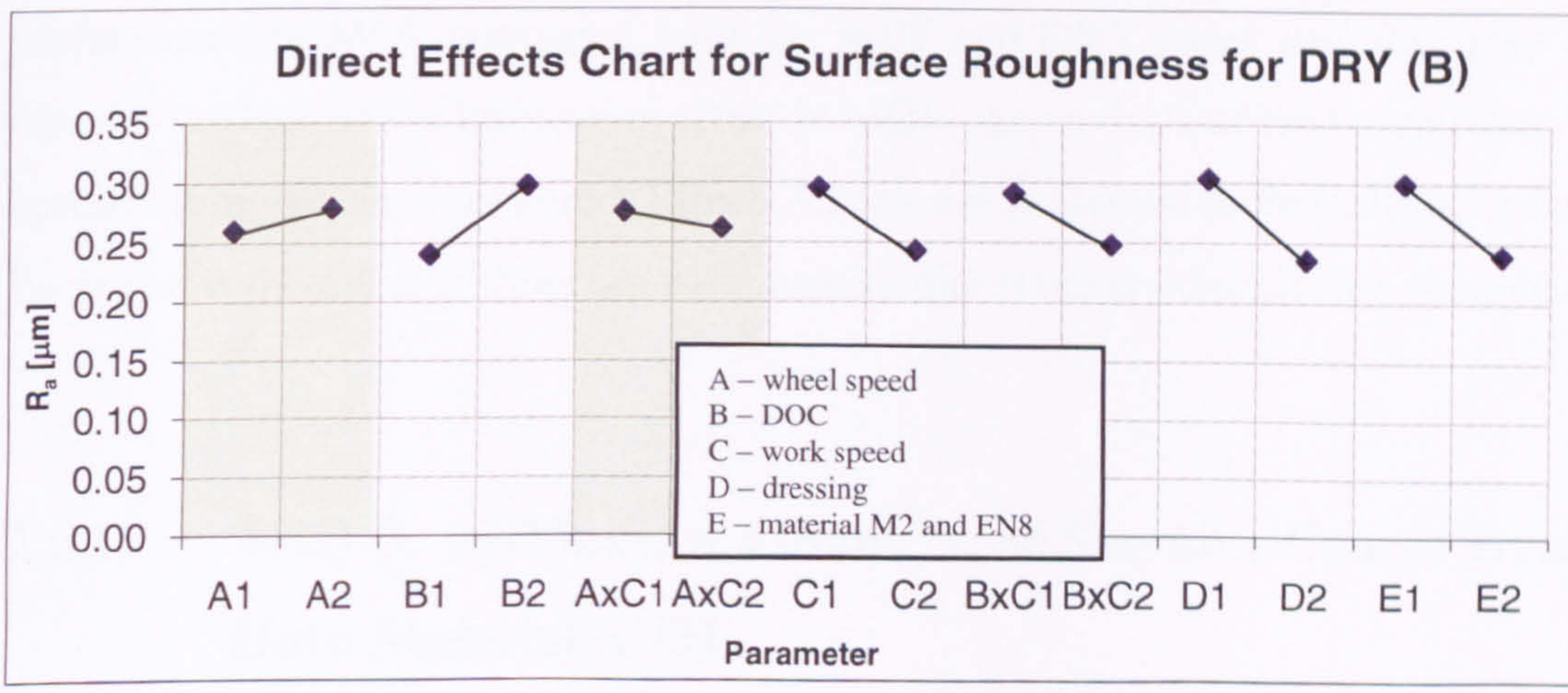

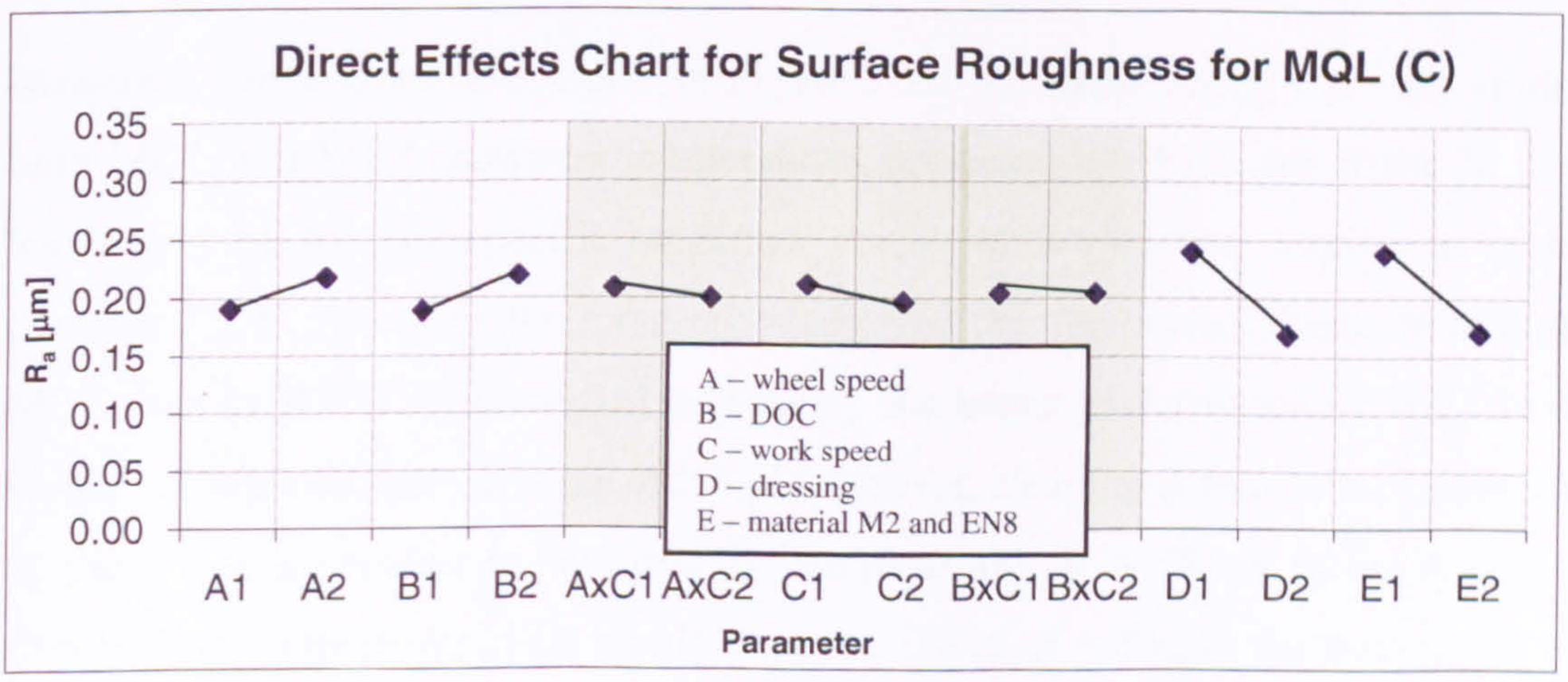

Figure 7-25. Direct effects chart for surface roughness with M2 and EN8.

7.5. Grinding Process Temperature

The temperature generated in grinding can be the limiting factor to target. The high temperatures produced by grinding can cause various types of thermal damage to the workpiece, such as burning, phase transformations, softening (tempering) of the surface layer with possible re-hardening (of hardened workpiece), reduced fatigue strength due to the unfavourable residual tensile stresses and cracks. Furthermore, thermal expansion of the workpiece during grinding contributes to inaccuracies and distortions in the final product.

Grinding contact temperature was measured during the tests. The measurement method was described fully in Chapter 6.3.5. This allowed an assessment of the thermal performance of MQL compared with the WET and DRY cases and also gave insight into the strength of the lubrication effect in MQL. An analysis of the temperature versus specific removal rate and Direct Effects Charts are presented in the following sections. Each plot is the mean of three separate measurements obtained under the same settings.

7.5.1. Trial 3: v_s=25m/s, a_e=15μm, v_w=6.5m/min, Coarse Dressing, Hard Material EN31

Measured temperatures are shown in Figure 7-26. The achieved Q'_w is very similar for both MQL and WET, however temperatures produced by WET are about 20 per cent lower than MQL. The specific tangential forces were also very similar in each case (Section 7.2.3). However, the force ratio indicated that the normal forces were higher in MQL than in WET. As identified previously the better performance of WET is due to higher cutting efficiency and the effect of improved cleaning action of the larger volume of fluid. It is interesting to note that the temperatures in WET are in the region of the film boiling temperature. This would have the effect of reducing the convection ability of the fluid and hence give rise to higher local temperatures.

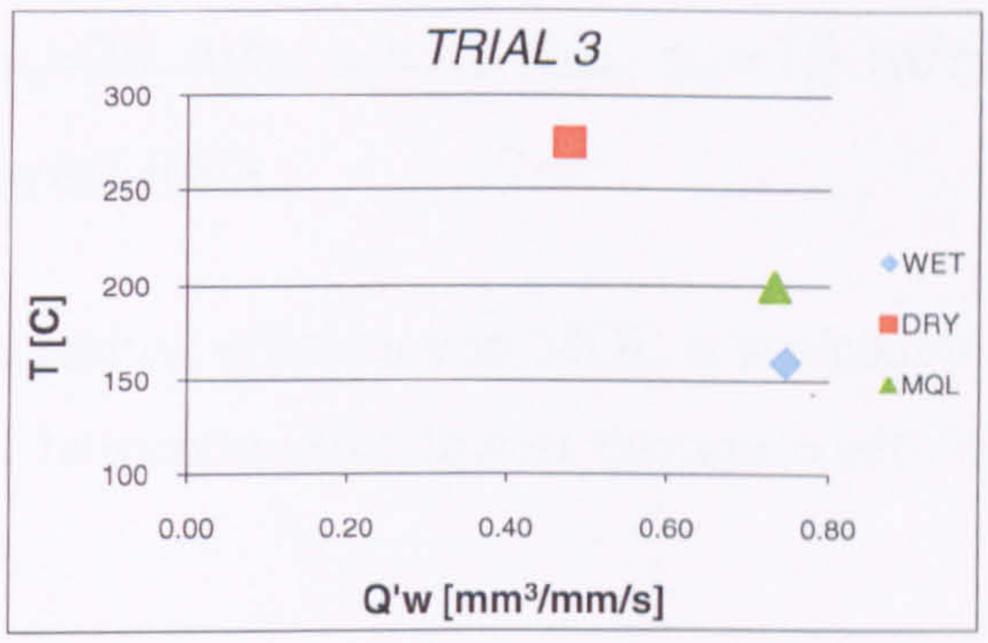

Figure 7-26. Temperature as a function of specific removal rate Q'_w for hard material EN31.

7.5.2. Trials 3: v_s=25m/s, a_e=15μm, v_w=6.5m/min, Coarse Dressing, Hard Material M2

Results are presented for M2 steel in Figure 7-27. In this trial, performance under all conditions is seen to improve.

It is also seen that M2 steel is an easier to machine material than EN31 (the HRC value is approximately 10 lower than that of EN31) and in general returns better results (i.e. lower temperatures) for MQL and DRY. This may also be due to the different material properties, especially thermal conductivity and specific heat capacity. This will be explored in further detail in the following Chapter.

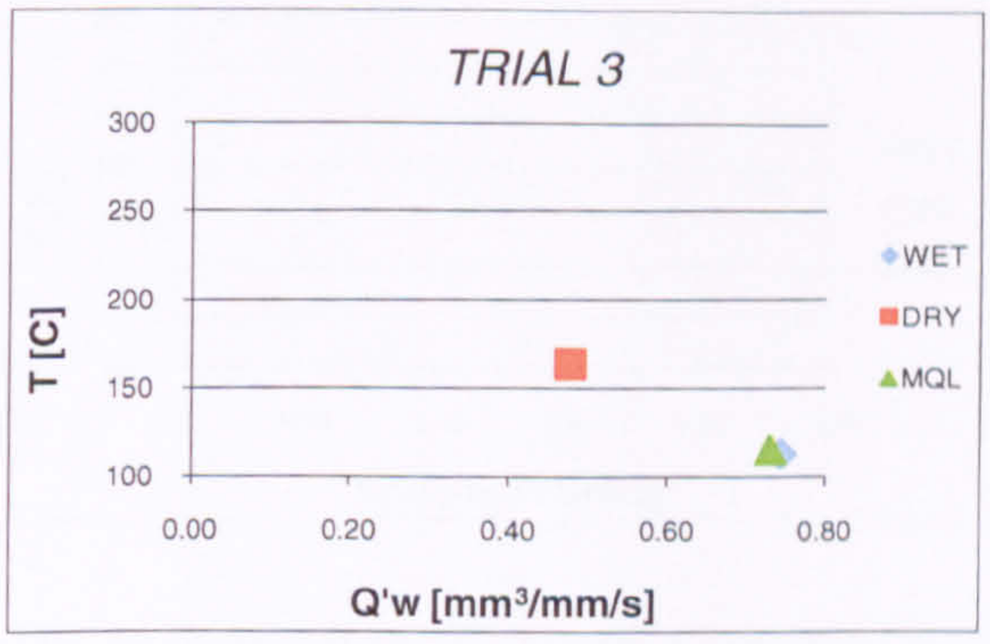

Figure 7-27. Temperature as a function of specific removal rate Q'_w for hard material M2.

A similar value of Q'_w is achieved in both WET and MQL and importantly a very similar temperature results. This indicates a comparable, and almost equal, performance of MQL to WET for the stated conditions.

7.5.3. Trial 4: v_s=25 m/s, a_e=15 μm, v_w=15 m/min, Fine Dressing, Soft Material EN8

In Trial 4 the improved cutting efficiency in MQL is noticeable. This is due largely to the combined effects of lubrication (the lowest friction coefficient was recorded under MQL) and soft material.

In the case of DRY, where the process was highly inefficient, the grinding temperature was relatively high for the low Q'_w value achieved. The reason for low cutting efficiency was reasoned to be the fine dressing parameters and soft material. There is additionally a problem with lack of wheel cleaning in DRY.

The wheel (fine abrasive and low porosity) tended to struggle with performance under the WET condition as it was not suited to this application. In this situation, material would flow plastically upwards and sideways but not be removed productively (i.e. sliding and ploughing components dominate). This would result in higher temperatures, again exceeding those of film boiling.

The high value of Q'_w achieved in MQL indicates a very effective and efficient grinding situation. This demonstrates strong promise for MQL in this region.

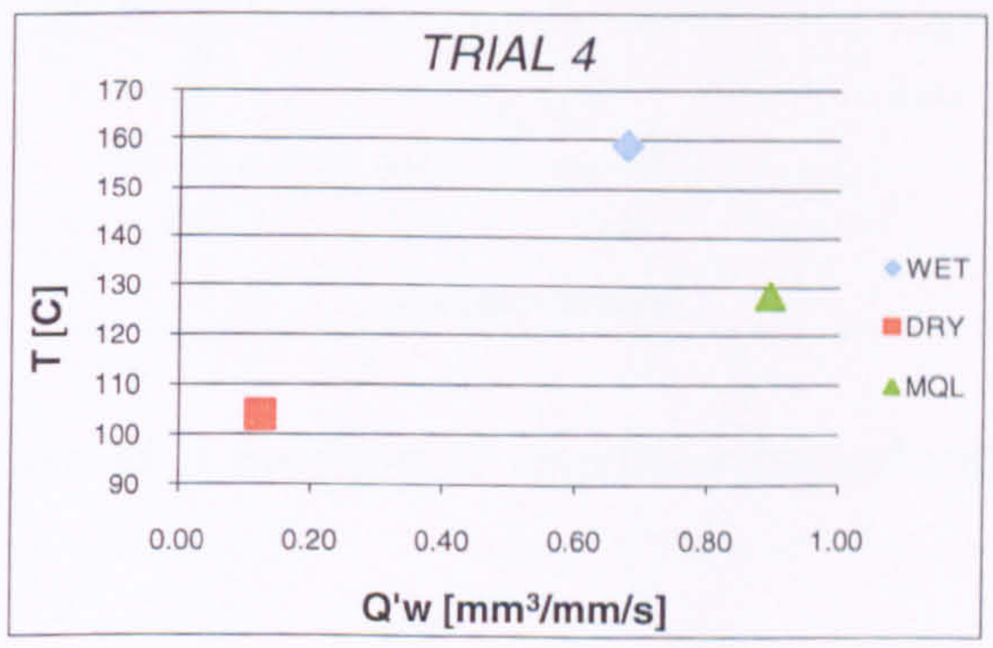

Figure 7-28. Temperature as a function of specific removal rate Q'_w for soft material EN8.

7.5.4. Trial 7: v_s=45m/s, a_e=15μm, v_w=6.5m/min, Fine Dressing, Soft Material EN8

In Trial 7 the highest temperature occurred under WET, and lowest under MQL. The low temperature in MQL was reasoned to be due to the better lubrication conditions (again, the lowest friction coefficient was recorded in MQL).

The highest temperature was recorded under WET, which also achieved the highest value of Q'_w value. The WET temperature, which was 25 per cent greater than that in DRY, would imply film boiling but with effective flushing aiding the achievement of a higher Q'_w than in DRY.

The value of Q'_w was similar for both DRY and MQL, the lower temperature in MQL resulting from the effects of lubrication.

It is of note that WET and DRY cases produced relatively high temperatures and were at a value associated with a high risk of thermal damage.

Figure 7-29. Temperature as a function of specific removal rate Q'_w for soft material EN8.

7.5.5. Trial 8: v_s=45m/s, a_e=15μm, v_w=15m/min, Coarse Dressing, Hard Material EN31

Results for Trial 8 are given in Figure 7-30. WET achieved the highest value of Q'_w, the performance of both MQL and DRY were similar. The lowest temperature also occurred in WET. The wheel favours (is designed for) the conditions of hard material,

high speed and coarse dressing in the WET situation and this would account for the good performance of WET and the lower resulting temperature.

The temperature in DRY is considerably higher than that in MQL. This is reasoned to be due to the wetting of the grains in MQL, which aids chip removal, reduces loading and hence results in more efficient grinding. This was evidenced through the lower force ratio and better surface finish measured for MQL.

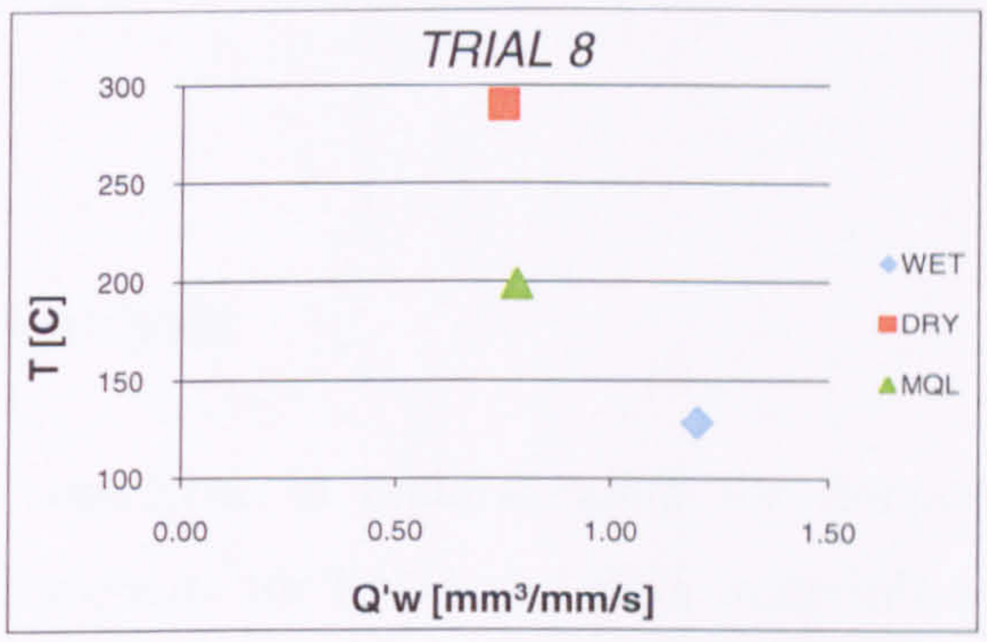

Figure 7-30. Temperature as a function of specific removal rate Q'_w for hard material EN31.

7.5.6. Trial 8: v_s=45m/s, a_e=15μm, v_w=15m/min, Coarse Dressing, Hard Material M2

Results are presented for M2 steel in Figure 7-31. It is seen again, that M2 steel is an easier to machine material than EN31 and in general produces lower temperatures for MQL and DRY.

In this trial, a large decrease in temperature is seen under DRY compared to the case for EN31. The surface finish and force ratio in MQL are each lower than that achieved in DRY. This is an unexpected result difficult to explain entirely through possible erratic thermocouple performance. Nor was it possible to see changes that may have occurred in subsequent tests because Trial 8 was the last of all tests and the results were analysed at a later date.

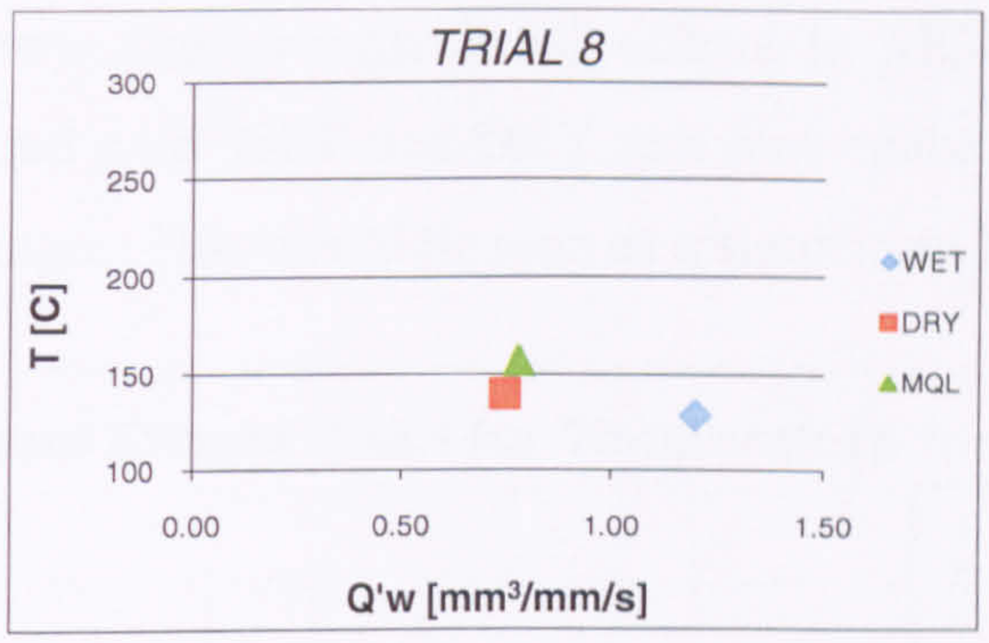

Figure 7-31.Temperature as a function of specific removal rate Q'_w for hard material M2.

7.5.7. Taguchi Analysis

Taguchi analysis may contribute to understanding the temperature results presented previously. Direct Effects charts for EN31 and EN8 materials are given in Figure 7-32 (A, B and C). As previously, significance of highlighted effects is below 95 per cent threshold.

Results (A), show that DOC has a strong effect on temperature in the case of conventional cooling. The second strongest effect is material type, and much lower temperatures occurred with the soft material under the condition of fine dressing and high wheel speed.

Further strong effects influencing grinding temperature are the dressing condition, wheelspeed and workpiece speed. Each of the interactions indicated a relatively strong effect on temperature and this would be consistent with the effects of the parameters singly.

In the case of DRY the most significant effect is DOC. Wheel speed and workspeed effects are also similar to those in WET and the tendency is in the same direction. However, the effects of dressing and material type have opposite tendencies to those observed in WET. A softer material and fine dressing is favoured in DRY.

The strongest effect in MQL is DOC. It is followed by interactions of workpiece speed and wheel speed, and then wheel speed-workpiece speed. Further effects are all reduced compared to the cases of WET and DRY (the effect of dressing is assumed unimportant

according to Fisher test). The strength of all effects in MQL (excepting DOC) is relatively weak compared with WET and DRY and may make the MQL process less sensitive to process changes. This would be seen as a significant benefit.

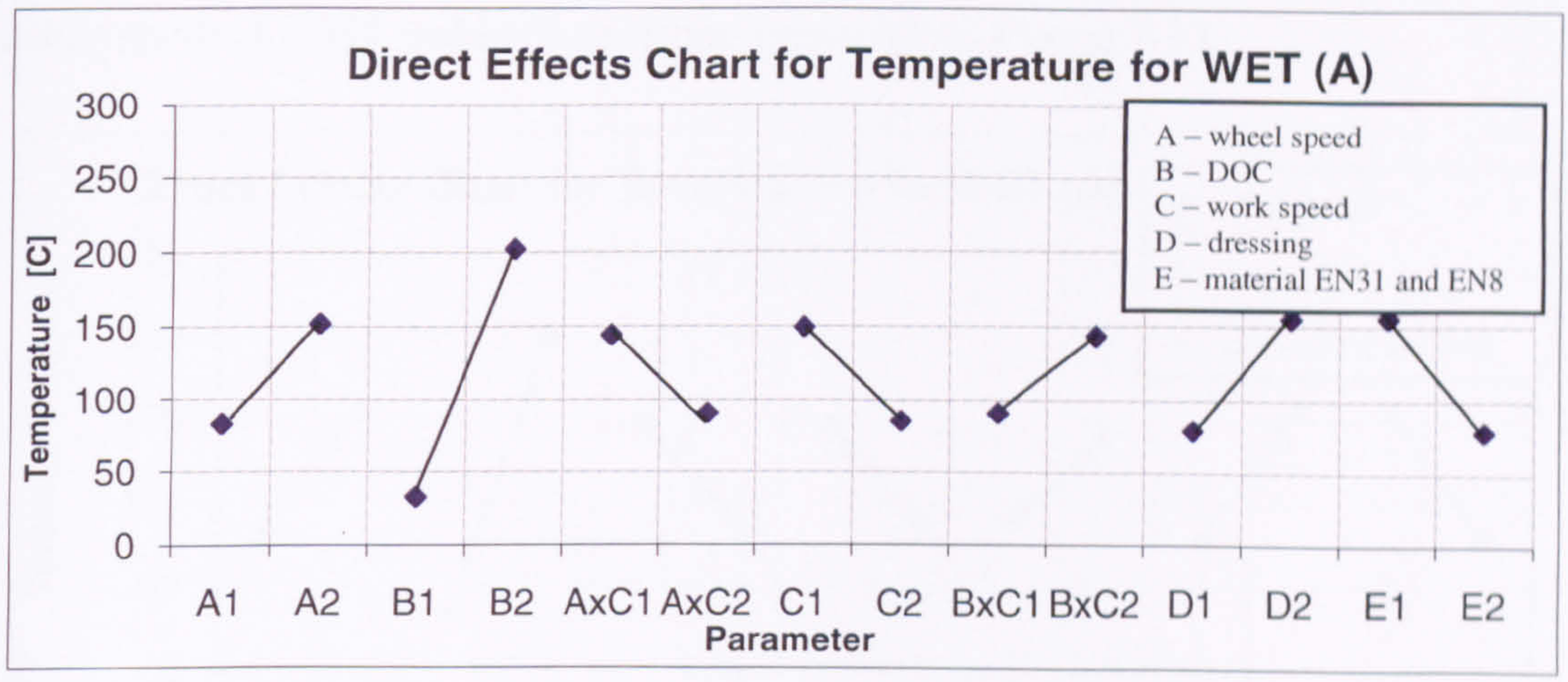

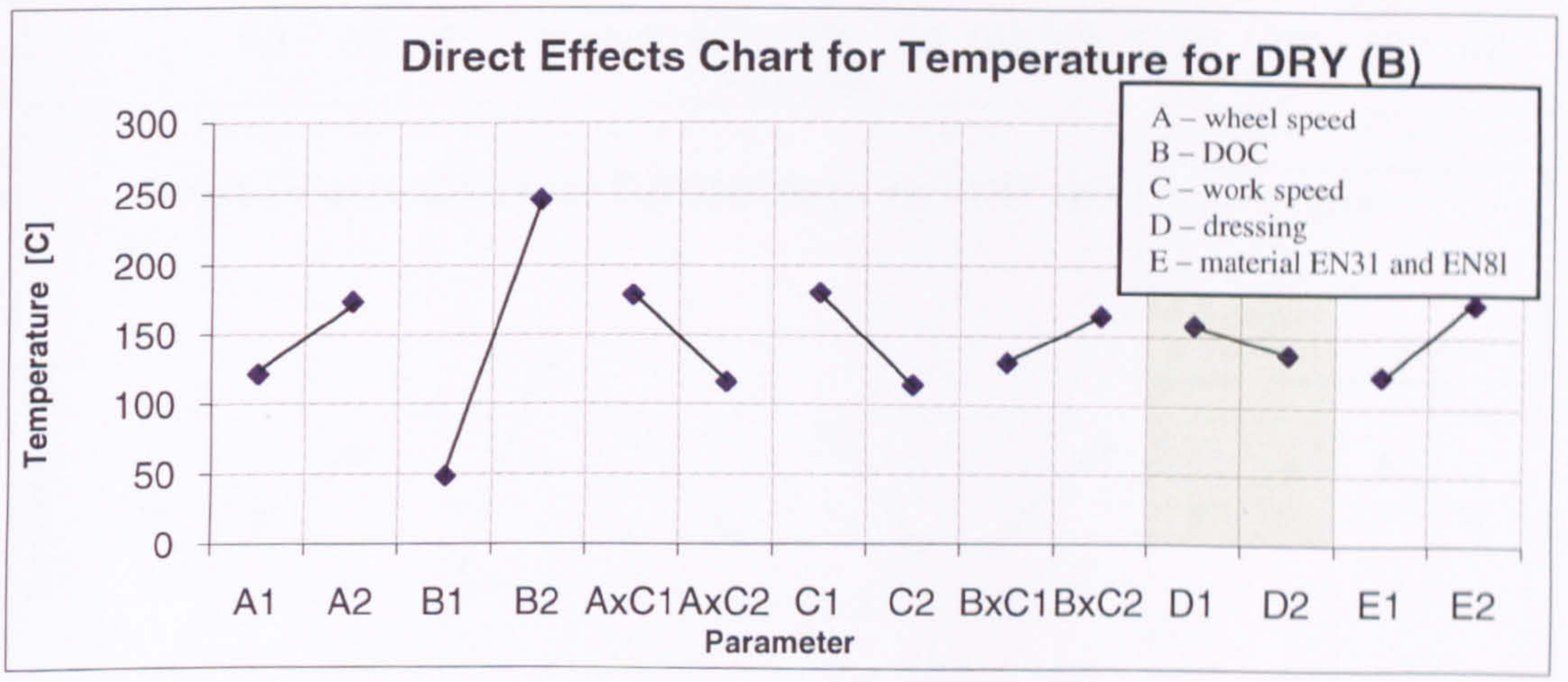

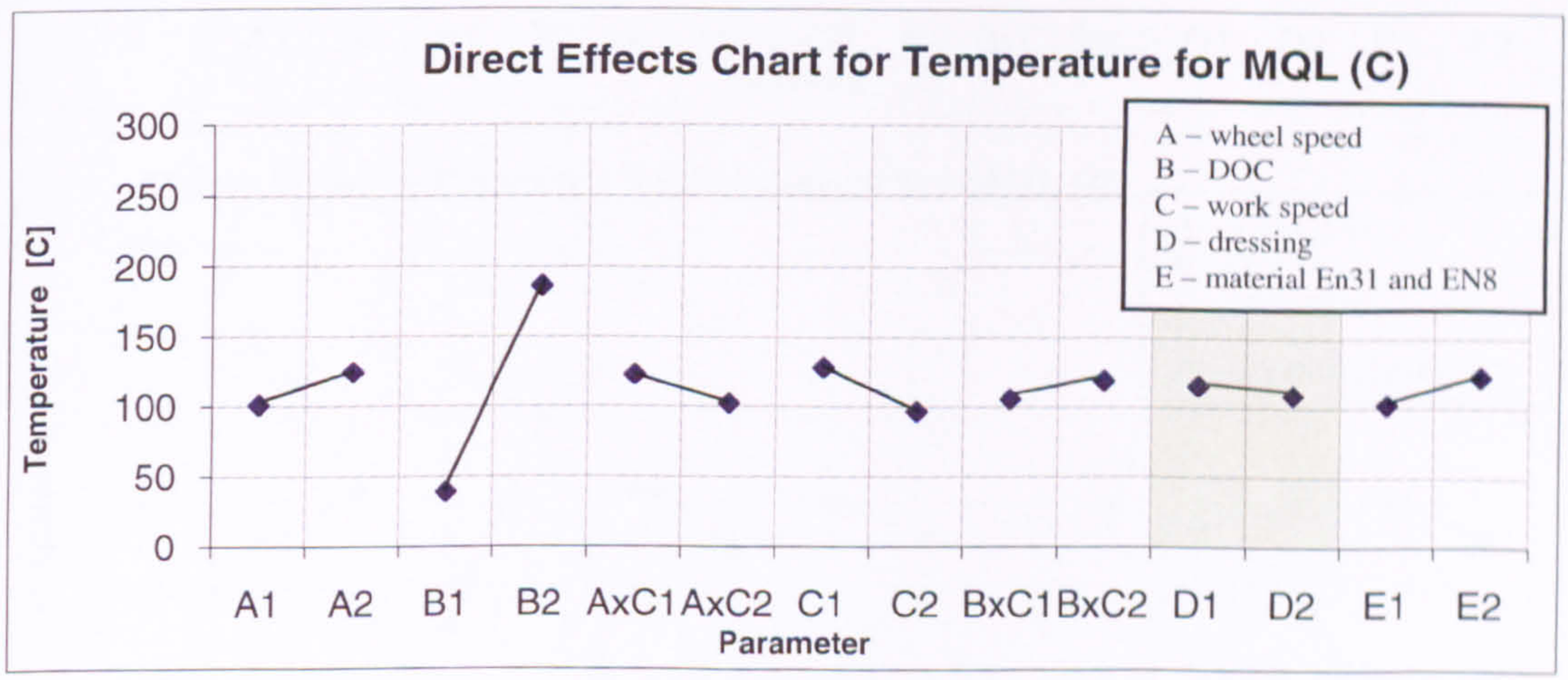

Figure 7-32. Direct effects chart for temperature with EN31 and EN8.

What can also be seen from the above Direct Effects Charts is that the DOC is strong in all cases and strongest in DRY. This is consistent with the kinematics of the process.

The effects of dressing type and material type are in opposite directions for WET compared to DRY and MQL. This is reasoned to be due to the better wheel cleaning capacity of WET and the wheel grade.

Further results for M2 and EN8 steels are presented in Figure 7-33.

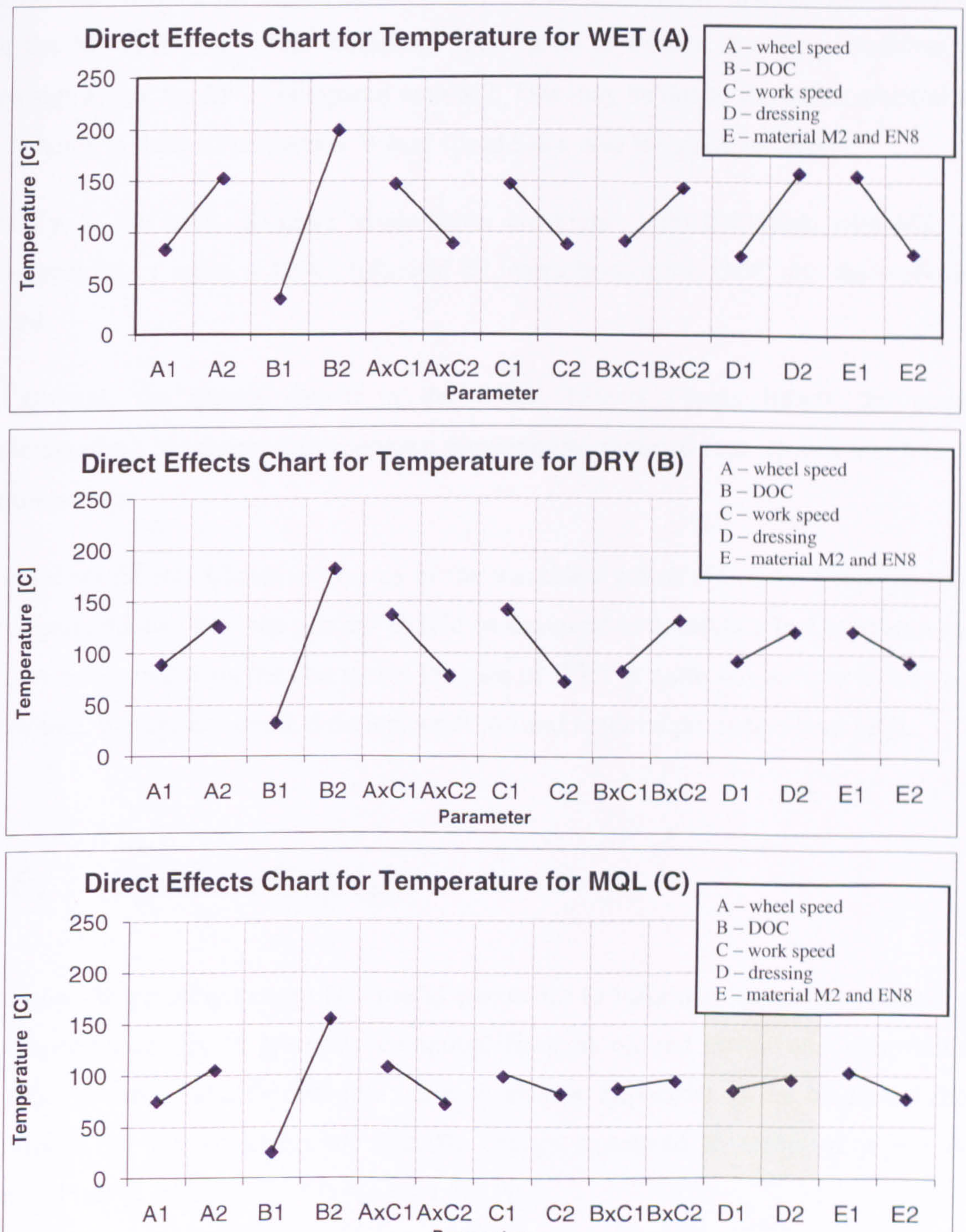

Figure 7-33. Direct effects chart for temperature with M2 and EN8.

It appears that for WET the significance levels are very similar when compared with EN31 steel. According to ANOVA the significance of effects is in following order: the DOC, dressing condition, material, followed by the wheel speed, the workpiece speed, and the two interactions.

In the case of DRY the significance of DOC for the EN31-EN8 is much lower than that for the M2-EN8 pair, while workpiece speed level is similar. Dressing condition was less significant for EN31 compared with M2. This may be due to the softer material and difference in thermal properties. Wheel speed has a near insignificant effect.

Finally, in the MQL grinding temperatures are higher with EN31than with M2. The strongest effect again is DOC, followed by interaction of the DOC and the workpiece speed.

In general, the results shown in the Direct Effects Charts follow the general understanding of relationships between temperature, removal rate, speeds and material hardness/type.

The Direct Effects Charts inform us of the variables, which affect the temperature the strongest and also how the process should be designed to generate a low temperature. It is also noticeable from the charts that the case of WET is more sensitive to factors such as: wheel, workpiece speed, dressing condition and material properties than MQL.

7.6. Specific Energy

The specific grinding energy is a useful parameter to inform us of process efficiency. The specific energy is generally computed from monitored power and programmed material removal rate. Grinding power may also be expressed as the tangential force multiplied by the wheel speed. Specific energy expressed in terms of power and removal rate is (equation (4.13), Chapter 4.3.1):

$$e_c = \frac{P}{Q_w}$$

where Q_w (material removal rate) and is defined by (equation (4.14)):

$$Q_w = v_w \, a_e \, b$$

It can readily be deduced that graphs for specific energy against specific removal rate give the same trends as the specific tangential force results. However, the results for Taguchi differ and provide further insight into the comparative performance of MQL and thus it is of value to focus on these results. It has been shown previously that the performance of DRY grinding does not compare favourably with either WET or MQL in almost all tests and reasons for this have been discussed. This section therefore concentrates on the performance of only WET and MQL as it brings into focus very neatly the efficiency of each case under the situations tested.

Table 7-2 presents results for specific energy obtained from the monitored power and achieved removal rate.

Trial number	**WET**		**MQL**	
	e_c J/mm^3	**a_e** µm	**e_c** J/mm^3	**a_e** µm
Trial 1	187.59	0.92	154.14	0.71
Trial 2	128.96	0.50	94.63	0.50
Trial 3	56.18	6.88	57.26	6.75
Trial 4	152.40	2.71	65.91	3.58
Trial 5	586.80	0.42	251.33	0.58
Trial 6	151.99	0.54	77.61	0.50
Trial 7	112.61	13.04	87.73	9.83
Trial 8	59.07	4.79	73.73	3.13

Table 7-2. Specific energy values for WET and MQL – where red highlighted values are those computed for the case of applied DOC = 5 µm, non-highlighted values represent applied DOC = 15 µm.

The results from the Taguchi analysis for materials EN31 and EN8 are presented in Figure 7-34.

For WET the strongest effects are DOC, followed by the interactions of wheelspeed and workpiece speed, and workpiece speed and DOC. The independent effects of the wheel speed and workpiece speed are less significant on this parameter.

MQL appears to present an attractive alternative to flood delivery as there is less sensitivity to variation in the value of the parameters. As a general assessment, MQL does perform reasonably well across the situations investigated, however there appears to be little opportunity to optimise the process. This may however, be simply that the chosen conditions happen to be those most favoured by MQL.

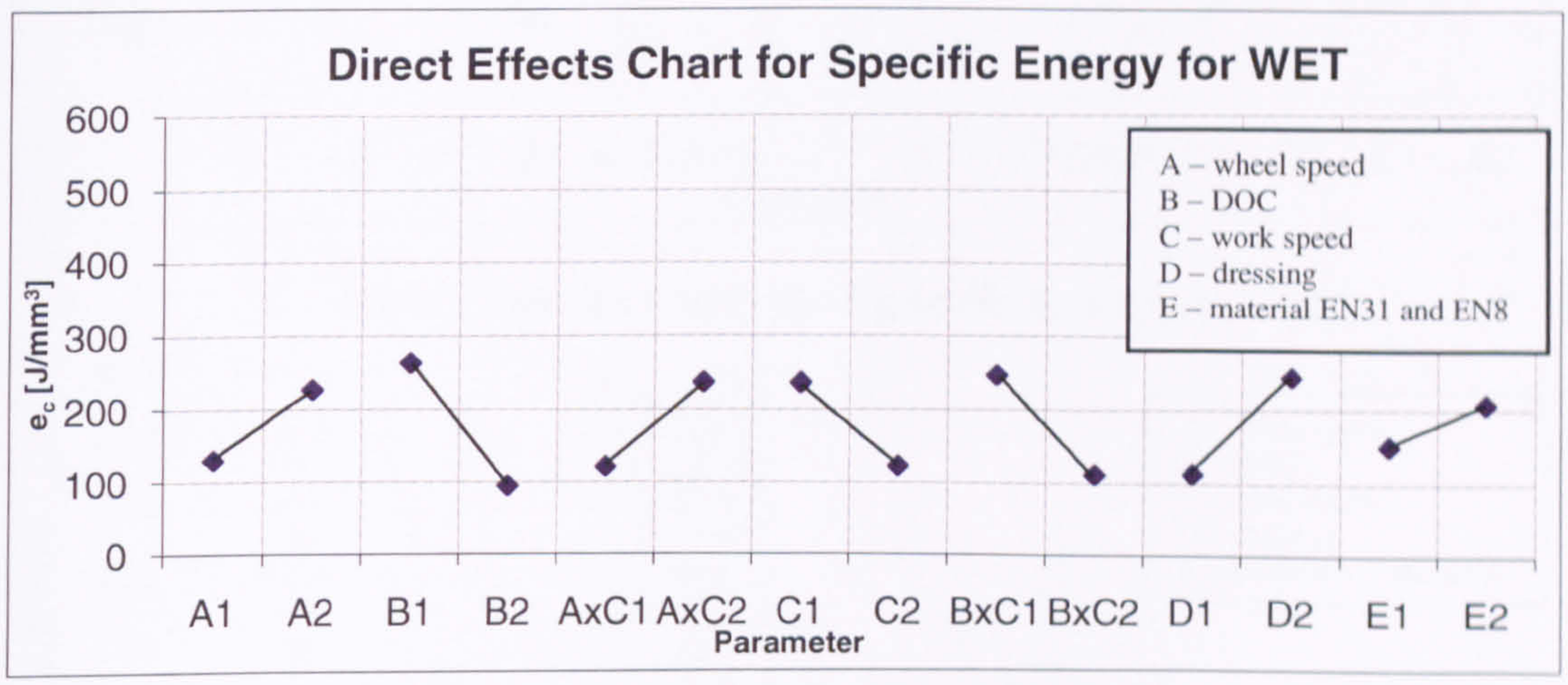

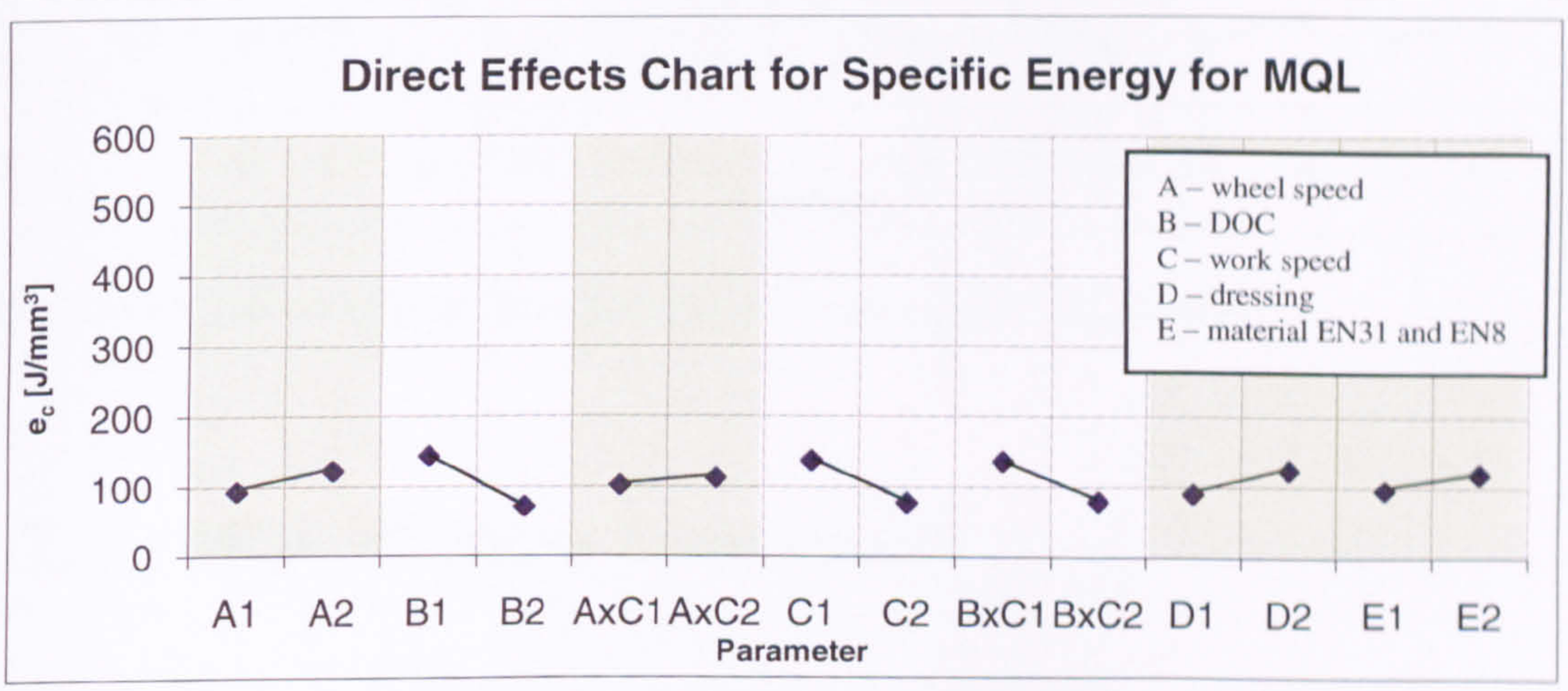

Figure 7-34. Direct effects chart for specific energy with EN31 and EN8.

The strongest effect, as with other results, is the DOC, followed by the workpiece speed and the interaction of workpiece speed and DOC. The wheel speed and the dressing conditions influence the MQL grinding process in a similar way and the interaction of wheel speed and workpiece speed and the material hardness are less significant.

The results for materials M2 and EN8 are shown in Figure 7-35. The outcomes are similar to those for the EN31-EN8 pair, however the strength of the effects in WET are stronger while for MQL they are weaker. This is reasoned to be an indication of the MQL preference (ease of cutting) for M2 and EN8 materials.

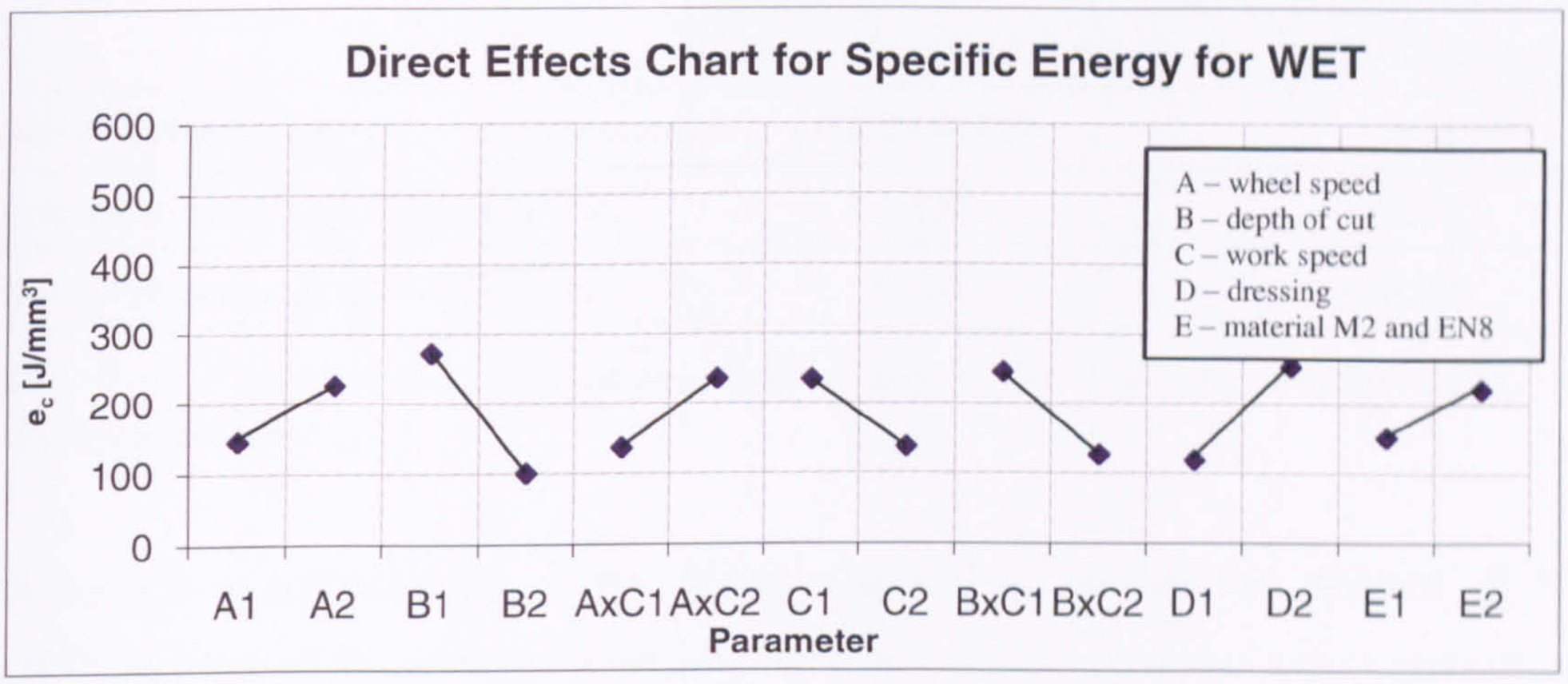

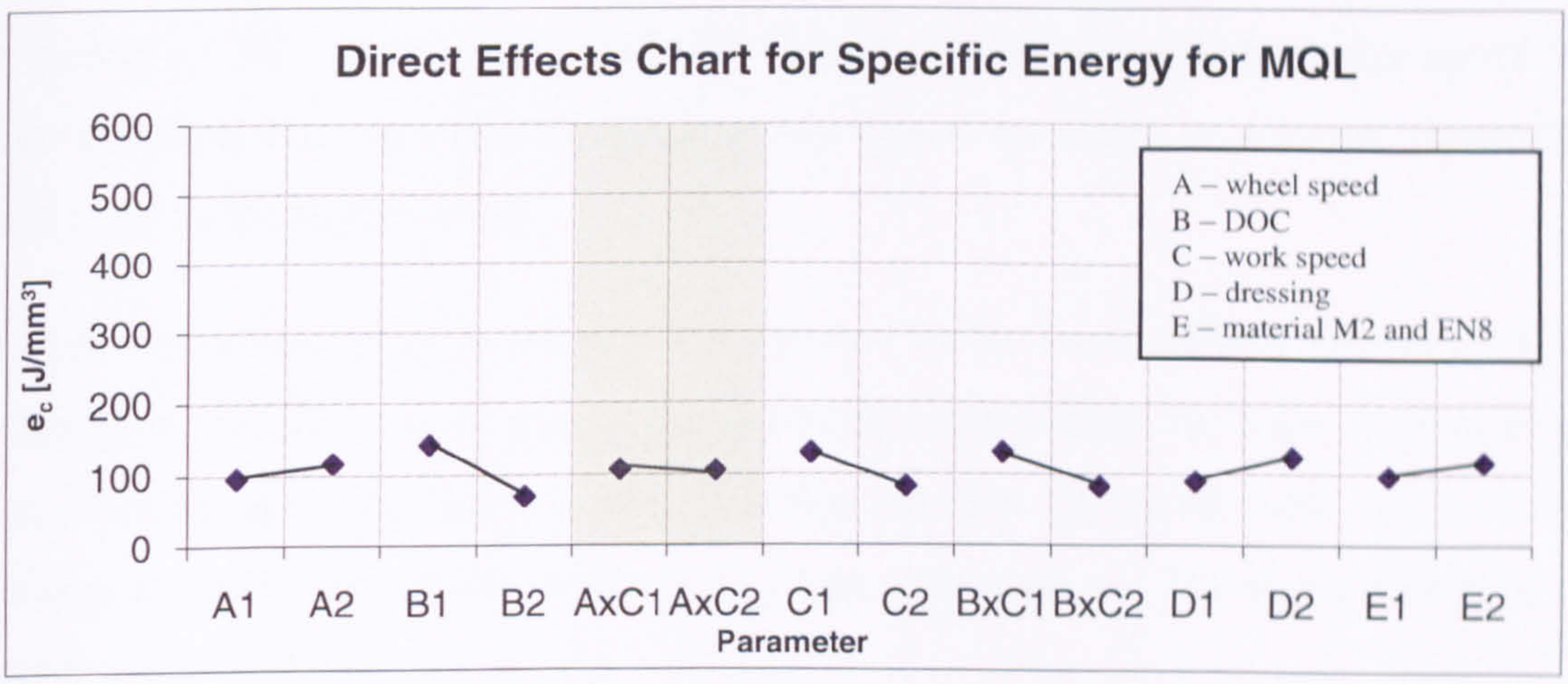

Figure 7-35. Direct effects chart for specific energy with M2 and EN8.

7.7. MQL Process Economics

7.7.1. A Summary of MQL Process Economics

Below in Table 7-3 is a summary of fluid usage and power consumption for the two cases under comparison, MQL and conventional flow. The figures provided are those obtained from the experimental tests completed for this study. The 'Fluid delivered' figures are expressed in ml and represent the total volume used to complete all tests. Delivery rate under MQL was ~ 33 ml/h, equating to a total of approximately 80 grinds. In production terms this would equate to approximately 3.25 hours of continuous machine time.

	Conventional delivery	MQL system
Fluid delivered [ml]	~ 1 944 000	~ 100
Process power consumption [kWh]	~ 1.8	~ 0.15
Total power consumption [kWh]	~ 5.8	~ 0.30

Table 7-3. Fluid usage and power consumption for the two cases: MQL and conventional flow.

Process power consumption is the power required to deliver the volume of fluid identified above. This value was obtained from an estimation of compressor power over the period of 3.25 hours, that is 0.5 kW (based on a local portable compressor). The value obtained for conventional delivery was based on usage of a larger compressor supplying the laboratory lines.

Total power consumption is the power consumed by the fluid delivery system using the assumption that the system was running continuously during the experimental period even when the machine tool was idle. This was the case for conventional delivery only. The experimental period was summed as 70 days continuous. The production day was assumed to be 8 hours.

The size and footprint of the equipment are compared, see Figure 7-36. Both pictures are to scale.

Figure 7-36. Comparison of fluid delivery systems (in scale) – conventional system (A), MQL system (B) and amounts of fluid used – i.e. bottle compared to barrel (C).

7.7.2. Economic Comparison of MQL Versus Emulsion Delivery in Industrial Conditions

A basic comparison of the economics of conventional and MQL fluid delivery systems in a hypothetical industrial application is presented. This comparison is only indicative and was based on book titled: Cutting and grinding fluids: selection and application, published by Society of Manufacturing Engineers (1992). The following assumptions for the calculations are made:

- 10 machine tools (each costs £40k with coolant reservoirs – WET and £35k without reservoirs and MQL system installed – MQL),
- parts processed per one machine per day – 200 (per year – 50 000),
- 8 hours per shift, two shifts per day, five days per week, fifty weeks per year,
- labour rate is: £9.50 per hour,
- coolant cost is: £2.50/l,
- the waste disposal and collection charges are: £0.20/l,
- each WET machine has 400 litre coolant capacity. At the end of each week approximately 3800 litre of cutting fluid, from all 10 machines, is a waste.

Table 7-4 shows the summary results calculated from figures referred to above.

	WET	MQL
Machine operator labour	£0.2280	£0.2280
Cutting fluid	£0.0554	£0.0150
Storage cost	£0.0150	£0.0030
System maintenance	£0.0095	£0.0002
Waste disposal	£0.0760	£0.0020
Equipment costs	£0.0100	£0.0010
Return for machine investment	£0.0800	£0.0700
Power consumption	£0.0128	£0.0010
Production stop costs	£0.2000	£0.0020
Tool costs	£0.0600	£0.0600
Purchased raw materials	£0.2000	£0.2000
Total cost per piece	**£0.9467**	**£0.5822**
Savings per year	**£182,250.00**	

Table 7-4. Cost comparison in production conditions – local systems.

Machine operator labour – this cost includes the cost of labour and maintenance on 'as needed' basis.

Cutting fluid – this includes fluid concentrate purchase and delivery cost, water, topping up, additives. Storage cost – this is a cost of storage of fluids and waste coolants (assumed 10 m^2 room for WET and 2 m^2 for MQL, £3.00 a square meter a day).

System maintenance – this includes maintenance of the fluid delivery system, fluid change and top up.

Waste disposal – this is includes waste collection and disposal.

Equipment costs – this includes the cost of filters, pumps and other equipment required for the delivery system to work properly.

Return for machine investment – this is based on 10 per cent set aside of the original cost of investment per year as return on capital invested.

Power consumption – this is the cost of power consumed by delivery systems.

Production stop costs – this is the cost of production stops. This includes the times when machines are maintained, repaired, fluid is topped up, etc.

Tool costs – this is the cost of the tools.

Purchased raw materials – materials purchase costs and preparation for this process.

Total cost per piece – this is the total cost of fabrication of the single workpiece.

There are potentially further savings expected from tool costs, however these are hard to calculate as there is no direct study for grinding, proving tool life is elongated when MQL is used.

For the case presented, there is a difference of £0.3645 per workpiece. At 500, 000 parts per annum, this would result in a total saving of **£182,250.00** per year.

Such analysis is for independent systems only.

The following example is for a centralised system, with efficient filtration, fluid quality control, buffers and tool life extending additives, together with machine feed and speeds optimised for a minimum cost. In this case workpiece costs are estimated to be approximately 25 per cent lower.

Total savings in this case are summarised in Table 7-5.

	WET	MQL
Total cost per piece	**£0.7100**	**£0.5822**
Difference per piece	£0.1278	
Savings per year	**£63,900.00**	

Table 7-5. Cost comparison in production condition – centralised facility.

The saving per year would reduce to £63,900.00. However, this still represents significant savings to the company.

Importantly however, in both cases there would be significant benefit to the natural environment.

7.8. Discussion

Very similar performance in terms of $F_t'/DOC/\ Q'_w\ /h_{eq}$ is seen in Trial 3. In Trial 4 MQL was seen to outperform WET in these measures. This provides strong evidence that MQL has potential to compete with WET under this latter combination of material, wheel and machining parameters. From this test, it appears that MQL favours lower workpiece speed with soft materials, when grinding with fine, medium hardness, vitrified, aluminium oxide abrasive. The very good performance in Trial 4 may be a result of the combined effects of wheel specification, speed ratio and workpiece material hardness, which was relatively low in this trial and good lubrication properties of the MQL oil.

The strongest effect on specific tangential force in MQL was DOC with the highest magnitudes in WET. This result implies that MQL is less prone to changes in the

grinding condition than WET under specific conditions. Further, it was also found that the highest h_{eq} was achieved with MQL.

The values of friction coefficient, as other results, were consistent with values published in literature for fine grinding, high precision operations.

The lowest F_t/F_n ratio was recorded for MQL and this was consistent throughout all trials. This outcome is important as this is indicative of a situation of good lubrication, relatively high specific material removal and reasonable penetration depth. Moreover, the value of μ in MQL is not as strongly affected as the other cases by the dressing condition, speeds or material hardness. The performance of MQL appears to have been relatively stable compared to both DRY and WET throughout the trials, again suggesting that MQL is less prone to changes in the grinding condition than WET.

In case of steels EN31 and M2 the small discrepancies do not allow identification of any clear trend. However, the results inform us that there is no strong effect due to a difference in material hardness.

Only small differences in R_a values were recorded between WET, DRY and MQL and all were approximately within expected surface quality. However, in some cases differences were strongly in favour of MQL – Trials 4 and 7.

The cutting efficiency in MQL is due largely to the combined effects of lubrication and appropriateness of the wheel and workpiece combinations. This was demonstrated in Trial 4 and Trial 7, which show an efficient grinding situation together with low temperatures and better general performance (R_a, force ratio) than the WET case. This is strong evidence that MQL has promise in this region.

Though MQL was not always able to match WET performance it was always very close. More importantly, there was no situation in any of trials where MQL temperatures exceeded film boiling that would result in essentially dry conditions. The highest temperature under MQL approached 200 °C, which is below the threshold temperature for damage to the workpiece.

The strongest effect on MQL process temperature was DOC and was rather expected. The change of other process parameters returned a relatively weak response, making the

MQL process less sensitive to process changes compared with WET and DRY. This would be seen as a significant benefit.

In terms of specific energy, MQL again appears to present an attractive alternative to conventional flood cooling. It was also less sensitive to variation in the value of the parameters used. As a general assessment, MQL does perform reasonably well across the situations investigated, however there appears to be little opportunity to optimise the process. This may however, be simply that the chosen conditions happen to be those most favoured by MQL.

It is important to recognise that the experimental conditions employed were defined to help facilitate the comparative study and were therefore not optimised for either the WET or DRY cases.

7.9. Summary

In the Results chapter, results for specific tangential force, force ratio, surface roughness, temperatures and specific energy were presented. In addition, an indicative analysis of process economics was made and as a result the range of savings achieved when using MQL systems rather than conventional fluid delivery systems can be seen.

In general, results indicated the applicable regime for MQL to perform well, i.e. similar or better than conventional delivery. There was a case when MQL did not perform as well as WET, however this was explained by favourable conditions for the grinding wheel in wet grinding.

Detailed discussion and conclusions were presented at the end of this chapter.

In the next chapter thermal analysis is provided, where the temperature obtained during the study is compared against the temperature predicted by a thermal model.

Chapter 8. THERMAL ANALYSIS

8.1. Introduction

In most cases temperature prediction is based on either measured power or grinding force levels, from which specific energy can be determined. This parameter can be obtained for a particular grinding wheel, workpiece combination under varying grinding conditions. For the purpose of the study the thermal model of Rowe and Morgan (1995), Marinescu *et al* (2004) and Rowe (2009) was used to obtain theoretical temperatures. Results from experiment are compared with those predicted by theory.

The model used for this study has been developed for conventional grinding processes. However, it has not previously been applied to the prediction of temperatures in MQL. A key feature of this work is to validate the model for this case.

8.2. Calculations of Estimated Temperature

Model parameters relating to workpiece materials, grinding wheel and fluids properties can be found in Appendix 11.

For the purpose of validation, experimental conditions selected arbitrarily, were as follows:

(Trials: z31, z32, z33)			
Fluid delivery	WET (conventional)	**Effective grain contact radius**	$r_0 = 15$ µm
Material	EN31	**Fluid convection factor**	$h_f = 10000$ W/m^2 K
Wheelspeed	$v_s = 25$ m/s	**Average tangential force**	$F_t = 33.50$ N
Wheel diameter	$d_s = 288$ mm	**Average normal force**	$F_n = 90.91$ N
Workpiece speed	$v_w = 6.5$ m/min (0.108 m/s)	**Average real DOC**	$a_e = 6.88$ µm
Workpiece width/contact width	$b_w = 20$ mm	**Average temperature**	$T = 123$ °C

Table 8-1. Experimental conditions values.

8.2.1. Contact Length

For the case given above the geometric contact length calculated from equation (4.1) is:

$$l_g = \sqrt{a_e\, d_s} = 1.408\, mm = 1.41 \cdot 10^{-3} m$$

The Roughness factor R_r has been shown to have a strong influence on the contact length predicted from theory. This parameter is related to the analysis of contact of rough surfaces under an applied force and it is the ratio of the smooth and rough contact lengths. The following equations provide inverse solution of this factor based on the assumption of $l_c = 2\, lg$ (Rowe *et al*, 1998):

$$l_c = 2\, l_g = 2.816\, mm = 2.82 \cdot 10^{-3} m$$

The contact length due to the deformation as a result of the applied force from equation (4.7) is therefore:

$$l_f = \sqrt{l_c^2 - l_g^2} = 2.439\, mm = 2.44 \cdot 10^{-3} m$$

The parameter relating Young's modulus E and Poisson's ratio υ for contacting materials is given by (equation (4.4)):

$$\frac{1}{E^*} = \frac{1 - \upsilon_s^2}{E_s} + \frac{1 - \upsilon_w^2}{E_w} = 2.35 \cdot 10^{-11}\, Pa$$

Thus E^* will equal:

$$E^* = 4.25 \cdot 10^{10}\, Pa = 42.52\, GPa$$

The specific normal force is calculated from equation (7.2):

$$F_n' = \frac{F_n}{b_w} = 4545.50\, \frac{N}{m}$$

The roughness factor for which we have now solved is calculated from equation (4.10):

$$R_r = \sqrt{\frac{l_f^2\ \pi\ E^*}{8\ F_n^{'}\ d_s}} = 8.71$$

This calculated value is consistent with values reported in literature (Marinescu *et al*, 2004, 2007). This is a typical value for the shallow cut operation under wet grinding of steel variants. This value in practice however will vary typically between $5 < R_r < 15$ and is related to a wide range of process variables.

8.2.2. Power, Material Removal Rate and Specific Energy

The grinding power is given by equation (4.12) and for the case examined, is:

$$P = F_t\ v_s = 837.50\ W$$

Material removal rate is then (equation (4.14)):

$$Q_w = v_w\ b_w\ a_e = 1.49 \cdot 10^{-8}\ \frac{m^3}{s} = 14.91\ \frac{mm^3}{s}$$

And the specific energy given by equation (4.13):

$$e_c = \frac{P}{Q_w} = 5.62 \cdot 10^{10}\ \frac{J}{m^3} = 56.21\ \frac{J}{mm^3}$$

This value, though typical for shallow cut grinding, illustrates the relative energy inefficiency of grinding compared to other material removal processes, which have typical values of the order of 2 to 10 J/mm^3 (Filipowski and Marciniak, 2000).

8.2.3. Thermal Partition Model

The total process heat flux from (Marinescu *et al*, 2004) is:

$$q_t = \frac{e_c\ Q_w}{b_w\ l_c} = \frac{P}{b_w\ l_c} = 14.87\ \frac{W}{mm^2} \qquad (8.1)$$

The specific energy to the chips is expressed as (Marinescu *et al*, 2004):

$$e_{ch} = \rho_w \, c_w \, \Theta_{mp} = 5.83 \, \frac{\mathrm{J}}{\mathrm{mm}^3} \tag{8.2}$$

The energy to the chips represented as heat flux is (Marinescu *et al*, 2004):

$$q_{ch} = \frac{e_{ch} \, Q_w}{b_w \, l_c} = \frac{e_{ch} \, v_w \, a_e}{l_c} = 1.54 \, \frac{W}{mm^2} \tag{8.3}$$

Workpiece material diffusivity is (Marinescu *et al*, 2004):

$$\alpha = \frac{k_w}{\rho_w \, c_w} = 8.60 \cdot 10^{-6} \, \frac{m^2}{s} \tag{8.4}$$

The Peclet number is a dimensionless parameter relating the advection of a flow to the thermal diffusivity. For grinding, Peclet number typically has a value in the range $0 \leq \mathrm{Pe} \leq 100$ (Marinescu *et al*, 2004), and is given by:

$$Pe = \frac{v_w \, l_c}{4\alpha} = 8.85 \tag{8.5}$$

The thermal constant C is determined from the Peclet number (Rowe *et al*, 1995):

Pe	C
>10	1.06
0.2 < Pe < 10	$\frac{0.95}{\pi} \cdot \sqrt{2\pi + \frac{Pe}{2}}$
< 0.2	0.76

Thus for the case considered the value of C equals (Marinescu *et al*, 2004):

$$C = \frac{0.95}{\pi} \sqrt{2\pi + \frac{Pe}{2}} = 0.99 \tag{8.6}$$

The geometric mean thermal property (GMTP) β_w is given by (Marinescu *et al*, 2004):

$$\beta_w = \sqrt{k_w \, \rho_w \, c_w} = 11595.23 \, \frac{J}{m^2 s^{0.5} K} \tag{8.7}$$

The workpiece convection factor is calculated as (Marinescu *et al*, 2004):

$$h_w = \frac{\beta_w}{C}\sqrt{\frac{v_w}{l_c}} = 72482.20\ \frac{W}{m^2K} \tag{8.8}$$

The partition ratio for heat flow to the workpiece and abrasive is (Marinescu *et al*, 2004):

$$R_{ws} = \left[1 + \frac{0.97\ k_g}{\beta_w\sqrt{r_0\ v_s}}\right]^{-1} = 0.90 \tag{8.9}$$

This value is again consistent with values published in literature for similar grinding conditions (Marinescu *et al*, 2007).

The maximum temperature for grinding is calculated to be (Marinescu *et al*, 2004):

$$\theta_{max} = \frac{q_t - q_{ch}}{\frac{h_w}{R_{ws}} + h_f} = 147.23\ °C \tag{8.10}$$

This value correlates well with the value measured from experiment (123° C) and supports the analytical approach employed. The model approach employed is known to be overly conservative to provide assurance of damage avoidance. The fine tuning can be undertaken in the production environment or under laboratory conditions.

8.3. Results From Measured and Predicted Temperature

To avoid thermal damage to the workpiece it is crucial to grind below a predetermined critical temperature. It is not possible to measure temperature directly in practice hence the need for predictive models. These models take into account many process factors derived directly from grinding mechanics and heat transfer theory. The most useful of these models (Rowe *et al*, 1991) is that developed by Rowe and Morgan (1995). This has been shown to be reliable and robust and requires a minimum input from the user. It is important to note that the model provides for the two cases: wet and dry, has not been

validated under MQL conditions. It is not anticipated that the thermal analysis will differ greatly for the case of MQL however, fluid convection values will be lower for MQL than in WET grinding and for highly accurate predictions partitioning to the fluid may have to be defined. In reported studies (Rowe *et al*, 1998) partitioning to the fluid in conventional operations under WET grinding was typically of the order of 5 to 10 per cent. As a consequence the DRY model is used for MQL and a slightly higher temperature for damage is predicted. This errs on the side of safety.

8.3.1. Results for Hardened Steel EN31

Tests at a low DOC are presented in Figure 8-1 (A). A large difference is observed between the experimental and predicted temperature results for WET grinding. The very low temperature measured suggests that the thermocouple may not have been working properly in this instance. In fine cut the single pole thermocouple junction may not be made as firmly as in the case of deeper cuts. This however was difficult to ascertain with confidence from the signal as it requires some amount of personal interpretation.

The net grinding power measurement is also difficult to obtain in fine cut operations due to the small percentage increase in the power level from the no-load value. This is potentially problematic when the power monitoring system is tuned to a higher power range. Importantly however, power measurement errors of this nature were eliminated in the tests described due to acquisition of grinding forces. The mean value of three measurements was taken as the value for the power calculation. The three values were generally in close agreement. In the case of WET grinding net power requirements may be higher than in the case of DRY due to effects of fluid acceleration (or wheel braking) and power needed to overcome the boundary film layer.

The DRY case exhibits a different tendency. The measured temperature is higher than predicted. It is hard to explain the reason for such a situation but it may occur due to the value of material properties employed. For the material EN31 there exists in the literature a wide range of values of material properties (For example: AISI E 52100, BS 534 A 99).

In the case of MQL the measured and predicted temperatures correlate reasonably well and fall between the WET and DRY values. Importantly, the applied DOC presented difficulties in achievement of grinding. In each situation only 0.5 μm was achieved with the applied DOC of 5 μm.

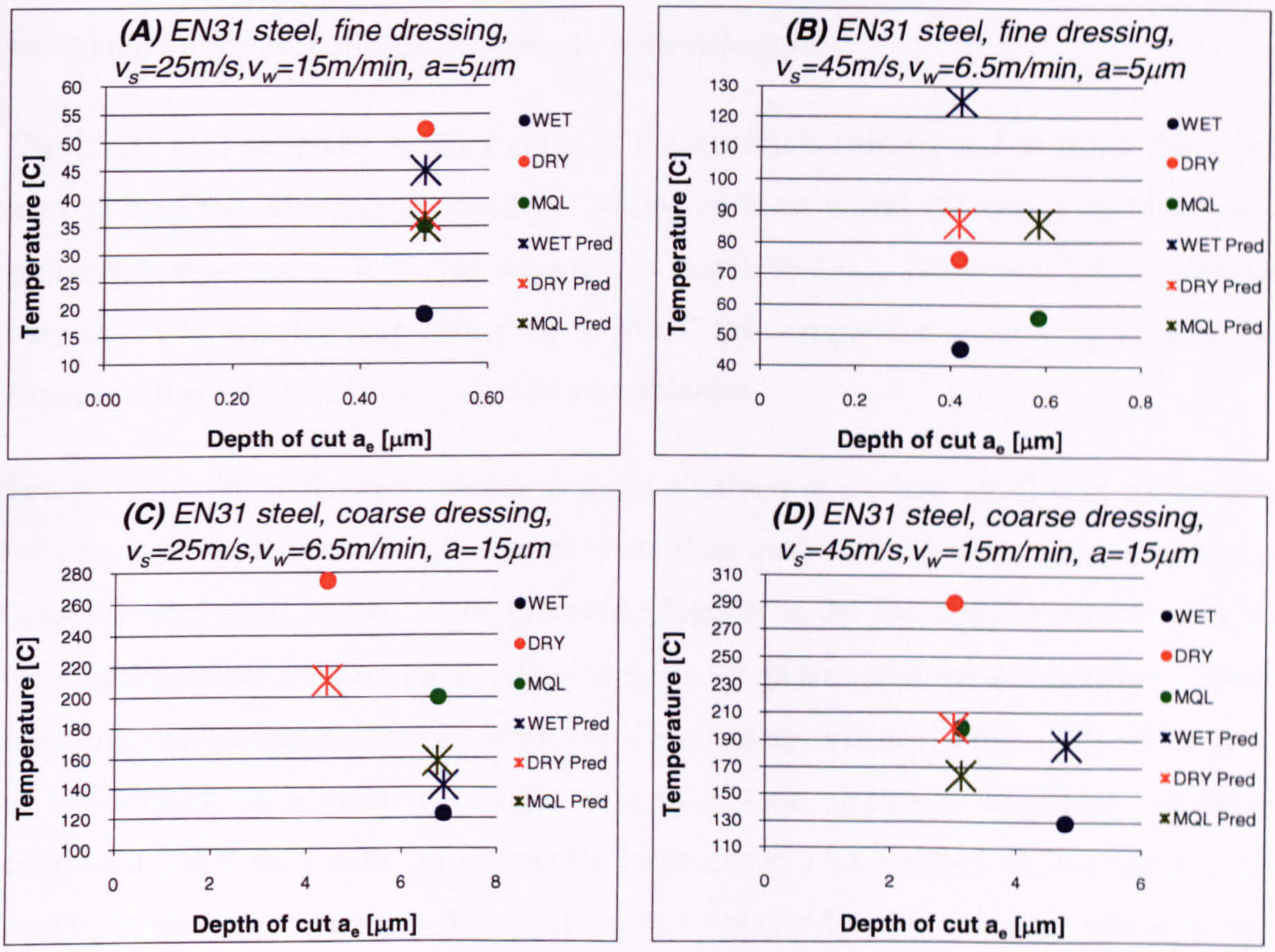

Figure 8-1. Experimental and predicted temperature as a function of DOC for EN31 steel.

In Figure 8-1 (B) (5 μm, DOC) the measured temperatures are considerably lower than those predicted from theory, with no easy to distinguish or conflicting tendencies. It is reasoned that since results for 5 μm DOC are hard to interpret in respect of temperature measurement, any results at this DOC are not considered further. However all results obtained can be found in Appendix 12.

In Figure 8-1 (C) and (D) results are presented for 15 μm DOC at different speed ratios. For both situations the lowest measured temperature was for the case of WET and a reasonable correlation with theory is observed.

The DRY case with the EN31 material (62 HRC) produced a much higher measured value than predicted. The experimental temperature is quite high and would indicate a rather good connection of the thermocouple with the workpiece. The higher temperature would be expected with more difficult to machine materials than the softer materials due to the mechanism of material removal. The ploughing and sliding components would tend to be proportionally higher in such situations.

The EN31 also generates smaller chips of the materials studied and as result the chips tend to load the wheel more rapidly. Loading reduces wheel efficiency and increases grinding temperatures. It is also reported in literature (Tso, 1995) that DRY grinding may result in smaller chip size than in WET for comparable machining conditions. However, this issue was not studied in this instance.

Temperatures in MQL were similar to those obtained at the low DOC with theoretical temperatures approximately 20 per cent lower than measured. However, it is to be noted that each plot value shown in the preceding Figures is the mean value computed from three independent measurements. This was so for power and for temperature. These three independent measurements were not always in accordance, particularly in the case of temperature. It is clear that in the case of a wide dispersion in values the mean computed value may have an inherently large error. This method of interpreting the results in this way using all three values was reasoned to be the most suited to the experimental results and selective choosing of data was not considered appropriate. Selective choosing of data has been shown to yield improved correlation with a number of the results shown, however, the validity of the comparison remains in question.

8.3.2. Results for Hardened Steel M2

The grinding conditions for to the hardened material M2 trials were identical to those for EN31 and the results are presented below.

In Figure 8-2 (A) in all cases a higher predicted value is shown to that measured. The DOC is still relatively small with applied DOC being 15 μm and achieved DOC of the order 3 < DOC < 7 μm. Reasonable correlation is observed with MQL however results

for the cases of DRY and WET are contradictory. It is interesting to note from Figure 8-2 (A) that temperatures measured in both WET and MQL were very similar. This points to a very similar level of performance. The temperature predicted for MQL assumes the DRY situation. This has the effect of increasing theoretical temperatures.

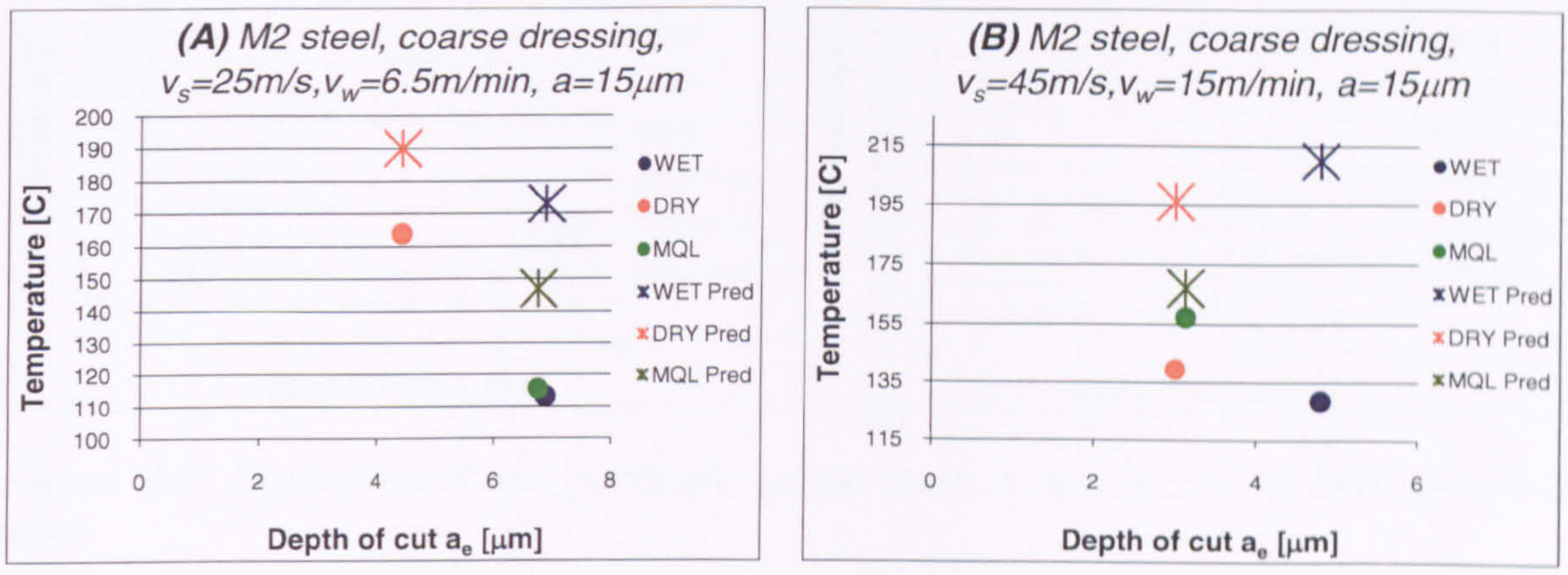

Figure 8-2. Experimental and predicted temperature as a function of DOC for M2 steel.

A further set of results for M2 steel is presented in Figure 8-2 (B), where wheel, workpiece velocities and DOC are relatively high. As for previous trials there is a large difference between predicted and experimental values in the cases of WET and DRY. There is however good correlation for MQL values. Of further interest are the temperature values predicted for both MQL and DRY. The lower temperatures for MQL align with results one would expect from the process mechanics.

8.3.3. Results for Mild Steel EN8

The third set of results are those for mild steel, EN8. The first set of trials is presented in Figure 8-3 (A). A good correlation is observed between predicted and experimental temperatures for the case of WET with a difference of approximately 20 per cent. The case of DRY does not exhibit a good match however the DOC achieved is very low and at such low depths of cut the reliability of the thermocouple is put to question. MQL produced a very close match for predicted and experimental temperature, however the measured temperature is marginally higher than predicted. This suggests that the DRY assumption may be inappropriate for MQL as it is reasoned that the difference may be attributable to effects of fluid convection. It is also interesting to note that the lowest

temperature generated in these tests was for MQL despite the DOC achieved being the highest in this case.

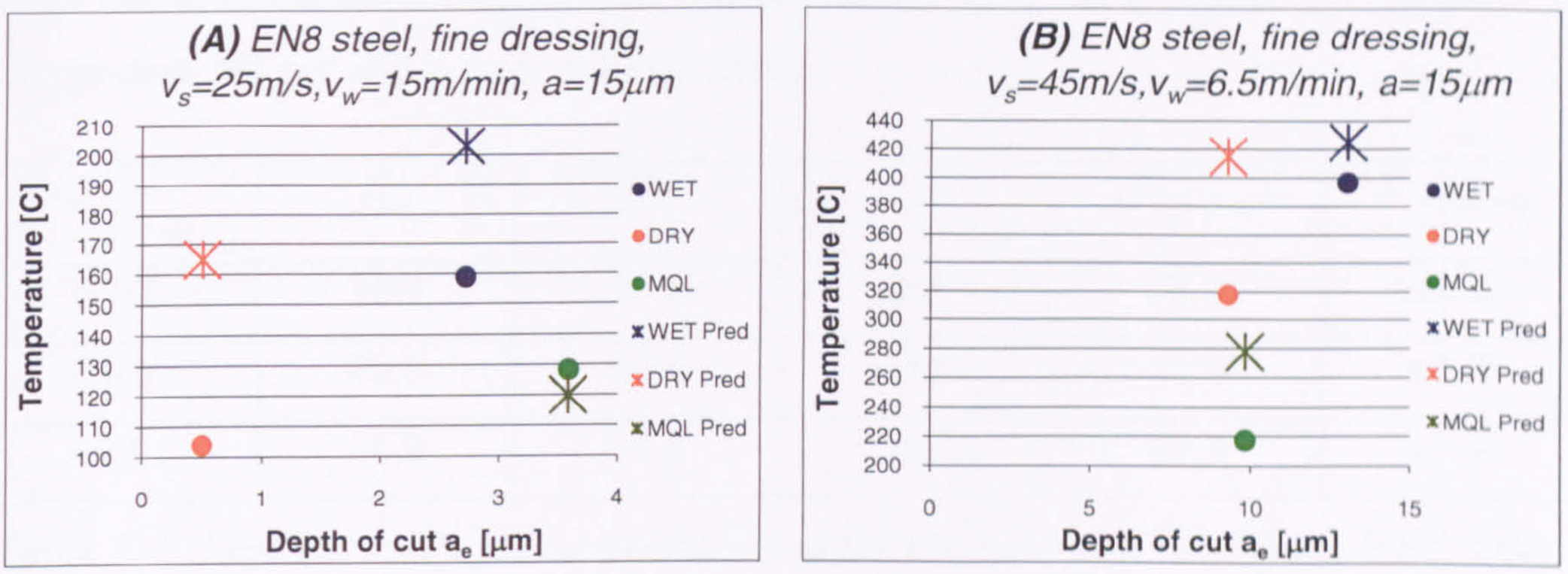

Figure 8-3. Experimental and predicted temperature as a function of DOC for EN8 steel.

The final set of results are presented in Figure 8-3 (B). For the first time a very close match can be seen for the case of WET with a difference of less than 7 per cent. This result suggests that the problems experienced with the thermocouple junction being 'made' may occur more readily at the lower grinding temperatures. At the higher temperatures, associated with the deeper cuts, the thermocouple measurements are more consistent. For the case of DRY the difference between predicted and experimental temperatures is reasonable at less than 25 per cent. The results for MQL are similar to DRY differing by approximately 20 per cent. The lowest temperatures are again identified for the case of MQL. However, it is reasoned that there should be little difference between the temperatures under WET and MQL at the same achieved DOC and it could in fact be the case that the lowest temperature occurs under MQL. It is to be emphasised that the DRY model was used for prediction of temperatures in MQL and further work on the thermal analysis of MQL is required.

8.4. Analysis of Predicted Temperatures Under Varying Assumptions

Each test result shown is the mean value of three measurements. The tangential force measurements exhibit good consistency and only slight variation is identified in the

results. This difference typically leads to variance of 8 per cent in the value of tangential force used in the analysis (however error calculated from Student's distribution is quite large due to small amount of samples and at probability of 95 per cent, error is about ± 20 per cent; 99 per cent – error ± 40 per cent).

	F_{t1}	F_{t2}	F_{t3}	$F_{t\,mean}$	$F_{t\,mean\,var}$
WET	35.9	33.8	30.7	33.5	±7 %
DRY	40.0	42.1	45.2	42.4	±5 %
MQL	36.9	31.8	31.8	33.5	±7 %

Table 8-2. Typical results for tangential force for the same test conditions WET, DRY, MQL.

The measured temperature results however show a much wider dispersion. In some cases this can lead to a large variance in the data. It has been reasoned previously that it is not considered appropriate to be selective with data used and as a consequence the errors reported can be as high as 20 per cent (as above – error will be large due to low number of samples and variance between samples seems to be more appropriate). This is the maximum error (worst case) and typically, variance was computed to be in the region of 4-8 per cent.

	θ_1	θ_2	θ_3	θ_{mean}	$\theta_{mean\,var}$
Worst	107	171	109	129	±19 %
Typical	136	125	126	129	±4 %

Table 8-3. Worst and typical case values of temperature.

The effect of the sometimes wide variation in measured temperature yields some interesting insight into the thermal analysis. An example is given (Table 8-3) for a typical test result, data has a variance in the 'typical' range. Assuming the two extreme values of temperature and inversely solving for model parameters the following Table can be generated.

$\theta_{m\ Ext\ min}$ 107 °C		
	Literature value for the model	Value obtained with inverse solving
κ_s [W/m K]	35	375
r_0 [m]	$1.5 \cdot 10^{-5}$	$1.3 \cdot 10^{-7}$
β_w [J/m^2 s$^{0.5}$ K]	9770	912
Yields wheel-workpiece partition ratio:		
R_{ws}	0.9	0.4

$\theta_{m\ Ext\ max}$ 171 °C		
	Literature value for the model	Value obtained with inverse solving
κ_s [W/m K]	35	172
r_0 [m]	$1.5 \cdot 10^{-5}$	$6.2 \cdot 10^{-7}$
β_w [J/m^2 s$^{0.5}$ K]	9770	1985
Yields wheel-workpiece partition ratio:		
R_{ws}	0.9	0.6

Table 8-4. Literature and obtained values comparison for two temperature extreme values.

The above example is for one of the more extreme cases from the tests. The parameters selected are seen to be sensitive to the temperature value employed and this confirms the importance of accurate and repeatable temperature measurements for theoretical validations. Importantly, however, the data highlights the challenge of thermocouple measurement at very low depths of cut on a relatively flexible machine tool. The large temperature differences measured obtained under similar conditions were seen to vary significantly with only small changes in achieved DOC.

8.5. Discussion

The thermal model is a useful tool for the prediction of grinding temperature. The model used (Rowe and Morgan model) has been shown to be quite efficient for the cases of WET and DRY grinding. The difference in results obtained for the case of WET were attributed to a number of factors. The key factor was thermocouple reliability, a further factor was the value of model parameters employed particularly those of the fluid and workpiece material.

The thermal analysis worked very well with MQL. This may suggest that earlier assumptions for evaporation being responsible for a small, but significant cooling performance may not be entirely correct, as the evaporation of oil will occur only when the grinding temperature exceeds the film boiling temperature. Generally, no such high temperatures were obtained under MQL though a quantitative assessment of the effects of convection remain unclear. This requires further research and model development but current results tend to indicate that the MQL phenomena comes directly from decreased friction.

The analytical model does not provide for direct cooling effects resulting from the high speed air jet, though it has been proved such an effect exists (Nguyen and Zhang, 2003). This aspect should be taken into account in future studies.

The temperature model has been shown to produce results that correlate well for the cases of WET and DRY. Results for MQL also correlate well and taking into account current model limitations (grinding under oil boiling temperature and using surrounding temperature air and oil), it is proposed that the model can be successfully used for maximum grinding temperature prediction. Nevertheless additional work is required with other grinding cases, to accommodate use of different wheels, materials to confirm the model validity with MQL.

8.6. Summary

A Thermal model and corresponding calculations of estimated temperature were presented in this chapter. A short introduction is followed by calculations of predicted (estimated) temperature, based on Morgan and Rowe model. The calculation is provided in respect of real contact length.

Also results for estimated temperature are presented within this chapter for EN31, M2 and M8 steels. In case of the presented temperature model, results correlate well for the cases of WET and DRY. In case of MQL correlation is well but requires that current model limitations (grinding under oil boiling temperature and using surrounding temperature air and oil) be taken into account. It is concluded that additional work is

required with other grinding cases, to accommodate use of different wheels and materials to confirm the model validity with MQL.

The following two chapters will be conclusions and future work. The conclusions chapter will summarise thoughts regarding the study and its results, whereas in the the chapter titled Future Work, directions for further study are presented.

Chapter 9. CONCLUSIONS

The study has helped explain many previously unanswered questions regarding MQL in grinding and a number of key contributions have been achieved:

- ✓ This work provides an advanced understanding of MQL performance and provides evidence that MQL can be effective in the fine grinding surface grinding regime (5 μm < DOC < 15 μm).

- ✓ Results for tangential and normal force were obtained in terms of real DOC which has been shown to be critically important for the analysis of fine grinding operations. It is worthy to note that the applied DOC was used in the majority of prior researches, which depending on process conditions, would lead to experimental errors and incorrect conclusions.

- ✓ Grinding temperatures at the contact arc were measured for the first time in MQL and compared against existing thermal models. This is a further innovative approach to improved understanding of the MQL technique and has only been achieved in AMTReL.

- ✓ An applicable regime for MQL was established in fine grinding operations and a summary Table generated (Table 9-1).

- ✓ The conditions under which dressing is performed 'dry', 'wet' or 'MQL' have also been identified as having a strong influence on process performance.

- ✓ A new MQL nozzle was designed for the tests reported.

The results for WET and MQL have been presented collectively in tabular form to provide an easy-to-use view of the performance under WET and MQL delivery methods. What can be seen very clearly is that MQL performed better than WET in most areas (i.e. 42 of the 56 elements) and in 5 of the 56 elements performance was similar. However to understand this table better a further description on how to use it is provided. It is important that consideration is given to the real DOC when reading these results.

The Table 9-1 presents different grinding configurations and performance measures. If the process performed best under specific conditions, a letter describing it was put in the

table. 'W' is used to represent conventional fluid delivery (WET), 'M' is used to represent MQL and 'S' informs us of a similar processes performance.

Trial no	v_s m/s	a_e mm **W**	a_e mm **M**	v_w m/min	Dre -	Mat -	Q'_w	F_t' N/mm	F_t/F_n -	R_a µm	T °C	T_{pred} °C	e_c
1	25	0.9	0.7	6.5	C	S	W	M	M	M	W	M	M
2	25	0.5	0.5	15	F	H	S	M	M	M	W	M	M
3	25	6.9	6.8	6.5	C	H	S	S	M	M	M	M	S
4	25	2.7	3.6	15	F	S	M	M	M	M	M	M	M
5	45	0.4	0.6	6.5	F	H	M	M	M	M	W	M	M
6	45	0.5	0.5	15	C	S	S	M	M	M	M	M	M
7	45	13.0	9.8	6.5	F	S	W	M	M	M	M	M	M
8	45	4.8	3.1	15	C	H	W	M	M	W	W	M	W

Table 9-1. Table showing MQL and WET grinding process performance.

The favourable conditions for MQL are highlighted in Green, for example conditions used in Trials 4 and 5.

The Blue colour indicates conditions under which MQL performed less well than WET, but still reasonable, for example conditions used in Trials 1 and 8.

The Yellow colour indicates conditions under which MQL and WET performed very similarly, e.g. within a 2 per cent difference in values.

It is seen that in Trials 2 to 7 the performance of MQL is extremely good and in only 5 of 42 cases did WET (W) achieve a comparable performance to MQL (M).

The Table above provides a useful reference for further studies in MQL and defines the useful regime under stated grinding conditions. For a correct reading of this chart it is important to take DOC into consideration. However, it is not obligatory – and for instance if the DOC per pass is not an issue but it is important to grind cool and energy efficient, then the DOC may be omitted.

What distinguishes the MQL technique and makes it highly desirable for industry is its environmental and economic efficiency. In conventional operations large quantities of fluid are consumed and require disposal. This incurs a high environmental and economic cost. For MQL operations these costs are reduced significantly. Purchase

costs of MQL systems (delivery and filtration), power consumption and footprint are also relatively small compared to conventional systems, providing potential for further cost savings. However all environmental and economic benefits need further clarification.

The following conclusions are reached based on results of this study:

- ✓ MQL can be successfully employed either as a fine finishing process or as a high precision shallow cut grinding process. In surface operations with conventional alumina abrasive and for a range of steels, this would achieve: Fine Finishing (< 5 μm applied DOC), delivering 0.2 μm < R_a < 0.25 μm and Shallow-cut processes (5 > applied DOC < 15 μm), with similar R_a values.

- ✓ Convective cooling with MQL is negligible compared with high volume flood delivery and is limited to convection resulting from latent heat of evaporation of the mist volume. It is therefore clear that effective lubrication developed with efficient aerosol delivery is largely responsible for MQL performance capability.

- ✓ Grinding temperatures in the contact arc measured for the first time in MQL and compared with temperatures predicted from existing thermal models showed that:

  - ➢ Surface temperatures in MQL are very similar to those generated in the WET flood delivery condition throughout the range of machining conditions investigated.
  - ➢ MQL temperatures are almost always lower than those measured in the DRY situation.
  - ➢ Predicted temperatures demonstrate that the existing thermal analysis is appropriate for MQL and results suggest that the DRY model can be employed.

- ✓ In terms of performance, measured by specific removal rate, specific tangential force, and grinding temperature MQL grinding is seen to outperform DRY grinding in almost all conditions investigated.
- ✓ In MQL grinding wheel speed has a greater influence on the process with harder materials than with softer materials.

- ✓ At higher wheel speeds, MQL grinding is more suitable than WET grinding for soft material in shallow-cut grinding with fine dressing.

MQL grinding appears to present an attractive alternative to flood delivery as there is less sensitivity to variation in the value of the parameters. As a general assessment, MQL grinding performs reasonably well across the range of situations investigated, although there was no opportunity to optimise the process. It is possible that the chosen conditions happened to be most favourable for MQL.

Results of this study prove very good applicability of MQL grinding in finishing conditions – up to 5 μm per cut. However, higher cuts up to 15 μm DOC, provides results with MQL grinding that are either slightly poorer for the hard material case or slightly better than conventional flood cooling for soft material conditions. It is considered possible that MQL grinding efficiency may be greatly improved in future development to such an extent that grinding performance for hard materials will also be better than conventional grinding.

In general, MQL led to lower friction with many cases resulting in temperatures sufficiently low to avoid thermal damage.

Chapter 10. FUTURE WORK

Areas requiring further development and research are summarised below.

This study was constrained to one abrasive type. It is highly recommended that further research be undertaken to study the effect of different wheel types on MQL process efficiency including CBN which is known to produce lower forces and which is extremely beneficial in poor cooling conditions. Wheels of different porosities, bonds and hardness should be introduced into the investigation. Such research would confirm which wheel types are best suited to the MQL process and which have the best workpiece price-quality ratio.

A successful grind (good workpiece quality and long wheel life) requires correct dressing. Further research is required to establish appropriate wheel dressing conditions for MQL grinding over a range of wheel variants.

A wider range of grinding conditions should also be studied. The technique should be investigated in different grinding regimes including: micro-grinding, high speed grinding and HEDG. The range of work material should also be extended to include brittle materials and common metal variants.

The MQL system used in this PhD study was developed to allow flexibility in air or oil pressure settings, together with flexibility in the quantities delivered. However, a more accurate computerised system would increase system efficiency and enable the meeting of more specific requirements.

Currently there are two types of MQL systems available. The first MQL system mixes oil and air in a reservoir. The second delivers air and oil separately to the nozzle where a mixture of those two fluids is created. The efficiency, advantages and disadvantages, of the two systems should be compared.

The success of MQL depends in great part on the nozzle and, in particular, the mixing of oil and air in the nozzle. Further research is required to establish ideal mix conditions and optimal nozzle direction and distance from the grinding arc/wheel.

The MQL system parameters should be explored further including delivery volume, delivery flowrate, mix-ratio and delivery temperature. A wider range of oils should also be investigated including vegetable based and ester based oils.

It would also be beneficial to study further the behaviour of the flows in the grinding arc and in the area immediately prior to the contact region to aid further understanding of MQL phenomena. The AMTReL has developed the LDA technique for fluid analysis in grinding and this could be applied to MQL. FEM stimulation could also be employed to investigate interior nozzle flows and flows at the nozzle outlet. FEM stimulation could be used as a comparison for the LDA.

Unlike in conventional flood cooling, in MQL grinding there is no active wheel cleaning during grinding. It is often critical that the wheel is cleaned of any contamination, especially if the wheel is rarely dressed, such as in CBN grinding. Thus, there is a need for the research and development of a dedicated wheel cleaning system for MQL.

Work area cleaning is also important as it was found that the area became contaminated with fine debris, chips and MQL fluid, quite readily. This led to pre-cleaning issues prior to surface measurements. A working solution, such as water based detergent, needs to be developed that meets grinding process requirements. From an environmental point of view and where it is important to collect and recycle grinding deposits, the whole recycling process should be designed to match the MQL grinding process.

It would be beneficial to research the live monitoring of DOC as this would save large amounts of time spent on measuring values that are rarely obtained in grinding practice.

The physiochemical effects on surface energy of the work material should also be studied. This would improve understanding of the tribology of the process and help explain MQL performance at the nano- and microscale.

Further studies should be undertaken to quantify the economics of MQL.

References

Alves, S.A., Gomes de Oliveira, J.F. (2006) Development of new cutting fluid for grinding process adjusting mechanical performance and environmental impact. Journal of Materials Processing Technology, 179, 185–189

Autret, R., Liang, S.Y., Woodruff, G.W. (2003) Minimum Quantity Lubrication in Finish Hard Turning, HNICEM

Attanasio, A., Gelfi, M., Giardini, C., Remino, C. (2005) Minimal quantity lubrication in turning. Wear, 260, 333-338

Babic, D., Murray, D.B., Torrance, A.A. (2005) Mist jet cooling of grinding processes. Machine Tools & Manufacture, 45, 1171-1177

Bains-Jones, V.B., Morgan, M.N., Allanson, D.R., Batako, A.D.L (2005) Grinding fluid delivery system design – nozzle optimisation. GERI Annual Research Symposium.

Batako, A.D., Rowe, W.B., Morgan, M.N. (2005) Temperature measurement in high efficiency deep grinding. Machine Tools & Manufacture, 45, 1231-1245

Braga, D.U., Diniz, A.E. (2002) Using a minimum quantity of lubricant (MQL) and a diamond coated tool in the drilling of aluminium–silicon alloys. Journal of Materials Processing Technology, 122, 127-138

Brinksmeier E., Werner F. (1992) Monitoring of Grinding Wheel Wear. CIRP Annals - Manufacturing Technology, 41/1, 373-376

Brinksmeier, E., Eckebrecht, J., Buhr, H. (1994) Improving ecological aspects of the grinding process by effective waste management. Journal of Materials Processing Technology, 44, 171-178

Brinksmeier, E., Brockhoff, T., Walter, A. (1997) Minimum quantity lubrication in grinding. In Proceedings of 2nd International Machining and Grinding Conference, Dearborn, Michigan

Brinksmeier, E., Heinzel, C., Wittmann, M. (1999) Friction, Cooling and Lubrication in Grinding. Annals of the CIRP. 48/2, 581-598

Brinksmeier, E., Walter, A., Janssen, R., Diersen, P. (1999) Aspects of cooling lubrication reduction in machining advanced materials. Proceedings of the Institution of Mechanical Engineers, 213, Part B, 769-778

Burnat, L. (1962) Szlifowanie i dogładzanie ścierne metali. Wydawnicta Naukowo-Techniczne

Buttery, T.C., Statham, A., Percival, J.B. (1978) Some effects of dressing on grinding performance. Wear, 55, 195-219

Challis, H. and Stanton, Ch. (1982) Grinding. Research on the problems of Grinding Technology. SERC

Chang, C.C., Szeri, A.Z. (1998) A thermal analysis of grinding. Wear, 216, 77-86

Chen, X., Rowe, W.B. (1996) Analysis and simulation of the grinding process. Part I: generation of the grinding wheel surface. International Journal of Machine Tools & Manufacture, 36, 871-882

Chen, X., Rowe, W.B. Analysis and simulation of the grinding process. Part IV: effects of wheel wear. International Journal of Machine Tools & Manufacture, 38, 41-49

Dmochowski, J. (1983) Podstawy obróbki skrawaniem. PWN

Ebbrell, S., Woolley, N.H., Tridimas, Y.D., Allanson, D.R., Rowe, W.B. (2000) The effects of cutting fluid application methods on the grinding process. International Journal of Machine Tools & Manufacture, 40, 209-223

Filipowski, R., Marciniak, M. (2000) Techniki obróbki mechanicznej I erozyjnej. OWPW

Gotou, E., Touge, M. (1996) Monitoring of wear of abrasive grains. Journal of Materials Processing Technology, 62, 408-414

Grove, D.M., Davis, T.P., (1992) Engineering quality and experimental design. Longman Scientific & Technical

Guo, C., Wu, Y., Varaghese, V., Malkin, S. (1999) Temperatures and Energy Partition for Grinding with Vitrified CBN Wheels. Annals of the CIRP, 48/1, 247-250

Hahn, R.S. (1966) On The Mechanics of The Grinding Process Under Plunge Cut Conditions. Trans ASME, Journal of Engineering for Industry, 72-80

Hebda, M., Wachal, A. (1980) Trybologia. Wydawnictwa Naukowo-Techniczne

Heisel, U., Lutz, M., Spath, D., Wassmer, R., (1994) Application of Minimum Quantity Cooling Lubrication Technology in Cutting Process, Production Engineering II/1, 49-54

Heston, T. (2007) The near dry sawing advantage. Fabricating & Metalworking. The Business of Metal Manufacturing

Hou, Z.B., Komanduri, R. (2003) On the mechanics of the grinding process, Part I - Stochastic nature of the grinding process. International Journal of Machine Tools & Manufacture, 43, 1579-1593

Jackson, A., (2008) An Investigation of Useful Fluid Flow in Grinding, PhD Thesis, LJMU

Jin, T., Stephenson, D.J. (2006) Heat flux distributions and convective heat transfer in deep grinding. International Journal of Machine Tools & Manufacture, 46, 1862–1868

Kaczmarek, J. (1971) Podstawy obróbki wiórowej, ściernej i erozyjnej. WNT

Kannapan, S., Malkin, S. (1972) Effects of Grain Size and Operating Parameters on the Mechanics of Grinding. Trans ASME, Journal of Engineering for Industry, 94, 833-842

Kasprowicz, A. (2007) Thermal analysis of the angle approach face and Shoulder grinding operation, M.Sc. Thesis, LJMU

King, R.I., Hahn, R.S., (1986) Handbook of modern grinding technology. Chapman and Hall Ltd.

Kim, N.K., Guo, S., Malkon, S. (1997) Heat Flux Distribution and Energy Partition in Creep-Feed Grinding. Annals of the CIRP, 46/1, 227-232

Kim, H.J., Kim, N.K., Kwak, J.S. (2006) Heat flux distribution model by sequential algorithm of inverse heat transfer for determining workpiece temperature in creep feed grinding. International Journal of Machine Tools & Manufacture, 46, 2086–2093

Klocke, F., Beck, T., Eisenblatter, G., Lung, D. (2000) Minimal Quantity of Lubrication (MQL) – Motivation, Fundamentals, Vistas. 12th International Colloquium, 929-942

Klocke, F., Beck, T., Hoppe, S., Krieg. T., Muller, N., Nothe, T., Raedt, H., Sweency, K., (2002) Examples of FEM Application in Manufacturing Technology, Journal of Materials Processing Technology, 120, 450-457

Liao, Y.S., Lin, H.M. (2007) International Journal of Machine Tools & Manufacture, 47, 1660–1666

Liao, W.T., Tang, F., Qu, J., Blau, P.J. (2007) A wavelet-based methodology for grinding wheel condition monitoring. International Journal of Machine Tools and Manufacture, 47, 580-592

Liao, W.T., Tang, F., Qu, J., Blau, P.J. (2008) Grinding wheel condition monitoring with boosted minimum distance classifiers. Mechanical Systems and Signal Processing, 22, 217-232

Makiyama, T. (2000) Advanced near dry machining system. 4th Annual NCMS Fall Workshop Series

Malkin, S. (1989) Grinding technology. Theory and applications of machining with abrasives. Society of Mechanical and Industrial Engineering, University of Massachusetts

Marinescu, I.D., Rowe, W.B., Dimitrow, B., Inasaki, I. (2004) Tribology of abrasive machining process. William Andrew publishing

Morgan, M., (1995) Modelling for the prediction of thermal damage in grinding. PhD Thesis, LJMU

Morgan, M.N., Rowe, W.B., Black, S.C.E. & Allanson, D.R. (1998) Effective thermal properties of grinding wheels and grains. Journal of Engineering Manufacture, 212/B8, 661-669

Mortimer, J. (2005) Less coolant can be more. Machinery, 5, 25-28

Nee, A.Y.C. (1979) The effect of grinding fluid additives on diamond abrasive wheel efficiency. International Journal of Machine Tools and Manufacture, 19, 21-31

Oczoś, K., Porzycki, J. (1986), Szlifowanie. Podstawy i technika. WNT

Ott, H.W. (1991), Zuführsysteme für Kühlschmierunstoff beim Schleifen. Seminar "Kühlschmierstoffe in der spanenden Fertigung", Deutsches Industrieforum für Technologie (DIF)

Peace, G.S., (1993) Taguchi methods. A hands-on approach. Addison-Wesley Publishing Company, Inc.

Rahman, M., Kumar, A.S., M-Ul-Salam (2001) Evaluation of minimal quantities of Lubricant in end milling. The International Journal of Advanced Manufacturing Technology, 18, 235-241

Rahman, M., Senthil, K.A., Salam, M.U. (2002) Experimental evaluation on the effect of minimal quantities of lubricant in milling. International Journal of Machine Tools & Manufacture, 42, 539-547

Ross, P.J. (1988) Taguchi techniques for quality engineering. McGraw-Hill Book Company, 1988

Rowe, W.B., Morgan, M.N., Allanson D.A. (1991) An Advance in the Modelling of Thermal Effects in the Grinding Process. CIRP Annals – Manufacturing Technology, 40/1, 339-342

Rowe, W.B., Qi, H.S., Morgan, M.N., Zheng, H.W. (1993) The effect of deformation on the contact area in grinding. CIRP Annals, 42/2, 409-413

Rowe, W.B., Black, S.C.E., Mills, B., Qi, H.S., Morgan, M.N. (1995) Experimental investigation of heat transfer in grinding. Annals of the CIRP, 44/1, 329-332

Rowe, W.B., Li, Y., Chen, X., Mills, B. (1997) An Intelligent Multiagent Approach for Selection of Grinding Conditions. CIRP Annals - Manufacturing Technology, 46/1, 233-238

Rowe. W.B., Ebbrell, S., Morgan, M.N. (2004) Process Requirements for Cost-Effective Precision Grinding. CIRP Annals - Manufacturing Technology, 53/1, 255-258

Rowe, W.B., Morgan, M.N., Black, S.C.E. (1998) Validation of Thermal Properties in Grinding. CIRP Annals - Manufacturing Technology, 47/1, 275-279

Rowe, W.B. (2001) Thermal analysis of high efficiency deep grinding. International Journal of Machine Tools & Manufacture, 41, 1-19

Rowe, W.B. (2009) Principles of modern grinding technology. Norwich, NY: William Andrew

Rubinstein, C. (1972) The mechanics of grinding. Pergamon Press

Shaji, S., Radhakrishnan, V. (2002) An investigation on surface grinding using graphite as lubricant. International Journal of Machine Tools & Manufacture, 42, 733-740

Shaji, S., Radhakrishnan, V. (2003) Analysis of process parameters in surface grinding with graphite as lubricant based on the Taguchi method. Journal of Materials Processing Technology, 141, 51-59

Shaji, S., Radhakrishnan, V. (2003) An investigation on solid lubricant moulded grinding wheels. International Journal of Machine Tools & Manufacture, 43, 965–972

Shaw, M.C. (1994) A production engineering approach to grinding temperatures. Journal of Materials Processing Technology, 44, 159-169

Shaw, M.C., (1996) Principles of abrasive processing. Oxford Science Publications

Shennan, J.L. (1983) Selection and evaluation of biocides for aqueous metal-working fluids. Tribology International, 16/6, 317-330

Silva, L.R., Bianchi, E.C., Catai, R.E., Fusse, R.Y., França, T.V., Aguiar, P.R. (2001) Study on the behaviour of the Minimum Quantity Lubricany - MQL technique under

different lubricating and cooling conditions when grinding ABNT 4340 steel. Journal of the Brazilian Society of Mechanical Science & Engineering, 2, 192-199

Silvaa, L.R., Bianchi, E.C., Fusse, R.Y., Catai, R.E., Franc, T.V., Aguiar, P.R. (2007) Analysis of surface integrainy for minimum quantity lubricant - MQL in grinding. International Journal of Machine Tools & Manufacture, 47, 412-418

Skuratov, D.L., Ratis, Y.L., Seleznewa, I.A. (2007) Mathematical modelling and analytical solution for workpiece temperature in grinding. Applied Mathematical Modelling, 31, 1039–1047

Sokovic, M., Mijanovic, K. (2001) Ecological aspects of the cutting fluids and its influence on quantifiable parameters of the cutting processes. Journal of Materials Processing Technology 109, 181-189

Sreejith, P.S. (2008) Machining of 6061 aluminium alloy with MQL, dry and flooded lubricant conditions. Materials Letters, 62/2, 276-278

Tawakoli, T., Westkamper, E., Rabiey, M., Rasifard, A. (2007) Influence of the type of coolant lubricant in grinding with CBN tools. International Journal of Machine Tools & Manufacture, 47, 734–739

The Omega. Transactions and Vol. MM Master Index (2000)

Trmal, G., Kaliszer, H. (1976) Delivery of cutting fluids in grinding. Institution of Mechnical Engineers, 95-100

Tso, P-L. (1995) An investigation of chip types in grinding. Journal of Materials Processing Technology 53, 521-532

Unist, Inc. (2005) Modern Application News

Unist, Inc. (2006) Case study 20060202S

Unist, Inc. (2006) Case study 20070208S

Walton, I.M., Stephenson, D.J., Baldwin, A. (2006) The measurement of grinding temperatures at high specific material removal rates. International Journal of Machine Tools & Manufacture, 46, 1617-1625

Webster, J.A., Cui, C & Mindek Jr., R.B. (1995), Grinding Fluid Application System Design, Annals of the CIRP - Manufacturing Technology, 44/1, 333-338

Webster, J., Tricard, M. (2004) Innovations in Abrasive Products for Precision Grinding. CIRP Annals – Manufacturing Technology, 53/2, 597-617

Weiner, K., Inasaki, I., Sutherland, J.W., Wakabayashi, T. (2004) Dry Machining and Minimum Quantity Lubrication. CIRP Annals – Manufacturing Technology, 53/2, 511-537

Wójcik, R., Kruszyński, B. (2003) Szlifowanie powierzchni płaskich z zastosowaniem minimalnego wydatku cieczy obróbkowej. XXVI Naukowa Szkoła Obróbki Ściernej, 221-225

Wu, H. (2009) Investigation of fluid flow in grinding using LDA techniques and CFD simulation. PhD Thesis, LJMU

Bibliography

Alfares, M., Elsharkawy, A. (2000) Effect of grinding forces on the vibration of grinding machine spindle system. International Journal of Machine Tools & Manufacture, 2003–2030

Brinksmeier, E., Aurich J.C., Govekar, E., Heinzel, C. Hoffmeister, H.W., Klocke, F., J. Peters, R. Rentsch, D. J. Stephenson, E. Uhlmann, K. Weinert, M. Wittmann (2006) Advances in Modelling and Simulation of Grinding Processes. Annals of the CIRP, 55/2, 667-696

Broese van Groenou, A. (1977) The high speed size effect in grinding: the role of heat generation. Wear, 44/2, 203-211

Buttery, T.C., Hamed, M.S. (1977) Some factors affecting the efficiency of individual grains in simulated grinding experiments. Wear, 44/2, 231-245

Chen, X., Rowe, W.B. (1996) Analysis and simulation of the grinding process. Part II: mechanics of grinding, International Journal of Machine Tools and Manufacture. 36/8, 883-896

Chen, X., Rowe, W.B. (1996) Analysis and simulation of the grinding process. Part III: comparison with experiment. International Journal of Machine Tools and Manufacture, 36/8, 897-906

Couey, J.A., Marsh, E.R., Knappb, B.R., Vallance, R.R. (2005) Monitoring force in precision cylindrical grinding. Engineering, 29/3, 307-314

Dhar, N.R., Kamruzzaman, M., Ahmed, M.T. (2006) Effect of minimum quantity lubrication (MQL) on tool wear and surface roughness in turning AISI-4340 steel. Journal of Materials Processing Technology, 172/2, 299-304

Dhar, N.R., Ahmed, M.T., Islam, S. (2007) An experimental investigation on effect of minimum quantity lubrication in machining AISI 1040 steel. International Journal of Machine Tools and Manufacture, 47/5, 748-753

Dhar, N.R., Islam, M.W., Islam, S., Mithu M.A.H. (2006) The influence of minimum quantity of lubrication (MQL) on cutting temperature, chip and dimensional accuracy in turning AISI-1040 steel. Journal of Materials Processing Technology, 171/1, 93-99

Dhavlikara, M.N., Kulkarnib, M.S., Mariappan, V. (2003) Combined Taguchi and dual response method for optimization of a centerless grinding operation. Journal of Materials Processing Technology, 132/1-3, 90-94

Drew, S.J., Mannan, M.A., Ong, K.L., Stone, B.J. (2001) The measurement of forces in grinding in the presence of vibration International Journal of Machine Tools and Manufacture, Volume 41, Issue 4, March, Pages 509-520

Fu, H., Matthews, M.A., Warner, L.S., (1998) Recycling steel from grinding swarf Waste Management, Volume 18, Issue 5, August, Pages 321-329

Gao, Y., Tse, S., Mak, H. (2003) An active coolant cooling system for applications in surface grinding Applied Thermal Engineering, 2/5, 523-537

Graham, W., Abdullahi, A.T. (1975) The nature wheel-workpiece contact is surface grinding. International Journal of Machine Tool Design and Research, Volume 15, Issue 3, November, Pages 153-160

Gviniashvil, V.K., Wooley, N.H., Rowe, W.B. (2004) Useful coolant flowrate in grinding. International Journal of Machine Tools and Manufacture, Volume 44, Issue 6, May, Pages 629-636

Hamdi, H., Zahouani, H., Berhgeau, J.M. (2004) Residual stresses computation in a grinding process. Journal of Materials Processing Technology, Volume 147, Issue 3, 20 April, Pages 277-285

Hamed, M.S., Buttery, T.C. (1979) Grinding forces and surface finish control using a theoretical model of the process. Precision Engineering, Volume 1, Issue 1, January, Pages 29-30

Hekman, K.A., Liang, S.Y. (1999) Feed rate optimization and depth of cut control for productivity and part parallelism in grinding. Mechatronics, 9/5, 447-462

Hou, Z.B., Komanduri, R. (2004) On the mechanics of the grinding process, Part II - thermal analysis of fine grinding. International Journal of Machine Tools and Manufacture, 44/2-3, 247-270

Hou, Z.B., Komanduri, R. (2004) On the mechanics of the grinding process, Part III - thermal analysis of the abrasive cut-off operation. International Journal of Machine Tools and Manufacture, 44/2-3, 271-289

Howes, T. (1990) Assessment of the cooling and lubricative properties of grinding fluids. CIRP Annals - Manufacturing Technology, 39/1, 313-316

Itoigawa, F., Childs, T.H.C., Nakamura, T., Belluco, W. (2006) Effects and mechanisms in minimal quantity lubrication machining of an aluminium alloy. Wear, 260/3, 339-344

Ko, T.J., Park, S.H., Kim, H.S. (2003) Experimental verification of the mist generation mechanism in turning. International Journal of Machine Tools and Manufacture, 43/2, 115-120

Kopac, J., Krajnik, P.J. (2006) High-performance grinding - A review. Journal of Materials Processing Technology, 175/1-3, 278-284

Kopalinsky, E.M. (1984) A new approach to calculating the workpiece temperature distributions in grinding. Wear, 94/3, 295-322

Krajnik, P., Kopac, J., Sluga, A. (2005) Design of grinding factors based on response surface methodology. Journal of Materials Processing Technology, 162-163, 629-636

Kuriyagawa, T.K., Syoji, H., Ohshita, S. (2003) Grinding temperature within contact arc between wheel and workpiece in high-efficiency grinding of ultrahard cutting tool materials. Journal of Materials Processing Technology, 136/1-3, 39-47

Kwak, J.S. (2005) Application of Taguchi and response surface methodologies for geometric error in surface grinding process. International Journal of Machine Tools and Manufacture, 45/3, 327-334

Lee, E.S., Kim, J.D. (1997) A study on the analysis of grinding mechanism and development of dressing system by using optimum in-process electrolytic dressing. International Journal of Machine Tools and Manufacture, 37/12, 1673-1689

Lee, E.S. (2000) A study on the mirror-like grinding of die steel with optimum in-process electrolytic dressing. Journal of Materials Processing Technology, 100/1-3, 200-208

Lefebvrea, A., Vievilleb, P., Lipinskia, P., Lescalier, C. (2006) Numerical analysis of grinding temperature measurement by the foil/workpiece thermocouple method. International Journal of Machine Tools and Manufacture, 46/14, 1716-1726

Li, Z.C., Lin, B., Xu, Y.S, Hu, J. (2002) Experimental studies on grinding forces and force ratio of the unsteady-state grinding technique. Journal of Materials Processing Technology, 129/1-3, 76-80

Liu, C.H., Chenb, A., Chenc, C.A., Wang, Y.T. (2005) Grinding force control in an automatic surface finishing system. Journal of Materials Processing Technology, 170/1-2, 367-373

Lortz, W. (1979) A model of the cutting mechanism in grinding. Wear, 53/1, 115-128

Midha, P.S., Zhu, C.B., Trmal, G.J. (1991) Optimum selection of grinding parameters using process modelling and knowledge based system approach. Journal of Materials Processing Technology, 28/1-2, 189-198

Mokbela, A.A., Maksoud, T.M.A. (2000) Monitoring of the condition of diamond grinding wheels using acoustic emission technique. Journal of Materials Processing Technology, 101/1-3, 292-297

Murthya, J.K.N., Chattopadhyayb, A.B., Chakrabarti, A.K. (2000) Studies on the grindability of some alloy steels. Journal of Materials Processing Technology, 104/1-2, 59-66

Nandi, A.K., Pratihar, D.K. (2004) Automatic design of fuzzy logic controller using a genetic algorithm to predict power requirement and surface finish in grinding. Journal of Materials Processing Technology, 148/3, 288-300

Nee, A.Y.C., Tay, A.O. (1981) On the measurement of surface grinding temperature. International Journal of Machine Tool Design and Research, 21/3-4, 279-291

Obikawaa, T., Kamataa, Y., Shinozuka, J. (2006) High-speed grooving with applying MQL. International Journal of Machine Tools and Manufacture, 46/14, 1854-1861

Outwater, J.O., Shaw, M.C. (1952) Surface temperatures in grinding. Transactions of the ASME. January Issue

Pande, S.J., Lal, G.K. (1979) Effect of dressing on grinding wheel performance. International Journal of Machine Tool Design and Research, 19/3, 171-179

Pande, S.J., Halder, S.N., Lal, G.K. (1980) Evaluation of grinding wheel performance. Wear, 58/2, 237-248

Qi, H.S., Rowe, W.B., Mills, B. (1997) Experimental investigation of contact behaviour in grinding. Tribology International, 30/4, 283-294

Quaile, R. (2005) Understanding MQL. Modern Machine Shop. January Issue

Razavi, H.A., Kurfess, T.R., Danyluk, S. (2003) Force control grinding of gamma titanium aluminide. International Journal of Machine Tools and Manufacture, 43/2, 185-191

Shamim, A. and C.F. Kettleborough (1995) Aerosol Aspects of Oil Mist Lubrication Generation and Penetration in Supply Line. Tribology Symposium, ASME, New York, 72, 133–140

Torrance, A.A. (1990) The correlation of process parameters in grinding. Wear, 139/ 2, 383-401

Tso, P.L., Wu, S.H. (1999) Analysis of grinding quantities through chip sizes. Journal of Materials Processing Technology, 95/1-3, 1-7

Venkatesh, K., Bobji, M.S., Biswas, S.K. (1998) Roughness due to workpiece wear generated in surface grinding of metals. Tribology International, 31/12, 771-778

Xiao, K.Q., Zhang, L.C. (2006) The effect of compressed cold air and vegetable oil on the subsurface residual stress of ground tool steel. Journal of Materials Processing Technology, 178/1-3, 9-13

Xu, Y.S., Hu, J., Lin, B., Lin, Z.C. (2002) Studies on surface quality of the unsteady-state grinding technique. Journal of Materials Processing Technology, 129/1-3, 364-368

Xu, X.S. (2001) Experimental study on temperatures and energy partition at the diamond–granite interface in grinding. Tribology International, 34/6, 419-426

Yui, A., Lee, H.S. (1996) Surface grinding with ultra high speed CBN wheel. Journal of Materials Processing Technology, 62/4, 393-396

Zhang, L.C., Suto, T., Noguchi, H. (2003) Applied mechanics in grinding part I: Modelling of elastic modulus of wheels and interface forces. International Journal of Machine Tools and Manufacture, 43/15, 1579-1593

Zhang, L.C., Suto, T., Noguchi, H. (1993) Applied mechanics in grinding part II. International Journal of Machine Tools and Manufacture, 33/2, 245-255

Zhang, L.C., Suto, T., Noguchi, H. (1993) Applied mechanics in grinding part III. International Journal of Machine Tools and Manufacture, 33/4, 587-597

Zhang, L.C., Mahdi, M. (1995) Applied mechanics in grinding part IV. International Journal of Machine Tools and Manufacture, 35/10, 1397-1409

Mahdi, M., Zhang, L.C. (1997) Applied mechanics in grinding part V. International Journal of Machine Tools and Manufacture, 37/5, 619-633

Mahdi, M., Zhang, L.C. (1998) Applied mechanics in grinding part VI. International Journal of Machine Tools and Manufacture, 38/10-11, 1289-1304

Mahdi, M., Zhang, L.C. (1999) Applied mechanics in grinding part VII. International Journal of Machine Tools and Manufacture, 39/8, 1285-1298

Zhang, N., Kirpitchenko, I., Liu, D.K. (2005) Dynamic model of the grinding process. Journal of Sound and Vibration, 280/1-2, 425-432

APPENDIXES

Appendix 1. Standard Marking System

An example of standard marking system used commonly in the world is presented in Figure A-1. The first number (prefix) is optional and represents the manufacturer's symbol indicating the exact quantity of abrasive utilised. The letter A (abrasive type) indicates aluminium oxide or the letter C a silicon carbide abrasive material. There are many types of abrasive based on synthetic aluminium oxide plus two common types of silicon carbide with different compositions and usually manufacturer's prefix indicates the particular type of alumina or silicon carbide used. The number to the right of the abrasive type letter indicates the abrasive grain size by a mesh number, where a larger mesh number indicates a finer grain size. Since each nominal grain size includes a range of abrasive grain sizes, the grain dimension corresponding to a particular grain size number may be characterized by an average value (Marinescu *et al*, 2004).

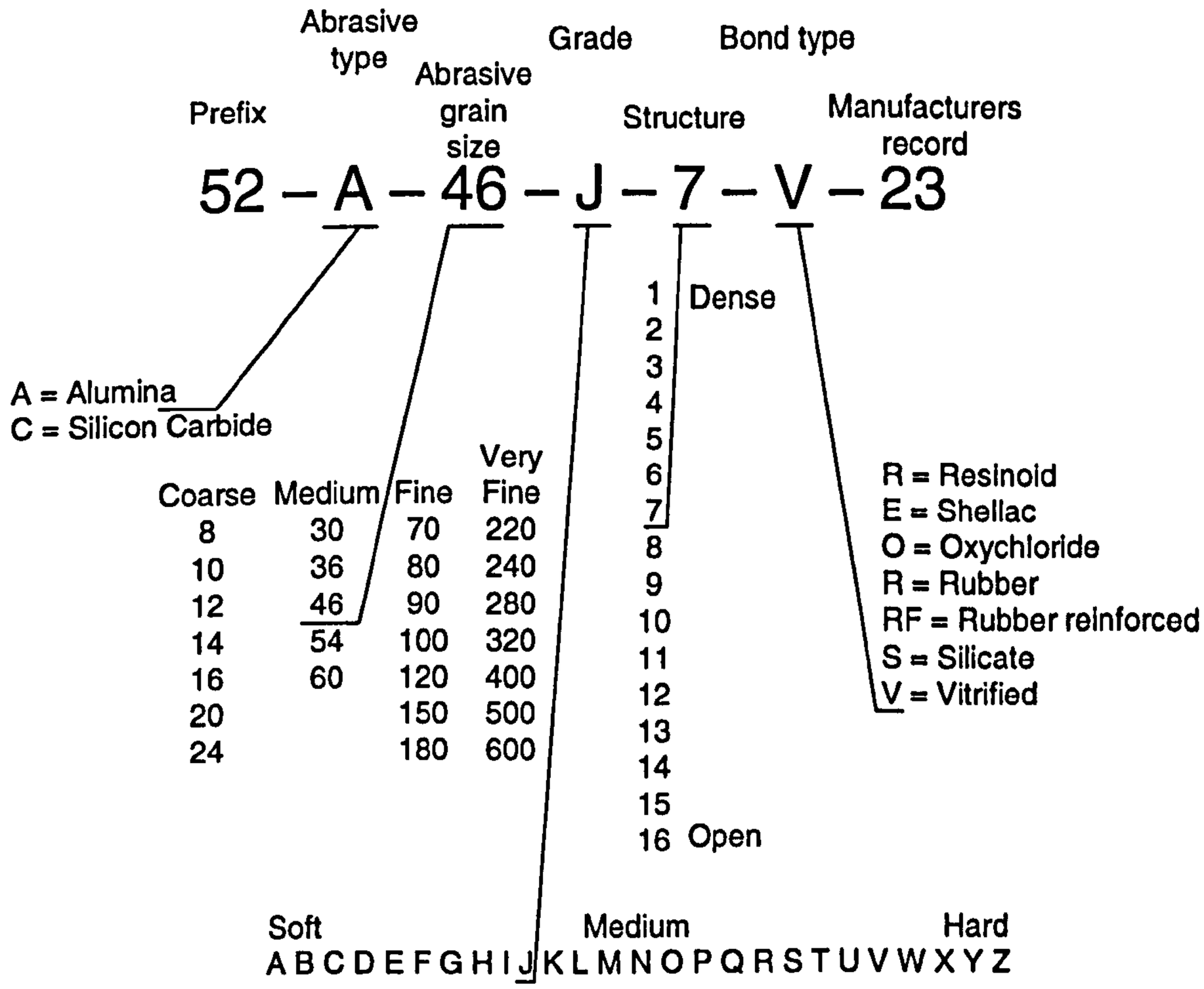

Figure A-1. An example of grinding wheel standard marking system for Alumina and Silicon wheels with explanation of terms (Jackson, 2008).

In world industry there are different ways to classify abrasive, however the most common and the oldest one, has been introduced by Norton company. Norton's classification consists on marking grains according to the scale with numbers. Each number corresponds to the number mesh sieve in the length of one inch in the sieve and are classified as: coarse (may be divided into very coarse and coarse), medium, fine and very fine (may be divided into very fine and powder) (Oczos and Porzycki, 1986).

The way how wheel hardness is marked is standardised, and again most commonly is Norton's scale that take into account 23 grades of hardness with following letters for A the softest and Z the hardest wheel (Oczos and Porzycki, 1986).

Appendix 2. MQL System

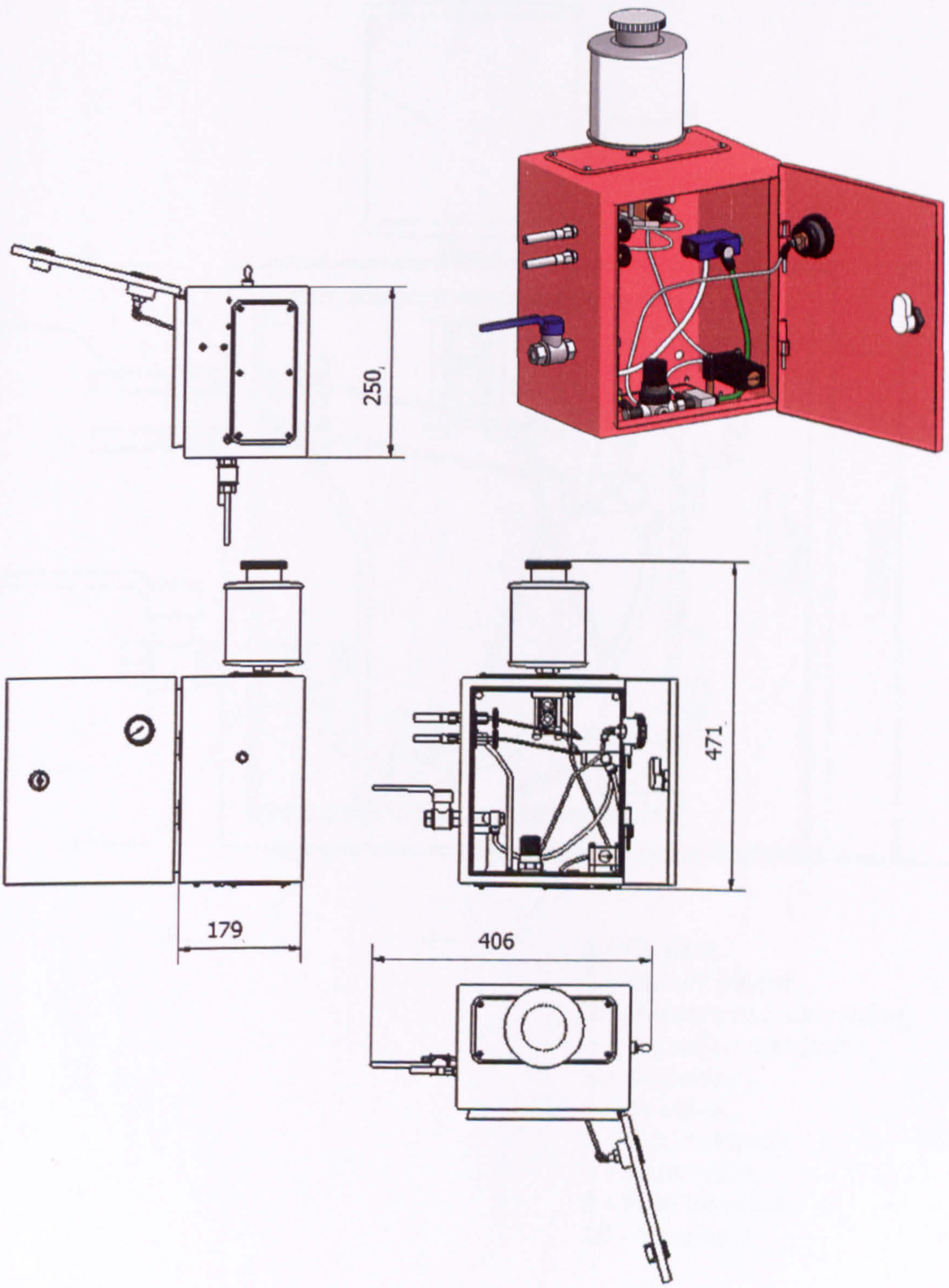

Figure A-2. General view of MQL system and its basic dimensions.

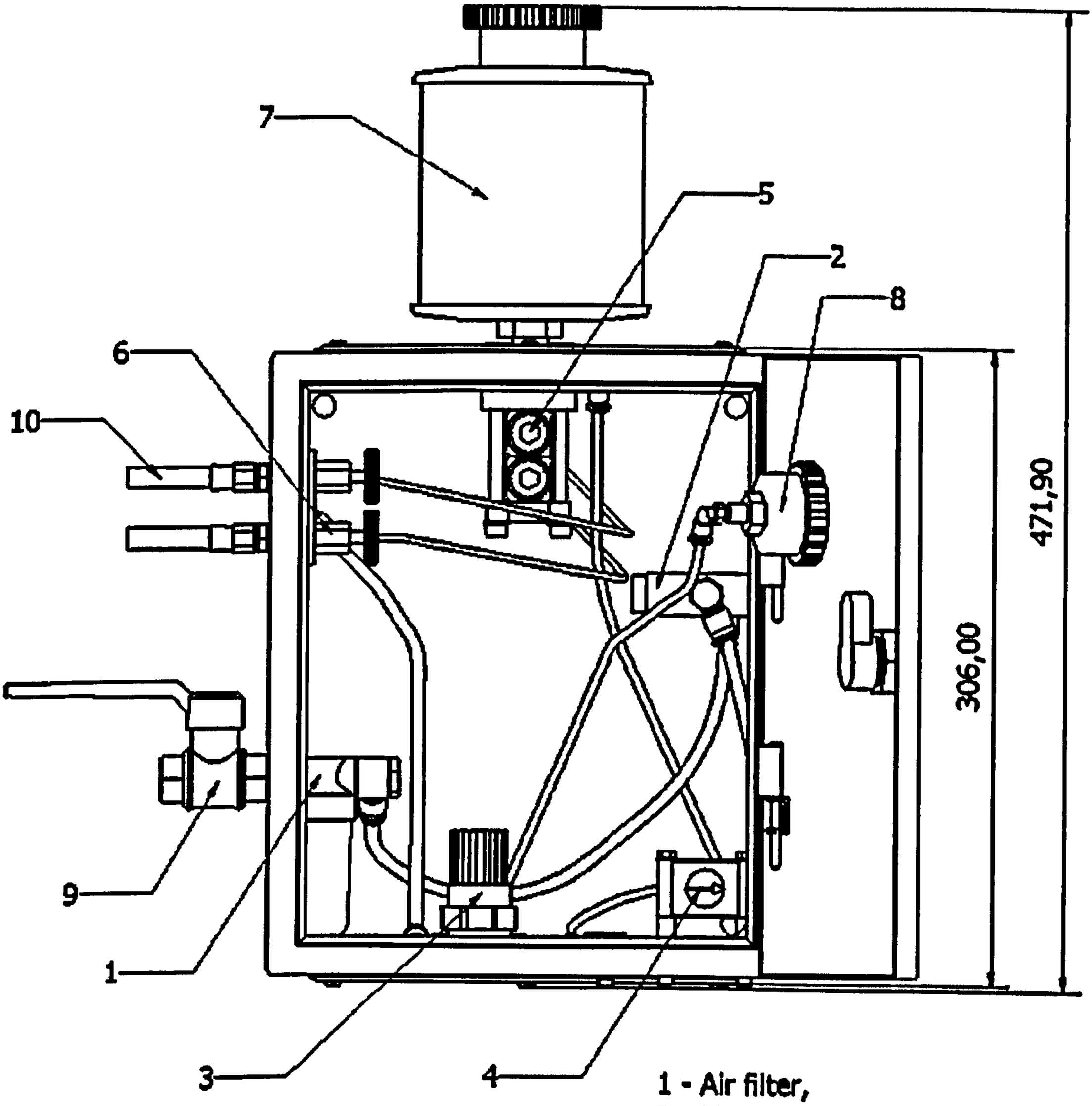

1 - Air filter,
2 - Manual trigger,
3 - Pressure reducing valve,
4 - Pulsation generator,
5 - Oil pump,
6 - Air valve,
7 - Fluid reservoir,
8 - Manometer,
9 - Main air valve,
10 - Feed tube

Figure A-3. Description of elemensts of MQL system.

SOME PARTS
EXCLUDED
UNDER
INSTRUCTION
FROM THE
UNIVERSITY